

2015

Investigation of AASHTOWare Pavement ME Design/Darwin-ME™ Performance Prediction Models for Iowa Pavement Analysis and Design

Orhan Kaya
Iowa State University

Follow this and additional works at: <https://lib.dr.iastate.edu/etd>

 Part of the [Civil Engineering Commons](#)

Recommended Citation

Kaya, Orhan, "Investigation of AASHTOWare Pavement ME Design/Darwin-ME™ Performance Prediction Models for Iowa Pavement Analysis and Design" (2015). *Graduate Theses and Dissertations*. 14840.
<https://lib.dr.iastate.edu/etd/14840>

This Thesis is brought to you for free and open access by the Iowa State University Capstones, Theses and Dissertations at Iowa State University Digital Repository. It has been accepted for inclusion in Graduate Theses and Dissertations by an authorized administrator of Iowa State University Digital Repository. For more information, please contact digirep@iastate.edu.

Investigation of AASHTOWare Pavement ME Design/Darwin-ME™ performance prediction models for Iowa pavement analysis and design

by

Orhan Kaya

A thesis submitted to the graduate faculty
in partial fulfillment of the requirements for the degree of
MASTER OF SCIENCE

Major: Civil Engineering (Transportation Engineering)

Program of Study Committee:
Halil Ceylan, Major Professor
Jing Dong
Kasthurirangan Gopalakrishnan
Sunghwan Kim
Paul G. Spry
Peter C. Taylor

Iowa State University

Ames, Iowa

2015

Copyright © Orhan Kaya, 2015. All rights reserved.

TABLE OF CONTENTS

	Page
LIST OF FIGURES	iv
LIST OF TABLES	iv
ACKNOWLEDGMENTS	xiii
ABSTRACT	xiv
CHAPTER 1. INTRODUCTION	1
Background	1
Objectives	4
Thesis Organization	4
CHAPTER 2. SUMMARY OF LITERATURE REVIEW RESULTS	6
CHAPTER 3. REVIEW OF PAVEMENT ME DESIGN SOFTWARE.....	16
Evaluation of Pavement ME Design Software: Comparison between Pavement ME Design and MEPDG Pavement Performance Predictions	21
CHAPTER 4. LOCAL CALIBRATION METHODOLOGY	27
Description of Iowa Pavement Sites Selected	27
Description of Calibration Database for Iowa Pavement Systems	33
Description of Optimization Approaches	39
Accuracy Evaluation Criteria.....	43
CHAPTER 5. LOCAL CALIBRATION RESULTS	46
JPCP	46
HMA	66
HMA over JPCP	90
CHAPTER 6. CONCLUSIONS, DISCUSSIONS AND RECOMMENDATIONS	105
Discussion on Future Enhancements of Pavement ME Design.....	105
Conclusions and Recommendations	107
Contributions of this study to the literature and state of the art practices related with the local calibration of Pavement ME Design	115
Recommendations: Future Research.....	116

REFERENCES	117
APPENDIX A: LITERATURE REVIEW RESULTS	125
Summary of National Level Projects for MEPDG Local Calibration	125
MEPDG/Pavement ME Design Local Calibration Studies in State Level	151
APPENDIX B. DESIGN EXAMPLES OF NEW JPCP, NEW HMA AND HMA OVER JPCP PAVEMENTS USING PAVEMENT ME SOFTWARE	178
New Rigid Pavement	178
New HMA Pavement.....	187
HMA over JPCP Pavement.....	195
APPENDIX C: SENSITIVITY ANALYSIS OF LOCAL CALIBRATION COEFFICIENTS .	204
New Rigid Pavement	205
New HMA and HMA over JPCP.....	206

LIST OF FIGURES

	Page
Figure 1. Flow chart of mechanistic-empirical pavement design concept (TRB 2012)	1
Figure 2. Flow chart of thesis organization	5
Figure 3. Summary of agency MEPDG implementation status (NCHRP 2014).....	9
Figure 4. Iowa pavements by AADTT distribution (as of 2014): (a) JPCPs, (b) HMA pavements, and (c) HMA over JPCPs.....	29
Figure 5. Geographical locations of selected Iowa pavement sites: (a) JPCPs, (b) HMA pavements, and (c) HMA over JPCPs.....	30
Figure 6. Iowa pavements by the distribution of construction years (as of 2014): (a) JPCPs, (b) HMA pavements, (c) initial JPCPs construction years of HMA over JPCPs, (d) HMA resurfacing years of HMA over JPCPs	31
Figure 7. Iowa pavements by the distribution of surface thicknesses (as of 2014): (a) PCC surface thickness for JPCPs, (b) HMA surface thickness for HMA pavements, (c) HMA overlay thicknesses for HMA over JPCPs, and (d) PCC thicknesses for HMA over JPCPs.....	32
Figure 8. Iowa pavements by the distribution of base thicknesses as of 2014 (as of 2014): (a) JPCPs, (b) HMA pavements, (c) HMA over JPCPs	33
Figure 9. JPCP performance data distribution (as of 2014): (a) faulting, (b) transverse cracking and (c) IRI	36
Figure 10. HMA performance data distribution (as of 2014): (a) total rutting, (b) HMA rutting, (c) granular base rutting, (d) subgrade rutting, (e) longitudinal cracking, (f) alligator cracking, (g) transverse cracking and (h) IRI	37
Figure 11. HMA over JPCP performance data distribution (as of 2014): (a) total rutting, (b) longitudinal cracking, (c) alligator cracking, (d) transverse cracking and (e) IRI.....	38
Figure 12. Optimization procedures to identify local calibration coefficients	40
Figure 13. Faulting values comparison between Pavement ME Design output and calculated values	50
Figure 14. Overall accuracy summary of JPCP faulting model using calibration set	52
Figure 15. Overall accuracy summary of JPCP faulting model using validation set	52
Figure 16. Overall accuracy summary of JPCP transverse cracking model using calibration set.....	56

Figure 17. Overall accuracy summary of JPCP transverse cracking model using validation set ..	57
Figure 18. Fatigue damage prediction comparisons	58
Figure 19. Comparison of calculated and Pavement ME Desing outputted IRI values	61
Figure 20. Overall accuracy summary of the JPCP IRI model using calibration set (Approach 1)	63
Figure 21. Overall accuracy summary of the JPCP IRI model using validation set (Approach 1)	63
Figure 22. Overall accuracy summary of JPCP IRI model using calibration set (Approach 2)	65
Figure 23. Overall accuracy summary of JPCP IRI model using validation set (Approach 2)	65
Figure 24. Overall accuracy summary of HMA rutting model using calibration set	71
Figure 25. Overall accuracy summary of HMA rutting model using validation set.....	71
Figure 26. Overall accuracy summary of HMA alligator (bottom-up) cracking model using calibration set	77
Figure 27. Overall accuracy summary of HMA alligator (bottom-up) cracking model using validation set	77
Figure 28. Overall accuracy summary of HMA longitudinal (top-down) cracking model using calibration set	78
Figure 29. Overall accuracy summary of HMA longitudinal (top-down) cracking model using validation set	79
Figure 30. Overall accuracy summary of HMA transverse cracking model using calibration set	82
Figure 31. Overall accuracy summary of HMA transverse cracking model using validation set .	83
Figure 32. Overall accuracy summary of HMA IRI model using calibration set (Approach 1) ...	87
Figure 33. Overall accuracy summary of HMA IRI model using validation set (Approach 1)	87
Figure 34. Overall accuracy summary of HMA IRI model using calibration set (Approach 2) ...	89
Figure 35. Overall accuracy summary of HMA IRI model using validation set (Approach 2)	90
Figure 36. Overall accuracy summary of HMA layer rutting model of HMA over JPCP pavements using calibration set	92
Figure 37. Overall accuracy summary of HMA layer rutting model of HMA over JPCP pavements using calibration set	92

Figure 38. Overall accuracy summary of HMA alligator (bottom-up) cracking model of HMA over JPCP pavements using calibration set	94
Figure 39. Overall accuracy summary of HMA alligator (bottom-up) cracking model of HMA over JPCP pavements using validation set	94
Figure 40. Overall accuracy summary of HMA longitudinal (top-down) cracking model of HMA over JPCP pavements using calibration set	95
Figure 41. Overall accuracy summary of HMA longitudinal (top-down) cracking model of HMA over JPCP pavements using validation set	96
Figure 42. Overall accuracy summary of HMA transverse cracking model of HMA over JPCP pavements using validation set.....	98
Figure 43. Overall accuracy summary of HMA transverse cracking model of HMA over JPCP pavements using validation set.....	98
Figure 44. Overall accuracy summary of HMA over JPCPs IRI model for calibration set (Approach 1)	101
Figure 45. Overall accuracy summary of HMA over JPCPs IRI model for validation set (Approach 1)	101
Figure A.1. The Bias and the residual error (Von Quintus 2008a).....	127
Figure A.2. Flow chart for the procedure and steps suggested for local calibration: steps 1-5 (NCHRP 2009).....	128
Figure A.3. Flow chart for the procedure and steps suggested for local calibration: steps 6-11 (NCHRP 2009)	129
Figure A.4. LTPP transverse cracking (Miller and Bellinger 2003).....	134
Figure A.5. Comparison of predicted and measured rut depths using the global calibration in KSDOT study (NCHRP 2009)	137
Figure A.6. Comparison of the intercept and slope estimators to the line of equality for the predicted and measured rut depths using the global calibration values in KSDOT study (NCHRP 2009).....	138
Figure A.7. Screen Shot of the MEPDG Software for the local calibration and agency specific values (Von Quintus 2008b).....	139
Figure A.8. Comparison of the standard error of the estimate for the global-calibrated and local-calibrated transfer function in KSDOT study (NCHRP 2009).....	143
Figure A.9. Regional and state level calibration coefficients of HMA rutting depth transfer function for Texas (Banerjee et al. 2009)	162

Figure A.10. 2007 and 2011 thickness designs for 13 projects at two levels of traffic each.....	177
Figure B.1. General inputs, design criteria and reliability	180
Figure B.2. Traffic inputs used in the design.....	180
Figure B.3. Vehicle class distribution and growth used in the design	181
Figure B.4. Climate input used in the design.....	181
Figure B.5. JPCP design properties	182
Figure B.6. Pavement structure input	182
Figure B.7. Layer design properties.....	183
Figure B.8. Modification of layer design properties.....	183
Figure B.9. Inputting local calibration coefficients	184
Figure B.10. Running the software	184
Figure B.11. Output reports	185
Figure B.12. PDF output report	186
Figure B.13. Optimization tool.....	187
Figure B.14. General inputs, design criteria and reliability	189
Figure B.15. Traffic inputs.....	190
Figure B.16. Truck traffic classification.....	190
Figure B.17. Climate inputs	191
Figure B.18. Pavement structure input for new HMA.....	192
Figure B.19. AC layer properties	192
Figure B.20. Layer design properties.....	193
Figure B.21. Modification of layer design properties of new HMA pavement.....	193
Figure B.22. Inputting HMA local calibration coefficients.....	194
Figure B.23. PDF output report for new HMA pavement	194
Figure B.24. General inputs, design criteria and reliability	197

Figure B.25. Traffic inputs.....	198
Figure B.26. Climate inputs	198
Figure B.27. JPCP design properties for the HMA over JPCP pavement	199
Figure B.28. Existing JPCP condition of the HMA over JPCP pavement	199
Figure B.29. AC layer design properties	200
Figure B.30. Pavement structure input for the HMA over JPCP pavement	200
Figure B.31. Choosing layer design properties of the HMA over JPCP pavement.....	201
Figure B.32. Modification of layer design properties.....	201
Figure B.33. Use of Back calculation Node	202
Figure B.34. Running the software	202
Figure B.35. PDF output report for the HMA over JPCP pavement	203

LIST OF TABLES

	Page
Table 1. Summary of agency local calibration efforts —Asphalt pavement performance models	9
Table 2. Agency local calibration—Concrete models	10
Table 3. Local calibration coefficients for JPCP pavement systems	12
Table 4. Local calibration coefficients for flexible and HMA overlaid pavement systems	13
Table 5. 15 total base cases used in NCHRP 1-47 project (NCHRP 2011).....	21
Table 6. Climate categories used in NCHRP 1-47 project (NCHRP 2011)	22
Table 7. Traffic levels used in NCHRP 1-47 project (NCHRP 2011).....	22
Table 8. Pavement performance prediction comparisons for new JPCP cases.....	23
Table 9. Pavement performance prediction comparisons for new JPCP over stiff foundation cases	23
Table 10. Pavement performance prediction comparisons for new HMA cases: cracking	24
Table 11. Pavement performance prediction comparisons for new HMA cases: rutting and IRI .	25
Table 12. Pavement performance prediction comparisons for HMA over stiff foundation cases: cracking	26
Table 13. Pavement performance prediction comparisons for HMA over stiff foundation cases: rutting and IRI	26
Table 14. Site selection summary information	28
Table 15. Optimization techniques used for different pavement distresses.....	41
Table 16. Sensitivity analysis results of transverse cracking calibration coefficients	55
Table 17. Sensitivity analysis results of HMA rutting calibration coefficients	69
Table 18. Experimental matrix for local calibration of HMA rutting model.....	70
Table 19. Sensitivity analysis results of HMA fatigue model calibration coefficients	75
Table 20. Sensitivity analysis results of HMA alligator (bottom-up) cracking model calibration coefficients.....	75

Table 21. Sensitivity analysis results of HMA longitudinal (top-down) cracking model calibration coefficients.....	75
Table 22. Sensitivity analysis results of HMA and thermal cracking calibration coefficients.....	81
Table 23. Trial calibration coefficients for HMA thermal cracking model.....	81
Table 24. Pair t test results for HMA IRI model (Approach 1).....	86
Table 25. Pair t test results for HMA IRI model (Approach 2).....	89
Table 26. Experimental matrix for local calibration of HMA layer rutting model of HMA over JPCP pavements.....	91
Table 27. Trial calibration coefficients for HMA over JPCP thermal cracking model.....	97
Table 28. Pair t test results for HMA IRI model for selected HMA over JPCP pavement sections (Approach 1).....	100
Table 29. Pair t test results for HMA IRI model for selected HMA over JPCP pavement sections (Approach 2).....	103
Table 30. Pavement and distress types the new reflection cracking affects (AASHTO 2015) ...	106
Table A.1. Calibration parameters to be adjusted for eliminating bias and reducing the standard error of the flexible pavement transfer functions (NCHRP 2009).....	140
Table A.2. Agency Use of Pavement Design Methods (NCHRP 2014).....	145
Table A.3. Summary of MEPDG Use or Planned Use by Pavement Type (NCHRP 2014).....	146
Table A.4. Agency Local Calibration Coefficients—Concrete (NCHRP 2014).....	147
Table A.5. Agency Local Calibration Coefficients—Asphalt (NCHRP 2014).....	148
Table A.6. List of assumptions in MEPDG local calibration of NC under FHWA HIF-11-026 research project (FHWA 2010).....	150
Table A.7. Listing of local validation-calibration projects (Von Quintus 2008b).....	154
Table A.8. Summary of local calibration values for the rut depth transfer function (Von Quintus 2008b).....	155
Table A.9. Summary of local calibration values for the area fatigue cracking transfer function (Von Quintus 2008b).....	156
Table A.10. Summary of the local calibration values for the thermal cracking transfer function (Von Quintus 2008b).....	157

Table A.11. HMA overlaid rigid pavements' IRI calibration coefficients for surface layer thickness within ADTT (Schram and Abdelrahman 2006)	158
Table A.12. JPCP IRI calibration coefficients for surface layer thickness within ADTT (Schram and Abdelrahman 2006)	159
Table A.13. North Carolina local calibration factors of rutting and alligator cracking transfer functions (Muthadi and Kim 2008)	160
Table A.14. Local calibrated coefficient results of typical Washington State flexible pavement systems (Li et al. 2009)	161
Table A.15. Calibration coefficients of the MEPDG flexible pavement distress models in Arizona conditions (Souliman et al. 2010)	163
Table A.16. Summary of calibration factors (Hall et al. 2011)	165
Table A.17. Comparison between local calibration coefficients from Approach 1 and 2 (Jadoun 2011).....	166
Table A.18. Local calibration summary for JPCP pavement systems (Mu et al. 2015).....	169
Table A.19. Calibration coefficients of the MEPDG (Version 0.9) rigid pavement distress models in the State of Washington (Li et al. 2006)	170
Table A.20. New local calibration coefficients of the MEPDG rigid pavement distress models in the State of Ohio (Titus-Glover and Mallela 2009)	172
Table A.21. New local calibration coefficients of the MEPDG rigid pavement distress models in the State of Missouri (Mallela et al. 2009).....	172
Table A.22. Recalibrated local calibration coefficients of the MEPDG for transverse cracking model models in the State of Washington (Li et al. 2010).....	173
Table A.23. Comparison of accuracy between global and ADOT calibrated MEPDG models for Arizona JPCP systems (Darter et al. 2014)	175
Table A.24. Comparison of erroneous CTEs (NCHRP 1-40D) and corrected CTEs (NCHRP 20-07) (Mallela et al. 2015).....	176
Table A.25. Revised calibrated joint faulting model coefficients (Mallela et al. 2015).....	177
Table C.1. Summary of calibration coefficient sensitivity indices for JPCP faulting model	206
Table C.2. Summary of calibration coefficient sensitivity indices for JPCP transverse cracking model.....	206

Table C.3. Summary of calibration coefficient sensitivity indices for JPCP IRI model	206
Table C.4. Summary of calibration coefficient sensitivity indices for HMA rutting model	207
Table C.5. Summary of calibration coefficient sensitivity indices for HMA subgrade rutting model.....	207
Table C.6. Summary of calibration coefficient sensitivity indices for HMA fatigue model.....	208
Table C.7. Summary of calibration coefficient sensitivity indices for HMA alligator (bottom-up) cracking model	208
Table C.8. Summary of calibration coefficient sensitivity indices for HMA longitudinal (top-down) cracking model.....	208
Table C.9. Summary of calibration coefficient sensitivity indices for HMA thermal (transverse) cracking model.....	208
Table C.10. Summary of calibration coefficient sensitivity indices for HMA IRI model.....	209

ACKNOWLEDGMENTS

First of all, I would like to thank my major professor, Dr. Halil Ceylan, for his support in this study. I especially admire his great technical knowledge, academic dedication and ability to successfully manage many tasks together.

Furthermore, I would like to acknowledge my committee members Drs. Kasthurirangan Gopalakrishnan, Sunghwan Kim, Jing Dong, Peter C. Taylor, and Paul G. Spry for their guidance and constructive comments for their guidance and support throughout the course of this research. Special thanks are extended to Drs. Kasthurirangan Gopalakrishnan and Sunghwan Kim for their extra invaluable assistance to my research. Dr. Kim inspired me with his diligence on work discipline, academic dedication and patience. Also, Dr. Gopalakrishnan inspired me with his great technical knowledge, professionalism and humbleness.

In addition, I would like to thank the Ministry of National Education of Turkey for providing me a scholarship and education opportunity in the U.S.

I also would like to acknowledge the Iowa DOT to support this study. Special thanks are extended to the Iowa DOT and ARA, Inc. engineers, who helped me throughout my study.

I would also like to thank my friends, colleagues, the department faculty and staff for making my time at Iowa State University a wonderful experience.

Last but not the least, I would like to thank my family for supporting me throughout writing this thesis and my life in general.

ABSTRACT

The Mechanistic Empirical Pavement Design Guide (MEPDG) was developed under the National Cooperative Highway Research Program (NCHRP) Project 1-37A as a novel mechanical-empirical procedure for analysis and design of pavements. The MEPDG was subsequently renamed the DarWin-ME in April 2011 and, most recently, marketed as the AASHTOWare Pavement ME Design as of February 2013. Although the core design process and computational engine have remained the same over the years, some enhancements to the pavement performance prediction models were implemented along with other documented changes as the MEPDG transitioned to the AASHTOWare Pavement ME Design.

Preliminary studies were carried out to determine possible differences between AASHTOWare Pavement ME Design, MEPDG (version 1.1) and DARWin-ME (version 1.1) performance predictions for new Jointed Plain Concrete Pavement (JPCP), new Hot-Mix Asphalt (HMA), and HMA over JPCP pavement systems. Differences were indeed observed between the pavement performance predictions produced by these software versions. Further investigation was needed to verify these differences and to evaluate whether identified local calibration factors from the latest MEPDG (version 1.1) were acceptable for use with the latest version (version 2.1.24) of AASTHOWare Pavement ME Design at the time this research was conducted. The primary objective of this research was to examine AASHTOWare Pavement ME Design performance predictions using previously-identified MEPDG calibration factors (through Iowa DOT Project TR 401) and, if needed, refine local calibration coefficients of AASHTOWare Pavement ME Design pavement performance predictions for Iowa pavement systems using linear and nonlinear optimization procedures. A total of 130 representative sections across Iowa consisting of JPCP, new HMA and HMA over JPCP sections are used. The local calibration

results of Pavement ME Design are presented and compared with national and MEPDG locally calibrated models.

CHAPTER 1. INTRODUCTION

Background

The Mechanistic-Empirical Pavement Design Guide (MEPDG) was completed under National Cooperative Highway Research Program 1-37A project (NCHRP 2004) and NCHRP project 1-40 (AASHTO 2010). This MEPDG provides a novel pavement analysis and design tool employing mechanistic structural response models to calculate pavement responses (stresses, strains, and deflection) and nationally-calibrated empirical distress transfer functions to predict pavement performance. This new pavement design concept is called mechanistic-empirical pavement design (M-E). Figure 1 shows the flow chart of mechanistic-empirical pavement design concept.

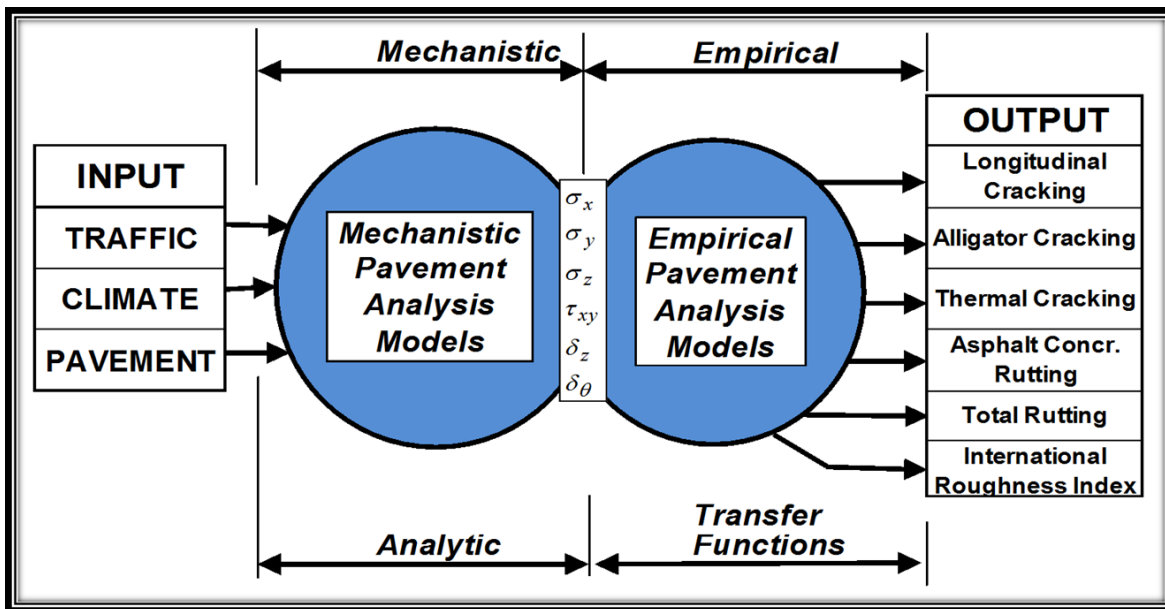


Figure 1. Flow chart of mechanistic-empirical pavement design concept (TRB 2012)

Following the release of NCHRP (2004), to implement MEPDG, pavement analysis and design software (MEPDG version 1.1) was also released along with the report for research purposes. The software has since been improved by adding new pavement performance

prediction models as well as by advancing existing models. MEPDG software has been rebranded in 2011 as DARWin-ME™ after mainly improving the software interface to make it more intuitive and user-friendly; it has recently been marketed as AASHTOWare® Pavement ME Design. The latest version of Pavement ME Design software is version 2.2, released in August, 2015.

Upon completion of national calibrations of MEPDG pavement prediction models, NCHRP (2004) recommended that state highway agencies (SHAs) conduct local calibration of the models before fully implementing the software. Using the term ‘local calibration’ in the MEPDG concept, implying a mathematical process of reducing the bias and standard error between actual (measured) pavement distress measurements and pavement performance predictions, makes the software output easier to understand (AASHTO 2010). Moreover, local calibration is conducted by optimizing local calibration coefficients that the empirical distress transfer functions use to reduce bias and standard error. Such local-calibration studies are needed for states for which the national- calibrated pavement performance model predictions are insufficiently accurate. It is to be expected that nationally-calibrated performance models would not provide similarly accurate pavement performance predictions for each state since (1) in the national calibration of MEPDG, the Long Term Pavement Performance (LTPP) test sections, and very few other experimental test sections, were mostly used. Also, while some states had many different LTPP test sections used in the national calibration process, some states had very few sections involved. This means that local conditions of some states may not have been well represented in the national calibration process. Also, AASHTO (2010) documents state that “policies on pavement preservation and maintenance, construction and material specifications, and materials vary across the United States and are not considered directly in the MEDPG”, so

AASHTO (2010) recommends employing local calibration studies to take into account these regional differences.

Following the release of NCHRP (2004), local calibration of MEPDG was extensively initiated by agencies separate from national-level follow-up research studies. The Iowa Department of Transportation (DOT) is also in the process of implementing the Mechanistic-Empirical Pavement Design Guide. Once the local calibration of the design guide for Iowa is finalized, it is expected that the guide would be used state-wise by state highway engineers and their private counterparts. Accurate prediction of distress in a pavement section during its service time is basically dependent on reliable pavement performance prediction models. It is quite possible that, by using locally-calibrated pavement prediction models, the Iowa DOT could save a great deal of money, because accurate prediction of such distress during the service life of a pavement section would enable engineers to take necessary and timely precautions as needed and determine the optimum pavement thickness for resisting all types of loading throughout its service life.

The primary goal of local calibration for Pavement ME Design is to identify optimized calibration coefficients of performance prediction models taking local conditions into account to reduce bias and standard error of predictions compared to actual distress measurements (AASHTO 2010). Therefore, optimizing calibration coefficients is a critical step in the local calibration process. However, most local calibration studies described in the literature have not discussed their optimization procedures in detail, instead reporting only local-calibration coefficient results. The procedure employed in previous studies (Darter et al. 2014, Wu et al. 2014, Williams and Shaidur 2013, Li et al. 2010 and Bustos et al. 2009) is mainly a trial-and-error approach requiring many MEPDG or Pavement ME Design software runs with ever-

changing calibration coefficients. The main reasons for use of a such limited approach in previous studies are related to (1) lack of understanding pavement-performance models comprised of numerous equations, (2) neglecting the review of numerous intermediate output files (mostly, text file format) produced along with final result summary output files (PDF and Excel file formats), and (3) pavement response results previously not provided by MEPDG software but now provided by Pavement ME Design software through intermediate output files.

In this study, the step-by-step procedure of local calibration was established and documented in detail. The local calibration results of Pavement ME Design were presented and compared with national and MEPDG local models.

Objectives

The first objective of this study is to evaluate the accuracy of nationally and MEPDG locally-calibrated pavement performance prediction models obtained through Iowa DOT project TR 401 (Ceylan et al. 2013). The second objective of this study is to conduct a recalibration of these models if their accuracy has been found insufficient. This recalibration process was implemented using AASHTOWare Pavement ME Design version 2.1.24, released in August 2014, with the assistance of linear and nonlinear optimization techniques for improving model prediction accuracy.

Thesis Organization

This thesis consists of six chapters. Chapter 1 introduces the background and objectives of this study. Chapter 2 provides a summary of literature review results related to local calibration of MEPDG. Chapter 3 presents a review of Pavement ME Design software along with an evaluation of Pavement ME Design software by comparing the pavement performance predictions of Pavement ME Design and MEPDG software. Chapter 4 documents the local

calibration methodology used in this study, including a description of Iowa pavement sites selected, a description of calibration databases for Iowa pavement systems, and a description of optimization approaches and accuracy evaluation criteria. Chapter 5 presents local calibration results for each pavement type are presented. Chapter 6 provides discussion on future enhancements of Pavement ME Design, conclusions and recommendations, contributions of this study to the literature, and state-of-the-art practices as well as recommendations for future research. Figure 2 shows the flow chart of thesis organization.

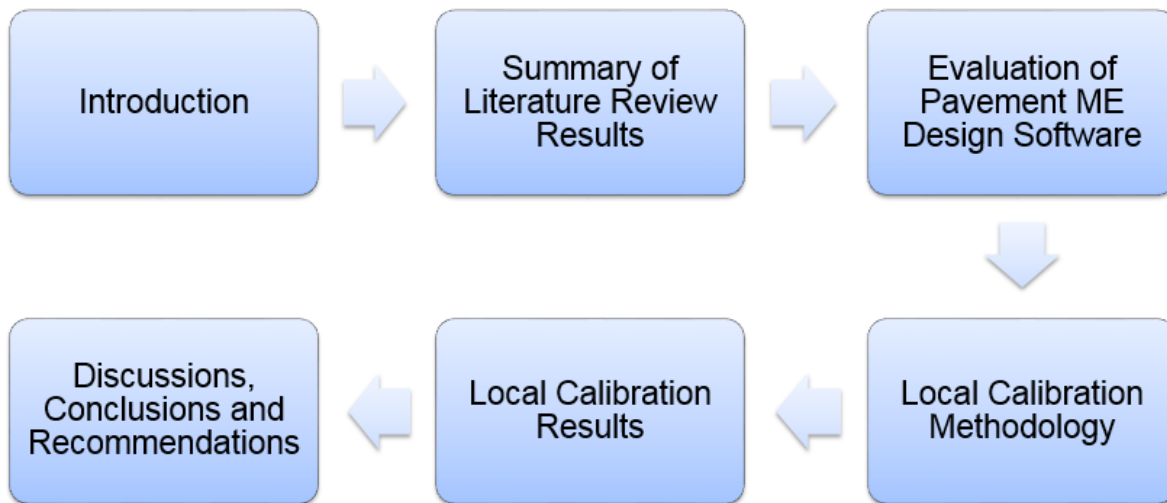


Figure 2. Flow chart of thesis organization

CHAPTER 2. SUMMARY OF LITERATURE REVIEW RESULTS

The national calibration-validation process was successfully completed for MEPDG and accompanying AASHTOWare Pavement ME Design software (NCHRP 2004, AASHTO 2010). Although these efforts were comprehensive, further calibration and validation studies to suit local conditions are highly recommended by MEPDG as a prudent step in implementing a new design procedure different from current procedures. Several national-level research studies supported by the NCHRP and FHWA have been conducted following the release of the original research version of the MEPDG software. Parallel to national-level research projects, many state/local agencies have either conducted or plan to undertake local calibration studies for their own pavement conditions. As part of the previous InTrans Project 11-401 “Iowa Calibration of MEPDG Performance Prediction Models”, Ceylan et al. (2013) reported comprehensive literature review results related to local calibration of MEPDG in both national and state level research studies prior to 2012. These results have been updated by incorporating newly reported study results at the time of this project (i.e., 2015) as described in Appendix A. Discussions of literature review results are presented here.

There are three NCHRP research projects that are closely related to local calibration of MEPDG and Pavement ME Design performance predictions. They are:

- (1) NCHRP 9-30 project (NCHRP 2003a, NCHRP 2003b), “Experimental Plan for Calibration and Validation of Hot Mix Asphalt Performance Models for Mix and Structural Design”
- (2) NCHRP 1-40B (Von Quintus et al. 2005, NCHRP 2007, Von Quintus et al. 2009a, Von Quintus et al. 2009b, NCHRP 2009, TRB 2010), “User Manual and Local Calibration Guide for the Mechanistic-Empirical Pavement Design Guide and Software”
- (3) NCHRP Synthesis 457 (NCHRP 2014), “Implementation of the AASHTO Mechanistic-Empirical Pavement Design Guide and Software”

Note that NCHRP 1-40B Project is a part of NCHRP 01-40 (accessed through the website <http://onlinepubs.trb.org> as of 2014) “Facilitating the Implementation of the Guide for the Design of New and Rehabilitated Pavement Structures” intended to ease the implementation and adoption of MEPDG by SHAs. Note that The AASHTOWare Pavement ME Design™ software is the final product of the NCHRP 1-40 study.

Under the NCHRP 9-30 project (NCHRP 2003b), pre-implementation studies involving verification and recalibration have been conducted to quantify the bias and residual error of the flexible-pavement distress models included in an initial version of MEPDG software from NCHRP 1-37A (Muthadi 2007). Similar to national recalibration of flexible pavement models, NCHRP 1-40 recalibrated the national calibration coefficients of rigid-pavement performance models by using more rigid-pavement sections than in NCHRP 1-37A. Nationally-recalibrated coefficients (referred to as Original National Calibration (ONC) in this report) for both flexible and rigid pavement performance models were incorporated into MEPDG version 1.0 and Pavement ME Design software. As a result of adapting new concrete coefficient of thermal expansion (CTE) testing procedures (AASHTO T336-09 2009), another set of national calibration coefficients (called New National Calibration (NNC)) for rigid-pavement models was determined in 2011 using CTE values determined from new test procedures without adjustment. Until the release of latest Pavement ME Design software (version 2.2), the ONC were being used as default national calibration coefficients. However, with the latest software version (version 2.2), users now can choose NNC values as default national calibration coefficients.

Based on findings of the NCHRP 9-30 study, the NCHRP 1-40B project has focused on preparing: (1) a user manual for the MEPDG and its software, and (2) a detailed, practical guide for highway agencies performing local or regional calibration of the distress models in the

MEPDG and its software. Both the manual and the guide have been presented in the form of draft AASHTO recommended practices, including two or more examples or case studies illustrating the step-by-step procedures. It has also been noted that the longitudinal cracking and reflection cracking models have not been much considered in local calibration guide development during the NCHRP 1-40B study because of lack of prediction accuracy (Muthadi 2007, Von Quintus and Moulthrop 2007). The NCHRP 1-40 B was completed in 2009 and published under the title, “Guide for the Local Calibration of the Mechanistic-Empirical Pavement Design Guide” through AASHTO (AASHTO 2010).

NCHRP synthesis 457 (NCHRP 2014) conducted a survey of 57 highway transportation agencies, with a 92% response rate from 48 U.S. state highway agencies and a 69% response rate from nine Canadian highway transportation agencies, to document strategies and lessons learned from state highway agencies in implementing MEPDG. Based on the results of these surveys, it was concluded that three agencies have fully implemented the MEPDG in their pavement designs, forty-six agencies have been in the act of implementing MEPDG, and eight agencies had no plan at survey time to implement MEPDG (See Figure 3). Twelve responding agencies also noted that MEPDG pavement performance prediction models were already locally-calibrated for their states. Arizona, Colorado, Hawaii, Indiana, Missouri, New Jersey, and Oregon implemented local calibration for HMA models, and Arizona, Colorado, Florida, Indiana, Missouri, North Dakota, and Oregon implemented local calibration for concrete models. Table 1 and Table 2 list the states conducting local calibration of HMA and concrete pavement performance prediction models and the models that were locally calibrated. Note in Table 1 that Arizona and Colorado locally calibrate the empirical reflective-cracking model originally

included in the MEPDG. Major challenges indicated by the surveyed agencies include software complexity, availability of needed data, defining input levels, and a need for local calibration.

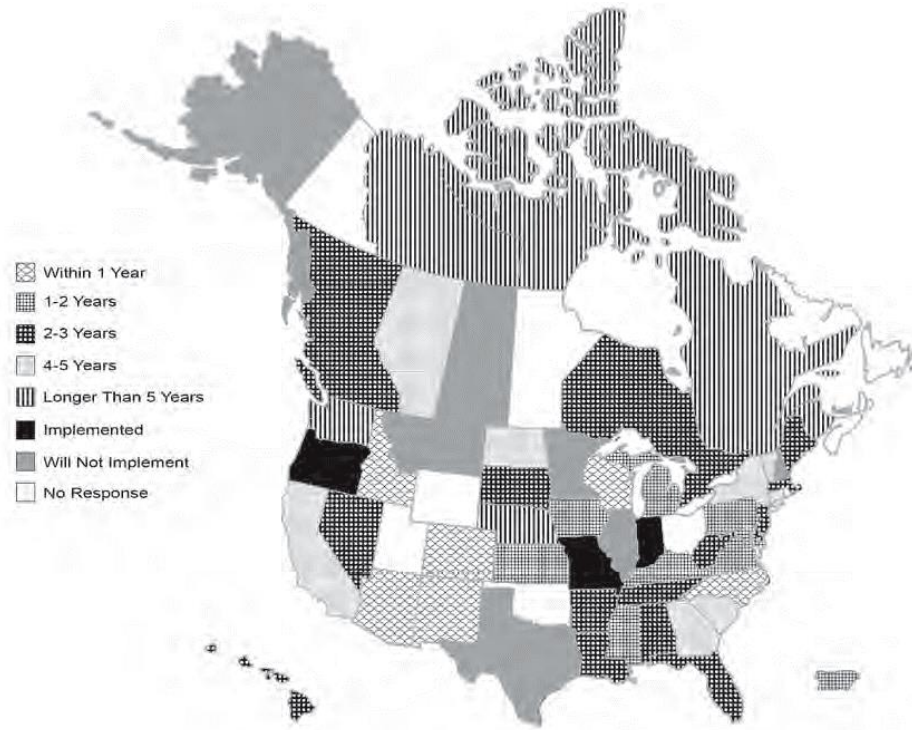


Figure 3. Summary of agency MEPDG implementation status (NCHRP 2014)

Table 1. Summary of agency local calibration efforts —Asphalt pavement performance models

Agency	IRI	Longitudinal Cracking	Alligator Cracking	Thermal Cracking	Rut Depth		Reflective Cracking
					Asphalt layer	Total	
Arizona	✓	Do not use	✓	MEPDG	✓	✓	✓
Colorado	✓	✓	✓	✓	✓	✓	✓
Hawaii	✓	1	1	1	1	1	1
Indiana	✓	Do not use	✓	MEPDG	MEPDG	Do not use	Do not use
Missouri	✓	MEPDG	MEPDG	✓	✓	✓	MEPDG
New Jersey	✓	1	1	1	1	1	1
Oregon	✓	✓	✓	✓	✓	✓	MEPDG

¹Future plans.

✓Indicates performance prediction models have been locally calibrated.

Table 2. Agency local calibration—Concrete models

Agency	JPCP			CRCP	
	IRI	Transverse cracking	Faulting	IRI	Punchouts
Arizona	✓	✓	✓	✓	✓
Colorado	✓	✓	✓	Do not use	Do not use
Florida	✓	✓	✓	Do not use	Do not use
Indiana	✓	<i>MEPDG</i>	<i>MEPDG</i>	Do not use	Do not use
Missouri	✓	<i>MEPDG</i>	<i>MEPDG</i>	Do not use	Do not use
North Dakota	✓	<i>MEPDG</i>	<i>MEPDG</i>	Do not use	Do not use
Oregon	✓	<i>MEPDG</i>	<i>MEPDG</i>	✓	✓

✓Indicates performance prediction models have been locally calibrated.

Two research studies supported by the FHWA have been conducted on using pavement management system (PMS) data for local calibration of MEPDG. The study “Using Pavement Management Data to Calibrate and Validate the New MEPDG, An Eight State Study” (FHWA 2006a, FHWA 2006b) evaluated the potential use of PMS for MEPDG local calibration. Eight states participated in this study: Florida, Kansas, Minnesota, Mississippi, New Mexico, North Carolina, Pennsylvania, and Washington. The study concluded that all participating states could feasibly use PMS data for MEPDG calibrations, and other states not participating in the study could do the same. It was further recommended that each SHA should develop a satellite pavement management/pavement design database for each project being designed and constructed using the MEPDG as part of the currently used PMS.

The second follow-up study, FHWA HIF-11-026, “The Local Calibration of MEPDG Using Pavement Management System” (FHWA 2010a, FHWA 2010b) was conducted to develop a framework for using existing PMS to calibrate MEPDG performance models. One state (North Carolina) was selected based on screening criteria to finalize and verify the MEPDG calibration framework based on a set of actual conditions. Using this developed framework, local

calibration for the selected state was demonstrated under the assumptions of both MEPDG performance predictions established from NCHRP 1-37 A as well as distress measurements from a selected state. Local/State level research studies have also been conducted in addition to national-level research studies. Studies on rigid-pavement performance prediction model calibration, primarily focusing on new JPCP, include the work by Li et al. (2006) in Washington; Schram and Abdelrahman (2006) in Nebraska; Darter et al. (2009) in Utah; Velasquez et al (2009) in Minnesota; Titus-Glover and Mallela (2009) in Ohio; Mallela et al. (2009) in Missouri; Kim et al. (2010) in Iowa; Bustos et al. (2009) in Argentina; and Delgadillo et al. (2011) in Chile; Li et al. (2011) in Washington; Mallela et al. (2013) in Colorado and Darter et al. (2014) in Arizona.

As results of these studies, eleven U.S. state highway agencies have approved use of nationally calibrated coefficients (either ONC or NNC) for new JPCP while eight agencies have adopted locally-calibrated coefficients (Mu et al. 2015). The states adapting nationally-calibrated coefficients are Utah, Wyoming, Delaware, Indiana, Kansas, New York, North Carolina, Oklahoma, Pennsylvania, South Dakota, and Virginia. The states of Arizona, Colorado, Louisiana, Missouri, Ohio, Washington, and Florida have decided to use at least one of the local calibration coefficients different from national ones for their JPCP pavement performance prediction models. Table 3 summarizes the calibration coefficients of the state highway agencies for JPCP pavement performance prediction models, along with optimization method, MEPDG version and project data source used in the local-calibration process.

Table 3. Local calibration coefficients for JPCP pavement systems

	Calibration coefficients	ONC	NNC	Arizona	Colorado	Lousiana	Missouri	Ohio	Washington	Florida
Cracking	C1	2		NNC	NNC	2.6	ONC	ONC	1.93	2.8389
	C2	1.22		NNC	NNC	ONC	ONC	ONC	1.177	0.9647
	C4	1	0.6	0.19	NNC	ONC	ONC	ONC	ONC	0.564
	C5	-1.98	-2.05	-2.067	NNC	ONC	ONC	ONC	ONC	-0.5946
Faulting	C1	1.0184	1.252632	0.0355	0.5104	ONC	ONC	ONC	ONC	4.0472
	C2	0.91656	1.1273688	0.1147	0.00838	ONC	ONC	ONC	ONC	ONC
	C3	0.002185	0.0026876	0.00436	0.00147	ONC	ONC	ONC	ONC	ONC
	C4	0.000884	0.001087	1.10E-07	0.008345	ONC	ONC	ONC	ONC	ONC
	C5	250		20000	5999	ONC	ONC	ONC	ONC	ONC
	C6	0.4		2.0389	0.8404	1.2	ONC	ONC	ONC	0.079
	C7	1.83312	9.1	0.189	5.9293	ONC	ONC	ONC	ONC	ONC
	C8	400		NNC	NNC	ONC	ONC	ONC	ONC	ONC
IRI	J1	0.8203		0.6	NNC	ONC	0.82	0.82	ONC	ONC
	J2	0.4417		3.48	NNC	ONC	1.17	3.7	ONC	ONC
	J3	1.4929		1.22	NNC	ONC	1.43	1.711	ONC	2.2555
	J4	25.24		45.2	NNC	ONC	66.8	5.703	ONC	ONC
Optimization techniques used in local calibration				Sensitivity Analysis	SAS Statistical Analysis	N/A	Statistical software	Statistical & non-statistical	Sensitivity Analysis/Trial error	N/A
MEPDG version used in local calibration				Darwin ME	Darwin ME	Pavement ME	N/A	N/A	MEPDG version 1.0	N/A
Project data source				LTPP and CDOT	LTPP and CDOT PMS	LA PMS	LTPP and MoDOT	LTPP	WSPMS	N/A

Note:

ONC: Original Calibration Coefficients

NNC: New National Calibration

LTPP: Long Term Pavement Performance Program

CDOT and MODOT: Colorado and Missouri Department of Transportation

LA PMS and WSPMS: Pavement Management Systems for Louisiana and Washington

The following studies have been conducted for new HMA pavement and HMA overlaid pavement systems: Galal and Chehab (2005) in Indiana; Von Quintus and Moulthrop (2007) in Montana; Kang et al. (2007) mainly in Wisconsin; Schram and Abdelrahman (2006) in Nebraska; Muthadi and Kim (2008), Corley-Lay et al. (2010), and Jadoun (2011) in North Carolina; Li et al. (2009) and Li et al. (2010) in Washington; Banerjee et al. (2010), and Banerjee et al. (2011) in Texas; Titus-Glover and Mallela (2009) in Ohio; Darter et al (2009) in Utah; Souliman et al. (2010) and Mamlouk and Zapata (2010) in Arizona; Kim et al. (2010) in Iowa; Khazanovich et al. (2008), Velasquez et al (2009) and Hoegh et al. (2010) in Minnesota; and Hall et al (2011) in Arkansas; Jadoun (2011) in North Carolina, Tarefder and Rodriguez-Ruiz (2013) in New Mexico, Mallela et al. (2013) in Colorado; Williams and Shaidur (2013) in Oregon; Zhou et al. (2013) in Tennessee and Darter et al. (2014) in Arizona.

Table 4 lists the locally-calibrated coefficients of new HMA and HMA overlaid pavement systems for Arizona, Colorado, Missouri, and Oregon as well as the corresponding optimization method, MEPDG version, and project data source for each study used in the local calibration process.

Table 4. Local calibration coefficients for flexible and HMA overlaid pavement systems

	Calibration coefficients	National default values	Arizona	Colorado	Missouri	Oregon
Cracking	C1 Bottom	1	National	0.07	National	0.56
	C1 Top	7	National	National	National	1.453
	C2 Bottom	1	4.5	2.35	National	0.225
	C2 Top	3.5	National	National	National	0.097
	C3 Bottom	6000	National	National	National	National
	C3 Top	0	National	National	National	National
	C4 Top	1000	National	National	National	National
Fatigue	BF1	1	249.00872	130.367	National	National
	BF2	1	National	National	National	National
	BF3	1	1.23341	1.2178	National	National
Thermal Fracture	Level 1	1.5	National	7.5	0.625	National
	Level 2	0.5	National	National	National	National
	Level 3	1.5	National	National	National	National
Rutting (asphalt)	BR1	1	0.69	1.34	1.07	1.48
	BR2	1	National	National	National	1
	BR3	1	National	National	National	0.9
Rutting (subgrade)	BS1 (fine)	1	0.37	0.84	0.4375	National
	BS1 (granular)	1	0.14	0.4	0.01	National
IRI	J1 (asphalt)	40	1.2281	35	17.7	National
	J2 (asphalt)	0.4	0.1175	0.3	0.975	National
	J3 (asphalt)	0.008	National	0.02	National	National
	J4 (asphalt)	0.015	0.028	0.019	0.01	National
	J1 (over concrete)	40.8	National	National	National	National
	J2 (over concrete)	0.575	National	National	National	National
	J3 (over concrete)	0.0014	National	National	National	National
J4 (over concrete)	0.00825	National	National	National	National	
Optimization techniques used			Sensitivity Analysis	SAS Statistical Analysis	Statistical and non-statistical	Trial error and MS Solver
MEPDG version used in local calibration			Darwin ME	Darwin ME	N/A	Darwin M-E version 1.1
Project data source			LTPP and CDOT PMS	LTPP and CDOT	WIM-IRD and LTPP	ODOT database

Along with local calibration efforts for the new HMA and HMA overlaid pavement-performance prediction models of the states in Table 4, some states implemented local calibration for some of the flexible and composite HMA overlaid pavement performance prediction models, as listed below:

- Ohio: HMA rutting, subgrade rutting, and IRI models
- Washington: Fatigue model, HMA rutting, subgrade rutting, alligator-cracking, and longitudinal-cracking models
- Montana: Thermal fracture models
- New Mexico: HMA rutting, subgrade rutting, alligator-cracking, and longitudinal-cracking models
- North Carolina: HMA rutting and subgrade-rutting models
- Texas: HMA rutting and subgrade-rutting models

The procedures and findings of all these studies related to both concrete-surfaced and asphalt-surfaced pavements are summarized in Appendix A. Several significant issues relevant to the present study are highlighted below:

- Rutting for asphalt-surfaced pavements: The accuracy of nationally-calibrated rutting models was evaluated in Arkansas, Colorado, Missouri, New Mexico, North Carolina, Ohio, Oregon, Texas, and Washington. Most state-level studies indicate that MEPDG over predicts total rut depth because significant rutting was predicted in unbound layers and embankment soils. However, rutting predictions could be improved through local calibration.
- The longitudinal (top-down) cracking for asphalt surfaced pavements: The accuracy of nationally longitudinal (top-down) cracking models was evaluated in Arkansas, Minnesota, Montana, New Mexico, Oregon, and Washington. Montana observed significant differences

between actual and MEPDG predicted longitudinal-cracking values and did not calibrate this model at the time of its MEPDG implementation. Other states performed local calibration of at least one of the calibration coefficients of this prediction model. However, no consistent trend in the longitudinal (top-down) cracking predictions could be identified that would reduce the bias and standard error and thereby improve the accuracy of this prediction model.

- Alligator (bottom-up) cracking for asphalt surfaced pavements: The accuracy of national alligator (bottom-up) cracking models was evaluated in Arkansas, Colorado, Minnesota, Missouri, Montana, New Mexico, Ohio, Oregon, and Washington. The Oregon study indicated that nationally-calibrated alligator (bottom-up) cracking was overpredicted when using Darwin ME version 1.1 software while a Missouri study found national alligator-model under predicting in HMA pavements. On the other hand, a Washington study also found the national model both under and over predicting alligator cracking. Washington, Arkansas, and New Mexico also used a locally-calibrated alligator-cracking model and, after local calibration, the model accuracy improved to some extent.
- Thermal (transverse) cracking for asphalt-surfaced pavements: The accuracy of national alligator (bottom-up) cracking models was evaluated in Colorado, Missouri, Montana, and Oregon.
- Reflection cracking for asphalt overlaid concrete pavements: Only one state (Arizona) attempted to calibrate the empirical reflection-cracking model of HMA overlaid concrete pavements using Pavement ME design software. However, the empirical reflection-cracking model was replaced by a mechanistic-based reflection-cracking model developed in the NCHRP 1-41 project (Lytton et al. 2010) and provided in the new version of Pavement ME Design (version 2.2) released in August 2015.

CHAPTER 3. REVIEW OF PAVEMENT ME DESIGN SOFTWARE

MEPDG has evolved since its first release in 2004 as a product of the National Cooperative Highway Research Program (NCHRP) 1-37A project (NCHRP 2004). The first version of the software was designated MEPDG version 1.1. New versions of the software have subsequently been released with new features and enhancements added. AASHTO's *MEPDG, Interim Edition: A Manual of Practice* was issued in 2008 to educate users about the design methodology software used (AASHTO 2008). As more features were added to the software, it was rebranded as Darwin-ME in 2011 and AASHTOWare Pavement ME Design in 2014.

After release of NCHRP (2004), the national recalibration of MEPDG was initiated under NCHRP project 1-40, using a larger number of pavement sections than was used in NCHRP (2004). National calibration coefficients resulting from NCHRP project 1-40 have been widely used since then and the previous calibration coefficients have been discarded.

Coefficient of thermal expansion (CTE) is an important parameter in determining the length change of concrete pavements under different thermal conditions. Crawford et al. (2010) found the CTE model incorporated in the MEPDG software produced erroneous results due to an error in the test procedure. The test procedure used in the characterization of CTE was initially AASHTO TP 60-00 (2004) and, using this test procedure, CTE values were found to be overpredicted. A new test procedure was accordingly developed (AASHTO T 336-09 2009) and new CTE values specified based on the new test procedure. The related distress models were nationally recalibrated in 2011 and the recalibrated coefficients (i.e., NNC) have recently been incorporated into the latest software version (version 2.2) as default national calibration coefficients. It was suggested to Pavement ME users that they use either ONC in using CTE values determined from the TP 60-00 method (AASHTO TP 60-00 2004) or NNC in using CTE

values determined from a newer test procedure (AASHTO T 336-09 2009). The CTE values used in this study were acquired from a previous MEPDG implementation study, Task 6: “Material Thermal Inputs for Iowa Materials” (Wang et al. 2008), that used AASHTO TP 60-00 (2004) in characterization of CTE values.

In the historical development of MEPDG software, as new features were added and available features expanded and improved, software incorporating the new enhancements on different bases has been released along with accompanying release notes to introduce these enhancements. The contents of all release notes issued are summarized below (<http://www.me-design.com/MEDesign/Documents.html>):

April 2011 (DARWin-ME Version 1.0)

In this release note, differences between MEPDG and Pavement ME Design (DARWin-ME) were documented. The major new capabilities included in the software are as follows:

- A completely redesigned user interface
- Enterprise database support for sharing and storing projects, materials, traffic and design considerations across the agency
- Ability to edit and run multiple design analyses simultaneously in batch, sensitivity, thickness optimization or back calculation modes
- Redesigned and improved output reports in both Excel and Adobe PDF formats
- Climate data editing tools
- Redesigned PDF help documents based on the new software and the Mechanistic-Empirical Pavement Design Guide, Interim Edition: A Manual of Practice
- Significant decreases in analyses run time

December 2011 (DARWin-ME Version 1.1.33)

- Some software issues were resolved.

February 2013 (Pavement ME Design Version 1.3.28)

- Some software issues were resolved.

July 2013 (Pavement ME Design Version 1.5.08, Educational Version 1.5.08)

- The educational version of the software can only be used for the design of new asphalt and concrete (JPCP and CRCP), AC/AC overlays, AC/JPCP Overlays, or Unbonded PCC overlays for a 30-year limited analysis period.
- Only 8 stations representing different climate zones around the country can be used in the educational version. Additionally, batch mode and sensitivity analysis cannot be used in this version. Unlike the conventional version, no access was provided to intermediate output files in the educational version.

January 2014 (Pavement ME Design Version 2.0.19, Educational Version 2.0.19)

- In this version, Citrix and Remote Desktop Services have been added.
- A layer-by-layer asphalt rutting coefficient can now be used for analysis
- In this version, The US Customary bins have been converted for rounded SI metric bins.
- Another new feature is the ability to input special axle traffic information by selecting a special traffic checkbox on the main project tab.
- The database was also improved to be more stable and provide enhanced selection and insert functionality.
- A file converter was also added to convert Version 1.1 files to the new 2.0 format before the software is run.

August 2014 (Pavement ME Design Version 2.1.24)

- With this version, users can receive back-calculation summary reports, enabling them to use back calculation with thickness optimization on each station project.
- Users can also use an automatic updater providing them with an option to automatically check for available system updates.
- Another enhancement in this version is capability for incorporating subgrade moduli in sensitivity analysis for any selected layer.

August 2015 (Pavement ME Design Version 2.2)

- A new reflection-cracking model developed from NCHRP 1-41 project was added to Pavement ME Design.
- With this version, Drainage Requirement In Pavements (DRIP) can be used as an accompanying tool to conduct hydraulic design computations for subsurface pavement drainage analysis.
- New calibration coefficients for JPCP cracking, JPCP faulting and CRCP punch-out models were added to Pavement ME Design.
- LTPP default axle load distributions could be imported in this software version.
- A MapME tool providing data from geographical information system data linkages to Pavement ME Design was also added.
- Semi-rigid pavement type replaced new AC over CTB design type in this software version.
- Level 1 and Level 2 input data AC overlays over AC rehabilitated pavements, Level 3 input data for AC overlays over intact JPCP rehabilitated pavements, and new Level 1, Level 2 and Level 3 inputs for PCC overlays over existing AC pavements are provided.

Training Webinar Series

A series of 13 webinars (each about 2 hours long) was prepared by the Federal Highway Administration (FHWA) in collaboration with the AASHTO Pavement ME Design Task Force to introduce different aspects of the software. Ten of these webinars were related to the material and design inputs used in the software and design of different pavement systems, and the remaining three webinars were related to software local calibration. The webinar series can be reached through (<http://www.me-design.com>) website. The titles in the webinar series are as follows:

- 1) Getting started with ME Design
- 2) Climatic Inputs
- 3) Traffic Inputs
- 4) Material and Design Inputs for New Pavement Design
- 5) Material and Design Inputs for Pavement Rehabilitation with Asphalt Overlays
- 6) Material and Design Inputs for Pavement Rehabilitation with Concrete Overlays
- 7) New Asphalt Pavement Structures
- 8) Asphalt Overlays of Asphalt Pavements
- 9) New Concrete Pavement Structures
- 10) Unbonded Concrete Overlays
- 11) Introduction to Local Calibration
- 12) Preparing for Local Calibration
- 13) Determining the Local Calibration Coefficients

This report presented design examples of new JPCP, new HMA, and HMA over JPCP pavements using Pavement ME Design (version 2.1.24) (See Appendix B). The design of such pavements were introduced in a step-by-step manner using screen shots from the software.

Evaluation of Pavement ME Design Software: Comparison between Pavement ME Design and MEPDG Pavement Performance Predictions

To compare pavement performance predictions of Pavement ME Design and MEPDG software, a set of 15 cases used in NCHRP 1-47 (NCHRP 2011) representing different climate and traffic conditions were presented. The case name and corresponding description of each case can be seen in Table 5.

Table 5. 15 total base cases used in NCHRP 1-47 project (NCHRP 2011)

Base Case Name	Description
CDL	Cold-Dry-Low-Traffic
CDM	Cold-Dry-Medium-Traffic
CDH	Cold-Dry-High-Traffic
CWL	Cold-Wet-Low-Traffic
CWM	Cold-Wet-Medium-Traffic
CWH	Cold-Wet-High-Traffic
TL	Temperate-Low-Traffic
TM	Temperate-Medium-Traffic
TH	Temperate-High-Traffic
HDL	Hot-Dry-Low-Traffic
HDM	Hot-Dry-Medium-Traffic
HDH	Hot-Dry-High-Traffic
HWL	Hot-Wet-Low-Traffic
HWM	Hot-Wet-Medium-Traffic
HWH	Hot-Wet-High-Traffic

To represent a variety of different climate conditions in the US, 5 different locations were determined representing such different climates. Climate category, location, weather station and total available climate data about each station are summarized in Table 6.

Table 6. Climate categories used in NCHRP 1-47 project (NCHRP 2011)

Climate Category	Location	Weather Station	Months of Data
Hot-Wet	Orlando FL	ORLANDO INTERNATIONAL	116
Hot-Dry	Phoenix AZ	PHOENIX SKY HARBOR INTL AP	116
Cold-Wet	Portland ME	PORTLAND INTL JETPORT	116
Cold-Dry	International Falls MN	FALLS INTERNATIONAL	112
Temperate	Los Angeles CA	LOS ANGELES INTL AIRPORT	108

To simulate different traffic conditions in the US, three categories of traffic conditions were presented: low, medium and high. Table 7 shows each traffic category and corresponding AADTT values, AADTT values in design lane, estimated ESALS for both flexible and rigid pavements, and AADTT range fitting each traffic category.

Table 7. Traffic levels used in NCHRP 1-47 project (NCHRP 2011)

Traffic Category	Baseline Inputs			AADTT Range
	AADTT	Est. ESALS (Flexible)	Est. ESALS (Rigid)	
Low	1,000	2M	5M	500-5,000
Medium	7,500	10M	25M	5,000-10,000
High	25,000	30M	75M	20,000-30,000

Using the same input parameters for all cases except for different climate and traffic conditions, MEPDG v.1.1, Pavement ME Design v.2.0 and Pavement ME Design v.2.1.24 were run. Table 8 summarizes the pavement performance predictions for new JPCP cases using MEPDG v.1.1, Pavement ME Design v.2.0, and Pavement ME Design v.2.1.24. As can be seen from the table, significant differences in transverse cracking and IRI predictions under cold climate zones between MEPDG v.1.1 and Pavement ME Design versions were observed. However, no significant differences between pavement performance predictions using Pavement ME Design v.2.0 and Pavement ME Design v.2.1 were observed.

Table 8. Pavement performance prediction comparisons for new JPCP cases

CaseType	CaseType2	Pavement age		Faulting (in) (MEPDG v.1.1)	Faulting (in) (Pavement ME v.2.0)	Faulting (in) (Pavement ME v.2.1.24)	Percent slabs cracked (MEPDG v.1.1)	Percent slabs cracked(Pavement ME v.2.0)	Percent slabs cracked(Pavement ME v.2.1.24)	IRI (in/mile) (MEPDG v.1.1)	IRI (in/mile) (Pavement ME v.2.0)	IRI (in/mile) (Pavement ME v.2.1.24)
		mo	yr									
CDL	New	300	25	0.01	0.01	0.01	16.8	13.0	13.0	141.10	184.45	184.45
CDM	New	300	25	0.05	0.05	0.05	5.5	3.4	3.4	152.30	195.84	195.84
CDH	New	300	25	0.13	0.13	0.13	1.6	1.0	1.0	186.00	230.63	230.63
CWL	New	300	25	0.02	0.02	0.02	10.7	10.1	10.1	106.00	130.91	130.91
CWM	New	300	25	0.09	0.09	0.09	2.4	2.3	2.3	133.40	160.81	160.81
CWH	New	300	25	0.17	0.17	0.17	0.6	0.6	0.6	171.70	199.02	199.02
HDL	New	300	25	0.01	0.01	0.01	14.7	14.2	14.2	80.80	80.79	80.79
HDM	New	300	25	0.05	0.05	0.05	6.6	5.6	5.6	96.30	96.25	96.25
HDH	New	300	25	0.16	0.16	0.16	1.9	1.4	1.4	146.40	146.86	146.86
HWL	New	300	25	0.01	0.01	0.01	5.1	5.1	5.1	72.80	73.04	73.04
HWM	New	300	25	0.05	0.05	0.05	1.9	1.8	1.8	89.30	90.34	90.34
HWH	New	300	25	0.13	0.13	0.13	0.4	0.4	0.4	132.20	133.24	133.24
TL	New	300	25	0.01	0.01	0.01	1.6	1.6	1.6	68.20	68.43	68.43
TM	New	300	25	0.03	0.03	0.03	0.3	0.3	0.3	80.60	81.51	81.51
TH	New	300	25	0.10	0.10	0.10	0.1	0.1	0.1	116.70	118.50	118.50

Table 9 summarizes pavement performance predictions for new JPCP over stiff foundation cases using MEPDG v.1.1, Pavement ME Design v.2.0, and Pavement ME Design v.2.1.24. As can be seen from the table, MEPDG v.1.1 overpredicts transverse cracking and underpredicts IRI for cold climate zones in comparison to Pavement ME versions. No significant differences between pavement performance predictions using Pavement ME Design v.2.0 and Pavement ME Design v.2.1.24 were observed.

Table 9. Pavement performance prediction comparisons for new JPCP over stiff foundation cases

CaseType	CaseType2	Pavement age		Faulting (in) (MEPDG v.1.1)	Faulting (in) (Pavement ME v.2.0)	Faulting (in) (Pavement ME v.2.1.24)	Percent slabs cracked (MEPDG v.1.1)	Percent slabs cracked(Pavement ME v.2.0)	Percent slabs cracked(Pavement ME v.2.1.24)	IRI (in/mile) (MEPDG v.1.1)	IRI (in/mile) (Pavement ME v.2.0)	IRI (in/mile) (Pavement ME v.2.1.24)
		mo	yr									
CDL	New	300	25	0.01	0.01	0.01	32.5	28.8	28.8	152.10	179.13	179.13
CDM	New	300	25	0.03	0.04	0.04	41.0	34.6	34.6	172.00	198.46	198.46
CDH	New	300	25	0.08	0.08	0.08	3.8	2.3	2.3	165.20	193.71	193.71
CWL	New	300	25	0.01	0.01	0.01	22.6	22.0	22.0	111.60	130.32	130.32
CWM	New	300	25	0.07	0.07	0.07	21.8	20.8	20.8	137.30	156.06	156.06
CWH	New	300	25	0.12	0.12	0.12	1.1	1.0	1.0	146.70	166.49	166.49
HDL	New	300	25	0.01	0.01	0.01	23.3	24.2	24.2	86.10	87.25	87.25
HDM	New	300	25	0.04	0.04	0.04	30.6	26.6	26.6	108.50	105.50	105.50
HDH	New	300	25	0.09	0.09	0.09	5.4	3.3	3.3	117.70	115.06	115.06
HWL	New	300	25	0.01	0.01	0.01	7.5	7.9	7.9	73.10	73.66	73.66
HWM	New	300	25	0.03	0.03	0.03	7.8	7.6	7.6	86.30	86.25	86.25
HWH	New	300	25	0.07	0.07	0.07	0.9	0.8	0.8	100.70	100.48	100.48
TL	New	300	25	0.00	0.00	0.00	0.0	2.2	2.2	65.00	67.54	67.54
TM	New	300	25	0.02	0.02	0.02	1.6	1.7	1.7	74.60	75.08	75.08
TH	New	300	25	0.04	0.04	0.04	0.1	0.1	0.1	87.10	87.38	87.38

Table 10 summarizes the cracking predictions of MEPDG v.1.1, Pavement ME v.2.0, and Pavement ME v.2.1.24 for new HMA cases. MEPDG v.1.1 underpredicts longitudinal cracking compared to Pavement ME Design versions for all climate zones. Some differences in alligator-cracking predictions under different climate zones were observed between MEPDG v.1.1 and Pavement ME Design versions. Also, note that in cold-wet weather conditions, MEPDG v.1.1 overpredicts transverse cracking compared to Pavement ME Design versions. No significant differences between pavement performance predictions using Pavement ME Design v.2.0 and Pavement ME Design v.2.1.24 were observed.

Table 10. Pavement performance prediction comparisons for new HMA cases: cracking

CaseType	CaseType2	Pavement age		Longitudinal Cracking (ft/mi) (MEPDG v.1.1)	Longitudinal Cracking (ft/mi) (Pavement ME v.2.0)	Longitudinal Cracking (ft/mi) (Pavement ME v.2.1.24)	Alligator Cracking (%) (MEPDG v.1.1)	Alligator Cracking (%) (Pavement ME v.2.0)	Alligator Cracking (%) (Pavement ME v.2.1.24)	Transverse Cracking (ft/mi) (MEPDG v.1.1)	Transvers Cracking (ft/mi) (Pavement ME v.2.0)	Transverse Cracking (ft/mi) (Pavement ME v.2.1.24)
		mo	yr									
CDL	New	180	15	1140	3280	3280	1.97	2.89	2.89	0	0	0
CDM	New	180	15	25.3	237	237	1.42	2.01	2.01	0	0	0
CDH	New	180	15	0.25	13.9	13.9	1.27	1.82	1.82	0	0	0
CWL	New	180	15	3130	2420	2420	3.57	2.28	2.28	0.3	0.02	0.02
CWM	New	180	15	168	125	125	2.51	1.55	1.55	0.2	0.01	0.01
CWH	New	180	15	1.5	3.83	3.83	2.22	1.37	1.37	0.1	0	0
HDL	New	180	15	1910	2030	2030	2.59	1.77	1.77	0	0	0
HDM	New	180	15	36.1	95.9	95.9	1.94	1.31	1.31	0	0	0
HDH	New	180	15	0.33	2.82	2.82	1.78	1.27	1.27	0	0	0
HWL	New	180	15	1060	1350	1350	2.55	1.87	1.87	0	0	0
HWM	New	180	15	2.5	9.43	9.43	1.88	1.31	1.31	0	0	0
HWH	New	180	15	0.07	0.76	0.76	1.8	1.23	1.23	0	0	0
TL	New	180	15	598	752	752	1.82	1.29	1.29	0	0	0
TM	New	180	15	1.45	4.98	4.98	1.34	0.934	0.934	0	0	0
TH	New	180	15	0.03	0.4	0.4	1.3	0.924	0.924	0	0	0

Table 11 summarizes the rutting and IRI predictions of MEPDG v.1.1, Pavement ME Design v.2.0 and Pavement ME Design v.2.1.24 for new HMA cases. Some differences in rutting and IRI predictions under different climate zones can be observed between MEPDG v.1.1 and Pavement ME Design versions. No significant differences between pavement performance predictions using Pavement ME Design v.2.0 and Pavement ME Design v.2.1.24 were observed.

Table 11. Pavement performance prediction comparisons for new HMA cases: rutting and IRI

CaseType	CaseType 2	Pavement age		AC Rutting (in) (MEPDG v.1.1)	AC Rutting (in) (Pavement ME v.2.0)	AC Rutting (in) (Pavement ME v.2.1.24)	Total Rutting (in) (MEPDG v.1.1)	Total Rutting (in) (Pavement ME v.2.0)	Total Rutting (in) (Pavement ME v.2.1.24)	IRI in/mile (MEPDG v.1.1)	IRI in/mile(Pa vement ME v.2.0)	IRI in/mile(Pa vement ME v.2.1.24)
		Fixed	Fixed									
CDL	New	180	15	0.17	0.20	0.20	0.50	0.58	0.58	103.9	111.9	111.9
CDM	New	180	15	0.38	0.44	0.44	0.70	0.80	0.80	111.5	118.4	118.4
CDH	New	180	15	0.51	0.57	0.57	0.81	0.92	0.92	115.8	123.2	123.2
CWL	New	180	15	0.23	0.19	0.19	0.59	0.52	0.52	110.5	108.4	108.4
CWM	New	180	15	0.51	0.41	0.41	0.86	0.73	0.73	120.5	115.3	115.3
CWH	New	180	15	0.68	0.54	0.54	1.01	0.85	0.85	126.2	119.7	119.7
HDL	New	180	15	0.30	0.29	0.29	0.61	0.58	0.58	102.1	101.8	101.8
HDM	New	180	15	0.64	0.64	0.64	0.95	0.92	0.92	115.0	114.2	114.2
HDH	New	180	15	0.84	0.82	0.82	1.14	1.10	1.10	122.6	121.1	121.1
HWL	New	180	15	0.17	0.20	0.20	0.50	0.50	0.50	101.2	102.0	102.0
HWM	New	180	15	0.37	0.44	0.44	0.69	0.74	0.74	108.3	110.4	110.4
HWH	New	180	15	0.50	0.57	0.57	0.81	0.86	0.86	113.0	114.9	114.9
TL	New	180	15	0.12	0.14	0.14	0.43	0.42	0.42	95.8	95.7	95.7
TM	New	180	15	0.26	0.32	0.32	0.56	0.59	0.59	100.7	101.9	101.9
TH	New	180	15	0.36	0.40	0.40	0.65	0.68	0.68	104.0	105.2	105.2

Table 12 summarizes cracking predictions of MEPDG v.1.1, Pavement ME Design v.2.0, and Pavement ME Design v.2.1.24 for HMA over stiff foundation cases. For all climate zones, MEPDG v.1.1 underpredicts longitudinal cracking compared to Pavement ME Design versions. Some differences in alligator-cracking predictions for different climate zones can be observed between MEPDG v.1.1 and Pavement ME Design versions. Also note that in cold-wet weather conditions, MEPDG v.1.1 overpredicts transverse cracking compared to Pavement ME Design versions. No significant differences between pavement performance predictions using Pavement ME Design v.2.0 and Pavement ME Design v.2.1.24 were observed.

Table 12. Pavement performance prediction comparisons for HMA over stiff foundation cases: cracking

CaseType	CaseType 2	Pavement age		Longitudinal Cracking (ft/mi) (MEPDG v.1.1)	Longitudinal Cracking (ft/mi) (Pavement ME v.2.0)	Longitudinal Cracking (ft/mi) (Pavement ME v.2.1.24)	Alligator Cracking (%) (MEPDG v.1.1)	Alligator Cracking (%) (Pavement ME v.2.0)	Alligator Cracking (%) (Pavement ME v.2.1.24)	Transverse Cracking (ft/mi) (MEPDG v.1.1)	Transverse Cracking (ft/mi) (Pavement ME v.2.0)	Transverse Cracking (ft/mi) (Pavement ME v.2.1.24)
		Fixed	Fixed									
CDL	New	180	15	0	0.06	0.06	0	4.48	4.48	0	0.01	0.01
CDM	New	180	15	0.01	7.22	7.22	0	4.49	4.49	0	0.01	0.01
CDH	New	180	15	0.34	30.8	30.8	0.032	4.70	4.70	0	0	0
CWL	New	180	15	0	0.002	0.002	0	4.48	4.48	0.5	0.06	0.06
CWM	New	180	15	0.02	0.05	0.05	0	4.49	4.49	0.4	0.04	0.04
CWH	New	180	15	1.73	7.71	7.71	0.0367	4.76	4.76	0.4	0.02	0.02
HDL	New	180	15	0.01	0.008	0.008	0	4.48	4.48	0	0	0
HDM	New	180	15	0.04	0.51	0.51	0.0001	4.49	4.49	0	0	0
HDH	New	180	15	0.36	53.8	53.8	0.0422	4.672	4.672	0	0	0
HWL	New	180	15	0	0.002	0.002	0	4.48	4.48	0	0	0
HWM	New	180	15	0.01	0.04	0.04	0	4.49	4.49	0	0	0
HWH	New	180	15	0	2.74	2.74	0.0347	4.67	4.67	0	0	0
TL	New	180	15	0	0.002	0.002	0	4.48	4.48	0	0	0
TM	New	180	15	0.01	0.03	0.03	0.0001	4.49	4.49	0	0	0
TH	New	180	15	0	2.87	2.87	0.0388	4.73	4.73	0	0	0

Table 13 summarizes the rutting and IRI predictions of MEPDG v.1.1, Pavement ME Design v.2.0, and Pavement ME Design v.2.1.24 for HMA over stiff foundation cases. Some differences in rutting and IRI predictions for different climate zones can be observed between MEPDG v.1.1 and Pavement ME Design versions. No significant differences between pavement performance predictions using Pavement ME Design v.2.0 and Pavement ME Design v.2.1.24 were observed.

Table 13. Pavement performance prediction comparisons for HMA over stiff foundation cases: rutting and IRI

CaseType	CaseType2	Pavement age		AC Rutting (in) (MEPDG v.1.1)	AC Rutting (in) (Pavement ME v.2.0)	AC Rutting (in) (Pavement ME v.2.1.24)	Total Rutting (in) (MEPDG v.1.1)	Total Rutting (in) (Pavement ME v.2.0)	Total Rutting (in) (Pavement ME v.2.1.24)	IRI in/mile (MEPDG v.1.1)	IRI in/mile (Pavement ME v.2.0)	IRI in/mile (Pavement ME v.2.1.24)
		Fixed	Fixed									
CDL	New	180	15	0.10	0.12	0.12	0.36	0.39	0.39	97.1	101.0	101.0
CDM	New	180	15	0.47	0.55	0.55	0.75	0.85	0.85	112.7	119.1	119.1
CDH	New	180	15	1.03	1.21	1.21	1.30	1.49	1.49	135.0	145.1	145.1
CWL	New	180	15	0.13	0.11	0.11	0.41	0.37	0.37	101.0	100.0	100.0
CWM	New	180	15	0.63	0.52	0.52	0.92	0.80	0.80	121.6	117.0	117.0
CWH	New	180	15	1.38	1.12	1.12	1.67	1.39	1.39	151.7	140.9	140.9
HDL	New	180	15	0.17	0.19	0.19	0.39	0.39	0.39	91.6	92.2	92.2
HDM	New	180	15	0.81	0.82	0.82	1.05	1.04	1.04	117.9	118.0	118.0
HDH	New	180	15	1.76	1.70	1.70	1.99	1.92	1.92	156.0	153.4	153.4
HWL	New	180	15	0.10	0.13	0.13	0.37	0.38	0.38	94.5	95.5	95.5
HWM	New	180	15	0.46	0.55	0.55	0.75	0.82	0.82	109.7	113.0	113.0
HWH	New	180	15	1.00	1.14	1.14	1.28	1.41	1.41	131.0	136.4	136.4
TL	New	180	15	0.08	0.10	0.10	0.32	0.32	0.32	90.2	90.5	90.5
TM	New	180	15	0.35	0.39	0.39	0.61	0.64	0.64	101.7	103.1	103.1
TH	New	180	15	0.75	0.81	0.81	1.00	1.05	1.05	117.5	119.9	119.9

CHAPTER 4. LOCAL CALIBRATION METHODOLOGY

Based on the literature review and consultations with Iowa DOT engineers, a set of procedures for local calibration of Pavement ME Design performance predictions for Iowa pavement systems was made. The following steps give details of this procedure:

- **Step 1:** Update and tabulate the Iowa pavement system database for Pavement ME Design local calibration based on the database developed in InTrans Project 11-401: Iowa Calibration of MEPDG Performance Prediction Models (Ceylan et al. 2013).
- **Step 2:** Conduct Pavement ME Design runs using (1) national and (2) MEPDG local calibration coefficients identified in InTrans Project 11-401 (Ceylan et al. 2013).
- **Step 3:** Evaluate the accuracy of both nationally and MEPDG-locally calibrated pavement performance prediction models.
- **Step 4:** If the accuracy of national or MEPDG local calibration coefficients for given Pavement ME Design performance prediction models were found to be adequate, these coefficients were determined to be acceptable for Iowa conditions.
- **Step 5:** If not, the calibration coefficients of Pavement ME Design can be refined using various optimization approaches
- **Step 6:** Evaluate adequacy of refined Pavement ME Design local calibration coefficients
- **Step 7:** Recommend Pavement ME Design calibration coefficients for Iowa conditions

Description of Iowa Pavement Sites Selected

A total of 130 representative pavement sites across Iowa, selected from InTrans Project 11-401 (Ceylan et al. 2013), were also used for Pavement ME Design local calibration. The selected pavement sites represent flexible, rigid, and composite pavement systems throughout Iowa at different geographical locations and different traffic levels.

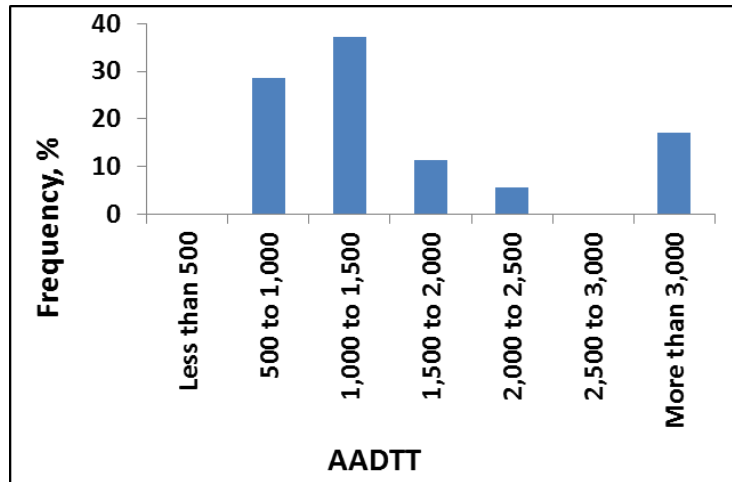
Table 14 lists the number of pavement sections selected for this study. A total of 35 sections for new JPCP (rigid pavements), a total of 35 sections for new HMA pavements (flexible pavements), and a total of 60 sections for HMA over JPCP (composite pavements) were selected. In the selected new JPCP and new HMA roadway segments, twenty-five sections were used for calibration and 10 sections were used for verification of identified calibration coefficients. In the selected HMA over JPCP roadway segments, forty-five sections were used for calibration and 15 sections were used for verification of identified calibration coefficients.

Table 14. Site selection summary information

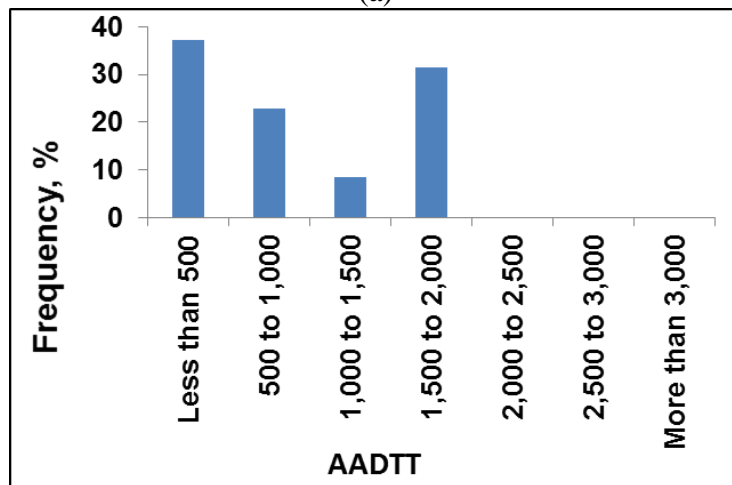
Type	Iowa PMIS Code	Number of Sites Selected	Iowa LTPP sections
JPCP	1	35	6
HMA	4	35	1
HMA over JPCP	3 and 3A	60	9

The descriptive information on selected pavement sites, developed in InTrans Project 11-401 (Ceylan et al. 2013), was updated by incorporating information from the new Iowa DOT PMIS database. Note that InTrans Project 11-401 (Ceylan et al. 2013) used the Iowa DOT PMIS database for 1998 to 2009 while this study used the one for 1992 to 2013.

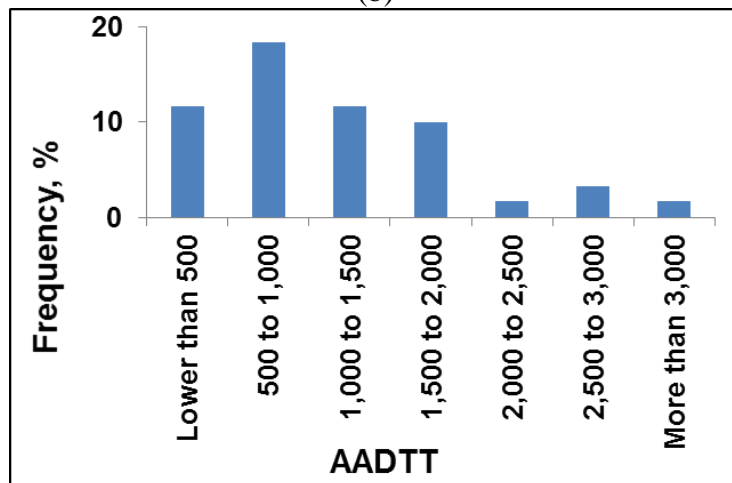
Figure 4 presents average annual daily truck traffic (AADTT) distributions for each type of Iowa pavement. As can be seen in this figure, HMA surface pavements are used more with lower AADTT and JPCPs are used more with higher AADTT. To include all Iowa traffic conditions, three categories of traffic levels were used in selecting calibration sites. An AADTT value less than 500 is categorized to be low traffic volume, between 500 and 1,000 is categorized as medium traffic volume, and higher than 1,000 is categorized as high traffic volume. The selected sections in Figure 5 also represent a variety of geographical locations across Iowa.



(a)

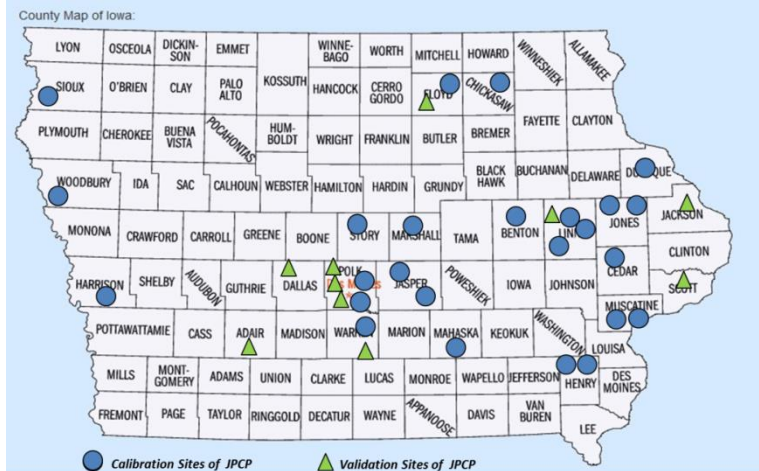


(b)

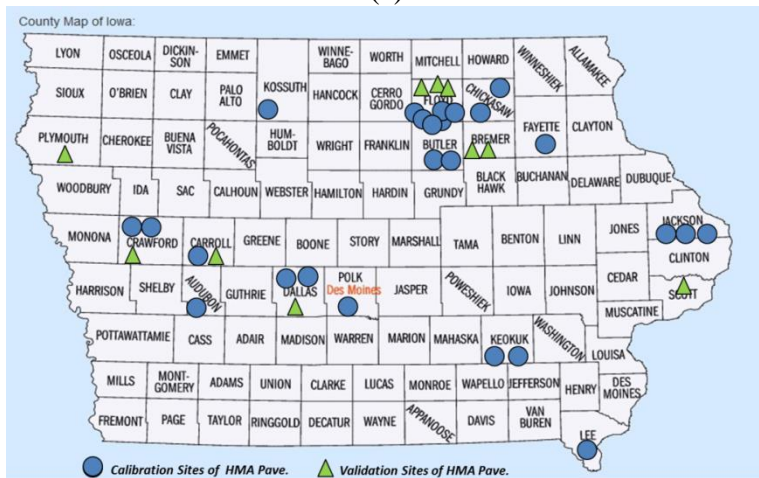


(c)

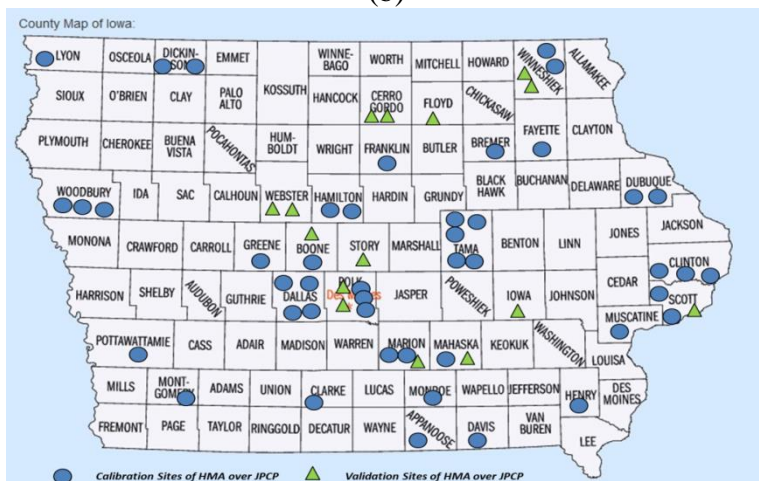
Figure 4. Iowa pavements by AADTT distribution (as of 2014): (a) JPCPs, (b) HMA pavements, and (c) HMA over JPCPs



(a)



(b)



(c)

Figure 5. Geographical locations of selected Iowa pavement sites: (a) JPCPs, (b) HMA pavements, and (c) HMA over JPCPs

The distribution of construction years for each type of pavement is depicted in Figure 6. HMA over JPCP pavement sections were categorized based on their JPCP construction and resurfacing years (Figure 6). As can be seen from the figure, most of the selected Iowa JPCPs were constructed between 1999 and 2002, while most of the selected HMA pavements were constructed after 1997. For Iowa HMA over JPCPs selected, most of the HMA resurfacings were conducted after 1999.

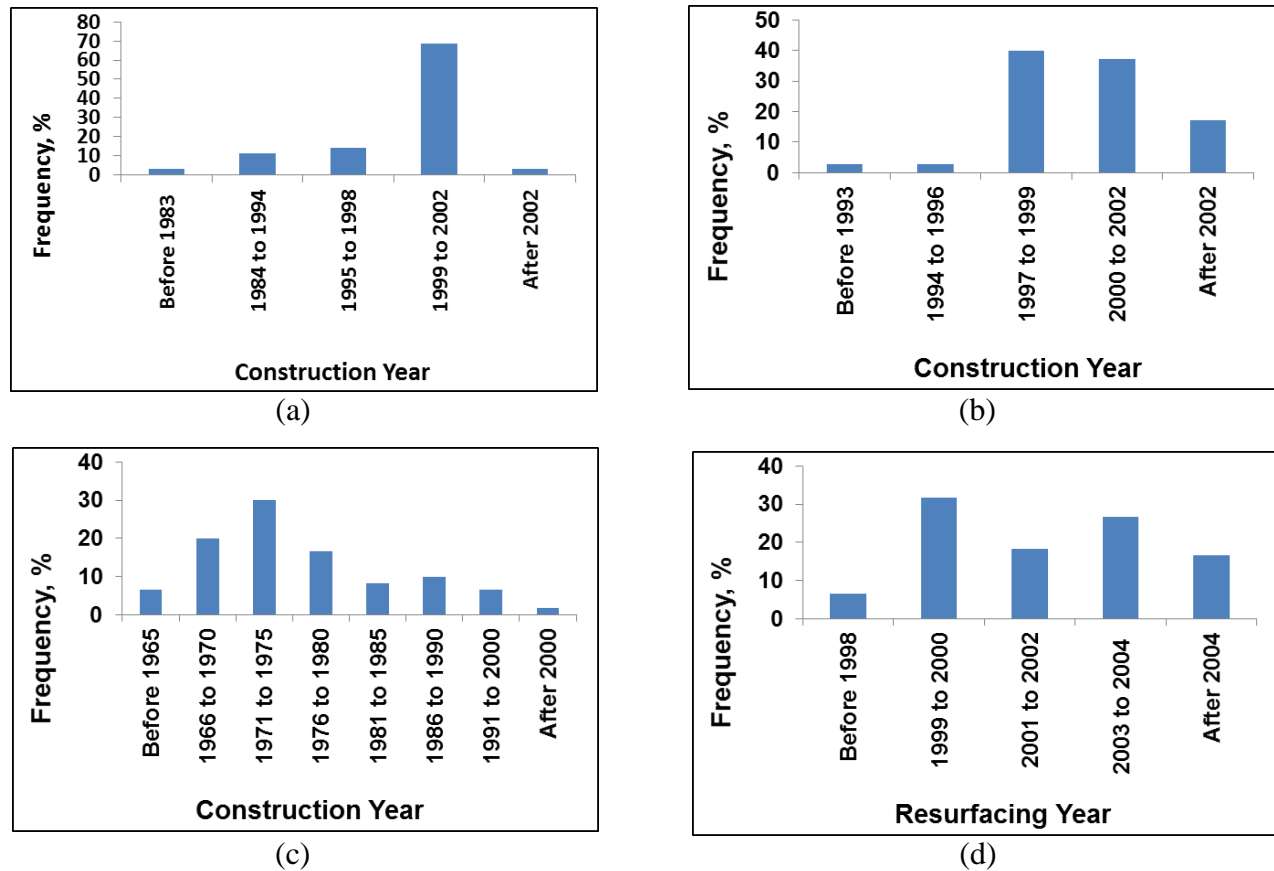


Figure 6. Iowa pavements by the distribution of construction years (as of 2014): (a) JPCPs, (b) HMA pavements, (c) initial JPCPs construction years of HMA over JPCPs, (d) HMA resurfacing years of HMA over JPCPs

Figure 7 depicts the distribution of PCC surface thicknesses for JPCPs, HMA surface thickness for HMA pavements, and HMA overlay and PCC thicknesses for HMA over JPCPs.

As can be seen from the figure, the PCC thickness for about 90% of selected JPCPs ranges from

9 to 11 in., while the HMA thicknesses for over 90% of selected HMA pavements is thicker than 10 in. It should also be noted that traffic volumes for JPCP pavements are higher than for HMA pavements (See Figure 4). Also, the HMA overlay thicknesses for over 90% of HMA over JPCP pavements range from 2 to 6 in. The distribution of base thicknesses for Iowa JPCP, HMA, and HMA over JPCP pavements is also presented in Figure 8. As can be seen from the figure, the most common base thicknesses for about 90% of JPCPs selected range from 9 to 11 in., while the HMA thicknesses for over 80 % of HMA pavements selected have no base layer. It can be concluded that more than 80 % of selected HMA pavements are full-depth HMA pavements. On the other hand, thicknesses for about 90% of HMA over JPCPs selected range from 0 to 5 in. Also note that there are no base layers thicker than 10 in. for selected HMA over JPCPs.

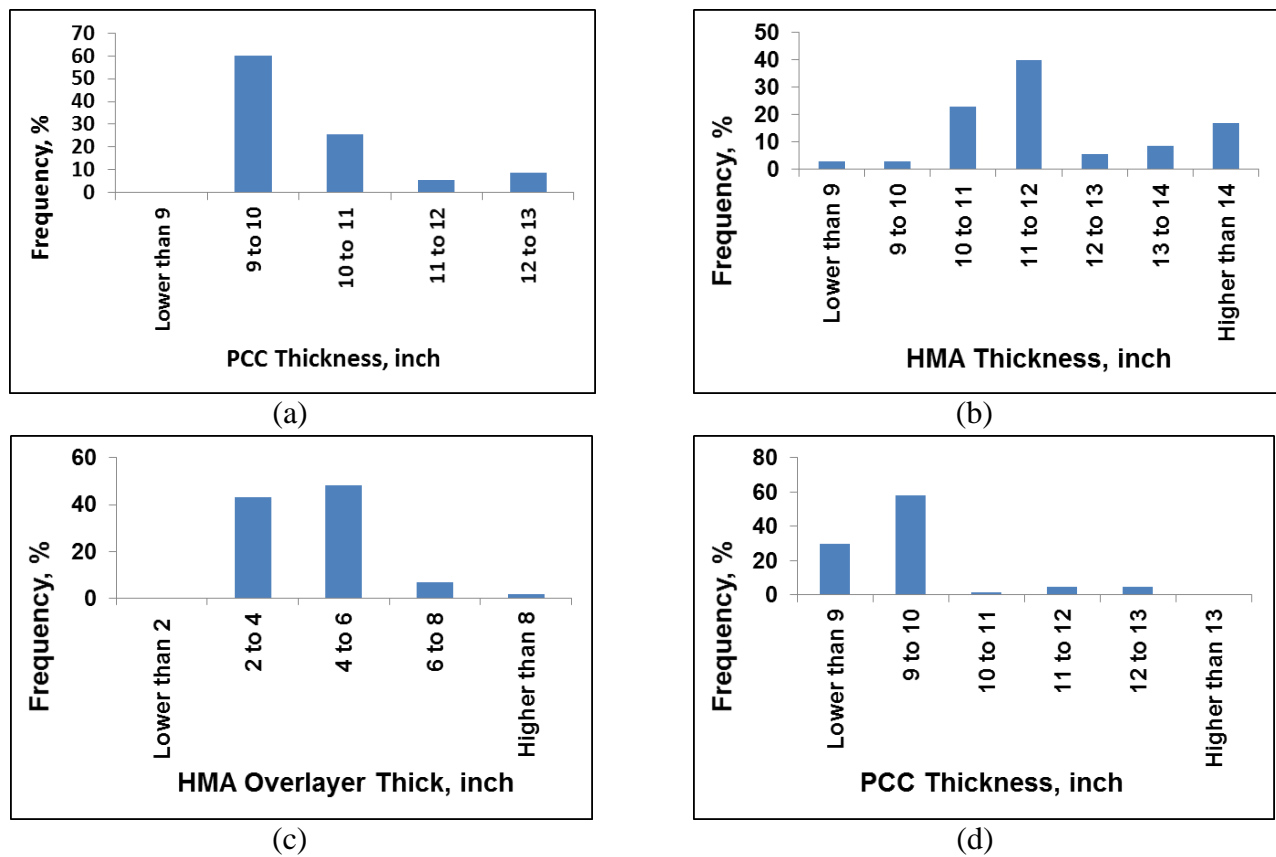


Figure 7. Iowa pavements by the distribution of surface thicknesses (as of 2014): (a) PCC surface thickness for JPCPs, (b) HMA surface thickness for HMA pavements, (c) HMA overlay thicknesses for HMA over JPCPs, and (d) PCC thicknesses for HMA over JPCPs

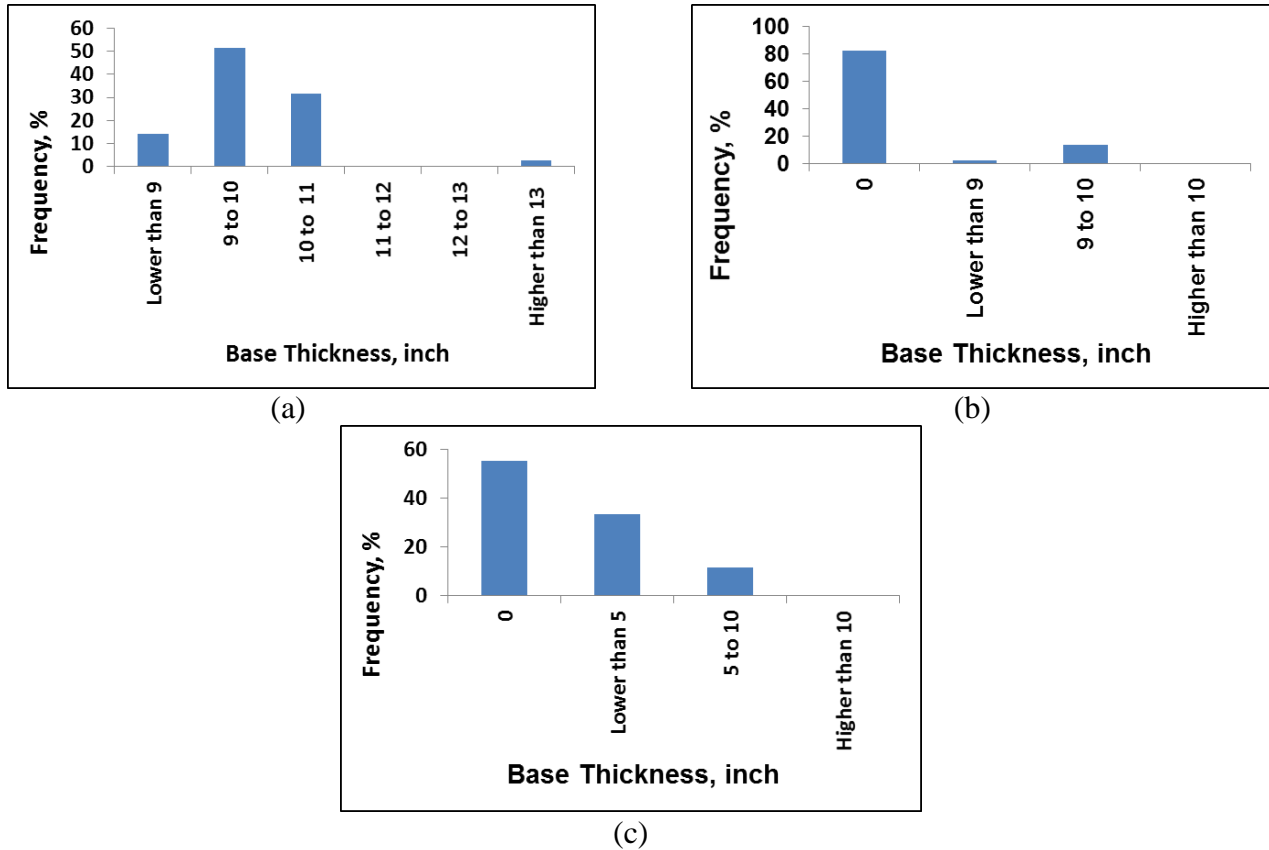


Figure 8. Iowa pavements by the distribution of base thicknesses as of 2014 (as of 2014): (a) JPCPs, (b) HMA pavements, (c) HMA over JPCPs

Description of Calibration Database for Iowa Pavement Systems

Input Database

The design input values required for Pavement ME Design runs were prepared from the design database developed in InTrans Project 11-401 (Ceylan et al. 2013). The data in the design input database were collected primarily from the Iowa DOT PMIS, material testing records, and previous project reports relevant to MEPDG implementation in Iowa. Detailed descriptions of the input database are provided in InTrans Project 11-401 report (Ceylan et al. 2013).

Pavement Distress Database

A database of historical performance data for the selected sections developed in InTrans Project 11-401 (Ceylan et al. 2013) were updated by incorporating data from the new Iowa DOT PMIS database. Note that the InTrans Project 11-401 (Ceylan et al. 2013) used the Iowa DOT PMIS database from 1998 to 2009 while this study used that from 1992 to 2013. As indicated in InTrans Project 11-401 (Ceylan et al. 2013), some differences between PMIS distress measures and Pavement ME Design performance predictions were still observed. For calibration of the performance prediction models, the identified differences were resolved by considering the following assumptions:

- Pavement ME Design provides rutting predictions for individual pavement layers while Iowa DOT PMIS provides only accumulated (total) rutting observed in HMA surfaces. Rutting measurements for individual layers were computed by applying the average percentage of total rutting for different pavement layers and subgrade recommended in the NCHRP 1-37A report (NCHRP 2004) on HMA surface rut measurements recorded in Iowa DOT PMIS.
- Pavement ME Design transverse cracking predictions for new HMA and HMA overlaid pavements are considered to reflect thermal cracking. The PMIS transverse cracking measurements for new HMA pavement could be considered as HMA thermal cracking, but those recorded for HMA overlaid pavements could be either reflection cracking or thermal cracking. However, transverse-cracking measurements in Iowa DOT PMIS for HMA overlaid pavements were not differentiated in that way. Considering the empirical nature of the reflection-cracking model implemented in Pavement ME Design (in the latest version available at the time of conducting this research), this study considered PMIS transverse cracking measurements for HMA overlaid pavements to be HMA thermal cracking to

calibrate the HMA thermal-cracking model rather than the reflection-cracking model.

- The units reported in PMIS for transverse cracking of JPCP and alligator and thermal (transverse) cracking of HMA and HMA overlaid pavements are different from those used in Pavement ME Design. These measured values of distress in PMIS are converted into the same units as those of Pavement ME Design predictions in accordance with the AASHTO guide for local calibration of the MEPDG (AASHTO 2010)
- Some irregularities in distress measures were identified in Iowa DOT PMIS. Occasionally, distress magnitudes appeared to decrease with time or show erratic patterns without explanation. In such cases, the distress measure history curves were modified to not to decrease with time.

Figure 9 presents the performance data distribution of selected JPCP sections for the faulting, transverse-cracking and IRI distresses, extracted from Iowa DOT PMIS database. Some performance measurements such as faulting measurements greater than 0.45 inch and transverse cracking greater than 80% for a 10-year JPCP service life are unusual when considering actual Iowa pavement performance practices and experiences. Such unusual measurements were considered to be outliers and eliminated in calibration producers.

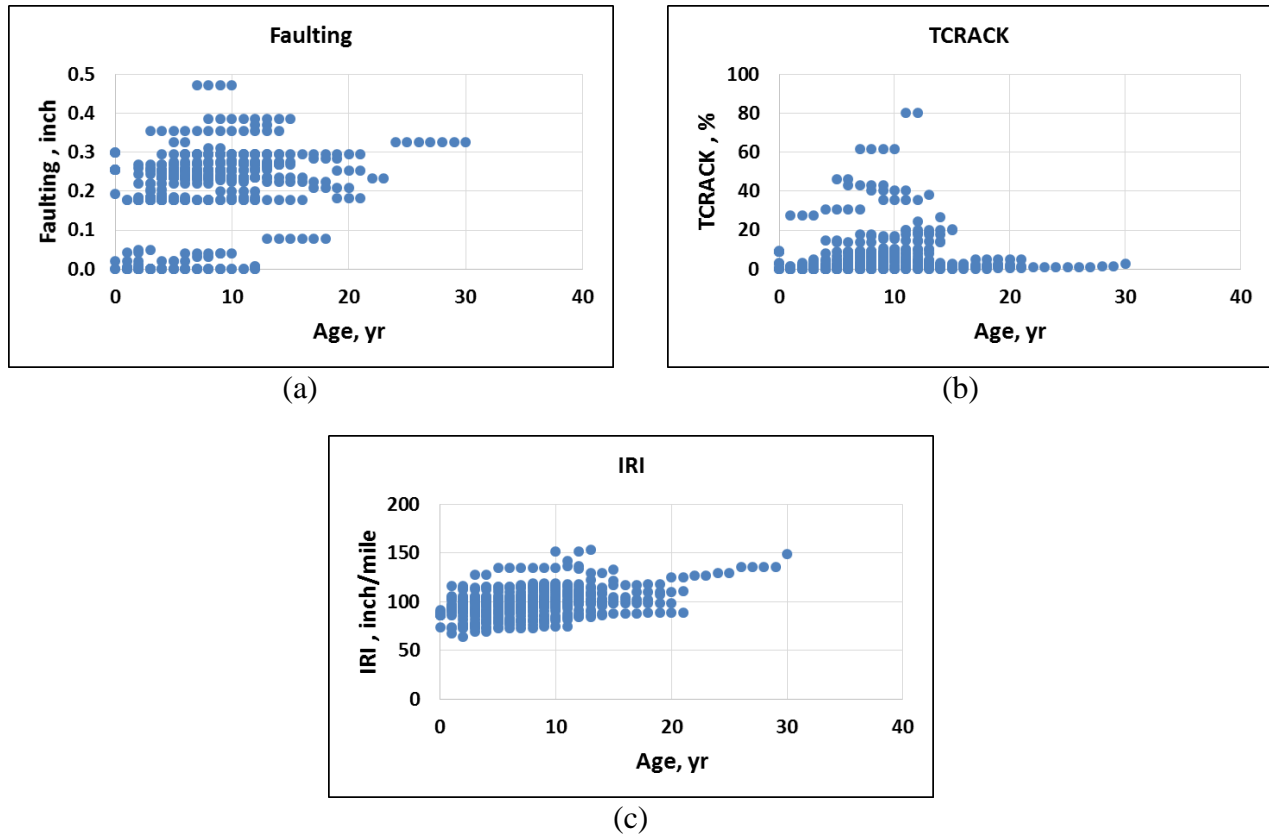


Figure 9. JPCP performance data distribution (as of 2014): (a) faulting, (b) transverse cracking and (c) IRI

Figure 10 presents performance data distribution for selected HMA pavement sections for total rutting, HMA rutting, granular-base rutting, subgrade rutting, longitudinal cracking, alligator cracking, transverse cracking and IRI. As can be seen in the figure, most total rutting occurs only coming from HMA rutting; the effect of granular base and subgrade rutting on total rutting is minimal. This is because most flexible pavements in Iowa are full-depth flexible pavements. Some performance measurements such as longitudinal-cracking measurements greater than 15,000 ft./mi. and transverse cracking greater than 7,000 ft./mi. before a 20-year HMA pavement service life are unusual when considering actual Iowa pavement performance practices and experiences. Such unusual measurements were considered to be outliers and eliminated in the calibration producers.

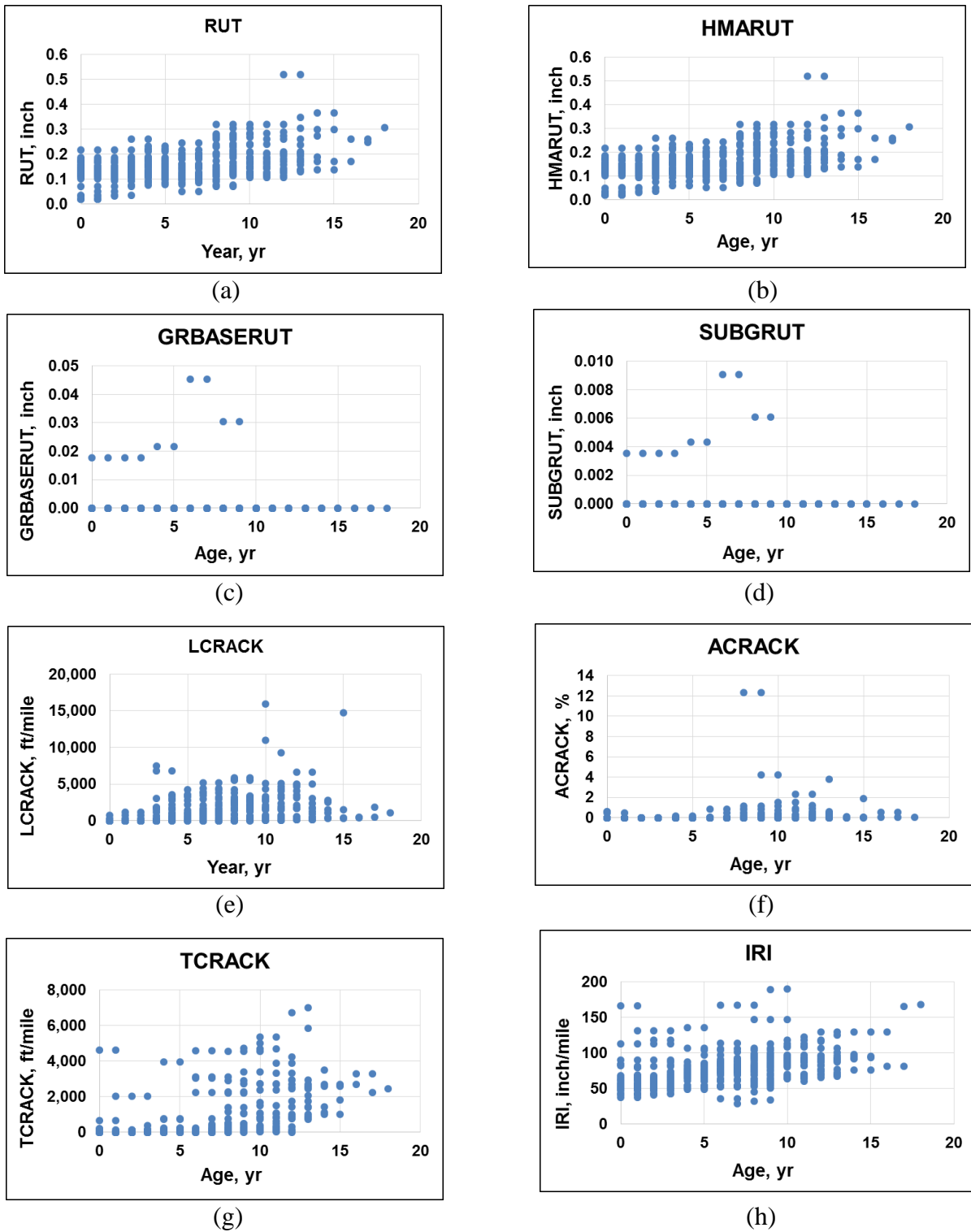


Figure 10. HMA performance data distribution (as of 2014): (a) total rutting, (b) HMA rutting, (c) granular base rutting, (d) subgrade rutting, (e) longitudinal cracking, (f) alligator cracking, (g) transverse cracking and (h) IRI

Figure 11 presents performance data distribution for selected HMA over JPCP sections for total rutting, longitudinal cracking, alligator cracking, transverse cracking and IRI. Some performance measurements such as longitudinal-cracking measurements greater than 8,000 ft./mi and transverse cracking greater than 10,000 ft./mi for a 10 year HMA over JPCP service life are unusual in considering actual Iowa pavement performance practices and experiences. Such unusual measurements were considered to be outliers and eliminated in calibration producers.

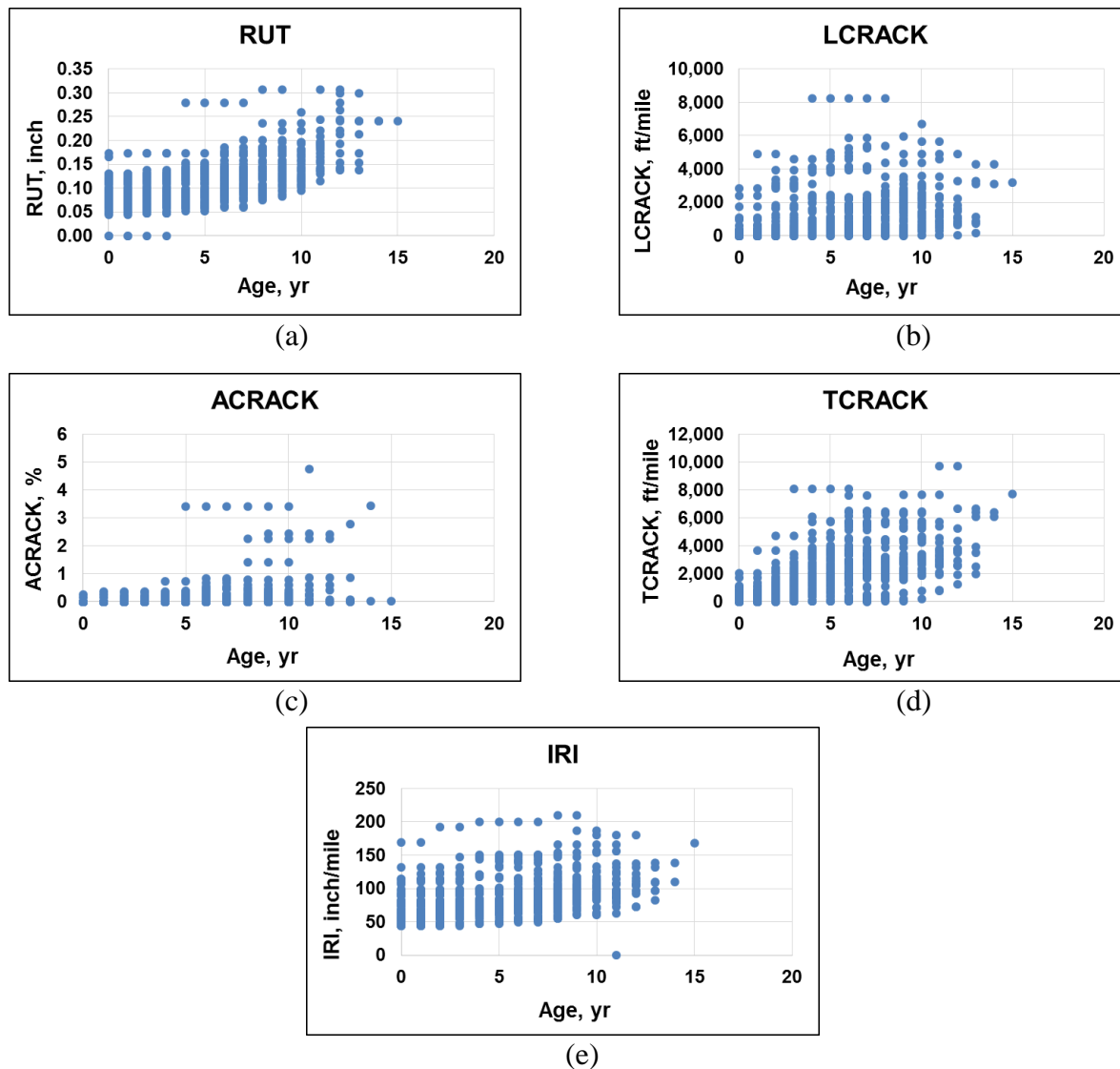


Figure 11. HMA over JPCP performance data distribution (as of 2014): (a) total rutting, (b) longitudinal cracking, (c) alligator cracking, (d) transverse cracking and (e) IRI

Description of Optimization Approaches

The purpose of Pavement ME Design local calibration is to identify a set of empirical transfer function coefficients (calibration coefficients) in pavement performance models to provide adequate accuracy for pavement performance predictions compared to actual pavement performance measurements (observations).

Figure 12 illustrates the flow of optimization procedures used to identify local-calibration coefficients having adequate accuracy for Iowa conditions. The local-calibration procedure starts with identification of transfer functions and their components. There are basically two types of transfer functions classified in Pavement ME Design: (1) functions directly calculating the magnitude of the pavement performance predictions, and (2) functions calculating the incremental damage over time relating such damage to the pavement performance predictions.

As can be seen in Figure 12, there are two approaches to optimizing pavement prediction models depending on whether the components of the transfer functions are known or not.

If all components of the transfer functions are provided by the software in intermediate files otherwise known to the designer, model predictions can be calculated outside the software using the transfer functions. In such a case, non-linear optimization techniques can be applied to calibrate pavement performance models.

If not all the components of the functions are known, the calibration can be achieved only through trial and error procedures by performing numerous Pavement ME Design runs to figure out the best combination of calibration coefficients in terms of goodness-of-fit accuracy. To minimize the number of Pavement ME Design runs, Ceylan et al. (2013) developed a linear optimization approach based on sensitivity analysis of calibration coefficients.

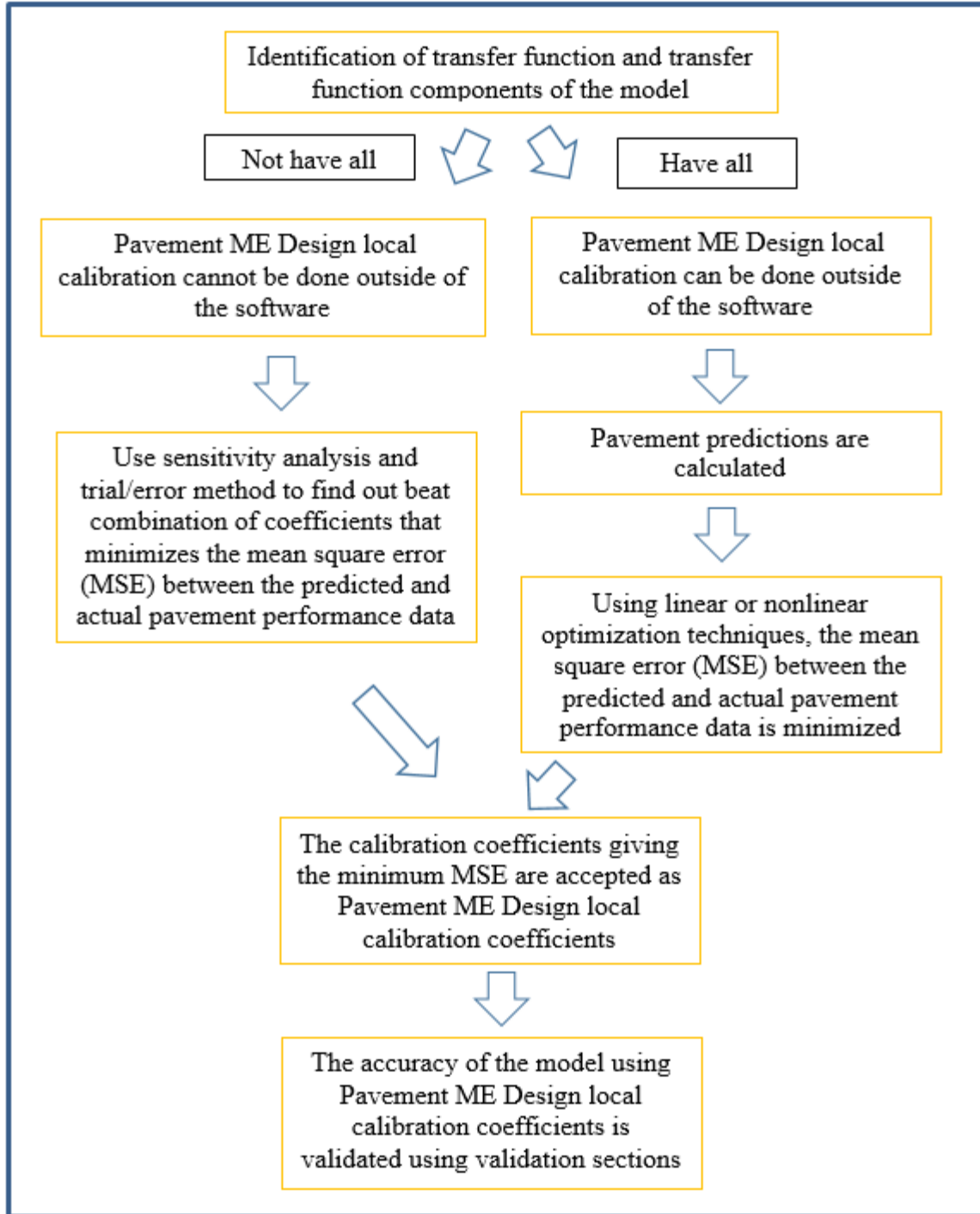


Figure 12. Optimization procedures to identify local calibration coefficients

In Pavement ME Design version 2.1.24, although some components of the transfer functions are provided in intermediate output files, many of them are not provided at all. This deficiency of the software was partially remedied in the latest version (version 2.2). For the

transfer function when not all the components are known, the calibration should be implemented within the software using sensitivity analysis and trial-and-error methods. These methods are extensively described in a previous report (Ceylan et al. 2013).

The optimization procedure is performed by minimizing the mean square error (MSE) between actual distress measurements and Pavement ME Design predicted values. (AASHTO 2010). Once the calibration coefficients are determined, the calibrated models are verified using the validation data set.

Various optimization methods utilized in this study are summarized in Table 15 and discussed in the following section.

Table 15. Optimization techniques used for different pavement distresses

Pavement Type	Distress	Optimization Technique Used
JPCP	Faulting	MS Excel® Solver, Brute Force and Lingo
	Transverse Cracking	MS Excel® Solver and Sensitivity Analysis
	IRI	MS Excel® Solver, Brute Force and Lingo
HMA	Rutting	Sensitivity Analysis
	Longitudinal Cracking	Sensitivity Analysis and MS Excel® Solver
	Alligator Cracking	Sensitivity Analysis and MS Excel® Solver
	Thermal Cracking	Sensitivity Analysis
	IRI	MS Excel® Solver, Brute Force and Lingo
HMA over JPCP	Rutting	Sensitivity Analysis
	Longitudinal Cracking	Sensitivity Analysis and MS Excel® Solver
	Alligator Cracking	Sensitivity Analysis and MS Excel® Solver
	Thermal Cracking	Sensitivity Analysis
	IRI	MS Excel® Solver, Brute Force and Lingo

Non-linear Optimization Methods

A nonlinear programming optimization technique provided as an MS Excel® solver routine has been commonly used to minimize the bias (ϵ) and the root mean square error (RMSE) between the actual distress measurements and the Pavement ME Design predicted

values (Velasquez et al. 2009, FHWA 2010a, Jadoun 2011). To use this approach, all input values required by the performance models are needed to satisfy closed-form solution requirements. Based on the linear or non-linear nature of the equation, MS Excel® solver uses three different methods: generalized reduced gradient (GRG), simplex (Simplex LP), and evolutionary. GRG is used for non-linear equations, Simplex LP is used for linear equations, and Evolutionary can be used for both non-linear and linear equations. GRG is a robust and fast tool for determining the best combination of calibration coefficients (Frontline Systems, Inc. 2015).

In addition to GRG in MS Excel® solver, a brute-force method (through Microsoft Visual Studio®) was implemented by trying all possible combinations of candidate numbers and checking to see whether any combinations satisfied the problem statement. This method is basically used this study to ensure that the results produced by MS Excel® solver are correct. Algorithms were composed using the transfer functions, constraints and increments were specified, and the best combinations of calibration coefficients minimizing the MSE between measured and predicted pavement performance values were determined. The disadvantage of this method would be that, as defined increments become smaller, the accuracy of the result increases. To make sure that the best combinations of coefficients have been determined, the increments should be minimized.

Along with other optimization methods, an optimization software tool, Lingo 15.0, was also used in this study. This software solves linear and non-linear optimization problems with great accuracy. It can determine global solutions to optimization problems for both convex and non-convex equations (LINDO Systems, Inc. 2015). Note that, using this software, you can find global solutions to the problem very quickly. Again, this software was also employed to ensure that the results provided by MS Solver are correct.

Linear Optimization Method

A linear optimization approach based on sensitivity analysis of calibration coefficients was developed (Ceylan et al. 2013) to reduce the computational burden of the trial-and-error procedure in a case where not all the transfer function components are known. In such a case, sensitivity analysis of each calibration coefficient is conducted and, based on the analysis results, a trial-and-error method is implemented to find the best combination of coefficients providing minimum MSE between measured and predicted pavement performance values. Details of this method can be found in Ceylan et al. (2013).

Accuracy Evaluation Criteria

The Pavement ME Design was executed using nationally and MEPDG locally-calibrated (through Ceylan et al. 2013)) model values to predict performance indicators for each selected PMIS roadway section. Predicted performance measures were then plotted relative to the measured values for the PMIS roadway sections. Based on the accuracy of performance predictions using the nationally and MEPDG locally-calibrated model coefficient values, determination as to whether or not it was necessary to modify the national and MEPDG local coefficient values for Iowa conditions was made. If needed, locally-calibrated model coefficients were identified to improve the accuracy of model predictions.

The accuracy of performance predictions was evaluated by plotting the measurements against the predictions on a 45-degree line representing equality, and also by observing the average bias, standard error, coefficient of determination (R^2) and mean absolute percentage error (MAPE) values. The accuracy indicators used in this study are defined as follows:

$$Ave\ Bias = \varepsilon_{ave} = \frac{\sum_{j=1}^n (y_j^{measured} - y_j^{predicted})}{n} \quad (1)$$

$$\text{Stand. Error} = \sqrt{\frac{\sum_{j=1}^n (y_j^{\text{measured}} - y_j^{\text{predicted}})^2}{n}} \quad (2)$$

$$R^2 = \left(\frac{1}{n} * \sum_{j=1}^n \frac{[(y_j^{\text{measured}} - y_{\text{mean}}^{\text{measured}}) * (y_j^{\text{predicted}} - y_{\text{mean}}^{\text{predicted}})]}{\sigma_{\text{measured}} * \sigma_{\text{predicted}}} \right)^2 \quad (3)$$

$$\text{LOE } R^2 = 1 - \frac{n-p}{n-1} * \left(\frac{S_e}{S_y} \right)^2 \quad (4)$$

$$\text{MAPE} = \frac{1}{n} * \sum_{j=1}^n \left| \frac{y_j^{\text{measured}} - y_j^{\text{predicted}}}{y_j^{\text{measured}}} \right| \quad (5)$$

Where,

- p = total number of explanatory variables in the model,
- n = number of data points in each distress comparison.
- y^{measured} = Measured distress data points
- $y^{\text{predicted}}$ = Measured distress data points
- σ_{measured} = Variance of measured distress data points
- $\sigma_{\text{predicted}}$ = Variance of predicted distress data points
- S_e = Standard error of the estimates
- S_y = Standard deviation of the estimates

The average bias basically shows the average of differences between measured and predicted values, while the standard error of estimate measures the differences between the predicted and measured values. In this study, two kinds of coefficients of determination were utilized: (1) line of equality (LOE) in which R^2 indicates how well the data fit the LOE, and (2) coefficient of determination, simply R^2 , indicating how well the data fit the regression line minimizing RMSE between the two data sets (i.e., measurements and predictions). Note that negative (LOE) R^2 simply means that the data points do not follow the associated model. Lower absolute values of average bias and standard error indicate better accuracy. A positive value for the average bias indicates underestimated predictions. Higher R^2 values show better accuracy. Also, for MAPE, the scale below is used to forecast accuracy (Lewis 1982):

- Highly accurate forecast: $MAPE < 0.1$ (10%)
- Good forecast: 0.1 (10%) $< MAPE < 0.2$ (20%)
- Reasonable forecast: 0.2 (20%) $< MAPE < 0.5$ (50%)
- Inaccurate forecast: $MAPE > 0.5$ (50%)

In addition to the accuracy indicators described, a paired t test was also performed. This test is used to compare the means of two populations to determine whether they differ from one another in a significant way under the assumptions that paired differences are independent and identically normally-distributed. In this test, the following null and alternative hypothesis are used:

- i. H_0 : Mean measured distress = mean predicted distress
- ii. H_A : Mean measured distress \neq mean predicted distress.

Equation 6 is used for the calculation of t values used in these test,

For $j=1:n$,

$$t = \frac{(y_j^{measured} - y_j^{predicted})_{mean}}{\frac{s_d}{\sqrt{n}}} \quad (6)$$

Where,

- n = number of paired data points
- $y^{measured}$ = Measured distress data points
- $y^{predicted}$ = Measured distress data points
- s_d = Standard deviation of paired data points

This statistic follows a t-distribution with $n - 1$ degrees of freedom.

The rejection of the null hypothesis (p -value < 0.05) implies that there are grounds for believing that there is a relationship between two phenomena and predicted distress prediction is thus unbiased.

CHAPTER 5. LOCAL CALIBRATION RESULTS

The pavement performance models adopted in Pavement ME Design for JPCP, HMA, and HMA over JPCP pavements are discussed here from a local calibration perspective. The step-by-step procedure of local calibration was documented by considering the availability of transfer function components. The Pavement ME Design calibration coefficients identified for Iowa pavement system and the corresponding model accuracies are presented and compared to MEPDG calibration coefficients identified by the InTrans Project 11-401 (Ceylan et al. 2013) and national calibration coefficients.

JPCP

The Pavement ME Design new JPCP performance predictions include mean joint-faulting, transverse slab-cracking and IRI performance models. The identification of transfer functions for these models was noted and the availability of each component of these functions for the local calibration were investigated. Based on the availability of these components, different optimization approaches were utilized and the calibration results from the utilized optimization approaches will be presented along with corresponding model accuracies.

Mean Transverse Joint Faulting

An incremental approach method was adapted (AASHTO 2008) for the calculation of mean transverse joint-faulting. Based on this method, faulting values for each month was calculated and summed, beginning with the traffic opening date, to determine the faulting value at any time.

Transverse joint faulting predictions can be calculated from the following set of equations:

$$Fault_m = \sum_{i=1}^m \Delta Fault_i \quad (7)$$

$$\Delta Fault_i = C_{34} * (FAULTMAX_{i-1} - Fault_{i-1})^2 * DE_i \quad (8)$$

$$FAULTMAX_i = FAULTMAX_{i-1} + (C_7/10^6) \sum_{j=1}^m DE_j * \log(1 + C_5 * 5^{EROD})^{C_6} \quad (9)$$

$$FAULTMAX_0 = C_{12} * \delta_{curling} * [\log(1 + C_5 * 5^{EROD}) * \log(\frac{P_{200} * Wet\ Days}{p_s})]^{C_6} \quad (10)$$

Where:

- $Fault_m$ = Mean joint faulting at the end of month m, inch
- $\Delta FAULT_i$ = Incremental change (monthly) in mean transverse joint faulting during month i, inch
- $FAULTMAX_i$ = Maximum mean transverse joint faulting for month i, inch
- $FAULTMAX_0$ = Initial maximum mean transverse joint faulting, inch
- $EROD$ = Base/subbase erodibility factor
- DE_i = Differential density of energy of subgrade deformation accumulated during month i
- $\delta_{curling}$ = Maximum mean monthly slab corner upward deflection PCC due to temperature curling and moisture warping
- P_s = Overburden on subgrade, lb
- P_{200} = Percent subgrade material passing #200 sieve
- $WetDays$ = Average annual number of wet days (greater than 0.1 in, rainfall), and
- $C_{1, 2, 3, 4, 5, 6, 7, 12, 34}$ = Calibration coefficients

C_{12} and C_{34} among calibration coefficients are defined by the following equations:

$$C_{12} = C_1 + C_2 * FR^{0.25} \quad (11)$$

$$C_{34} = C_3 + C_4 * FR^{0.25} \quad (12)$$

Where:

- FR = Base freezing index defined as percentage of time the top base temperature is below freezing (32°F) temperature.

Note that Equation 9 is presented in AASHTO *Mechanistic-Empirical Pavement Design Guide, Interim Edition: A Manual of Practice* (AASHTO 2008) as:

$$FAULTMAX_i = FAULTMAX_0 + (C_7) \sum_{j=1}^m DE_j * \log(1 + C_5 * 5^{EROD})^{C_6} \quad (13)$$

Using Equation 13 from the AASHTO *Mechanistic-Empirical Pavement Design Guide, Interim Edition: A Manual of Practice* (AASHTO 2008), the same mean transverse joint-faulting values reported in the software outputs could not be calculated. Communications with the

developers of Pavement ME Design software (ARA, personal communication, August 4, 2014) revealed the following clarifications:

- Division of C_7 by 10^6 in Equation 9 is hardcoded into the software, although this division was not shown in the equation (Refer to Equation 13).
- $FAULTMAX_{i-1}$ (See Equation 9) should be used instead of $FAULTMAX_0$ (See Equation 15)

The availability of each variable of the equations described above was carefully inspected. All were either extracted from the Pavement ME Design final and intermediate output files or calculated using the data provided by the Pavement ME Design output files. The reporting file location or calculation method for each variable are listed as follows:

- Erodibility = Used as input value, known or can be checked from the “Design Properties” tab in final result summary output file
- P200 = Used as input value, known or can be checked from the “Layer #” tab in the final result summary output file
- Wet days = Can be indirectly found in the intermediate output file of “MonthlyClimateSummary.csv” by summing all the wet days in all months and then multiplying by 12 to obtain annual wet day results
- $FAULTMAX_0$ = Provided in the first column and first row of the “JPCP_faulting.csv” intermediate file for each pavement section
- DE = Can be extracted from the “Faulting Data” tab in the final result summary output file
- Curling and warping deflection = knowing the $FAULTMAX_0$ value from the intermediate file, the curling deflection value can be calculated using the $FAULTMAX_0$ equation (See equation 13)
- P_s = Overburden pressure can be determined using the following equation:

$$P_s = 144 * (Gam_{PCC} * H_{PCC} + Gam_{base} * H_{base}) \quad (14)$$

Where:

- Gam_{PCC} = Unit weight of concrete (lb/in³)
- Gam_{base} = Unit weight of base (lb/in³)
- H_{PCC} = Concrete thickness (in.)
- H_{base} = base thickness (in.)

The step-by-step faulting calculation from available variables can be described as follows:

Step 1: Calculate $\delta_{curling}$ using Equation 12.

$$\delta_{curling} = \frac{FAULTMAX_0}{C_{12}} * [\log(1 + C_5 * 5^{EROD}) * \log(\frac{P_{200} * Wet\ Days}{p_s})]^{C_6} \quad (15)$$

Step 2: Using this $\delta_{curling}$ value, calculate the corrected value of the $FAULTMAX_0$ as follows:

$$FAULTMAX_0^{New} = C_{12}^{New} * \delta_{curling} * [\log(1 + C_5^{New} * 5^{EROD}) * \log(\frac{P_{200} * Wet\ Days}{p_s})]^{C_6^{New}} \quad (16)$$

Step 3: Using the corrected value of the initial maximum mean transverse joint faulting

$FAULTMAX_0^{New}$, calculate the maximum mean transverse joint faulting for each month as follows:

$$FAULTMAX_i^{New} = FAULTMAX_{i-1}^{New} + C_7^{New} / 10^6) \sum_{j=1}^m DE_j * \log(1 + C_5^{New} * 5^{EROD})^{C_6^{New}} \quad (17)$$

Step 4: Calculate the faulting increment as follows:

$$\Delta Fault_i^{New} = C_{34}^{New} * (FAULTMAX_{i-1}^{New} - Fault_{i-1}^{New})^2 * DE_i \quad i=1,2... \quad (18)$$

Step 5: Calculate the mean joint faulting at the end of month i as follows:

$$Fault_i^{New} = Fault_{i-1}^{New} + \Delta Fault_i^{New} \quad i = 1, 2 ... \quad (19)$$

Step 6: The calculated faulting values were compared with the ones produced by software to see

if the same values were obtained. Figure 13 shows the correlation between calculated and

software output faulting values.

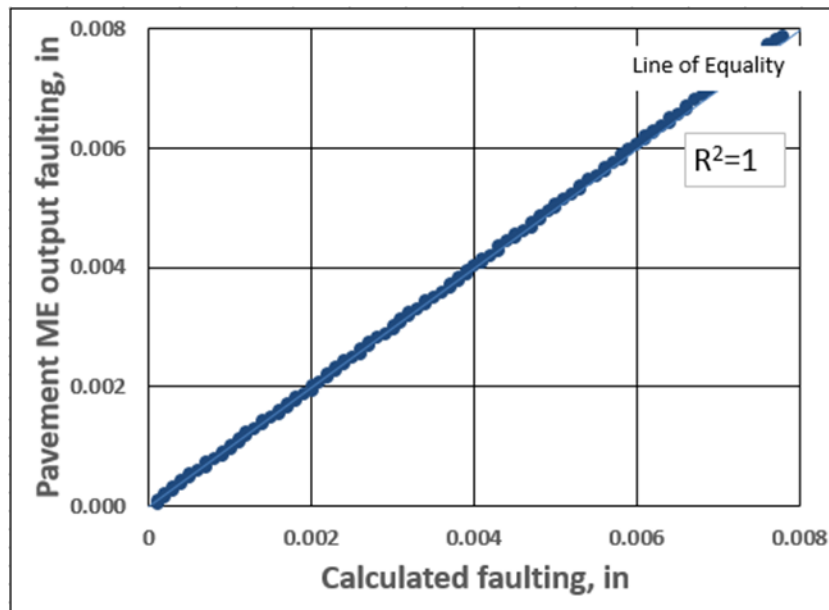


Figure 13. Faulting values comparison between Pavement ME Design output and calculated values

Calculated mean joint-faulting values were compared with the actual Iowa DOT PMIS faulting measurements of each section in the calibration data set. A local calibration coefficients optimization procedure was performed using different nonlinear optimization approaches (MS Excel Solver, Lingo, and Brute Force) to minimize the mean square error (MSE) between the predicted and actual mean joint-faulting values. The set of calibration coefficients determined from the optimization procedure was used as the set of local calibration coefficients. For validation purposes, the local calibration coefficient accuracy was evaluated using an independent validation data set.

Figure 14 and Figure 15 compare the faulting predictions using national, MEPDG local, and Pavement ME Design local calibration coefficients for calibration and validation data sets, respectively. Note that Pavement ME Design software was used for these comparisons by

changing each of the three calibration coefficient sets: ONC, local calibration coefficients determined from MEPDG runs by using trial-error based approach under previous study (Ceylan et al. 2013), and local calibration coefficients determined from Pavement ME Design software runs in this study.

As can be seen in these figures, the nationally-calibrated faulting model underpredicted distress for Iowa JPCPs. When using MEPDG local calibration coefficients determined through a trial-and-error based approach from a previous study (Ceylan et al. 2013), significant amount of standard error was still observed, although underprediction was mostly eliminated. As a result of the optimization procedure in the Pavement ME Design JPCP faulting model, 7 of 8 national calibration coefficients were optimized. Further accuracy improvement in the Pavement ME Design JPCP faulting model for Iowa JPCP could be achieved through nonlinear optimization approaches by using fully-optimized local calibration coefficients.

Faulting predictions from the locally-calibrated Pavement ME Design model are higher than those from the nationally-calibrated model. This finding implies that increases in pavement thickness and dowel diameter are recommended when the locally-calibrated Pavement ME Design faulting model is used rather than national one, given that faulting is the controlling failure mode. Using the Pavement ME Design locally-calibrated faulting model would make the design more realistic.

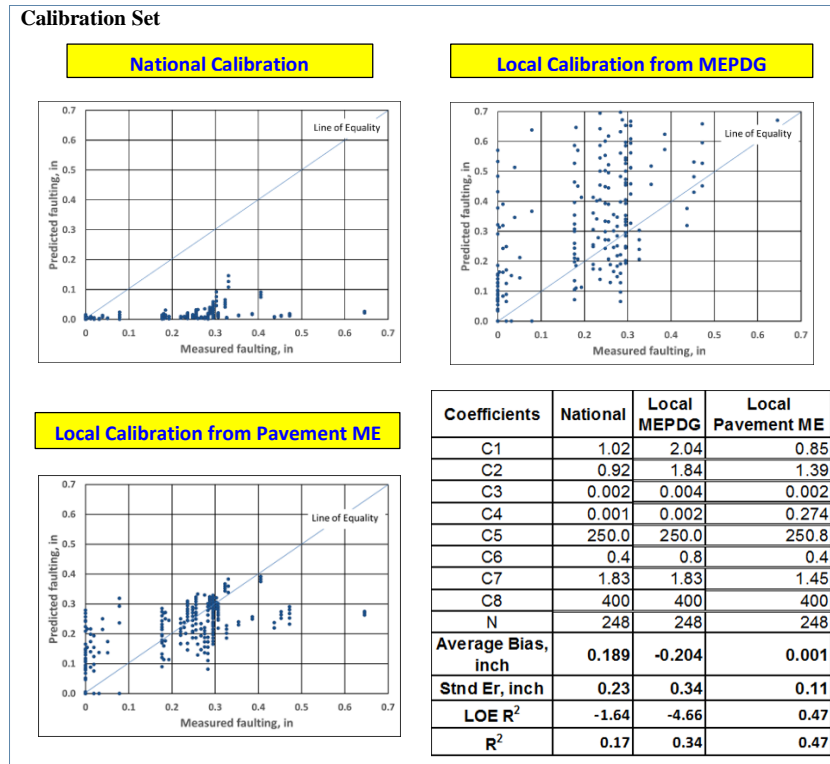


Figure 14. Overall accuracy summary of JPCP faulting model using calibration set

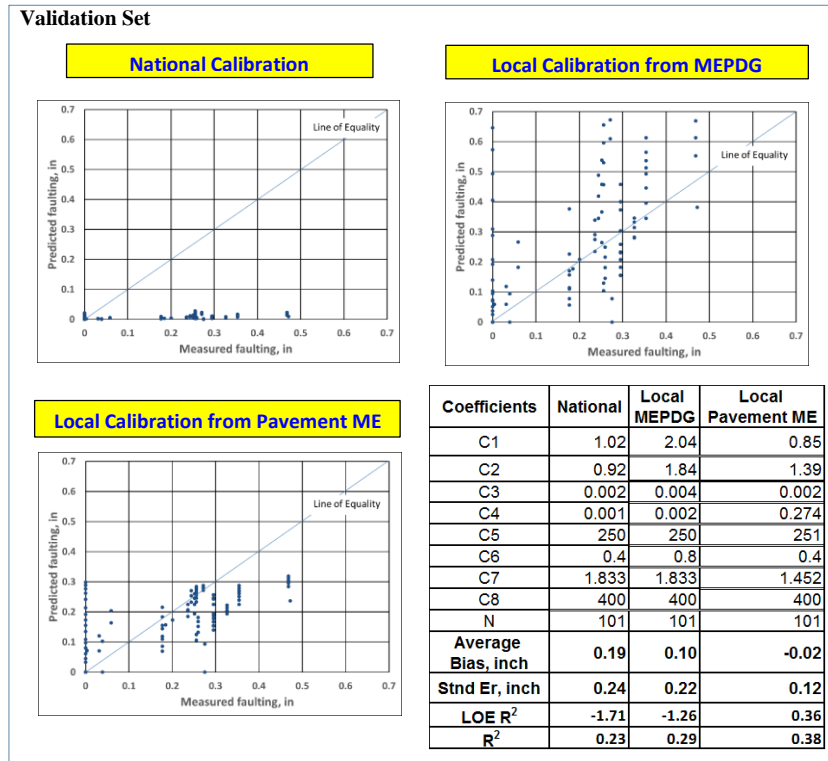


Figure 15. Overall accuracy summary of JPCP faulting model using validation set

Transverse Slab Cracking (Bottom-Up and Top-Down)

Transverse-cracking predictions were computed using two models: the fatigue damage model and transverse-cracking transfer functions. The fatigue damage model provides a fatigue damage estimate for the given conditions and the transverse-cracking transfer model converts fatigue damage estimation into transverse-cracking predictions equivalent to transverse-cracking measurements.

Transverse slab cracking predictions were calculated from a set of equations as follows (AASHTO 2008):

$$\log(N_{allowable}) = C_1 \left(\frac{MR}{\sigma} \right)^{C_2} \quad (20)$$

$$Crack = \frac{100}{1 + C_4 * FD^{C_5}} = \frac{100}{1 + C_4 * (N_{applied} / N_{allowable})^{C_5}} \quad (21)$$

Where:

- MR = Modulus of rupture of the concrete
- σ = Critical stress in the slab
- FD = Fatigue damage
- $N_{applied}$ = Applied number of load applications
- $N_{allowable}$ = Allowable number of load applications
- $C_{1, 2, 4, 5}$ = Calibration coefficients

The total slab-cracking prediction provided by Pavement ME Design software is the sum of bottom-up and top-down cracking prediction values because, in JPCP pavement systems, cracks can be initiated either from the bottom of the slab and propagate upwards or vice-versa but not both ways. Therefore, providing the combined cracking prediction is more meaningful than providing only bottom-up or top-down values (AASHTO 2008).

Total transverse cracking predictions are calculated as follows:

$$TCrack = (Crack_{Bottom-up} + Crack_{Top-down} - Crack_{Bottom-up} * Crack_{Top-down}) * 100 \quad (22)$$

Where:

- $TCrack$ = Total transverse cracking (percent, all severities)
- $CrackBottom-up$ = Predicted amount of Bottom-up transverse cracking (fraction)
- $CrackTop-down$ = Predicted amount of Top-down transverse cracking (fraction)

As can be seen from the equations, for this distress type, four calibration coefficients must be calibrated from Equation 20 and Equation 21. These four coefficients can be categorized into two groups: two (C_1 and C_2) are related to the stress ratio (M_R/σ) for fatigue damage estimation and the others (C_4 and C_5) are in the transverse-cracking transfer model to convert fatigue damage estimations into transverse-cracking predictions.

Searching for input variables for Equations 20, 21, and 22 revealed that $N_{applied}$ was not reported in any of the Pavement ME Design output files. Communications with software developers (ARA, personal communication, September 24, 2014) regarding this issue confirmed that the latest version of Pavement ME Design software (version 2.1) does not provide this information. It was concluded that it is impossible to calibrate coefficients (C_1 , C_2 , C_4 and C_5) all together for actual transverse-cracking measurements. Rather than using this approach, C_4 and C_5 could be optimized to actual transverse-cracking measurements through non-linear optimization approaches using the FD values reported under the “Cracking Data” tab in the final result summary output. However, without actual $N_{allowable}$ measurements, requiring many laboratory fatigue tests, C_1 and C_2 could not be calibrated even through non-linear optimization approaches, so alternative approaches such as trial-and-error based implemented using a linear optimization approach as a screening procedure (Ceylan et al. (2013), Kim et al. (2014)) were used to calibrate coefficients of C_1 and C_2 . The step-by-step procedure of JPCP transverse cracking model local calibration is described as follows:

Step 1: Sensitivity analysis of all transverse cracking model calibration coefficients was performed with the results shown in Table 16. Detailed descriptions this sensitivity analysis are provided in Appendix C. Based on the sensitivity analysis results, C_1 and C_2 coefficients in the fatigue damage model were found to be more sensitive to transverse slab-cracking predictions than C_4 and C_5 coefficients in the transverse-cracking transfer function. Taking this information into account, a set of C_1 and C_2 coefficients was selected from a linear optimization approach using the sensitivity index as a screening procedure to reduce the computational burden of the trial-and-error procedure. Among many sets of C_1 and C_2 coefficients selected, the C_1 and C_2 coefficients resulting in minimum mean square error (MSE) between transverse-cracking predictions and measurements were determined through a trial-and-error procedure using Pavement ME Design.

Table 16. Sensitivity analysis results of transverse cracking calibration coefficients

Calibration factors	Coefficient Sensitivity Index	Rank
C_1	-2.58	1
C_2	-2.52	2
C_4	-0.11	3
C_5	0.24	4

Step 2: The determined C_1 and C_2 coefficients were input into Pavement ME Design to execute its runs for each section to produce a calibration data set. Both bottom-up and top-down fatigue damage estimations from Pavement ME Design runs were extracted under the “Cracking Data” tab in the final result summary output files.

Step 3: Using these fatigue damage predictions, C_4 and C_5 calibration coefficients were calibrated with the help of various nonlinear optimization approaches (MS Excel Solver, Lingo and Brute Force) applied to Equations 21 and 22.

Figure 16 and Figure 17 compare the transverse cracking predictions using national, MEPDG local, and Pavement ME Design local-calibration coefficients for calibration and validation sets. As can be seen in the figure, the transverse-cracking model using national calibration coefficients could not accurately predict transverse-cracking distress in Iowa JPCP. This might be explained by the fact that typical Iowa JPCP has a joint spacing of 20 ft. while JPCP in most other states has less than 20 ft. of joint spacing, affecting LTPP data used for national calibration. Using MEPDG local calibration coefficients, the accuracy of model predictions was improved compared over using national calibration coefficients. Further accuracy improvement was attempted for Pavement ME Design by minimizing standard error. Significant accuracy enhancements can be accomplished using locally-calibrated Pavement ME Design transverse-cracking predictions (See Figure 16 and Figure 17).

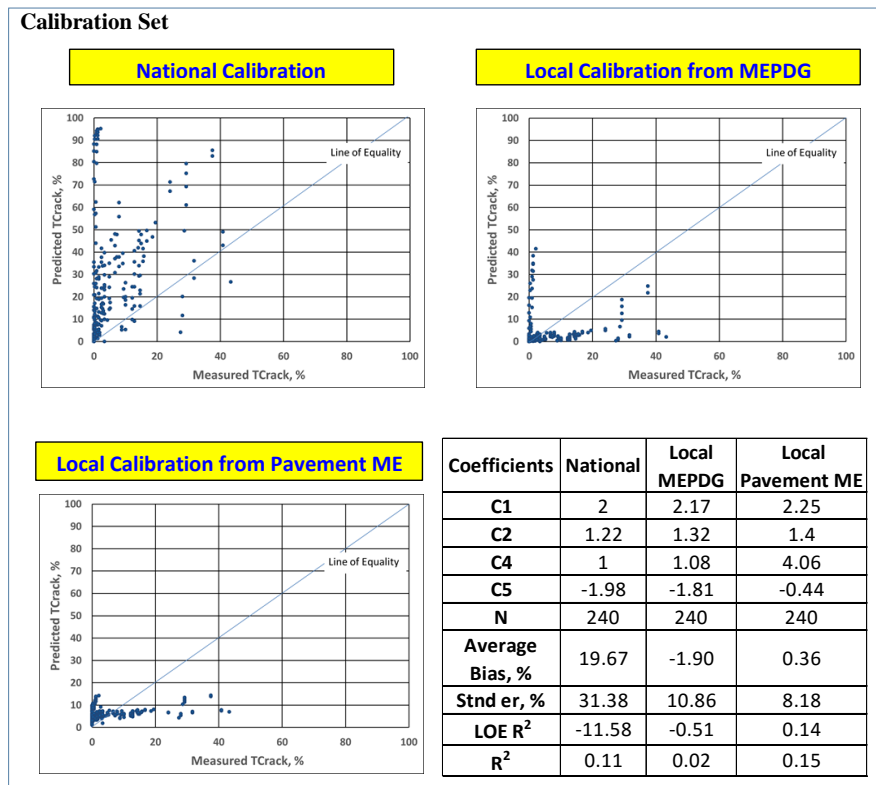


Figure 16. Overall accuracy summary of JPCP transverse cracking model using calibration set

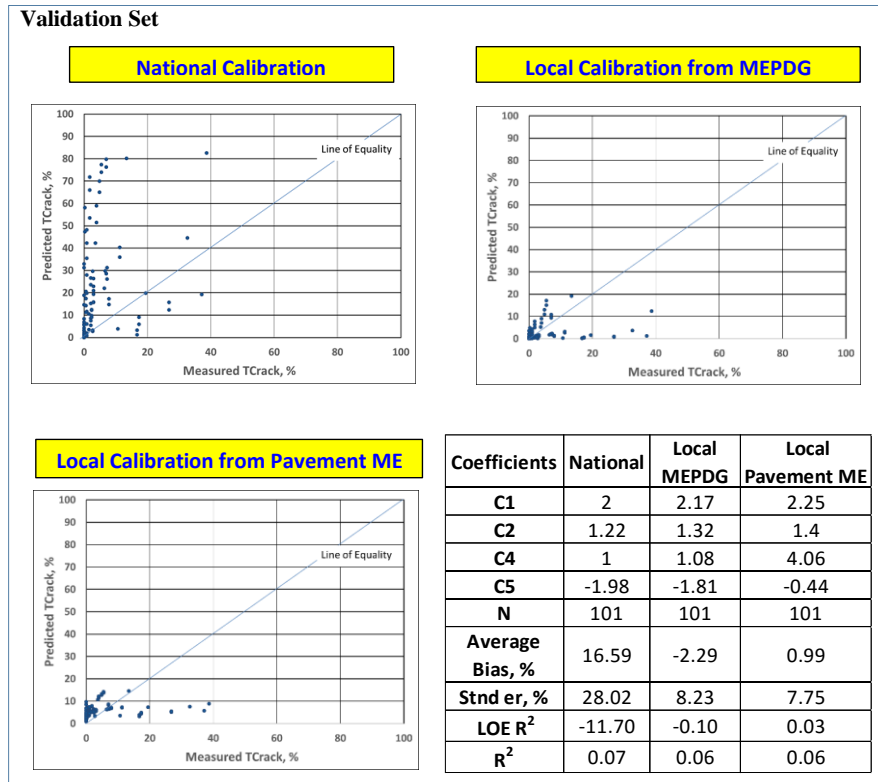


Figure 17. Overall accuracy summary of JPCP transverse cracking model using validation set

Figure 18 presents fatigue damage calculations using national, MEPDG local, and Pavement ME Design local-fatigue damage calibration coefficients (i.e., C1 and C2 coefficients). For the given stress/strain ratios (σ/MOR), using Pavement ME Design local-fatigue damage calibration coefficients can provide fewer damage calculations in comparison to using national and MEPDG local-fatigue damage calibration coefficients. This implies that using Pavement ME Design local fatigue damage calibration coefficients will lead to thinner pavement thickness and wider joint spacing in Iowa JPCP design than when using national and MEPDG local-fatigue damage calibration coefficients, given that the other coefficients (i.e., C4 and C5 coefficients) remain the same and transverse cracking is the controlling distress mode in JPCP design.

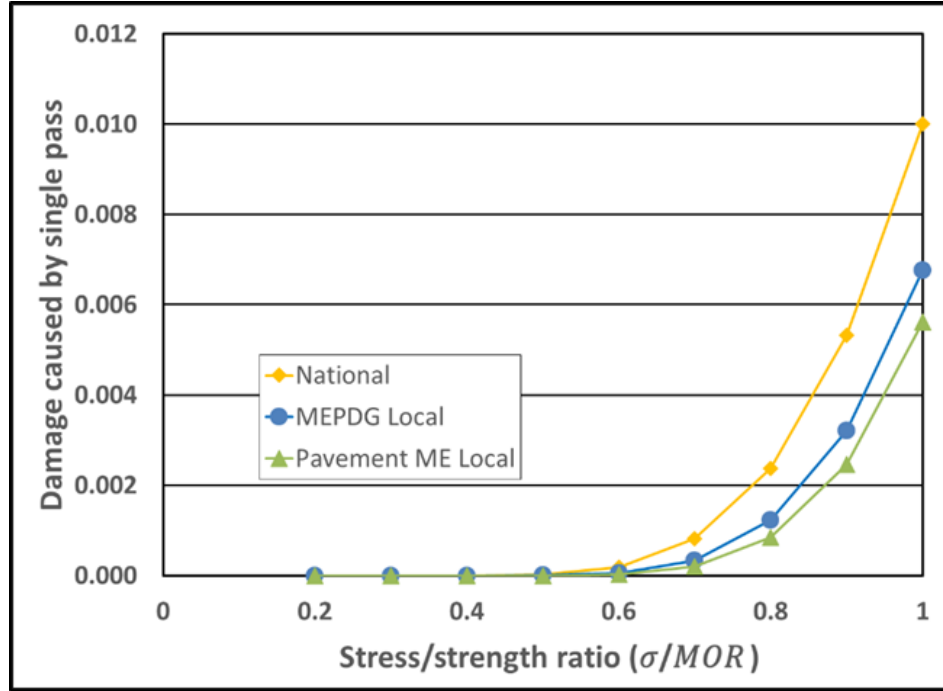


Figure 18. Fatigue damage prediction comparisons

Smoothness (IRI)

The International Roughness Index (IRI) is the smoothness performance index employed in Pavement ME design. The Pavement ME design IRI prediction model for JPCP consists of the transverse-cracking prediction, the joint-faulting prediction, the spalling prediction and a site factor, along with calibration coefficients. The AASHTO Mechanistic-Empirical Pavement Design Guide, Interim Edition: A Manual of Practice (AASHTO 2008) presents the JPCP IRI prediction equation employed in MEPDG as follows:

$$IRI = IRI_{ini} + C1 \times CRK + C2 \times SPALL + C3 \times TFAULT + C4 \times SF \quad (23)$$

Where:

- IRI = Predicted IRI, in./mi.
- IRI_{ini} = Initial smoothness measured as IRI, in./mi.
- CRK = Percent slabs with transverse cracks (all severities)
- $SPALL$ = Percentage of joints with spalling (medium and high severities)
- $TFAULT$ = Total joint faulting cumulated, in.

- SF = Site factor
- $C_{1,2,3,4}$ = Calibration coefficients

The site factor of Equation 20 can be calculated as follows:

$$SF = AGE(1 + 0.5556 \times FI)(1 + P_{200}) \times 10^{-6} \quad (24)$$

Where:

- AGE = Pavement age, yr
- FI = Freezing index, °F-days
- P_{200} = Percent subgrade material passing No. 200 sieve.

However, the JPCP IRI values reported in the Pavement ME Design software outputs could not be obtained using Equation 23. Communications with the Pavement ME design software developers (ARA, personal communication, July 7, 2015) resulted in the following corrected JPCP IRI equation used in Pavement ME Design:

$$IRI = IRI_{ini} + C1 \times CRK + C2 \times SPALL + C3 \times TFAULT \times 5280/JSP + C4 \times SF \quad (25)$$

Where:

- JSP = Joint spacing, (ft.)

Since in the calculation of IRI both percentage of transverse cracking and faulting were involved, either nationally-calibrated or locally-calibrated transverse-cracking and faulting models can be used for local calibration of IRI model. Two approaches for local calibration of the coefficients of IRI model were investigated as follows:

- **Approach 1:** Calibrate using either locally-calibrated or nationally-calibrated distress prediction models. Note that nationally-calibrated distress prediction models can be used when they provide good accuracy in distress measurements.
- **Approach 2:** Calibrate only using nationally-calibrated distress prediction models without considering accuracy of distress model predictions with respect to distress measurements

The purpose of using two approaches in the local calibration of IRI model is to determine whether the IRI model can be locally-calibrated with good accuracy without using the local-calibration procedure of each of distress models that expend cost and data resources.

The availability of each variable required for IRI calculation was carefully inspected. It was found that all the variables were either extracted from general or intermediate output files, or calculated using data provided by the output files. The location or calculation method of each variable can be described as follows:

- *IRIini*: input in the software as an initial IRI value. It can also be obtained from the final result summary output file.
- *CRK and TFAULT*: can be obtained from the “*Distress Data*” tab in the final result summary output file.
- *SPALL*: can be obtained from an intermediate output file ‘*Spalling.txt*’.
- *SF*: can be calculated using Equation 24.
- *FI for SF calculation*: can be obtained from the “*Climate Inputs*” tab in the final result summary output file.
- *P₂₀₀*: a used input value or can be taken from the *Layer #* tab in the final result summary output file.
- Note that Pavement ME Design uses an intermediate file ‘*JPCPIRIInput.txt*’ in calculating IRI predictions.

Figure 19 demonstrates that the JPCP IRI values calculated using Equation 25 are the same as those obtained from Pavement ME Design software output files.

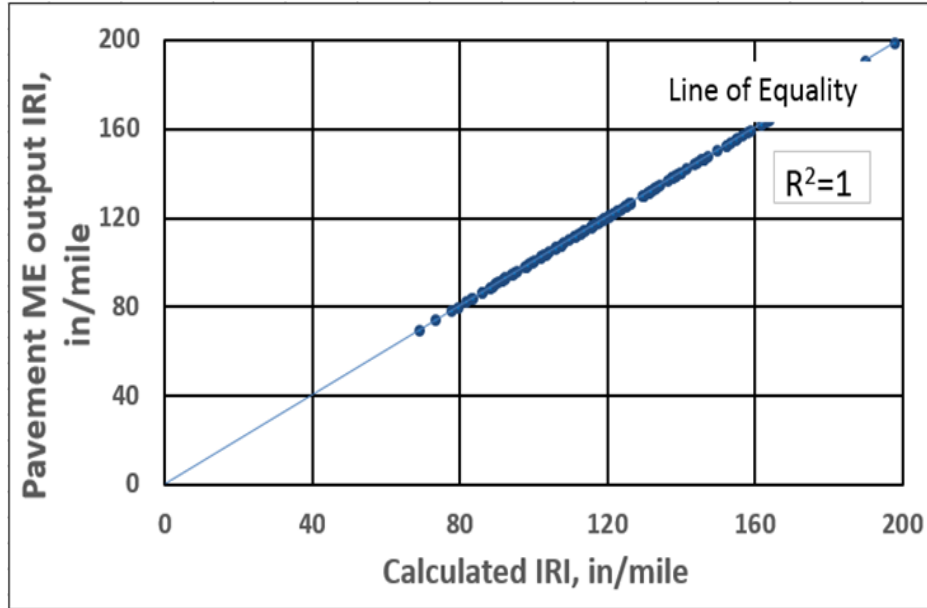


Figure 19. Comparison of calculated and Pavement ME Desing outputted IRI values

As can be seen in Equation 25, in the calculation of IRI both transverse-cracking and faulting predictions are involved. In this study, both locally and nationally-calibrated transverse-cracking and faulting predictions were used for local calibration of JPCP IRI model. The step-by-step procedure for local calibration of JPCP IRI model can be described as follows:

Step 1: Site factor values for each year of each pavement section in calibration data set were calculated using Equation 25. Using these values along with other input variables required by Equation 25, IRI predictions for each year and each pavement section were calculated. Note that locally-calibrated transverse cracking and faulting model predictions are used as inputs to the IRI equation in Approach 1, while nationally-calibrated transverse-cracking and faulting model predictions are used as inputs to the IRI equation in Approach 2. Initially, nationally-calibrated $C1$, $C2$, $C3$ and $C4$ coefficients were used in the calculation of IRI, and these coefficients were also used as input to the Pavement ME Design software runs to ensure that the calculated and Pavement ME Design output IRI values were the same (using Approach 1)

(Figure 19).

Step 2: Differences between IRI predictions and measurements of each pavement section in the calibration data set were calculated and summed to produce MSE.

Step 3: The optimization procedure for local calibration coefficients was performed using various nonlinear optimization approaches (MS Excel Solver, Lingo, and Brute Force) to minimize the mean square error (MSE) between predicted and actual IRI values. The set of calibration coefficients providing minimum MSE was in turn taken as the Pavement ME Design local calibration coefficient set for the IRI model.

Approach 1

Figure 20 and Figure 21 compare the IRI predictions using national, MEPDG local, and Pavement ME Design local calibration coefficients for calibration and validation sets. Approach 1 was used for local calibrations for both MEPDG and Pavement ME Design. As can be seen from the figures, both MEPDG and Pavement ME Design locally-calibrated models produce more accurate predictions than the national model. Model accuracy was further improved by Pavement ME Design local calibration compared to that of the MEPDG locally-calibrated model.

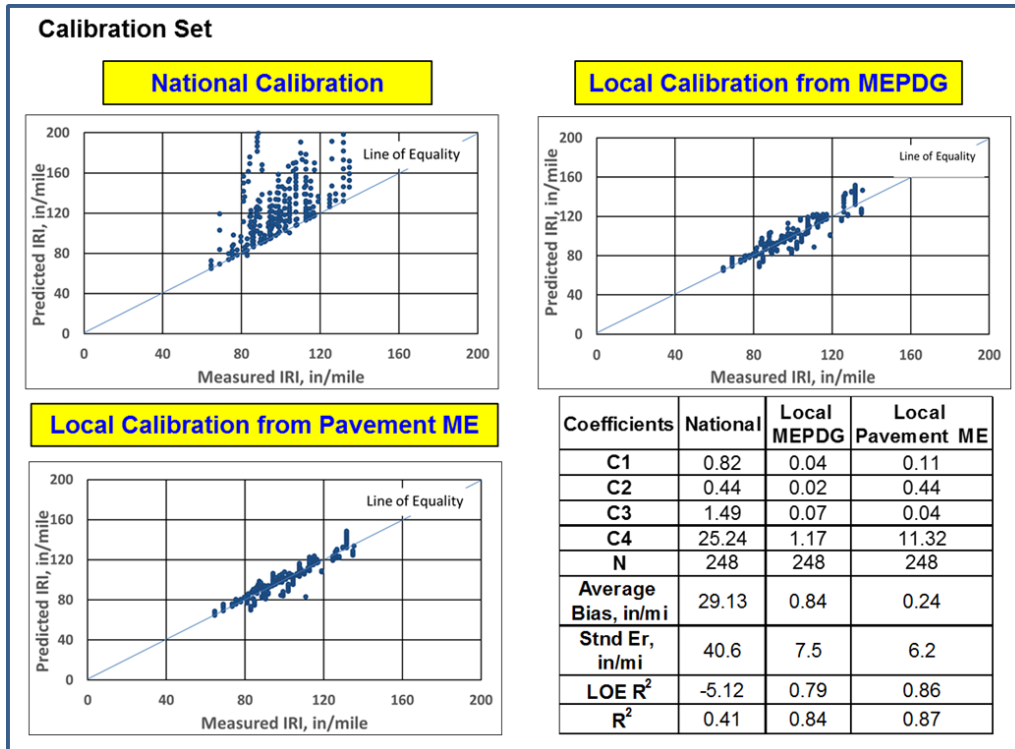


Figure 20. Overall accuracy summary of the JPCP IRI model using calibration set (Approach 1)

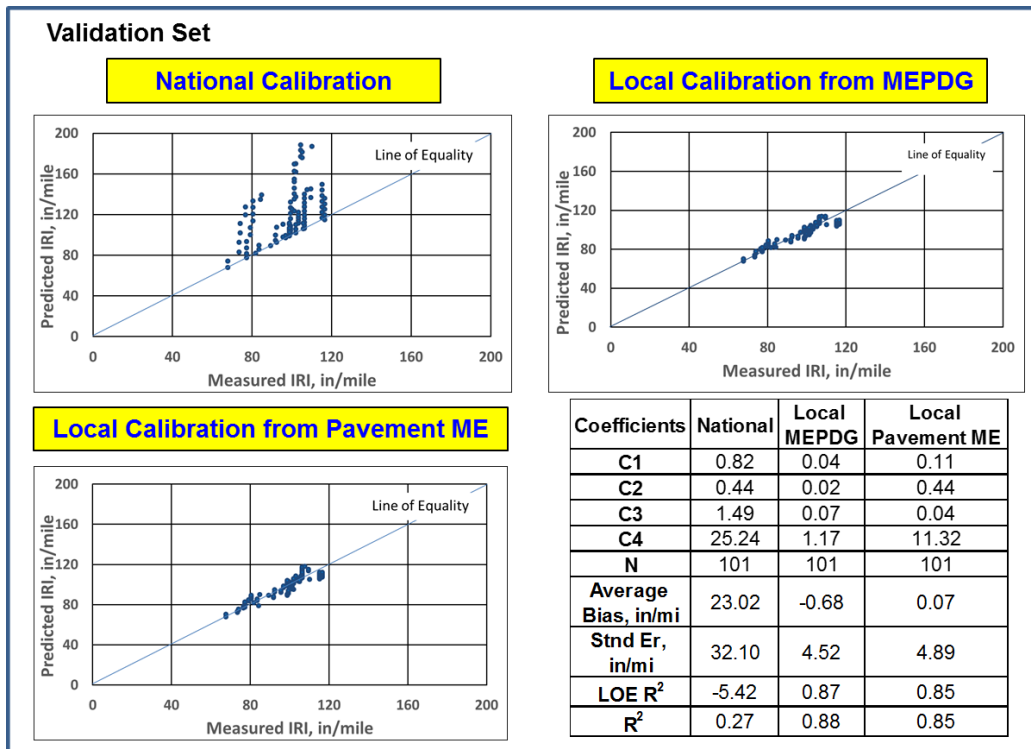


Figure 21. Overall accuracy summary of the JPCP IRI model using validation set (Approach 1)

Approach 2

An alternative approach (Approach 2) was also used to locally calibrate the IRI model using Pavement ME Design. In this approach, nationally-calibrated transverse-cracking and faulting model predictions were used as inputs to the IRI equation. As seen in Figure 22 and Figure 23, approach 2 can also significantly improve IRI predictions. The purpose of using two approaches in the local calibration of IRI model is to determine whether the IRI model can be locally calibrated with sufficient accuracy without the local calibration procedure of each distress models and thereby conserve cost and data resources. A locally-calibrated IRI model using Approach 2 would save significant amounts of time and funds. Use of Approach 2 in local calibration of the IRI model would be especially useful for those SHAs, if they are more interested in obtaining locally-calibrated IRI predictions rather than locally-calibrated transverse-cracking and faulting predictions. In this study, it was determined that Approach 2 with a locally-calibrated IRI model can predict this distress with sufficient accuracy for Iowa JPCP pavement systems.

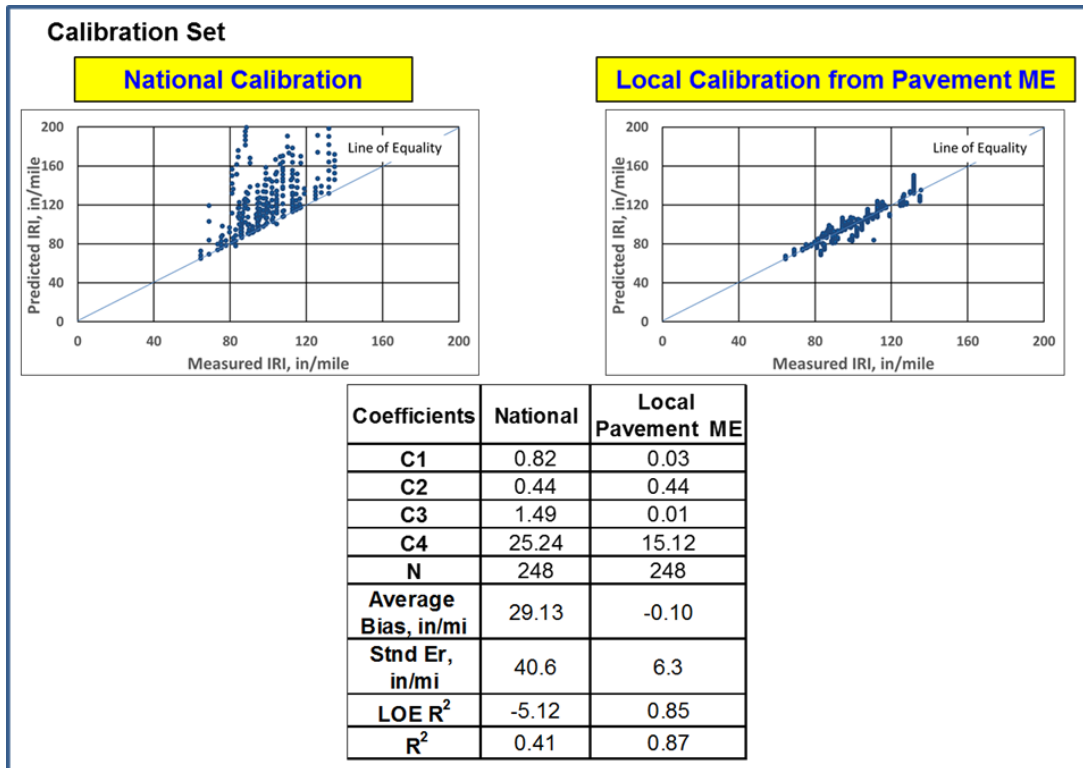


Figure 22. Overall accuracy summary of JPCP IRI model using calibration set (Approach 2)

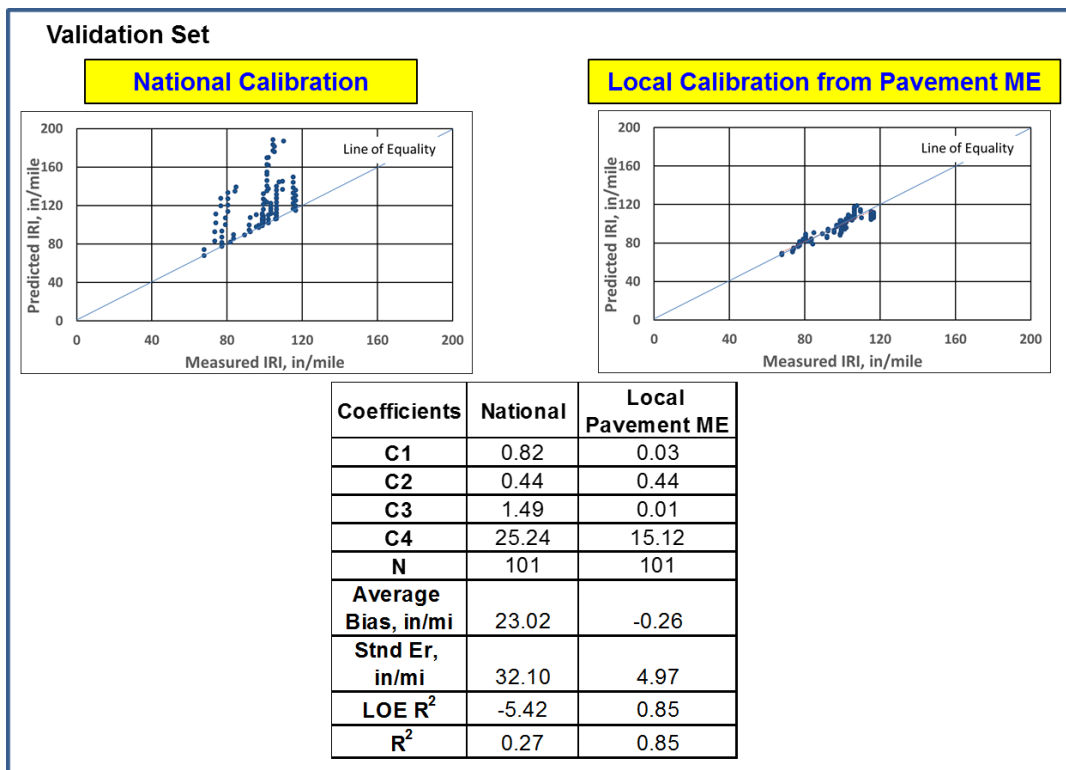


Figure 23. Overall accuracy summary of JPCP IRI model using validation set (Approach 2)

HMA

The Pavement ME Design new HMA pavement performance prediction models include rutting, longitudinal (top down) cracking, alligator-cracking (bottom up) cracking, thermal (transverse) cracking and IRI. Rutting predictions consist of HMA layer rutting, granular-base rutting, subgrade rutting and total surface rutting. Similar to JPCP, the HMA fatigue models use a damage estimate model along with fatigue-distress transfer function models to provide longitudinal-cracking and alligator-cracking predictions equivalent to actual cracking measurements.

Rut Depth

Pavement ME Design outputs rutting depth values in each sublayer, including an HMA surfaced layer, an unbound aggregate base layer, and a subgrade, as well as total rutting in HMA pavements. The total rut depth in Pavement ME Design is calculated as the summation of rutting depths at each sublayer. The accumulated permanent or plastic deformation in the HMA layer/sublayer is calculated using the following equations (AASHTO 2008):

$$\Delta_{p(HMA)} = \varepsilon_{p(HMA)} \times h_{HMA} = \beta_{1r} \times k_z \times \varepsilon_{r(HMA)} \times 10^{k_{1r}} \times n^{k_{2r}\beta_{2r}} \times T^{k_{3r}\beta_{3r}} \quad (26)$$

Where:

- $\Delta_{p(HMA)}$ = Accumulated permanent or plastic vertical deformation in the HMA layer/sublayer, in.
- $\varepsilon_{p(HMA)}$ = Accumulated permanent or plastic axial strain in the HMA layer/sublayer, in/in.
- $\varepsilon_{r(HMA)}$ = Resilient or elastic strain calculated by the structural response model at the mid-depth of each HMA sublayer, in/in.
- h_{HMA} = Thickness of the HMA layer/sublayer, in.
- n = Number of axle-load repetitions
- T = Mix or pavement temperature, °F
- k_z = Depth confinement factor
- $k_{1r,2r,3r}$ = Global field calibration parameters (from the NCHRP 1-40D recalibration;
- $k_{1r} = -3.35412, k_{2r} = 0.4791, k_{3r} = 1.5606$

- $\beta_{1r,2r,3r}$ = Local or mixture field calibration constants; for the global calibration, these constants were all set to 1.0

$$k_z = (C_1 + C_2 \times D) \times 0.328196^D \quad (27)$$

$$C_1 = -0.1039 \times H_{HMA}^2 + 2.4868 \times H_{HMA} - 17.342 \quad (28)$$

$$C_2 = 0.0172 \times H_{HMA}^2 - 1.7331 \times H_{HMA} + 27.428 \quad (29)$$

Where:

- D = Depth below the surface, in.
- H_{HMA} = Total HMA thickness, in.

The accumulated permanent or plastic deformation in the base/subgrade is calculated

using following equations (AASHTO 2008):

$$\Delta_{p(soil)} = \beta_{s1} \times k_{s1} \times \varepsilon_v \times h_{soil} \times \frac{\varepsilon_0}{\varepsilon_r} \times e^{-\left(\frac{\rho}{n}\right)^\beta} \quad (30)$$

Where:

- $\Delta_{p(soil)}$ = Permanent or plastic deformation for the layer/sublayer, in.
- n = Number of axle-load applications
- ε_0 = Intercept determined from laboratory repeated load permanent deformation tests, in/in
- ε_r = Resilient strain imposed in laboratory test to obtain material properties ε_0 , ε , and ρ , in/in
- ε_v = Average vertical resilient or elastic strain in the layer/sublayer and calculated by the structural response model, in/in
- h_{soil} = Thickness of the unbound layer/sublayer, in
- k_{s1} = Global calibration coefficients; $k_{s1} = 1.673$ for granular materials and 1.35 for fine-grained materials
- β_{s1} = A local calibration constant for rutting in the unbound layers; it was set to 1.0 for the global calibration procedure

$$\text{Log}\beta = -0.61119 - 0.017638 \times (W_c) \quad (31)$$

$$\rho = 10^9 \times \left(\frac{C_0}{1-(10^9)^\beta}\right)^{\frac{1}{\beta}} \quad (32)$$

$$C_0 = \text{Ln}\left(\frac{a_1 M_r^{b_1}}{a_9 M_r^{b_9}}\right) = 0.0075 \quad (33)$$

Where:

- W_c = Water content, %
- M_r = Resilient modulus of the unbound layer or sublayer, psi
- $a_{1,9}$ = Regression constants; $a_1 = 0.15$ and $a_9 = 20.0$
- $b_{1,9}$ = Regression constants; $b_1 = 0.0$ and $b_9 = 0.0$

Searching the equations in the Pavement ME Design outputs revealed that not all the variables required could have been determined by software output or from intermediate output files to conduct local calibration outside the software.

The availability and the location of each available variable for HMA rutting model can be described as follows:

- $\epsilon_{r(HMA)}$ = Not provided by the software
- h_{HMA} = Input value, known or can be checked from the “Grand Summary” tab in the final result summary output file
- n = Not provided by the software
- T = Not provided by the software
- k_z = Can be calculated using Equations 27, 28 and 29

Also, the availability and the location of each available variable for the subgrade-rutting model can be described as follows:

- n = Not provided by the software
- ϵ_0 = Not provided by the software
- ϵ_r = Not provided by the software
- ϵ_v = Not provided by the software
- h_{soil} = Input value, known or can be checked from the “Grand Summary” tab in the final result summary output file

- W_c = Input value, known or can be checked from the “Layer #” tab in the final result summary output file
- M_r = Input value, known or can be checked from the “Layer #” tab in the final result summary output file

Although Pavement ME Design provides a vertical strain output file ‘VertStrain.txt’ that reports different vertical strain values for different sub seasons, axle numbers, AC moduli, and load locations for each month, it is not known whether this reported vertical strain value is used in the equation during software execution. Mr. Titus-Glover of ARA (Leslie Titus-Glover, ARA, 2015) advised a procedure of conducting local calibration by software input of different combinations of calibration coefficients and choosing the combination that provides the most accurate prediction; sensitivity analysis of HMA rutting model calibration coefficients was conducted for that purpose with detailed descriptions provided in Appendix C. Table 17 shows the sensitivity analysis results:

Table 17. Sensitivity analysis results of HMA rutting calibration coefficients

Calibration factors	Coefficient Sensitivity Index	Rank
BR2	9.65	1
BR3	8.94	2
BR1	1.00	3

Based on sensitivity analysis results, an experimental matrix including different sets of calibration coefficients were prepared as shown in Table 18. After trying different sets of calibration coefficients, the set consisting of 1.1 and 1 for BR2 and BR3, respectively, resulted in the most accurate predictions (Table 18).

Table 18. Experimental matrix for local calibration of HMA rutting model

BR2	BR3	R ²
1.15	1	0.12
1.1	1.05	0.26
1.1	1	0.55
1.05	1.05	0.53

Rutting measurement estimations from Iowa DOT PMIS data indicated that almost all total rutting is a result of HMA layer rutting related to the fact that most selected HMA pavements are full-depth asphalt pavements reflecting present-day HMA pavement design and construction practices in Iowa. As a result, the local calibration coefficient for β_{s1} related to subgrade rutting, was chosen as 0.001 to minimize subgrade-rutting predictions.

Figure 24 and Figure 25 show the total rutting predictions using national, MEPDG local, and Pavement ME Design local calibration coefficients for both calibration and validation sets. As can be seen in the figures, although the MEPDG locally-calibrated rutting model gives more accurate predictions than the nationally-calibrated model, the accuracy further improved when using the Pavement ME Design locally-calibrated rutting model identified in this study (Figure 24 and Figure 25).

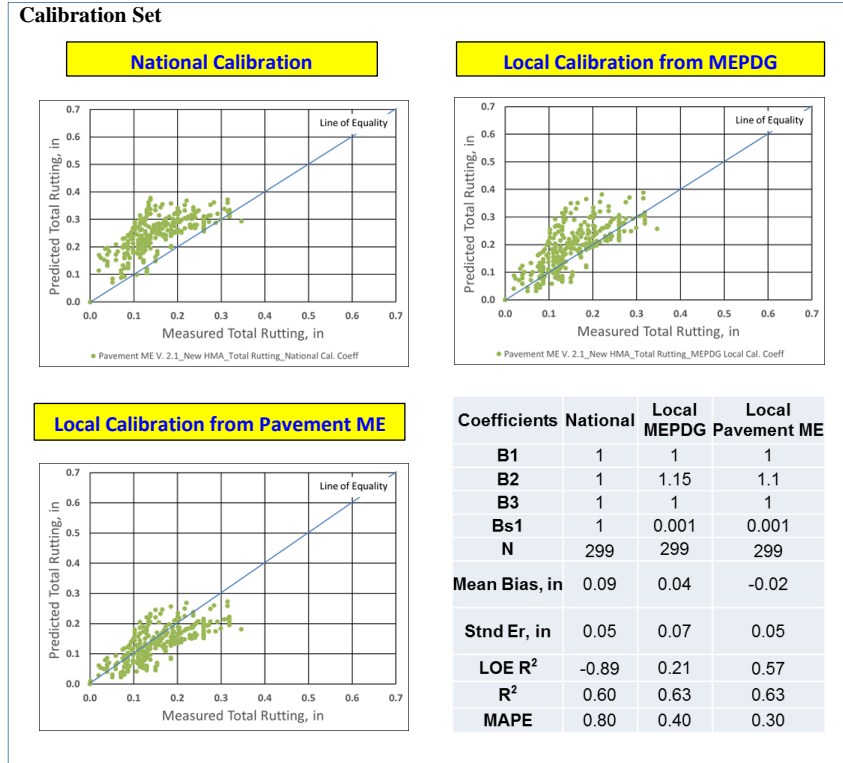


Figure 24. Overall accuracy summary of HMA rutting model using calibration set

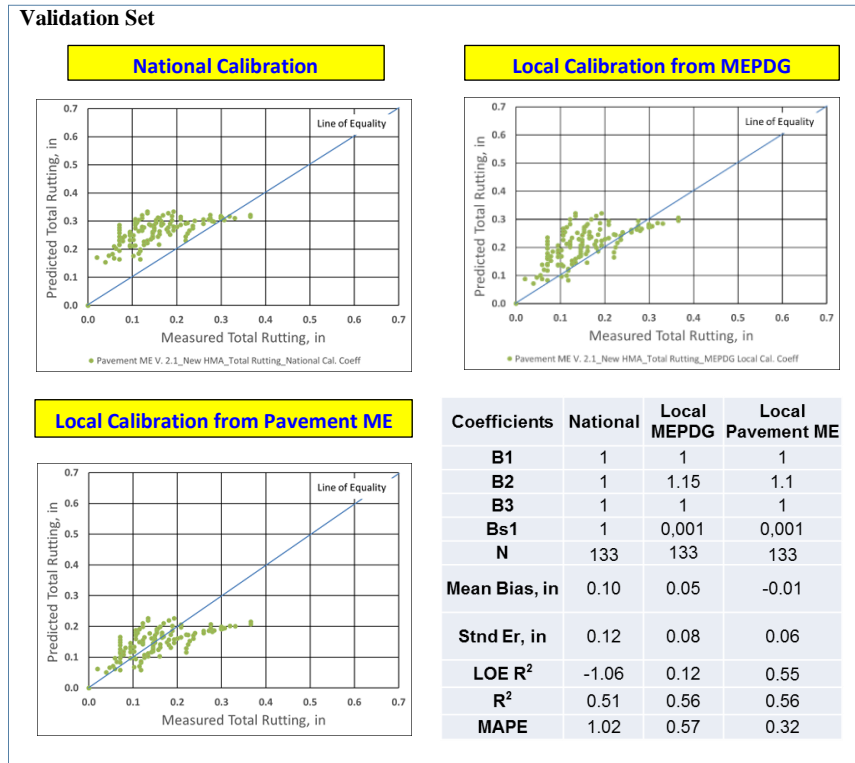


Figure 25. Overall accuracy summary of HMA rutting model using validation set

Load-Related Cracking

Pavement ME Design predicts two types of load-related cracking for flexible pavement systems: alligator cracking (bottom-up) and longitudinal cracking (top-down). The allowable number of axle-load applications required for evaluation of fatigue failure of the HMA layer can be calculated as follows (AASHTO 2008):

$$N_{f-HMA} = k_{f1} \times C \times C_H \times \beta_{f1} \times \varepsilon_t^{k_{f2}\beta_{f2}} \times E_{HMA}^{k_{f3}\beta_{f3}} \quad (34)$$

Where:

- N_{f-HMA} = Allowable number of axle-load applications for a flexible pavement and HMA overlays
- ε_t = Tensile strain at critical locations calculated by the structural response model, in/in
- E_{HMA} = Dynamic modulus of the HMA measured in compression, psi
- $k_{f1, f2, f3}$ = Global field calibration parameters (from the NCHRP 1-40D recalibration;
- $k_{f1} = 0.007566$, $k_{f2} = -3.9492$, and $k_{f3} = -1.281$)
- $\beta_{f1, f2, f3}$ = Local or mixture specific field calibration constants; for the global calibration effort, these constants were set to 1.0

$$C = 10^M \quad (35)$$

$$M = 4.84 \times \left(\frac{V_{be}}{V_a + V_b} - 0.69 \right) \quad (36)$$

Where:

- V_{be} = Effective asphalt content by volume, %
- V_a = Percent air voids in the HMA mixture, and
- C_H = Thickness correction term, dependent on type of cracking

For bottom-up or alligator cracking:

$$C_H = \frac{1}{0.000398 + \frac{0.003602}{1 + e^{(11.02 - 3.49 \times H_{HMA})}}} \quad (37)$$

For top-down or longitudinal cracking:

$$C_H = \frac{1}{0.01 + \frac{12.00}{1 + e^{(15.676 - 2.8186 \times H_{HMA})}}} \quad (38)$$

Where:

- H_{HMA} = Total HMA thickness, in

The cumulative damage index (DI) at critical locations is required for load-related cracking predictions and can be calculated by summing the incremental damages over time (Miner's hypothesis) as shown in the following equation.

$$DI = \sum(\Delta DI)_{j,m,l,p,T} = \sum\left(\frac{n}{N_{f-HMA}}\right)_{j,m,l,p,T} \quad (39)$$

Where:

- n = Actual number of axle-load applications within a specific time period
- j = Axle-load interval
- m = Axle-load type (single, tandem, tridem, quad, or special axle configuration)
- l = Truck type using the truck classification groups included in the MEPDG
- p = Month
- T = Median temperature for the five temperature intervals or quintiles used to subdivide each month, °F

Alligator-cracking and longitudinal-cracking predictions, in term of area and length, respectively, can be calculated using the cumulative damage index along with calibration coefficients of transfer function equations, as shown in the following equations (AASHTO 2008):

$$FC_{Bottom} = \frac{1}{60} \times \frac{C_4}{1 + e^{(C_1 \times C_1^* + C_2 \times C_2^* \times \text{Log}(DI_{Bottom} \times 100))}} \quad (40)$$

Where:

- FC_{Bottom} = Area of alligator cracking that initiates at the bottom of the HMA layers, % of total lane area
- DI_{Bottom} = Cumulative damage index at the bottom of the HMA layers
- $C_{1,2,4}$ = Transfer function regression constants

$$C_1^* = -2 \times C_2^* \quad (41)$$

$$C_2^* = -2.40874 - 39.748(1 + H_{HMA})^{-2.856} \quad (42)$$

Where:

- H_{HMA} = Total HMA thickness, in

$$FC_{Top} = 10.56 \times \frac{C_4}{1 + e^{(C_1 - C_2 \text{Log}(DI_{Top}))}} \quad (43)$$

Where:

- FC_{Top} = Length of longitudinal cracks that initiate at the top of the HMA layer, ft/mi
- DI_{Top} = Cumulative damage index near the top of the HMA surface
- $C_{1,2,4}$ = Transfer function regression constants

The availability of each variable of the equations above was carefully inspected. For this distress type, not all of the variables required could have been determined from software output or intermediate output files to conduct local calibration outside the software.

For fatigue model:

- ε_t = Not provided by the software
- E_{HMA} = Not provided by the software
- V_{be} = Input value, known or can be obtained from the “Layer #” tab in the final result summary output file
- V_a = Input value, known can be obtained from the “Layer #” tab in the final result summary output file
- H_{HMA} = Input value, known can be obtained from the “Layer #” tab in the final result summary output file
- n = Not provided by the software

For alligator and longitudinal-cracking transfer functions:

- DI_{Bottom} = Provided in the “Fatigue Data” tab of the final result summary output file

- DI_{Top} = Provided in the “Fatigue Data” tab of the final result summary output file

In both alligator and longitudinal-cracking prediction models, there are two sets of coefficients: one set comes from the fatigue model, the other comes from the top-down or bottom-up cracking transfer functions. Sensitivity analysis of HMA fatigue and determination of alligator and longitudinal-cracking model calibration coefficients were conducted to obtain an idea regarding the sensitivity of related calibration coefficients with results given in Appendix C. Table 19, Table 20, and Table 21 summarize the sensitivity analysis results of HMA fatigue, alligator (bottom-up), and longitudinal (top-down) cracking models, respectively.

Table 19. Sensitivity analysis results of HMA fatigue model calibration coefficients

Calibration factors	Coefficient Sensitivity Index	Rank
BF2	-5153.72	1
BF3	77.67	2
BF1	-1.04	3

Table 20. Sensitivity analysis results of HMA alligator (bottom-up) cracking model calibration coefficients

Calibration factors	Coefficient Sensitivity Index	Rank
C1_bottom	-5.65	1
C2_bottom	-1.24	2
C4_bottom	1.00	3

Table 21. Sensitivity analysis results of HMA longitudinal (top-down) cracking model calibration coefficients

Calibration factors	Coefficient Sensitivity Index	Rank
C1_Top	-9.54	1
C2_Top	-5.64	2
C4_Top	1.00	3

By considering the availability of each equation variable and using results of sensitivity analysis, this study has focused on recalibration of top-down and bottom-up transfer function coefficients rather than fatigue model coefficients. Note that fatigue-model calibration would require lab testing to yield accurate results. Nonlinear optimization techniques were used to calibrate both top-down and bottom-up transfer function coefficients. .

Figure 26 and Figure 27 compare HMA alligator (bottom-up) cracking predictions using national, MEPDG local, and Pavement ME Design local calibration coefficients for both calibration and validation sets. As can be seen in the figures, although the Pavement ME Design locally-calibrated model improves the alligator (bottom-up) cracking predictions compared to nationally and MEPDG locally-calibrated models, the improvement is insignificant. Neither national nor Pavement ME Design local alligator (bottom up) cracking models could provide high accuracy for this model. It can be concluded that the alligator (bottom-up) cracking model by itself is not able to simulate the field behavior of Iowa HMA pavements very well. Additionally, it should be realized that most of the tested pavement sections have 0 % alligator cracking measurements, while very few sections have as much as 1.1 % alligator cracking. These 0 % cracking data points lower the accuracy of the model. Also it should be noted that the measured alligator (bottom up) cracking values for Iowa HMA pavements are not high; therefore, it can be stated that Iowa HMA pavements do not generally have severe alligator (bottom-up) cracking problems (See Figure 26 and Figure 27).

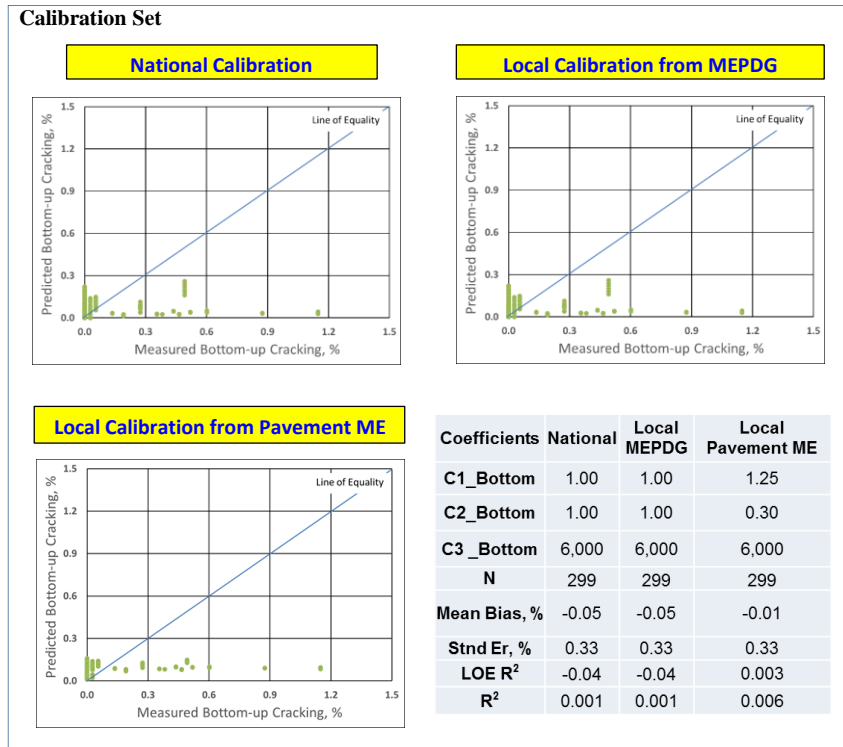


Figure 26. Overall accuracy summary of HMA alligator (bottom-up) cracking model using calibration set

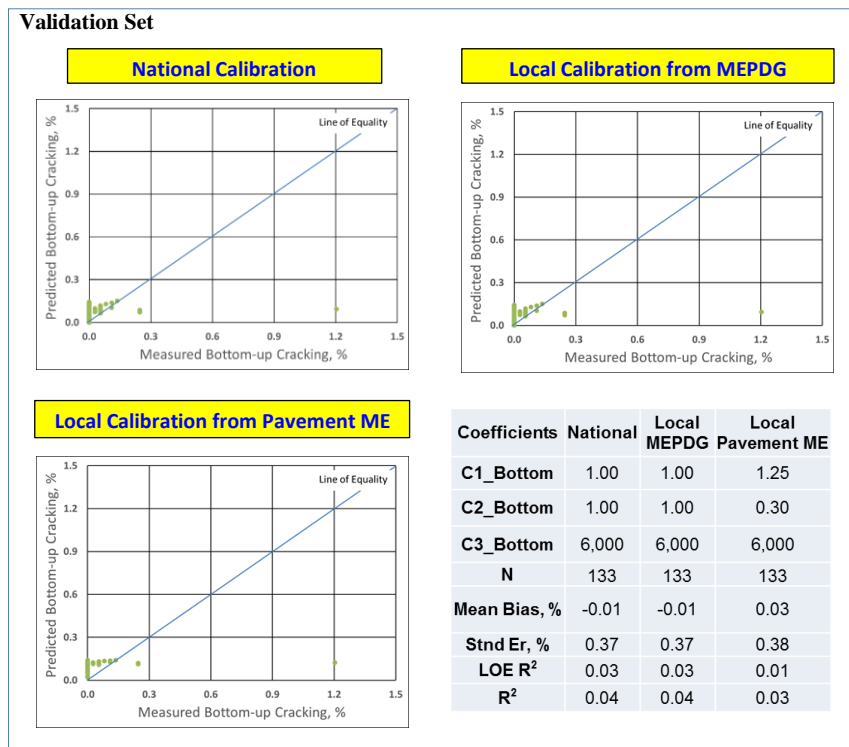


Figure 27. Overall accuracy summary of HMA alligator (bottom-up) cracking model using validation set

Figure 28 and Figure 29 compare HMA longitudinal (top-down) cracking predictions using national, MEPDG local, and Pavement ME Design local calibration coefficients for both calibration and validation sets. As can be seen in the figures, compared to the nationally calibrated model the MEPDG locally-calibrated model reduces the bias although even the MEPDG locally-calibrated model has a significant amount of standard error. The model was further improved with Pavement ME Design local calibration (See Figure 28 and Figure 29).

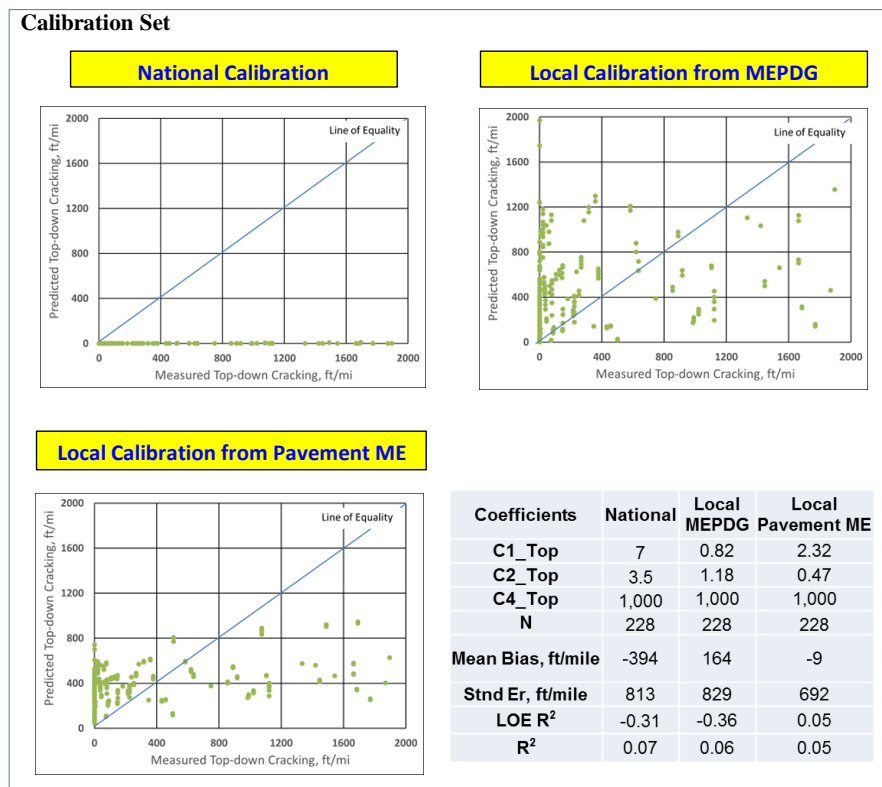


Figure 28. Overall accuracy summary of HMA longitudinal (top-down) cracking model using calibration set

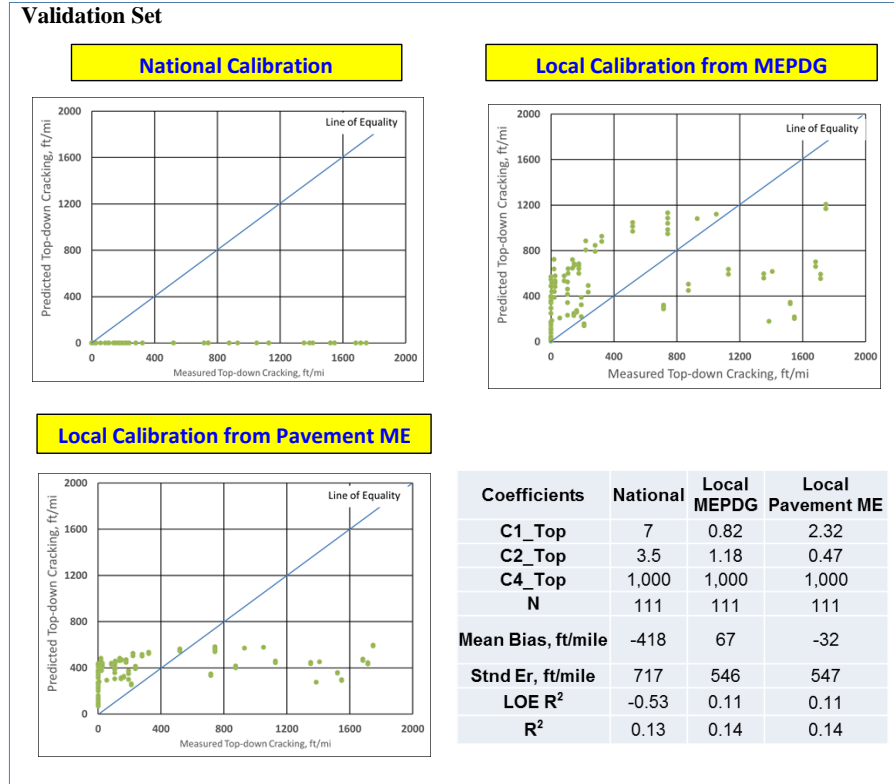


Figure 29. Overall accuracy summary of HMA longitudinal (top-down) cracking model using validation set

Transverse (Thermal) Cracking

According to (AASHTO 2008), the logarithmic ratio between the crack depth and HMA layer thickness plays the most important role in predicting the degree of transverse (thermal) cracking:

$$TC = \beta_{t1} \times N \times \left[\frac{1}{\sigma_d} \times \text{Log} \left(\frac{C_d}{H_{HMA}} \right) \right] \quad (44)$$

Where:

- TC = Observed amount of thermal cracking, ft/mi
- β_{t1} = Regression coefficient determined through global calibration (400)
- $N[z]$ = Standard normal distribution evaluated at $[z]$
- σ_d = Standard deviation of the log of the depth of cracks in the pavement
- C_d = Crack depth, in
- H_{HMA} = Thickness of HMA layers, in

$$\Delta C = (k \times \beta_t)^{n+1} \times A \times \Delta K^n \quad (45)$$

$$A = 10^{(4.389 - 2.52 \times \log(E \times \sigma_m \times n))} \quad (46)$$

Where:

- k = Regression coefficient determined through field calibration
- β_t = Calibration parameter
- A, n = Fracture parameters for the asphalt mixture
- ΔK = Change in the stress intensity factor due to a cooling cycle
- E = Mixture stiffness
- σ_m = Undamaged mixture tensile strength

The availability of each variable of the above equations was carefully inspected. For this distress type, not all the required variables could have been obtained from either software output or intermediate output files to conduct local calibration outside the software.

- $N[z]$ = Not provided by the software
- σ_d = It is a fixed number, 0.769 in.
- C_d = Available in the “Distress data” tab of the final result summary output file
- H_{HMA} = Input value, known or can be checked from “Grand Summary” tab in the final result summary output file
- A, n = Not provided by the software
- ΔK = Not provided by the software
- σ_m = Not provided by the software
- E = Input value, known or can be checked from “HMAInput.xlsx” intermediate output file for different temperature conditions

Local calibration of the transverse (thermal) cracking model within the software was followed using different calibration coefficients and choosing the best method (trial-and-error).

To do this, sensitivity analysis of the thermal cracking Level 3 coefficient was initially

performed. Table 22 shows this coefficient's sensitivity analysis result for this model. It could also be seen that the model with national calibration coefficients underpredicts thermal cracking for Iowa HMA pavements. Therefore, based on these sensitivity analysis results, a set of trial calibration coefficients was determined for use in local calibration; Table 23 shows these trial calibration coefficients. Running the software using these coefficients for 35 HMA sections, the calibration coefficient providing minimum mean-square error (MSE) between field-measured thermal cracking values and the software predictions in selected Iowa HMA pavements was determined. Also, using the validation set, accuracy verification of the transverse cracking model using this coefficient was performed. As a result of these analyses, the final local coefficient was determined to be 2 (Table 23).

Table 22. Sensitivity analysis results of HMA and thermal cracking calibration coefficients

Calibration factors	Coefficient Sensitivity Index	Rank
K_Level 3	3.17	1

Table 23. Trial calibration coefficients for HMA thermal cracking model

Coefficient	Trial value	R ²
K_Level 3	2	0.16
K_Level 3	2.5	0.07
K_Level 3	3	0.03

Figure 30 and Figure 31 compare HMA transverse (thermal) cracking predictions using national, MEPDG local, and Pavement ME Design local calibration coefficients for both calibration and validation sets. As can be seen from the figures, the national and MEPDG local model predictions are the same since they both have the same calibration coefficient. Both national and Pavement ME Design local HMA transverse (thermal) cracking models could not provide high accuracy for this model. It can be concluded that the HMA transverse (thermal)

cracking model itself is not very capable of simulating field behavior of Iowa HMA pavements. Additionally, we should realize that most of the pavement sections have less than 300 ft/mi thermal cracking measurements, and very few sections in a range as high as 600-900 ft/mi thermal for thermal cracking measurements. Data points in the range of 600-900 ft/mi thermal cracking data points would lower the accuracy of the model (See Figure 30 and Figure 31).

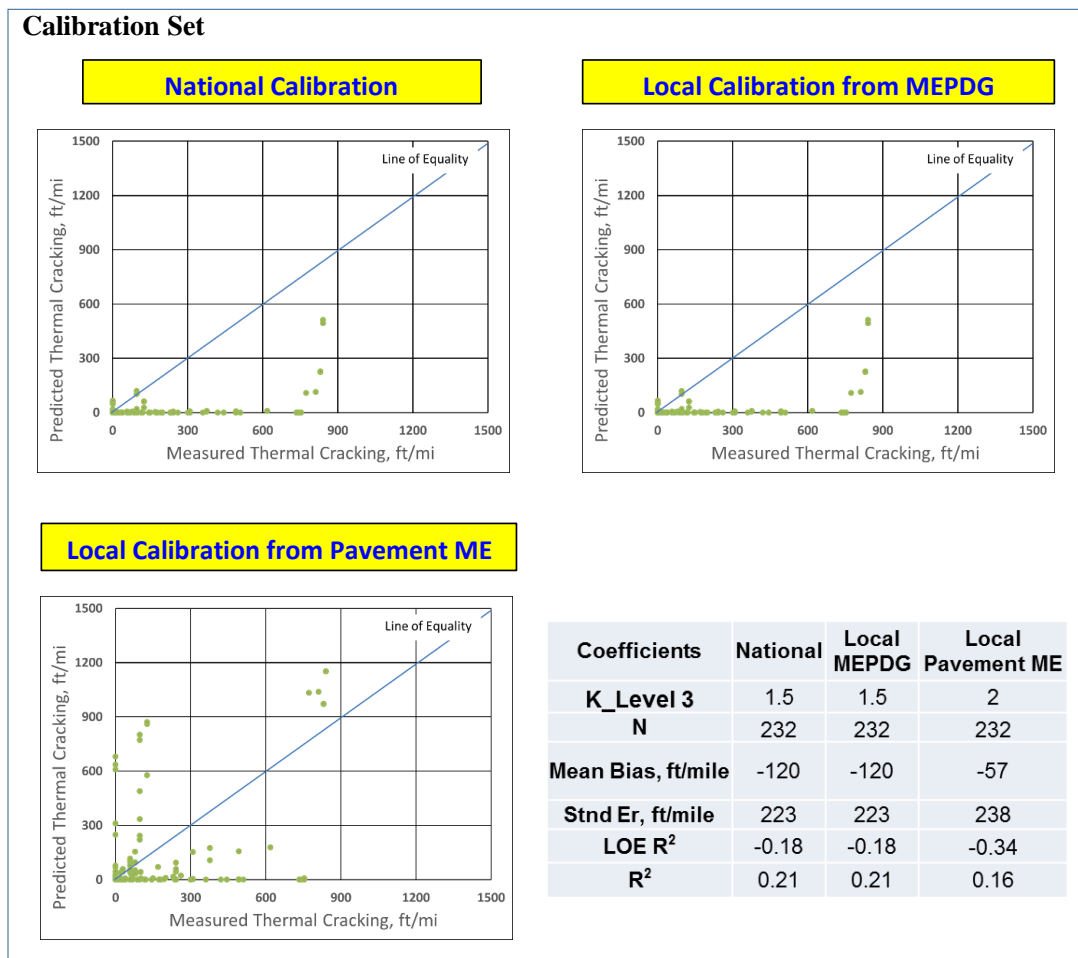


Figure 30. Overall accuracy summary of HMA transverse cracking model using calibration set

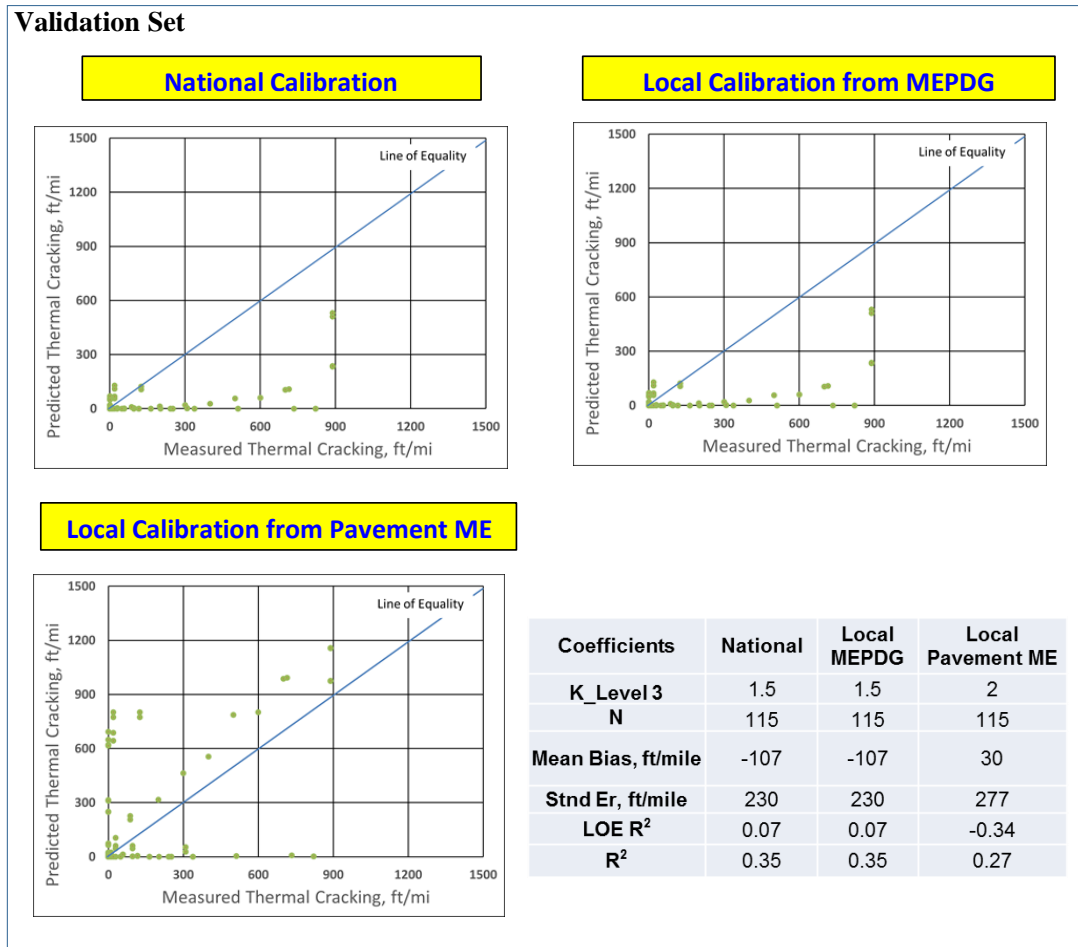


Figure 31. Overall accuracy summary of HMA transverse cracking model using validation set

Smoothness (IRI)

All surface-related distresses are involved when dealing with prediction of smoothness in HMA pavements.

The equation for the IRI transfer function for new HMA pavements is as follows:

$$IRI = IRI_0 + C_4 \times (SF) + C_2 \times (FC_{Total}) + C_3 \times (TC) + C_1 \times (RD) \quad (47)$$

Where:

- IRI_0 = Initial IRI after construction, in/mi
- SF = Site factor, refer to Equation 35
- FC_{Total} = Area of fatigue cracking (combined alligator, longitudinal, and reflection cracking in the wheel path), percent of total lane area. All load related cracks are

combined on an area. Basis-length of cracks is multiplied by 1 ft. to convert length into an area basis

- TC = Length of transverse cracking (including the reflection of transverse cracks in existing HMA pavements), ft./mi
- RD = Average rut depth, in.
- $C_{1,2,3,4}$ =Calibration coefficients; 40, 0.4, 0.008, 0.015 are national calibration coefficients, respectively

The site factor is calculated by:

$$SF = Age[0.02003(PI + 1) + 0.007947(Precip + 1) + 0.000636(FI + 1)] \quad (48)$$

Where:

- Age = Pavement age, year
- PI = Percent plasticity index of the soil
- FI = Average annual freezing index, °F days
- $Precip$ = Average annual precipitation or rainfall, in.

The availability of each variable of the IRI transfer function was carefully inspected. All variables were either extracted from general or intermediate output files, or calculated using the data provided by the output files. The location or calculation method used for each variable can be seen as follows:

- IRI_0 : : Input to the software as an initial IRI value, either known or capable of being found at the “Grand Summary” tab in the final result summary output file
- SF = Can be calculated using Equation 48
- FC_{Total} = Top-down and bottom-up cracking can be obtained from the “Distress” tab in the final result summary output file
- TC = Transverse cracking can be obtained from the “Distress” tab in the final result summary output file
- FI for SF calculation: Can be obtained from the climate output file titled “Climate Inputs”
- P_{200} : Can be obtained from the “Layer #” tab in the final result summary output file

The predicted IRI values were compared with the actual Iowa DOT PMIS IRI data for each section in each year. The local calibration procedure was performed until a combination of calibration coefficients producing the minimum mean square error (MSE) between the predicted and actual IRI values was found. This combination of calibration coefficients was announced as a set of local calibration coefficients. These announced local calibration coefficients were validated using validation pavement sections. Similar, to new JPCP IRI calibrations, two approaches were used for new HMA IRI calibrations:

- **Approach 1:** Calibrate using either locally-calibrated or nationally-calibrated distress prediction models. Note that nationally-calibrated distress prediction models can be used when they provide good accuracy in distress measurements
- **Approach 2:** Calibrate using only nationally-calibrated distress prediction models without considering accuracy of distress-model predictions

Approach 1

If the Pavement ME Design locally-calibrated distress prediction models could not produce accurate predictions in the calculation of IRI, nationally-calibrated models should be used. Note that, in the calculation of JPCP IRI model using Approach 1, all Pavement ME Design locally-calibrated faulting and cracking predictions were used because of their high accuracy. However, because HMA transverse (thermal) and bottom-up cracking predictions could not have provided accurate predictions, national models for these types of distress were utilized in the calculation of the HMA IRI model using Approach 1.

Figure 32 and Figure 33 compare the IRI predictions using national, MEPDG local, and Pavement ME Design local models for calibration and validation sets, respectively. The Pavement ME Design locally-calibrated IRI model shown in these figures was calibrated using

Approach 1; in the calculation of IRI predictions, Pavement ME Design used locally-calibrated rutting and top-down (longitudinal) cracking predictions. As can be seen from the figures, the MEPDG locally-calibrated IRI model improved accuracy compared to the national model. The model accuracy was further improved using the Pavement ME Design locally-calibrated IRI model, as can be seen from the figures.

Implementing a paired t-test using measured IRI values and Pavement ME Design locally-calibrated predictions for selected pavement sections, a p value was calculated as $P(T \leq t)$ two-tail = 0.88 > 0.05. This result implies that, with 95 % certainty, there is no significant difference between actual and Pavement ME Design predicted IRI values (Table 24).

Table 24. Pair t test results for HMA IRI model (Approach 1)

	<i>Actual IRI</i>	<i>Predicted IRI</i>
Mean	77.21715	77.08087
Variance	646.307	602.1901
Observations	432	432
Pearson Correlation	0.71164	
Hypothesized Mean Difference	0	
df	431	
t Stat	0.149166	
P(T<=t) one-tail	0.440746	
t Critical one-tail	1.648397	
P(T<=t) two-tail	0.881493	
t Critical two-tail	1.965483	

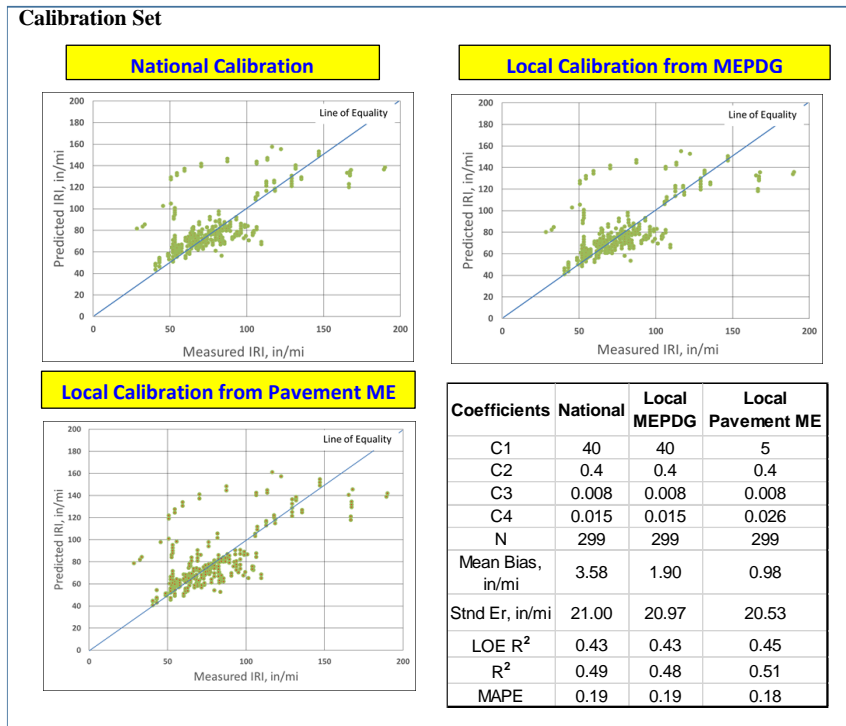


Figure 32. Overall accuracy summary of HMA IRI model using calibration set (Approach 1)

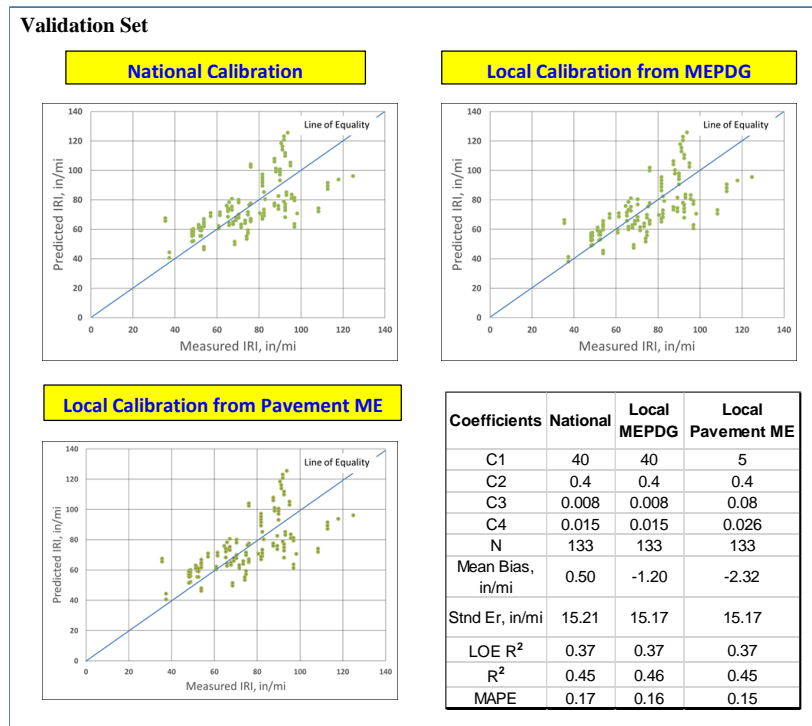


Figure 33. Overall accuracy summary of HMA IRI model using validation set (Approach 1)

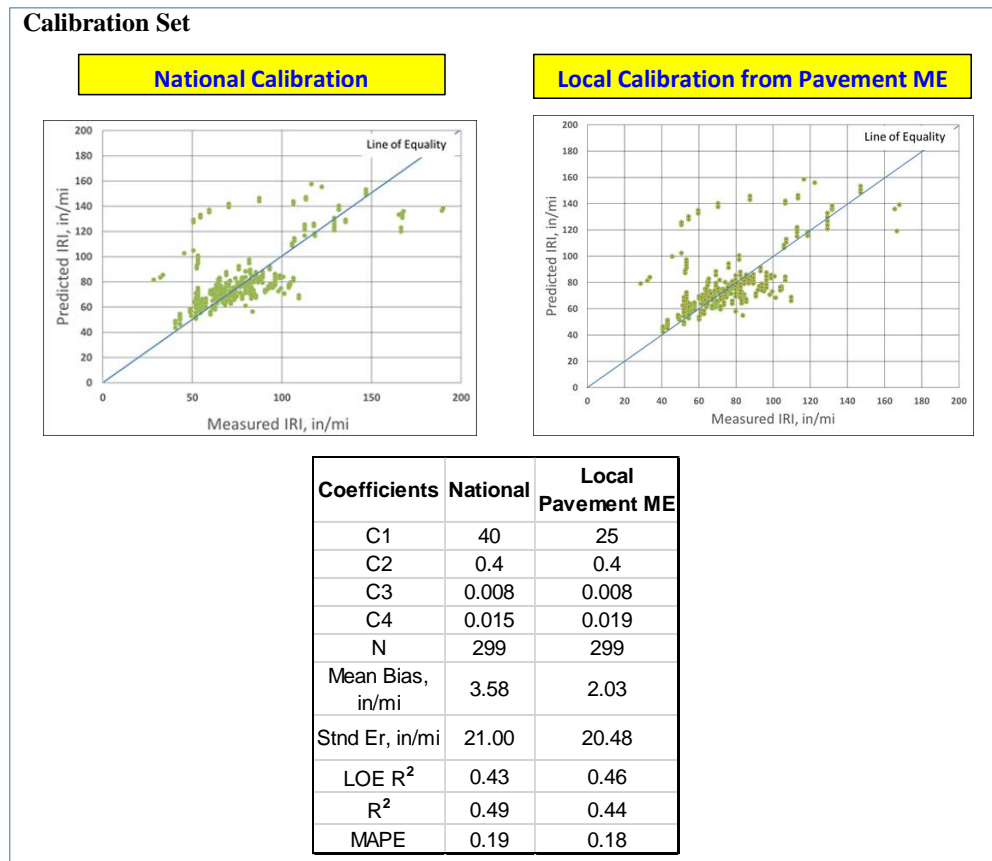
Approach 2

An alternative approach (Approach 2) was used to locally calibrate the IRI model using Pavement ME Design software. In this approach, with respect to the local calibration of the IRI model, nationally-calibrated rutting, transverse (thermal) and fatigue-cracking model predictions were used. Figure 34 and Figure 35 compares the local calibration results using national and Pavement ME local models in Approach 2. It is important to highlight that, although the rutting model was further improved using Pavement ME Design local-calibration coefficients, this improvement was not significant (Figure 34 and Figure 35). The purpose for using two approaches in the local calibration of IRI model was to figure out whether the IRI model could be locally calibrated with sufficient accuracy without need for the local calibration procedure of each of the distress models that would require significant additional cost and data resources. A local calibration IRI model using Approach 2 would save significant sources in terms of both time and funds. Use of Approach 2 in the local calibration of the IRI model would be especially useful for those SHAs, if they were only interested in attaining locally-calibrated IRI predictions rather than locally-calibrated rutting, fatigue and thermal-cracking predictions. In this study, it was determined that using Approach 2, a locally-calibrated IRI model can predict this distress with accuracy sufficient for Iowa HMA pavement systems.

Also, a paired t test was performed for this approach, and the p value was found to be $P(T \leq t) \text{ two-tail} = 0.25 > 0.05$. This result implies that, with 95 % certainty, there is no significant difference between national field-measured and Pavement ME Design predicted IRI values using Approach 2 (Table 25).

Table 25. Pair t test results for HMA IRI model (Approach 2)

	<i>Actual</i>	
	<i>IRI</i>	<i>IRI Av</i>
Mean	77.21715	78.27098
Variance	646.307	567.1067
Observations	432	432
Pearson Correlation	0.70723	
Hypothesized Mean Difference	0	
df	431	
t Stat	-1.15913	
P(T<=t) one-tail	0.123523	
t Critical one-tail	1.648397	
P(T<=t) two-tail	0.247047	
t Critical two-tail	1.965483	

**Figure 34. Overall accuracy summary of HMA IRI model using calibration set (Approach 2)**

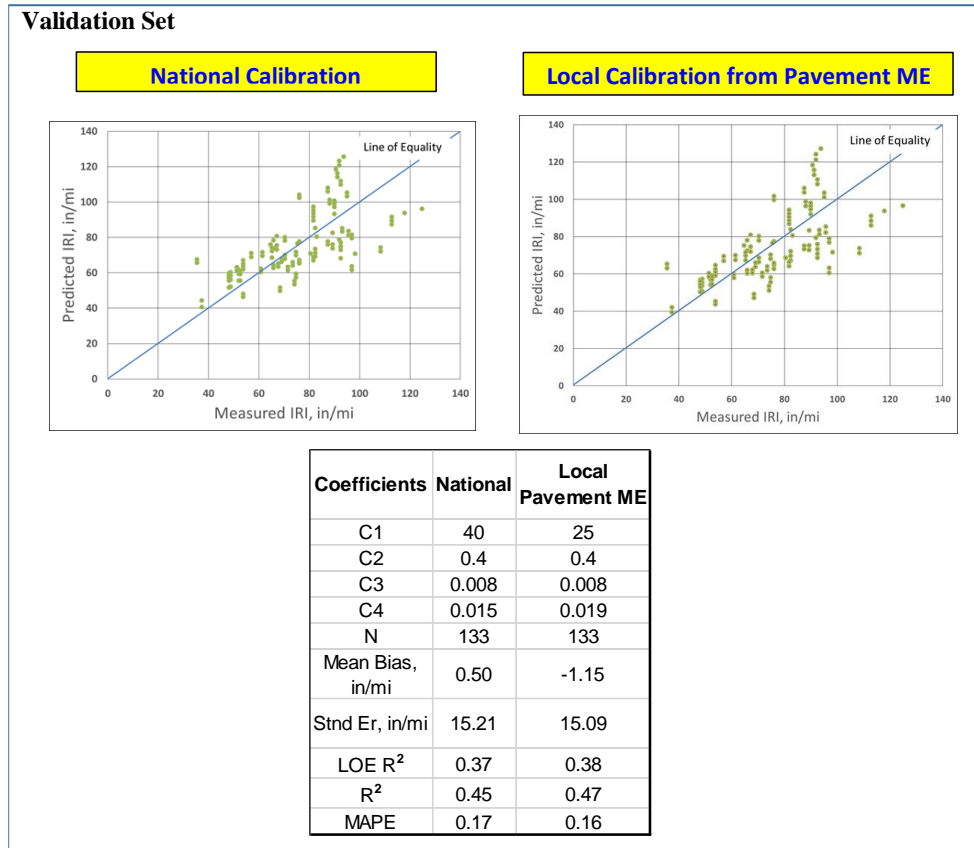


Figure 35. Overall accuracy summary of HMA IRI model using validation set (Approach 2)

HMA over JPCP

Pavement ME Design HMA over JPCP pavement performance predictions include rutting, longitudinal (top-down) cracking, alligator (bottom-up) cracking, thermal (transverse) cracking, reflective cracking, and IRI.

Rut Depth

The total rut depth in Pavement ME Design is calculated as the summation of vertical deformations in each sublayer. Rutting predictions are divided into HMA layer rutting, granular-base layer rutting, subgrade-layer rutting and total pavement rutting. However, most of the total rutting predictions come from the HMA layer because the existing JPCP can provide strong

foundation to HMA surface overlay to prevent granular-base and subgrade-layer rutting. The same HMA layer rutting equation (Equation 26) is used for HMA overlays as for HMA pavements. Also, the sensitivity of calibration coefficients used for HMA layer rutting in HMA pavements is the same as for HMA over JPCP pavements (Table 17).

Based on sensitivity analysis results, an experimental matrix including different sets of calibration coefficients was prepared and is shown in Table 26. Trying different sets of calibration coefficients, the set with values of 1.01 and 1 for BR2 and BR3, respectively, produced the most accurate predictions.

Table 26. Experimental matrix for local calibration of HMA layer rutting model of HMA over JPCP pavements

BR2	BR3	Mean Bias (in)
1.01	1	0.002
1.01	0.99	-0.004
0.99	1.01	-0.006

Figure 36 and Figure 37 compare the total rutting predictions using national, MEPDG local, and Pavement ME Design local calibration coefficients for both calibration and validation sets. As can be seen in the figures, while the MEPDG locally-calibrated rutting model gives more accurate predictions than the nationally calibrated model, the accuracy was further improved using the Pavement ME Design locally-calibrated rutting model (Figure 36 and Figure 37).

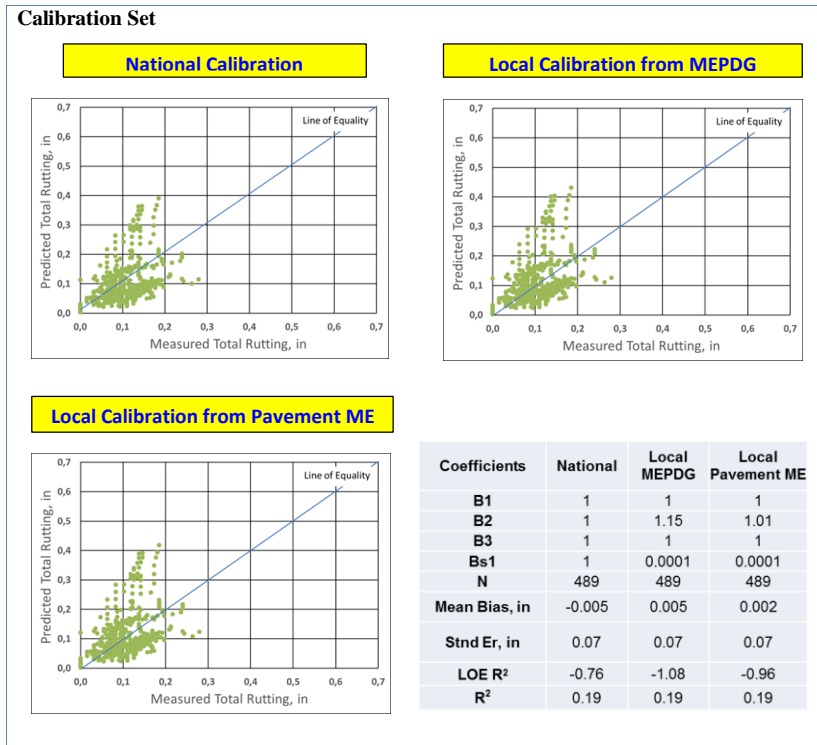


Figure 36. Overall accuracy summary of HMA layer rutting model of HMA over JPCP pavements using calibration set

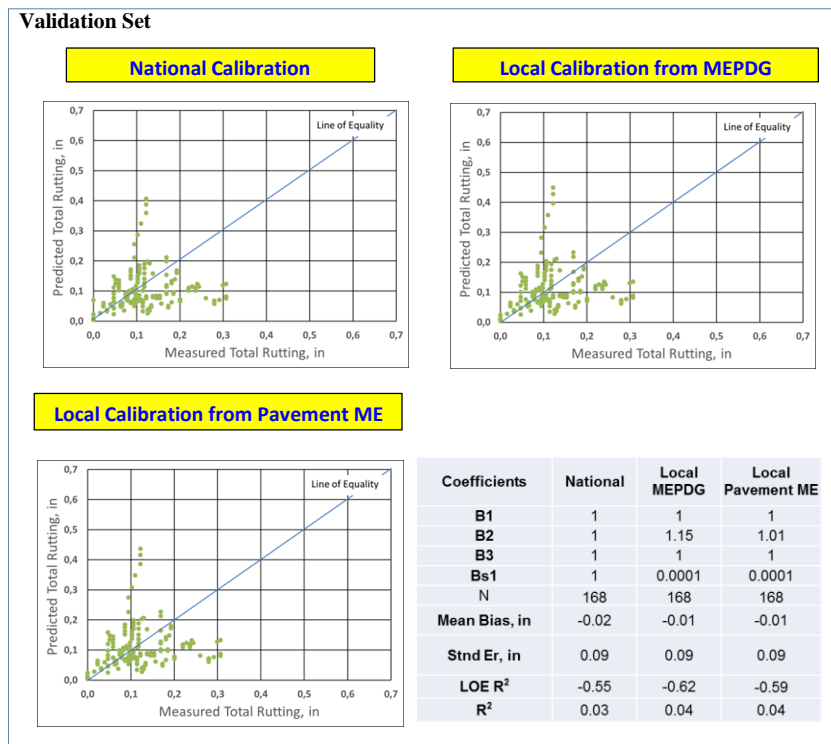


Figure 37. Overall accuracy summary of HMA layer rutting model of HMA over JPCP pavements using calibration set

Load-Related Cracking

Since load-related cracking is a distress type related to the HMA surface course, the same load-related cracking equations used for new HMA pavements are also used for HMA overlaid pavements. Fatigue models were used to estimate fatigue damage that were input into transfer functions of longitudinal-cracking and alligator-cracking predictions to obtain equivalent cracking measurements. Similarly, to HMA pavements, the fatigue model was not modified for HMA over JPCP pavement systems. Extracting fatigue damage predictions from the fatigue model, alligator (bottom-up) and longitudinal (top-down) cracking predictions were calculated using the related transfer functions (Equations 40 and 43). These transfer functions were locally calibrated using a non-linear optimization technique (MS Excel Solver).

Figure 38 and Figure 39 compare HMA alligator (bottom-up) cracking predictions for selected HMA over JPCP pavement sections using national, MEPDG local, and Pavement ME local calibration coefficients for both calibration and validation sets. As can be seen in the figures, although the Pavement ME Design locally-calibrated model improved the alligator (bottom-up) cracking predictions, the improvement was insignificant. Neither national and Pavement ME Design local alligator (bottom up) cracking models could provide high accuracy for this model. It can be concluded that the alligator (bottom-up) cracking model itself would not be able to simulate field behavior of Iowa HMA over JPCP pavements very well. Additionally, it should be noted that most pavement sections have fewer than 0.3 % measured alligator cracking measurements and very few sections exhibit a range of 0.6-1.4 % measured alligator cracking. Also note that the measured alligator (bottom-up) cracking values for Iowa HMA over JPCP pavements is not high; it can therefore be concluded that Iowa HMA over JPCP pavements do not have severe alligator (bottom-up) cracking problem.

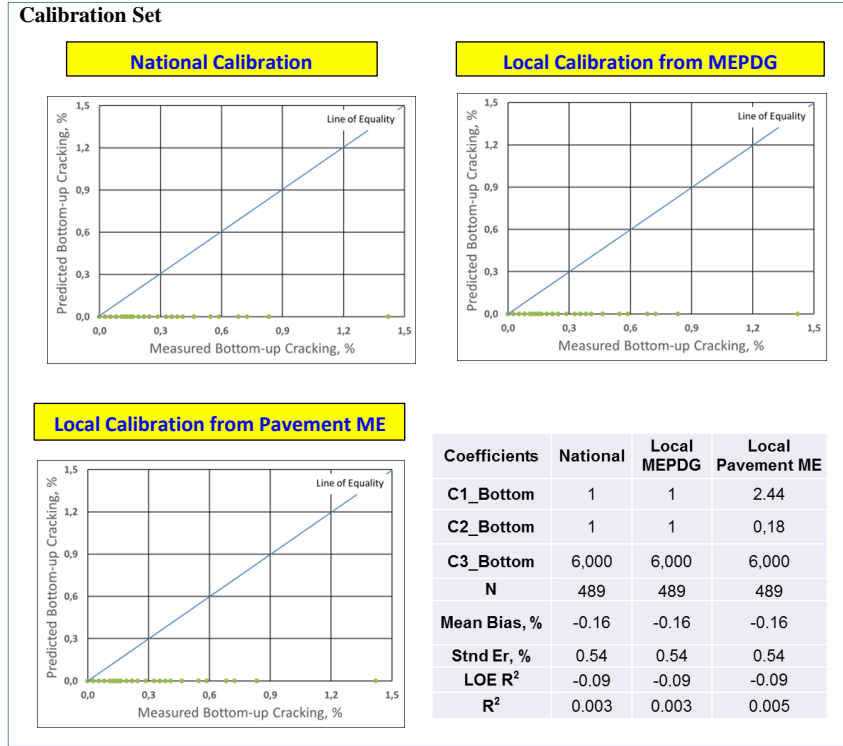


Figure 38. Overall accuracy summary of HMA alligator (bottom-up) cracking model of HMA over JPCP pavements using calibration set

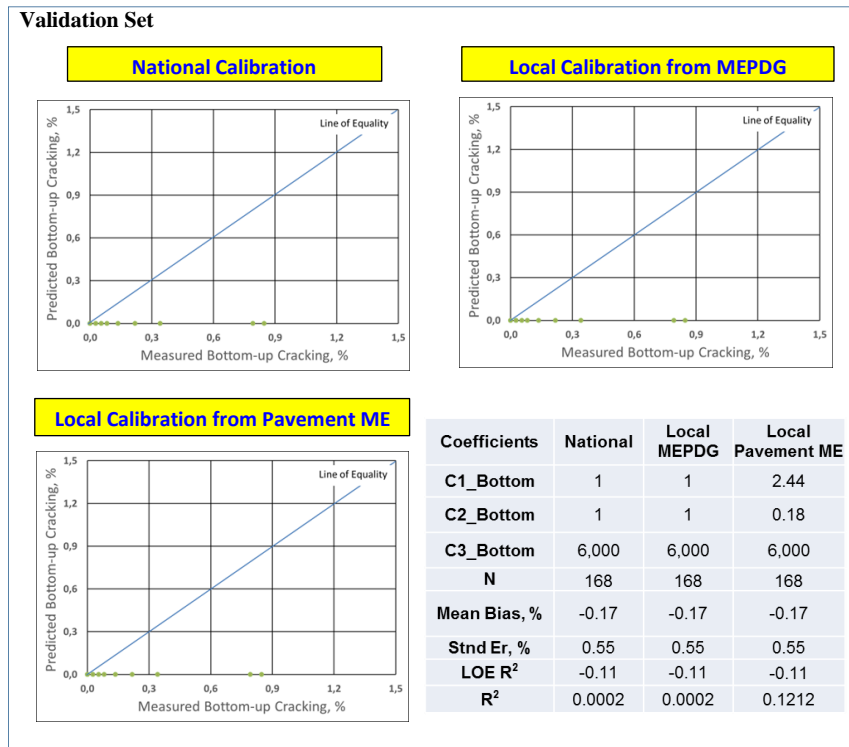


Figure 39. Overall accuracy summary of HMA alligator (bottom-up) cracking model of HMA over JPCP pavements using validation set

Figure 40 and Figure 41 compare HMA longitudinal (top-down) cracking predictions for selected HMA over JPCP pavement sections using national, MEPDG local, and Pavement ME Design local calibration coefficients for both calibration and validation sets. As can be seen from the figures, compared to the nationally-calibrated model, the MEPDG locally-calibrated model reduces the bias, although even the MEPDG locally-calibrated model exhibits a significant amount of standard error. The model was further improved with Pavement ME Design local calibration.

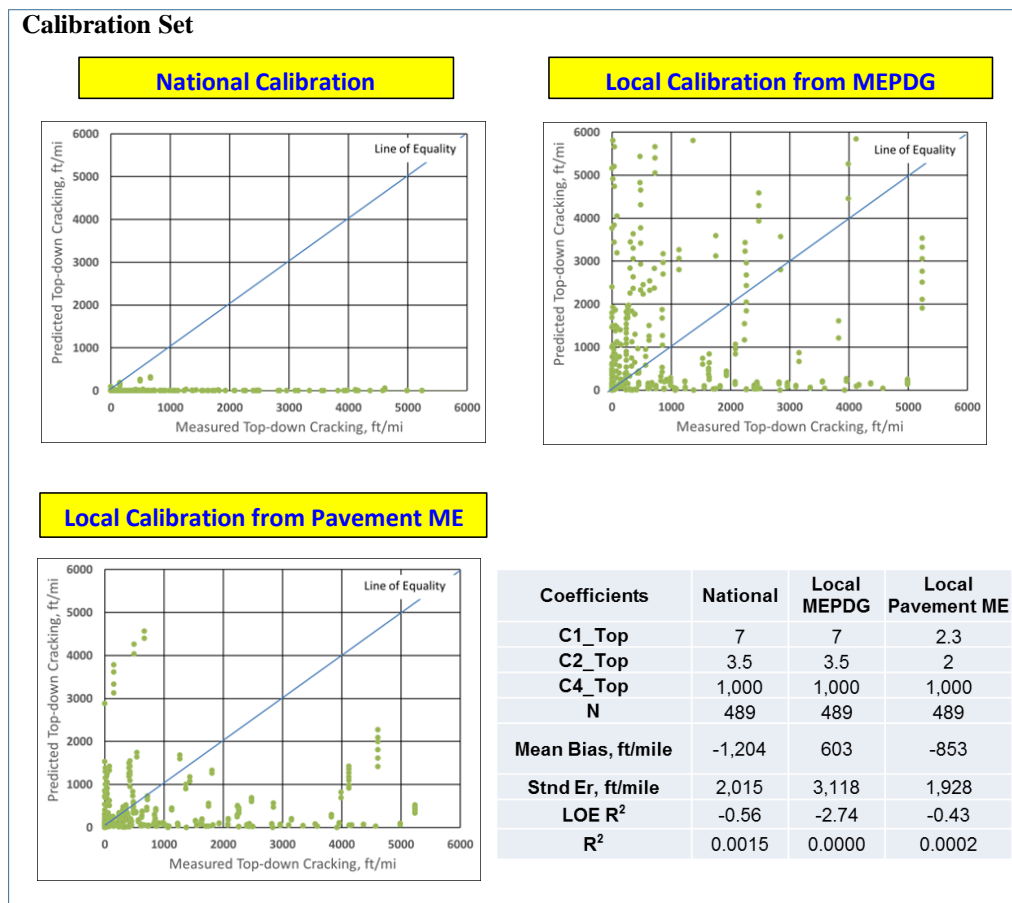


Figure 40. Overall accuracy summary of HMA longitudinal (top-down) cracking model of HMA over JPCP pavements using calibration set

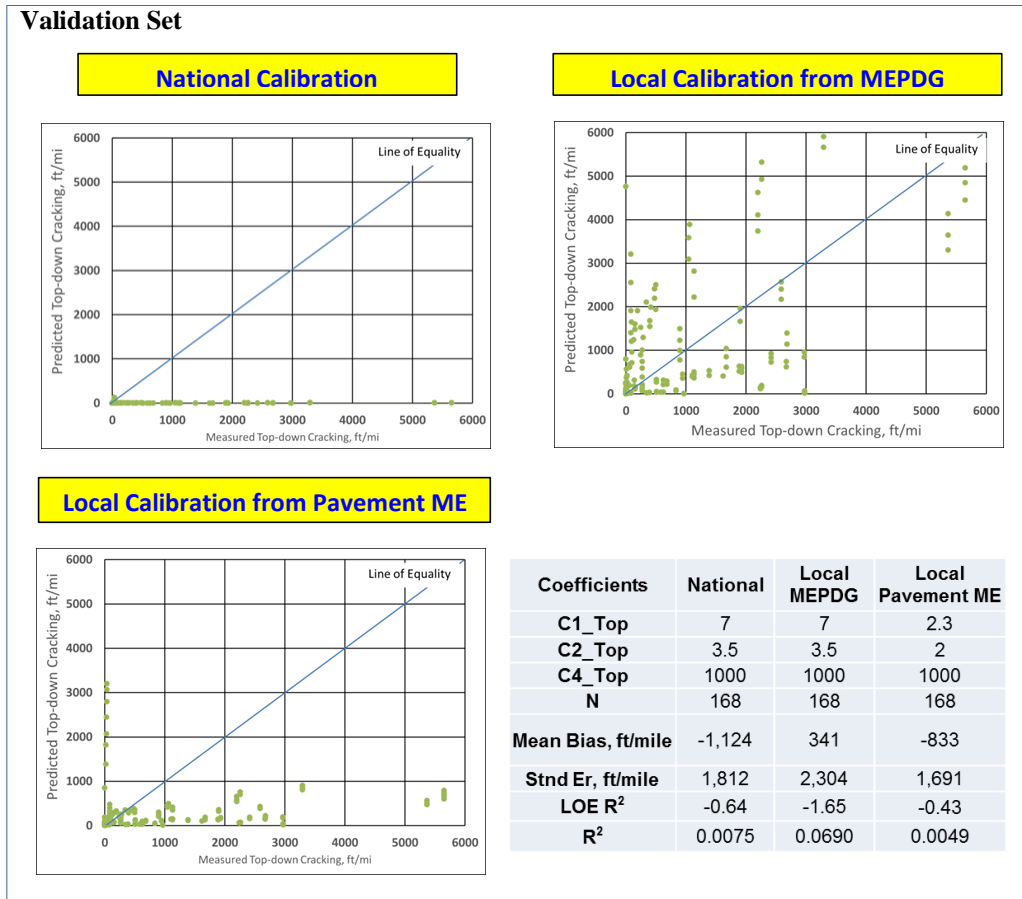


Figure 41. Overall accuracy summary of HMA longitudinal (top-down) cracking model of HMA over JPCP pavements using validation set

Transverse (Thermal) Cracking

Local calibration of transverse (thermal) cracking model was performed for selected HMA over JPCP pavements within the software by submitting various combinations of calibration coefficients to the software and choosing the combination providing the most accurate predictions (non-linear optimization). A set of calibration coefficients was used to determine the optimal set (Table 27). This analysis produced a final coefficient value of 2.7.

Table 27. Trial calibration coefficients for HMA over JPCP thermal cracking model

Coefficient	Trial value	R²	Mean bias, in
K_Level 3	1.8	0.018	-1,683
K_Level 3	2.1	0.025	-1,512
K_Level 3	2.4	0.027	-1,331
K_Level 3	2.7	0.027	-1,141

Figure 42 and Figure 43 compare HMA over JPCP transverse (thermal) cracking predictions for selected HMA over JPCP pavement sections using national, MEPDG local, and Pavement ME Design local-calibration coefficients for both calibration and validation sets. As can be seen from the figures, the national and MEPDG local model predictions are the same since they both use the same calibration coefficient. Both national and Pavement ME Design local HMA over JPCP transverse (thermal) cracking models could not provide high accuracy for this model. It can be concluded that the HMA over JPCP transverse (thermal) cracking model itself is unable to simulate the field behavior of Iowa HMA over JPCP pavements very well. It can also be concluded that the HMA over JPCP transverse (thermal) cracking model itself would be unable to simulate the field behavior of Iowa HMA over JPCP pavements very well. Additionally, most of the pavement sections have fewer than 4,000 ft/mi thermal cracking measurements, while very few sections have thermal cracking measurements in the range of 6,000-8,000 ft/mi. The data points in the range of 6,000-8,000 ft/mi thermal cracking data points would therefore lower the accuracy of the model. (See Figure 42 and Figure 43).

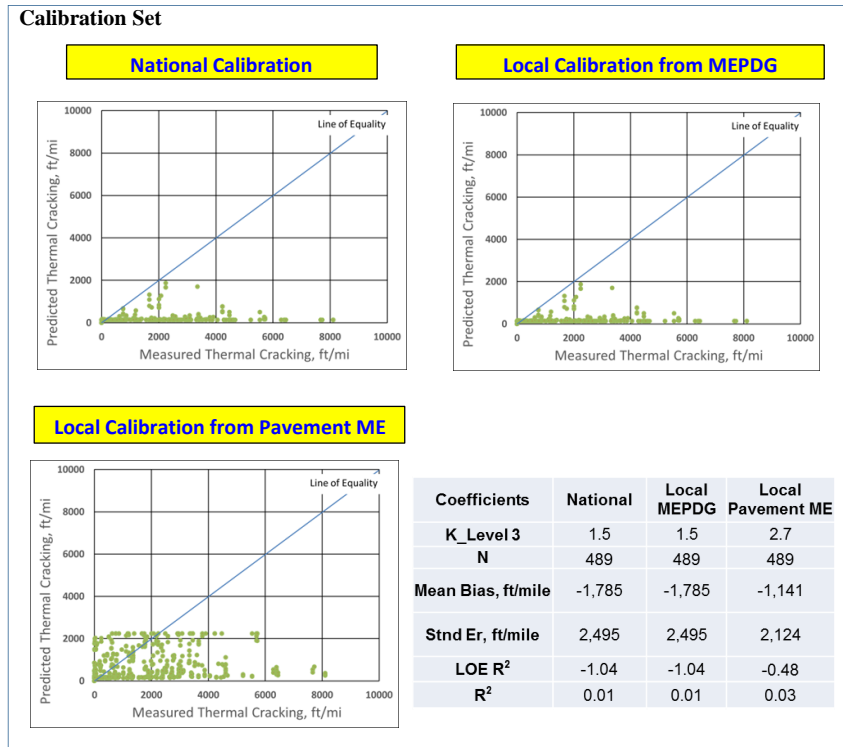


Figure 42. Overall accuracy summary of HMA transverse cracking model of HMA over JPCP pavements using validation set

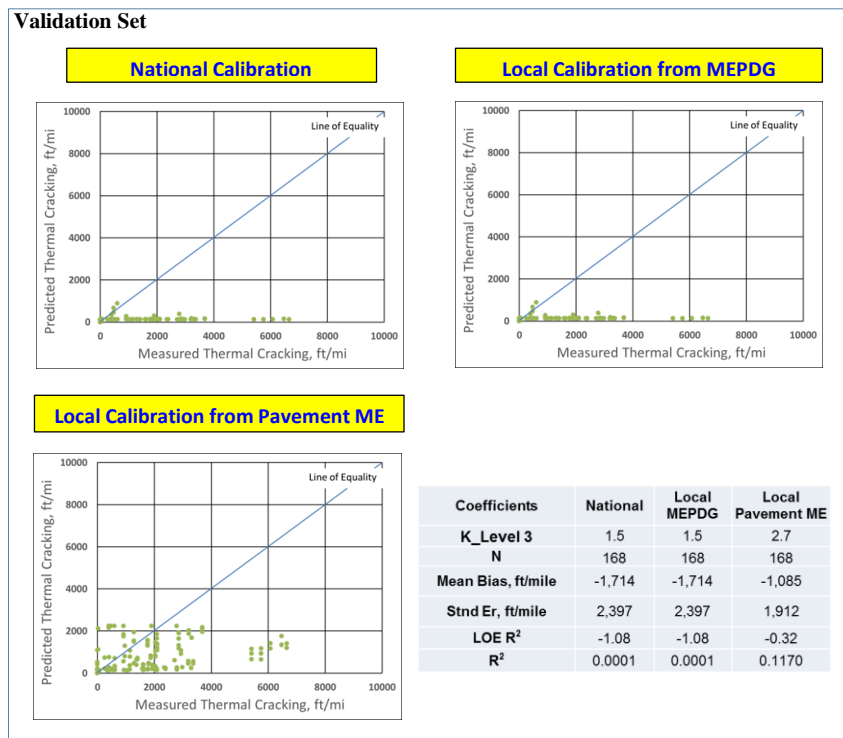


Figure 43. Overall accuracy summary of HMA transverse cracking model of HMA over JPCP pavements using validation set

Smoothness (IRI)

In IRI calculation, the equation used for HMA pavements is also used for HMA over JPCP pavements since the surface course in both pavement types is HMA. Only differences in the HMA over JPCP IRI model, reflective cracking predictions from empirical model, are included in the IRI equations as a part of total transverse-cracking predictions. Similarly to new HMA IRI calibrations, two approaches were used for HMA over JPCP IRI calibrations:

- **Approach 1:** In the calculation of IRI predictions, Pavement ME Design locally-calibrated rutting and longitudinal (top-down) cracking predictions and nationally-calibrated transverse (thermal), alligator (bottom-up) and reflective cracking predictions were used. Note that, in contrast to the HMA IRI model, reflective-cracking predictions were added to the model as a part of the area of total fatigue cracking (See Equation 47).
- **Approach 2:** In the calculation of IRI predictions, all nationally-calibrated rutting, longitudinal (top-down), alligator (bottom-up), transverse (thermal), and reflective cracking predictions were utilized. Note that, unlike the HMA IRI model, reflective cracking predictions were added to the model as a part of the area of total fatigue cracking (See Equation 47).

Approach 1

The IRI model was locally-calibrated using the MS Excel Solver optimization tool. Figure 44 and Figure 45 compare the IRI predictions using national, MEPDG local, and Pavement ME local models for calibration and validation sets, respectively. The Pavement ME Design locally-calibrated IRI model shown in these figures was calibrated using Approach 1: in the calculation of IRI predictions, Pavement ME Design locally-calibrated rutting and top-down (longitudinal) cracking predictions were used. As can be seen in the figures, the MEPDG locally-

calibrated IRI model improved the accuracy compared to the national model. The model accuracy was further improved using the Pavement ME Design locally-calibrated IRI model as can be seen from the figures.

Implementing a paired t-test using measured IRI values and Pavement ME Design locally-calibrated predictions for selected pavement sections, a p value was calculated as $P(T \leq t)_{two-tail} = 0.34 > 0.05$. This result implies that, with 95 % certainty, there are no significant differences between actual and Pavement ME Design predicted IRI values (Table 28).

Table 28. Pair t test results for HMA IRI model for selected HMA over JPCP pavement sections (Approach 1)

	<i>Actual IRI</i>	<i>IRI Av</i>
Mean	86.64803	86.05753
Variance	914.4023	710.8831
Observations	657	657
Pearson Correlation	0.85092	
Hypothesized Mean Difference	0	
df	656	
t Stat	0.951236	
P(T<=t) one-tail	0.170918	
t Critical one-tail	1.64718	
P(T<=t) two-tail	0.341835	
t Critical two-tail	1.963587	

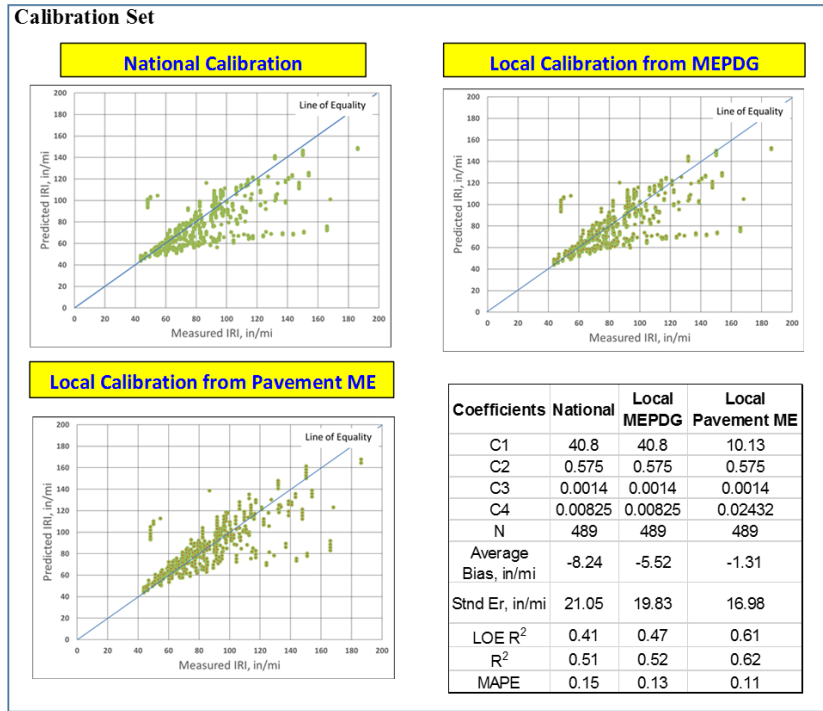


Figure 44. Overall accuracy summary of HMA over JPCPs IRI model for calibration set (Approach 1)

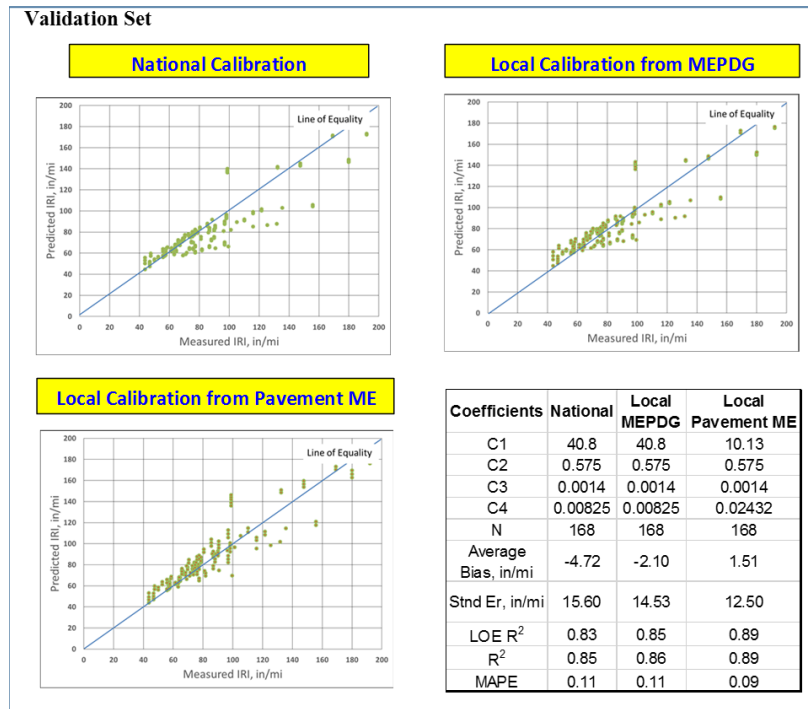


Figure 45. Overall accuracy summary of HMA over JPCPs IRI model for validation set (Approach 1)

Approach 2

Approach 2 was also used to locally calibrate the HMA over JPCP IRI model using Pavement ME Design software. In this approach, nationally calibrated rutting and fatigue cracking model predictions were used in local calibration of the IRI model.

Calibrating the IRI model in that way, similar model accuracies to those of Approach 1 were obtained. It was found out that the calibration coefficients established using Approach 1 also produced accurate predictions in this approach. This is because the most sensitive coefficient in the IRI transfer function is C4, related to the site factor, and the site factor values are the same in both approaches; using nationally-calibrated rutting and top-down (longitudinal) cracking models rather than Pavement ME Design locally-calibrated ones do not significantly change IRI predictions. Also note that the second most sensitive calibration coefficient for the IRI model is C1, related to rutting. It is important to highlight that, although the rutting model was further improved using Pavement ME Design local calibration coefficients, the difference between nationally-calibrated and Pavement ME Design locally-calibrated rutting model predictions was not significant, so the effect of using the nationally-calibrated rutting model rather than the Pavement ME Design locally-calibrated one was not significant. That would also mean that the local calibration of the IRI model for Iowa HMA over JPCP pavements could be performed with sufficient accuracy by nationally-calibrated rutting and top-down (longitudinal) cracking models. As can be seen from in figures Figure 46 and Figure 47, the Pavement ME Design locally-calibrated IRI model improved model accuracy significantly compared to the national model. Local calibration of the IRI model using Approach 2 would save significant resources, both time and funds. Use of Approach 2 in the local calibration of IRI model would be especially useful for those SHAs if they are mainly interested in only attaining locally-calibrated

IRI predictions rather than locally-calibrated rutting, fatigue, thermal, and thermal-cracking predictions. In this study, it was determined that using Approach 2, the locally-calibrated IRI model can predict this distress with sufficient accuracy for Iowa HMA over JPCP pavement systems.

A paired t test was also applied to this approach, and the calculated p value was $P(T \leq t)_{two-tail} = 0.11 > 0.05$. This result implies that, with 95 % certainty, there is no significant difference between national field-measured and Pavement ME predicted IRI values using Approach 2 (Table 29).

Table 29. Pair t test results for HMA IRI model for selected HMA over JPCP pavement sections (Approach 2)

	<i>Actual</i>	
	<i>IRI</i>	<i>IRI_{Av}</i>
Mean	86.64803	85.66045
Variance	914.4023	710.7439
Observations	657	657
Pearson Correlation	0.851534	
Hypothesized Mean Difference	0	
df	656	
t Stat	1.594009	
P(T<=t) one-tail	0.055708	
t Critical one-tail	1.64718	
P(T<=t) two-tail	0.111416	
t Critical two-tail	1.963587	

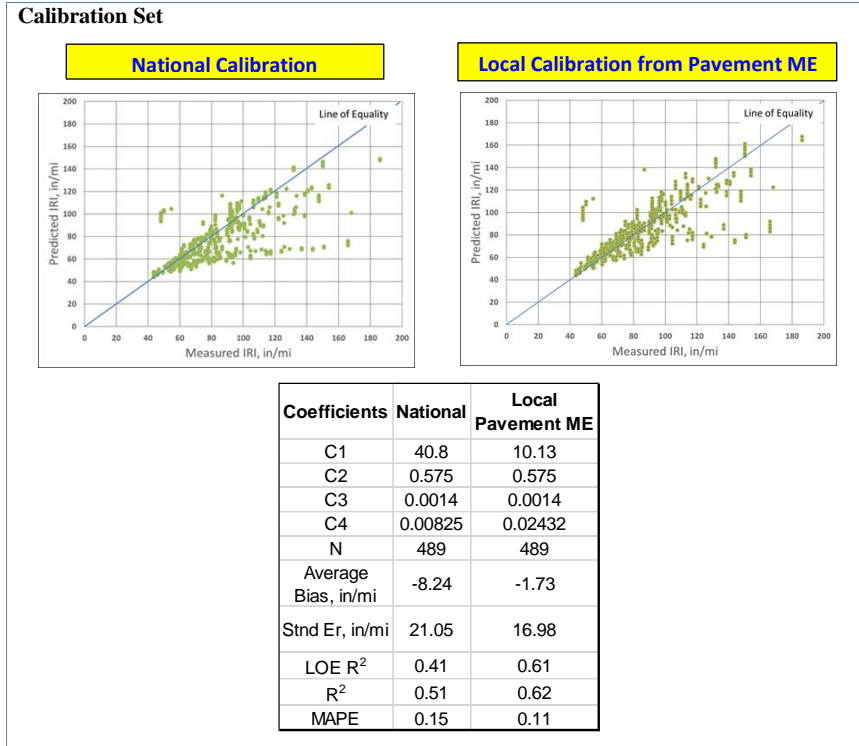


Figure 46. Overall accuracy summary of HMA over JPCPs IRI model for calibration set (Approach 2)

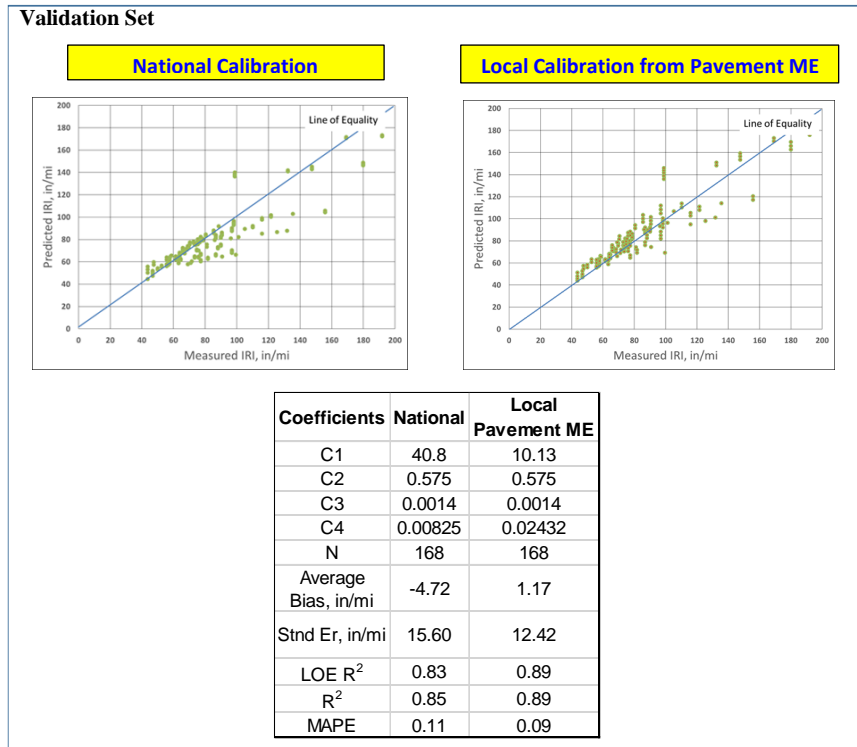


Figure 47. Overall accuracy summary of HMA over JPCPs IRI model for validation set (Approach 2)

CHAPTER 6. CONCLUSIONS, DISCUSSIONS AND RECOMMENDATIONS

Discussion on Future Enhancements of Pavement ME Design

AASHTO has a taskforce on Pavement ME Design to maintain system performance and keep up with technology, to implement new models, to develop enhancements, and to maintain communication and input from users (AASHTOWare Newsletter 2014). Under the support of AASHTO taskforce on Pavement ME Design, Pavement ME Design software continues to be upgraded. One of the enhancement items in the current work plan is the development of Application Programming Interfaces (APIs). APIs can provide Pavement ME Design users with the capability for interacting with the program and creating their own derivative applications, either to directly enhance the Pavement ME Design or for some other purpose. As discussed previously, full optimization of local calibration coefficients requires the availability of all input variables of various equations comprising each of the pavement performance models. For example, local calibration of the fatigue model for HMA surface pavements requires the values of ϵ_t (tensile strain in critical locations) to fully optimize coefficients (β_{f1} , β_{f2} , β_{f3} ,). However, this study has revealed that the version of Pavement ME Design software (version 2.1.24) used in this study does not provide these values. Incorporating APIs in Pavement ME Design would allow Pavement ME Design users to directly obtain such input values from APIs outputs and to implement them to achieve “true” local calibration. API tools are provided to Pavement ME Design users in the latest version of the software (version 2.2), released in August, 2015.

Along with API, there have been some other enhancements in the newly-released Pavement ME Design software (version 2.2) , including a DRIP tool for drainage assessment, LTPP high-quality traffic data, an improved reflection-cracking model, an enhanced climate dataset, MAPME, and level 1 and level 2 AC rehabilitation inputs for concrete overlays. Details of these enhancements are as follows (AASHTO 2015):

- A new reflection-cracking model was also incorporated into Pavement ME Design version 2.2. This model was documented in the NCHRP 1-41 study (NCHRP 2010). Table 30 gives pavement and distress types related to the new reflection cracking affects.

Table 30. Pavement and distress types the new reflection cracking affects (AASHTO 2015)

Pavement Type	Distress Type
AC OL over Existing AC (no interlayer, AC interlayer, seal coat)	Alligator Cracking
	Transverse Cracking
AC OL over Existing Intact JPCP	Transverse Cracking
AC OL over Existing Fractured JPCP or Intact CRCP	Transverse Cracking
Semi-Rigid (New AC over CTB)	Alligator Cracking
	Transverse Cracking

- The new calibration coefficients for JPCP cracking, JPCP faulting, and CRCP punch-out models using the coefficient of thermal expansion (CTE) values acquired using the new test specification (AASHTO T 336-09 2009) were added to the latest version of the software. Users having CTE values acquired using the AASHTO T 339-09 test method can use these new calibration coefficients for the aforementioned models. Also note that these new calibration coefficients are documented in NCHRP 20-07/327 study (Mallela et al. 2011).
- Drainage Requirement In Pavements (DRIP) is a Windows-based microcomputer program, used to conduct hydraulic design computations for subsurface drainage analysis of pavements. DRIP has many features such as roadway geometry calculations, sieve analysis calculations, inflow calculations, permeable base design, separator layer design, and edge drain design. DRIP can be applied to decision-making for drainage design by using its grain-

size distribution graphs and sensitivity analysis plots. DRIP can be downloaded from the ME-Design website (www.me-design.com).

- LTPP default axle load distributions can be imported and used in the new software version (version 2.2). The LTPP default axle load distributions are categorized into four groups in Pavement ME version 2.2: Global, Heavy, Typical and Light. Also note that the right-click choices “Single”, “Tandem”, Tridem, or “Quad” axle-load distribution are disabled in Pavement ME Design version 2.2.
- In Pavement ME Design version 2.2, an option for the users to define the climate data range was also added.
- MapME provides data from geographical information system data linkages to Pavement ME Design
- The semi-rigid pavement type replaced the new AC over CTB design type in Pavement ME Design version 2.2.
- Level 1 and Level 2 input data AC overlays over AC rehabilitated pavements, Level 3 input data for AC overlays over intact JPCP rehabilitated pavements, and new Level 1, Level 2 and Level 3 inputs for PCC overlays over existing AC pavements are provided in Pavement ME Design version 2.2.

Conclusions and Recommendations

The AASHTOWare Pavement ME Design local calibration for Iowa pavement system has been conducted by (1) evaluation of accuracy of the nationally-calibrated Pavement ME Design performance models and the locally-calibrated MEPDG performance models, identified through InTrans project TR 401 (Ceylan et al. 2013) and (2) recalibration of these models when the accuracies of the models was found to be insufficient. The recalibration of these models was

performed using AASHTOWare Pavement ME Design version 2.1.24 with the help of linear and nonlinear optimization techniques to improve the accuracy of model predictions. A step-by-step local calibration procedure was established for each pavement performance prediction model in this study by extensively reviewing transfer functions used in these models. The required components of transfer functions needed to implement local calibration were documented as well as well as their locations in intermediate and general output files and how to calculate them. More pavement performance measurements were used in this study than in the InTrans project TR 401 (Ceylan et al. 2013). Specific conclusions were drawn for each pavement type, and corresponding performance prediction models and recommendations for the use of identified local calibration coefficients as well as future research were provided.

Conclusions: JPCP

- Mean joint faulting, transverse-cracking and IRI models for Iowa JPCPs were significantly improved as a result of Pavement ME Design local calibration compared to national and MEPDG local counterparts.

Conclusions: HMA Pavements

- The identified Pavement ME Design local calibration factors significantly increased the accuracy of rutting models for Iowa HMAs compared to national and MEPDG local counterparts.
- The identified Pavement ME Design local calibration factors increased the accuracy of the IRI model for Iowa HMAs compared to nationally and MEPDG locally calibrated models, although nationally and MEPDG locally-calibrated IRI models also provided acceptable predictions.

- The nationally-calibrated longitudinal (top-down) cracking model underpredicted distress measurements while the MEPDG locally-calibrated model overpredicted distress measurements for Iowa HMA pavements. The accuracy of this model was improved as a result of Pavement ME Design local calibration.
- All the nationally, MEPDG and Pavement ME Design locally calibrated alligator (bottom-up) and thermal-cracking models provide acceptable predictions for Iowa HMA pavements.

Conclusions: HMA over JPCP

- The identified Pavement ME design local-calibration factors increased the accuracy of the rutting model for Iowa HMA over JPCP compared to nationally and MEPDG locally-calibrated models, although nationally and MEPDG locally-calibrated IRI models also provided acceptable predictions for this model.
- The identified local calibration factors significantly increased the accuracy of IRI predictions for Iowa HMA over JPCP.
- The nationally-calibrated model underpredicted the longitudinal (top-down) cracking model, while the MEPDG locally-calibrated model has excessive standard error for Iowa HMA over JPCPs. The accuracy of this model was improved as a result of Pavement ME Design local calibration.
- All of the nationally, MEPDG, and Pavement ME Design locally-calibrated alligator (bottom-up) cracking models and thermal-cracking models provided acceptable predictions for Iowa HMA over JPCPs.

Recommendations: The Use of Local Calibration Coefficients Identified

- The recommended local calibration coefficients to Iowa DOT to be used in design practice as alternatives to nationally-calibrated counterparts are summarized in Table 31 for Iowa JPCP,

Table 32 for Iowa HMA pavements, and Table 33 for Iowa HMA over JPCP. It should be noted that the recommended local calibration coefficients in red show that these numbers are different from their counterparts in nationally-calibrated models.

Table 31. Nationally and Pavement ME Design locally calibrated local calibration coefficients for Iowa JPCP pavement systems

Distress	Factors	National	Local
Faulting	C1	1.0184	0.85
	C2	0.91656	1.39
	C3	0.0021848	0.002
	C4	0.0008837	0.274
	C5	250	250.8
	C6	0.4	0.4
	C7	1.83312	1.45
	C8	400	400
Cracking	C1 (fatigue)	2	2.25
	C2 (fatigue)	1.22	1.4
	C4 (crack)	1	4.06
	C5 (crack)	-1.98	-0.44
IRI: Approach 1	C1	0.8203	0.11
	C2	0.4417	0.44
	C3	1.4929	0.04
	C4	25.24	11.32
IRI: Approach 2	C1	0.8203	0.03
	C2	0.4417	0.44
	C3	1.4929	0.01
	C4	25.24	15.12

Note: The recommended local calibration coefficients are red texted numbers

- The locally-calibrated JPCP performance models (faulting, transverse cracking, and IRI) identified in this study are recommended for use in Iowa JPCPs as alternatives to the nationally-calibrated ones.
- Since, in the calculation of IRI, both faulting and transverse-cracking predictions were involved, two approaches were utilized in the local calibration of the JPCP IRI model. In Approach 1, the IRI model was locally-calibrated using Pavement ME Design locally-

calibrated faulting and transverse-cracking model predictions, while in Approach 2, nationally-calibrated faulting and transverse-cracking model predictions were used.

- The use of two approaches in the local calibration of IRI model was intended to determine whether the IRI model could be locally calibrated with sufficient accuracy without using local calibration procedures for each distress model, thereby requiring additional cost and data resources. Local calibration of the IRI model using Approach 2 would save significant time and funds. Use of Approach 2 in the local calibration of the IRI model would be especially useful for the Iowa DOT, either whether they decided to use nationally-calibrated transverse-cracking and faulting models and locally calibrate the IRI model, or instead were more interested in attaining locally-calibrated IRI predictions rather than locally-calibrated transverse-cracking and faulting model predictions.
- In this study, it was determined that using Approach 2, a locally-calibrated IRI model can predict distress with sufficient accuracy for Iowa JPCP pavement systems.
- The locally-calibrated rutting, longitudinal (top-down) cracking and IRI prediction models identified in this study are recommended for use in Iowa HMAs as alternatives to nationally-calibrated models.
- The locally-calibrated rutting, longitudinal (top-down) cracking and IRI prediction models identified in this study are recommended for use in HMA over JPCPs as alternatives to nationally calibrated models.
- The nationally-calibrated alligator (bottom-up) and transverse (thermal) cracking prediction models are recommended for use in Iowa HMA systems, because even though the accuracy of these models were improved, the improvement was insignificant. Note that Iowa HMAs do not experience severe fatigue-related problems. It was also found that the HMA transverse

(thermal) cracking model would be unlikely to satisfactorily simulate this distress for Iowa HMA pavements.

Table 32. Nationally and Pavement ME locally calibrated local calibration coefficients for Iowa HMA pavement systems

Distress	Factors	National	Local
HMA Rut	B1	1	1
	B2	1	1.1
	B3	1	1
GB Rut	B1 Granular	1	0.001
SG Rut	B1 Fine-grain	1	0.001
Fatigue for ACrack and LCrack	B1	1	1
	B2	1	1
	B3	1	1
LCrack	C1 Top	7	2.32
	C2 Top	3.5	0.47
	C4 Top	1000	1000
ACrack	C1 Bottom	1	1
	C2 Bottom	1	1
	C4 Bottom	6000	6000
TCrack	K Level 3	1.5	1.5
IRI: Approach 1	C1	40	5
	C2	0.4	0.4
	C3	0.008	0.008
	C4	0.015	0.026
IRI: Approach 2	C1	40	25
	C2	0.4	0.4
	C3	0.008	0.008
	C4	0.015	0.019

Note: The recommended local calibration coefficients are red texted numbers

- The nationally-calibrated alligator (bottom-up) and thermal-cracking prediction models are recommended for use in Iowa HMA over JPCP systems, since even though the accuracy of these models were improved, the improvement was insignificant.
- In local calibration of the IRI model for Iowa HMAs and HMA over JPCPs, two approaches were followed. In Approach 1, the IRI model was locally-calibrated using Pavement ME

Design locally-calibrated rutting and top-down (longitudinal) cracking and nationally-calibrated alligator (bottom-up) and transverse (thermal) cracking predictions for HMAs and HMA over JPCPs, while in Approach 2 all nationally-calibrated model predictions were used. Note that, in contrast to the HMA IRI model, reflective cracking predictions were added to the IRI model as part of the area of total fatigue cracking in HMA over JPCPs. In both Approach 1 and Approach 2, nationally-calibrated reflection cracking predictions were employed.

- In this study, it was determined that, using Approach 2, a locally-calibrated IRI model can predict distress with sufficient accuracy for Iowa HMA and HMA over JPCP pavement systems.
- Preliminary studies were carried out to see whether there are any differences between the latest version of Pavement ME Design (version 2.2) released in August 2015 and the version used in this study, Pavement ME Design version 2.1.24. One significant change between these two versions is the prediction of Freezing Index Factor, a component of the IRI models. The results indicated some differences in IRI model predictions between these two software versions due to different Freezing Index Factor predictions. Note that Freezing Index Factors are predicted by the software using Enhanced Integrated Climatic Models (EICM) and automatically incorporated into the calculation of IRI predictions by the software. The Iowa DOT would deal with this issue by: (1) running the software input files provided by the researchers of this study, (2) based on the IRI predictions, locally calibrate the IRI model by modifying only the Freezing Index Factor following the steps documented in this report.

Table 33. Nationally and Pavement ME locally calibrated local calibration coefficients for Iowa HMA over JPCP pavement systems

Distress	Factors	National	Local
HMA Rut	B1	1	1
	B2	1	1.01
	B3	1	1
GB Rut	B1_Granular	1	0.001
SG Rut	B1_Fine-grain	1	0.001
Fatigue for ACrack and LCrack	B1	1	1
	B2	1	1
	B3	1	1
LCrack	C1_Top	7	2.3
	C2_Top	3.5	2
	C4_Top	1000	1000
ACrack	C1_Bottom	1	1
	C2_Bottom	1	1
	C4_Bottom	6000	6000
TCrack	K_Level 3	1.5	1.5
IRI: Approach 1	C1	40.8	10.13
	C2	0.575	0.575
	C3	0.0014	0.0014
	C4	0.00825	0.02432
IRI: Approach 2	C1	40.8	10.13
	C2	0.575	0.575
	C3	0.0014	0.0014
	C4	0.00825	0.02432

Note: The recommended local calibration coefficients are red texted numbers

Contributions of this Study to the Literature and State of the Art Practices Related with the Local Calibration of Pavement ME Design

Compared to previous studies regarding local calibration of MEPDG, there are many new approaches and advanced methods in this study that contribute to the available literature, including:

- Using Pavement ME Design version 2.1.24, the local calibration methodology of Pavement ME Design pavement prediction models for JPCP, HMA and HMA over JPCP pavements were documented in a detailed in step-by-step manner.
- Most of the pavement performance models were locally-calibrated outside the software by using nonlinear optimization techniques documented in great detail in this report. Different optimization techniques were employed in the local calibration procedure. Also, the availability of each equation variable of the transfer functions in the intermediate or general output files of Pavement ME Design was investigated to conduct local calibration.
- In the local calibration of the IRI models, two approaches were followed: (1) Calibrate using either locally-calibrated or nationally-calibrated distress prediction models. Note that nationally-calibrated distress prediction models can be used when they provide good accuracy in terms of distress measurements. (2) Calibrate using only nationally-calibrated distress prediction models without considering agreement of distress-model predictions with distress measurements.
- One of the latest versions of Pavement ME Design software was used in the local calibration procedure.
- The new features added to the software in Pavement ME Design version 2.2, released in August 2015, are summarized in this document.

- The accuracy improvements of the pavement prediction models as a result of local calibration were documented in great detail in this document.
- Pavement performance model predictions of different versions of MEPDG (version 1.1) and Pavement ME Design (versions 2.0 and 2.1.24) were compared to document any existing differences.

Recommendations: Future Research

Pavement ME Design software is still in the process of development. With every new version of the software, additional enhancements are added and sometimes the models are modified (e.g. Freezing Index). The following items would be valid topics for future research related to the local calibration of Pavement ME Design software:

- As mentioned earlier, a reflection-cracking model was added to the new version of the software, Pavement ME Design version 2.2. Local calibration of this model should be conducted.
- As new pavement performance models are added to the software or available models are modified, additional local calibration of Pavement ME Design studies should be conducted.

REFERENCES

- AASHTO. 2008. *Mechanistic-Empirical Pavement Design Guide, Interim Edition: A Manual of Practice*. Washington, DC.
- AASHTO. 2010. *Guide for the Local Calibration of the Mechanistic-Empirical Pavement Design Guide*. Washington, DC.
- AASHTO T 336-09.2009. *Standard Method of Test for Coefficient of Thermal Expansion of Hydraulic Cement Concrete*. Standard Specifications for Transportation Materials and Methods of Sampling and Testing, American Association of State Highway and Transportation Officials, Washington, DC.
- AASHTO TP 60-00. 2004. *Standard Method of Test for Coefficient of Thermal Expansion of Hydraulic Cement Concrete*. Standard Specifications for Transportation Materials and Methods of Sampling and Testing, American Association of State Highway and Transportation Officials, Washington, DC.
- AASHTO. *AASHTOWare Newsletter, October 2014*.
www.aashtoware.org/Pavement/Pages/Newsletter.aspx. Accessed July 15, 2015.
- AASHTO. *AASHTOWare Pavement ME Design Release Notes, August 2015*. <http://me-design.com/MEDesign/Documents.html>. Accessed September 15, 2015.
- Banerjee, A., J. A. Prozzi, and J. P. Aguiar-Moya. 2010. Calibrating the MEPDG permanent deformation performance model for different maintenance and rehabilitation strategies. Presented at the 89th annual meeting of the Transportation Research Board. Washington, DC: Transportation Research Board.
- Banerjee, A., J. A. Prozzi, and A. Freiman. 2011. Regional calibration of the permanent deformation performance models for rehabilitated flexible pavements. Presented at the Annual 90th annual meeting of the Transportation Research Board. Washington, DC: Transportation Research Board.
- Ceylan, H., S. Kim, K. Gopalakrishnan, and D. Ma. 2013. *Iowa Calibration of MEPDG Performance Prediction Models*. Iowa: Institute for Transportation, Iowa State University.

- Corley-Lay, J. B., F. Jadoun, J. Mastin, and R. Kim. 2010. Comparison of NCDOT and LTPP monitored flexible pavement distresses. *Transportation Research Record* 2153: 91-96. Washington DC: Transportation Research Board, National Research Council.
- Crawford, G., J. Gudimettla, and J. Tanesi. 2010. Inter-laboratory study on measuring coefficient of thermal expansion of concrete. Presented at the annual meeting of the Transportation Research Board. Washington, DC: Transportation Research Board.
- Darter, M. I., L. T. Glover, and H. L. Von Quintus. 2009. *Implementation of the Mechanistic-Empirical Pavement Design Guide in Utah: Validation, Calibration, and Development of the UDOT MEPDG User's Guide*. Report no. UT-09.11, IL: ARA, Inc.
- Darter, M. I., L. T. Glover, H. L. Von Quintus, B. Bhattacharya, and J. Mallela. 2014. *Calibration and Implementation of the AASHTO Mechanistic-Empirical Pavement Design Guide in Arizona*. IL: ARA, Inc.
- Delgadillo, R., C. Wahr, and J. P. Alarcón. 2011. Towards the implementation of the MEPDG in Latin America, preliminary work carried out in Chile. Presented at the 90th Annual Meeting of the Transportation. Washington, DC: Transportation Research Board, National Research Council.
- Federal Highway Administration (FHWA). 2006a. *Using Pavement Management Data to Calibrate and Validate the New MEPDG, An Eight State Study*. Final Report, Volume I, Washington, DC: Federal Highway Administration.
- Federal Highway Administration (FHWA). 2006b. *Using Pavement Management Data to Calibrate and Validate the New MEPDG, An Eight State Study*. Final Report, Volume II, Washington, DC: Federal Highway Administration.
- Federal Highway Administration (FHWA). 2010a. *Local Calibration of the MEPDG Using Pavement Management*. Final Report for FHWA Project DTFH61-07-R-00143, Volume I, Washington, DC: Federal Highway Administration.
- Federal Highway Administration (FHWA). 2010b. *Local Calibration of the MEPDG Using Pavement Management*. Final Report for FHWA Project DTFH61-07-R-00143, Volume II, Washington, DC: Federal Highway Administration.

Frontline Systems, Inc. <www.solver.com> (Accessed July 15, 2015).

Galal, K. A., and G. R. Chehab. 2005. Implementing the mechanistic-empirical design guide procedure for a Hot-Mix Asphalt-rehabilitated pavement in Indiana. *Transportation Research Record* 1919:121-133. Washington DC: Transportation Research Board, National Research Council.

Hall, K. D., D. X. Xiao, and K. C. P. Wang. 2011. Calibration of the MEPDG for flexible pavement design in Arkansas. *Transportation Research Record* 2226:135-141. Washington DC: Transportation Research Board, National Research Council.

Hoegh, K., L. Khazanovich, M. R. Jensen. 2010. Local calibration of MEPDG rutting model for MnROAD test section. *Transportation Research Record* 2180: 130-141. Washington DC: Transportation Research Board, National Research Council.

Jadoun, F. M. 2011. Calibration of the flexible pavement distress prediction models in the Mechanistic Empirical Pavement Design Guide (MEPDG) for North Carolina. PhD dissertation, North Carolina State University.

Kang, M., T. M. Adams, and H. Bahia. 2007. *Development of a Regional Pavement Performance Database of the AASHTO Mechanistic-Empirical Pavement Design Guide: Part 2: Validations and Local Calibration*. MRUTC 07-01. Wisconsin: Midwest Regional University Transportation Center, University of Wisconsin-Madison.

Khazanovich, L., L. Yut, S. Husein, C. Turgeon, and T. Burnham. 2008. Adaptation of Mechanistic–Empirical Pavement Design Guide for design of Minnesota low-volume Portland Cement Concrete Pavements. *Transportation Research Record* 2087: 57-67. Washington DC: Transportation Research Board, National Research Council.

Kim, S., H. Ceylan, K. Gopalakrishnan, and O. Smadi. 2010. Use of pavement management information system for verification of Mechanistic-Empirical Pavement Design Guide performance predictions. *Transportation Research Record* 2153: 30-39. Washington DC: Transportation Research Board, National Research Council.

Lewis, C. D. 1982. *Industrial and Business Forecasting Methods*. London: Butterworths.

- Li, J., S. T. Muench, J. P. Mahoney, N. Sivaneswaran, and L. M. Pierce. 2006. Calibration of NCHRP 1-37A software for the Washington State Department of Transportation: rigid pavement portion. *Transportation Research Record* 1949: 43-53. Washington DC: Transportation Research Board, National Research Council.
- Li, J., L. M. Pierce, and J. S. Uhlmeier. 2009. Calibration of flexible pavement in mechanistic-empirical pavement design guide for Washington State. *Transportation Research Record* 2095: 73-83. Washington DC: Transportation Research Board, National Research Council.
- Li, J., D. R. Luhr, and J. S. Uhlmeier. 2010. Pavement performance modeling using piecewise approximation. *Transportation Research Record* 2153: 24-29. Washington DC: Transportation Research Board, National Research Council.
- LINDO Systems, Inc. *Lingo 15.0*. <www.lindo.com> (Accessed July 15, 2015).
- Lytton, R. L., F. L. Tsai, S. Lee, R. Luo, S. Hu, and F. Zhou. 2010. *Models for Predicting Reflection Cracking of Hot-Mix Asphalt Overlays*. Research Report 669. National Cooperative Highway Research Program 1-41. Washington, DC: Transportation Research Board, National Research Council.
- Mallela, J., L. Titus-Glover, H. Von Quintus, M. I. Darter, M. Stanley, C. Rao, and S. Sadasivam. 2009. *Implementing the AASHTO Mechanistic-Empirical Pavement Design Guide in Missouri. Volume I: Study Findings, Conclusions, and Recommendations*. Applied Research Associates, Inc.
- Mallela, J., M. I. Darter, L. Titus-Glover, C. Rao, and B. Bhattacharya. 2011. *Recalibration of AASHTO-ME Rigid Pavement National Models Based on Corrected CTE Values*. NCHRP 20-07/Task 288, Transportation Research Board of the National Academies, Washington, D.C.
- Mallela, J. L. Titus-Glover, S. Sadasivam, B. B. Bhattacharya, M. I. Darter and H. Von Quintus. 2013. *Implementation of the AASHTO Mechanistic-Empirical Pavement Design Guide for Colorado*. Applied Research Associates, Inc.

- Mallela, J., L. Titus-Glover, B. B. Bhattacharya, A. Gotlif, and M. I. Darter. Recalibration of the JPCP cracking and faulting models in the AASHTO ME Design. *Transportation Research Record 5222*. Washington DC: Transportation Research Board, National Research Council.
- Mamlouk, M. S., and C. E. Zapata. 2010. Necessary assessment of use of state pavement management system data in mechanistic-empirical pavement design guide calibration process. *Transportation Research Record 2153*: 58-66. Washington DC: Transportation Research Board, National Research Council.
- Miller, J. S. and W. Y. Bellinger. 2003. *Distress Identification Manual for the Long-Term Pavement Performance (LTPP) Project*. FHWA-RD-03-031 (4th edition). Federal Highway Administration.
- Mu F., J. W. Mack, and R. A. Rodden. 2015. *Review of national and state-level calibrations of the AASHTOWare Pavement ME Design for new jointed plain concrete pavement*. Proceeding of ASCE Airfield and Highway Pavements: 708-719.
- Muthadi, N. R. 2007. Local calibration of the MEPDG for flexible pavement design. MS thesis, North Carolina State University.
- Muthadi, N. R., and R. Kim. 2008. Local calibration of mechanistic-empirical pavement design guide for flexible pavement design. *Transportation Research Record 2087*: 131-141. Washington DC: Transportation Research Board, National Research Council.
- NCHRP. 2003a. *Jackknife Testing—An Experimental Approach to Refine Model Calibration and Validation*. Research Results Digest 283. National Cooperative Highway Research Program 9-30. Washington, DC: Transportation Research Board, National Research Council.
- NCHRP. 2003b. *Refining the Calibration and Validation of Hot Mix Asphalt Performance Models: An Experimental Plan and Database*. Research Results Digest 284. National Cooperative Highway Research Program 9-30. Washington, DC: Transportation Research Board, National Research Council.
- NCHRP. 2004. *Guide for Mechanistic-Empirical Design of New and Rehabilitated Pavement Structures*. www.trb.org/mepdg., National Cooperative Highway Research Program 1-37 A. Washington, DC: Transportation Research Board, National Research Council.

- NCHRP. 2006a. *Independent Review of the Mechanistic-Empirical Pavement Design Guide and Software*. Research Results Digest 307. National Cooperative Highway Research Program 1-40 A. Washington, DC: Transportation Research Board, National Research Council.
- NCHRP. 2006b. *Changes to The Mechanistic-Empirical Pavement Design Guide Software Through Version 0.900-July, 2006*. Research Results Digest 308. National Cooperative Highway Research Program 1-40 D. Washington, DC: Transportation Research Board, National Research Council.
- NCHRP. 2007. *Recommended Practice for Local Calibration of the ME Pavement Design Guide*. National Cooperative Highway Research Program 1-40B Draft. Texas: ARA, Inc.
- NCHRP. 2009. *Standard Practice for Conducting Local or Regional Calibration Parameters for the MEPDG*. National Cooperative Highway Research Program Project 1- 40B Report, Washington, DC: Transportation Research Board, National Research Council.
- NCHRP. 2010. *Models for Predicting Reflection Cracking of Hot-Mix Asphalt Overlays*. National Cooperative Highway Research Program Project 1- 41 Report, Washington, DC: Transportation Research Board, National Research Council.
- NCHRP. 2011. *Sensitivity Evaluation of MEPDG Performance Prediction*. National Cooperative Highway Research Program Project 1- 47 Report, Washington, DC: Transportation Research Board, National Research Council.
- NCHRP. 2014. *Implementation of the AASHTO Mechanistic-Empirical Pavement Design Guide and Software: A Synthesis of Highway Practice*. Washington, DC: Transportation Research Board, National Research Council.
- Schram, S., and M. Abdelrahman. 2006. Improving prediction accuracy in mechanistic-empirical pavement design guide. *Transportation Research Record* 1947: 59-68. Washington DC: Transportation Research Board, National Research Council.
- Souliman, M. I., M. S. Mamlouk, M. M. El-Basyouny, and C. E. Zapata. 2010. Calibration of the AASHTO MEPDG for flexible pavement for Arizona conditions. Presented at the 89th Annual Meeting of the Transportation Research Board. Washington, DC: Transportation Research Board.

- Tarefder R. and J. I. Rodriguez-Ruiz. 2013. Local calibration of MEPDG for flexible pavements in New Mexico. *Journal of Transportation Engineering* 139:10.
- Titus-Glover, L. and J. Mallela. 2009. *Guidelines for Implementing NCHRP 1-37A M-E Design Procedures in Ohio Volume 4 - MEPDG Models Validation & Recalibration*. Applied Research Associates, Inc.
- Transportation Pooled Fund (TPF) Program. 2012. *Investigation of Low Temperature Cracking in Asphalt Pavements - Phase II (MnROAD Study)*.
www.pooledfund.org/Details/Study/395. Accessed April 2012.
- TRB. 2009. *NCHRP Projects*, <http://www.trb.org/CRP/NCHRP/NCHRPPProjects.asp>. Accessed February 2009.
- TRB. 2012. *Sensitivity Evaluation of the MEPDG for Flexible Pavements*. TRB Webinar.
<http://onlinepubs.trb.org/onlinepubs/webinars/120725.pdf>. Accessed October 2015.
- Velasquez, R., K. Hoegh, I. Yut, N. Funk, G. Cochran, M. Marasteanu, and L. Khazanovich. 2009. *Implementation of the MEPDG for New and Rehabilitated Pavement Structures for Design of Concrete and Asphalt Pavements in Minnesota*. MN/RC 2009-06, Minneapolis, Minnesota: University of Minnesota.
- Von Quintus, H. L., M. I. Darter, and J. Mallela. 2005. *Phase I – Local Calibration Adjustments for the HMA Distress Prediction Models in the M-E Pavement Design Guide Software*. Interim Report. National Cooperative Highway Research Program 1-40 B. Washington, DC: Transportation Research Board, National Research Council.
- Von Quintus, H. L. and J. S. Moulthrop. 2007. *Mechanistic-Empirical Pavement Design Guide Flexible Pavement Performance Prediction Models: Volume I- Executive Research Summary*. FHWA/MT-07-008/8158-1. Texas: Fugro Consultants, Inc.
- Von Quintus, H. L. 2008a. MEPDG overview & national perspective. Presented at North-Central MEPDG User Group, Ames, IA: February 19, 2008.
- Von Quintus, H. L. 2008b. Local calibration of MEPDG—An overview of selected studies. Presented at 2008 AAPT Symposium Session: Implementation of the New MEPDG, Philadelphia, PA: April 29 2008.

- Von Quintus, H. L., M. I. Darter, and J. Mallela. 2009a. *Recommended Practice for Local Calibration of the M-E Pavement Design Guide*. National Cooperative Highway Research Program Project 1- 40B Manual of Practice, Washington, DC: Transportation Research Board, National Research Council.
- Von Quintus, H. L., M. I. Darter, and J. Mallela. 2009b. *Examples Using the Recommended Practice for Local Calibration of the MEPDG Software*. National Cooperative Highway Research Program Project 1- 40B Manual of Practice, Washington, DC: Transportation Research Board, National Research Council.
- Williams R. C., and R. Shaidur. 2013. *Mechanistic-Empirical Pavement Design Guide Calibration for Pavement Rehabilitation*. Iowa: Institute for Transportation, Iowa State University.
- Wu Z., D. W. Xiao, Z. Zhang, and W. H. Temple. 2014. Evaluation of AASHTO Mechanistic-Empirical Pavement Design Guide for Designing Rigid Pavements in Louisiana. *International Journal of Pavement Research and Technology* 7(6): 405-416.
- Zapata, C. E. 2010. *A National Database of Subgrade Soil-Water Characteristic Curves and Selected Soil Properties for Use with the MEPDG*. National Cooperative Highway Research Program Project 9-23A Report (NCHRP Web Only Document 153), Washington, DC: Transportation Research Board, National Research Council.
- Zhou C., B. Huang, X. Shu, and Q. Dong. 2013. Validating MEPDG with Tennessee Pavement Performance Data. *Journal of Transportation Engineering* 139(3).
- Wang, K., J. Hu, and Z. Ge. 2008. *Task 6: Material Thermal Input for Iowa*. CTRE Project 06-272. Iowa: Center for Transportation Research and Education, Iowa State University.

APPENDIX A: LITERATURE REVIEW RESULTS

The national calibration-validation process was successfully completed for Mechanistic-Empirical Pavement Design Guide (MEPDG) (NCHRP 2004). Although this effort was comprehensive, a further validation study is highly recommended by the MEPDG or Pavement ME design as a prudent step in implementing a new design procedure that is so different from the current procedures. The objective of this task is to review all of available existing literature with regard to implementing the MEPDG and local calibration at national and local research levels. A comprehensive literature review was undertaken specifically to identify the following information:

- Identify local calibration steps detailed in national level research studies (National Cooperative Highway Research Program (NCHRP) and Federal Highway Administration (FHWA) research projects) for local calibration.
- Examine how State agencies apply the national level research projects' local calibration procedures in their pavement systems.
- Summarize MEPDG or Pavement ME Design pavement performance models' local calibration coefficients reported in literature.

Summary of National Level Projects for MEPDG Local Calibration

AASHTO Guide for the Local Calibration of the MEPDG Developed from NCHRP Projects

At the request of the American Association of State Highway and Transportation Officials (AASHTO) Joint Task Force on Pavements (JTTF), the NCHRP initiated the project, 1-40 "*Facilitating the Implementation of the Guide for the Design of New and Rehabilitated Pavement Structures*" following NCHRP 1-37A (NCHRP 2004) for implementation and adoption of the recommended MEPDG (TRB 2009). A key component of the NCHRP 1-40 is an

independent, third-party review to test the design guide’s underlying assumptions, evaluate its engineering reasonableness and design reliability, and to identify opportunities for its implementation in day-to-day design production work. Beyond this immediate requirement, NCHRP 1-40 includes a coordinated effort to acquaint state DOT pavement designers with the principles and concepts employed in the recommended guide, assist them with the interpretation and use of the guide and its software and technical documentation, develop step-by-step procedures to help State DOT engineers calibrate distress models on the basis of local and regional conditions for use in the recommended guide, and perform other activities to facilitate its acceptance and adoption.

There are two NCHRP research projects that are closely related to local calibration of MEPDG performance predictions. They are (1) NCHRP 9-30 project (NCHRP 2003a, NCHRP 2003b), “*Experimental Plan for Calibration and Validation of Hot Mix Asphalt Performance Models for Mix and Structural Design*” and (2) NCHRP 1-40B (Von Quintus et al. 2005, NCHRP 2007, Von Quintus et al. 2009a, Von Quintus et al. 2009b, NCHRP 2009, TRB 2010), “*User Manual and Local Calibration Guide for the Mechanistic-Empirical Pavement Design Guide and Software.*” Under the NCHRP 9-30 project, pre-implementation studies involving verification and recalibration have been conducted in order to quantify the bias and residual error of the flexible pavement distress models included in the MEPDG (Muthadi 2007). Based on the findings from the NCHRP 9-30 study, the NCHRP 1-40B project has focused on preparing (1) a user manual for the MEPDG and software and (2) detailed, practical guide for highway agencies for local or regional calibration of the distress models in the MEPDG and software. The manual and guide have been presented in the form of a draft AASHTO recommended practices; the guide shall contain two or more examples or case studies illustrating the step-by-step procedures.

It was also noted that the longitudinal cracking model be dropped from the local calibration guide development in NCHRP 1-40B study due to lack of accuracy in the predictions (Muthadi 2007, Von Quintus and Moulthrop 2007). NCHRP 1-40 B was completed in 2009 and now published as “Guide for the Local Calibration of the Mechanistic-Empirical Pavement Design Guide” in AASHTO.

NCHRP 1-40B study (NCHRP 2007) initially provided the primary three steps for calibrating MEPDG to local conditions and materials as follows:

Verification of MEPDG performance models with national calibration factors: Run the current version of the MEPDG software for new field sections using the best available materials and performance data. The accuracy of the prediction models was evaluated using the bias (defined as average over or under prediction) and the residual error (defined as the predicted minus observed distress) as illustrated in Figure A.1. If there is a significant bias and residual error, it is recommended to calibrate the models to local conditions leading to the second step.

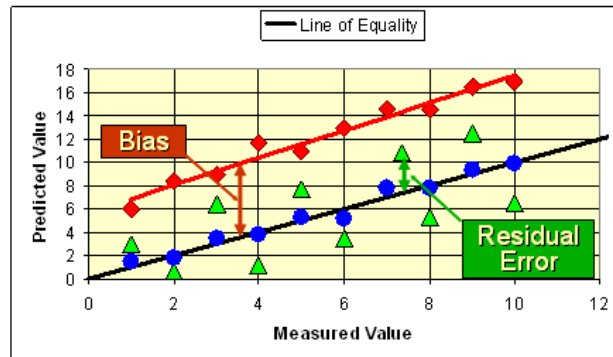


Figure A.1. The Bias and the residual error (Von Quintus 2008a)

Calibration of the model coefficients: eliminate the bias and minimize the standard error between the predicted and measured distresses.

Validation of MEPDG performance models with local calibration factors: Once the bias is eliminated and the standard error is within the agency’s acceptable level after the calibration,

validation is performed on the models to check for the reasonableness of the performance predictions. NCHRP 1-40B study (NCHRP 2009) has also detailed these steps more into 11 steps for local calibration of the MEPDG. These 11 steps are depicted in Figure A.2 and Figure A.3 below and each of the 11 steps is summarized in the following subsections.

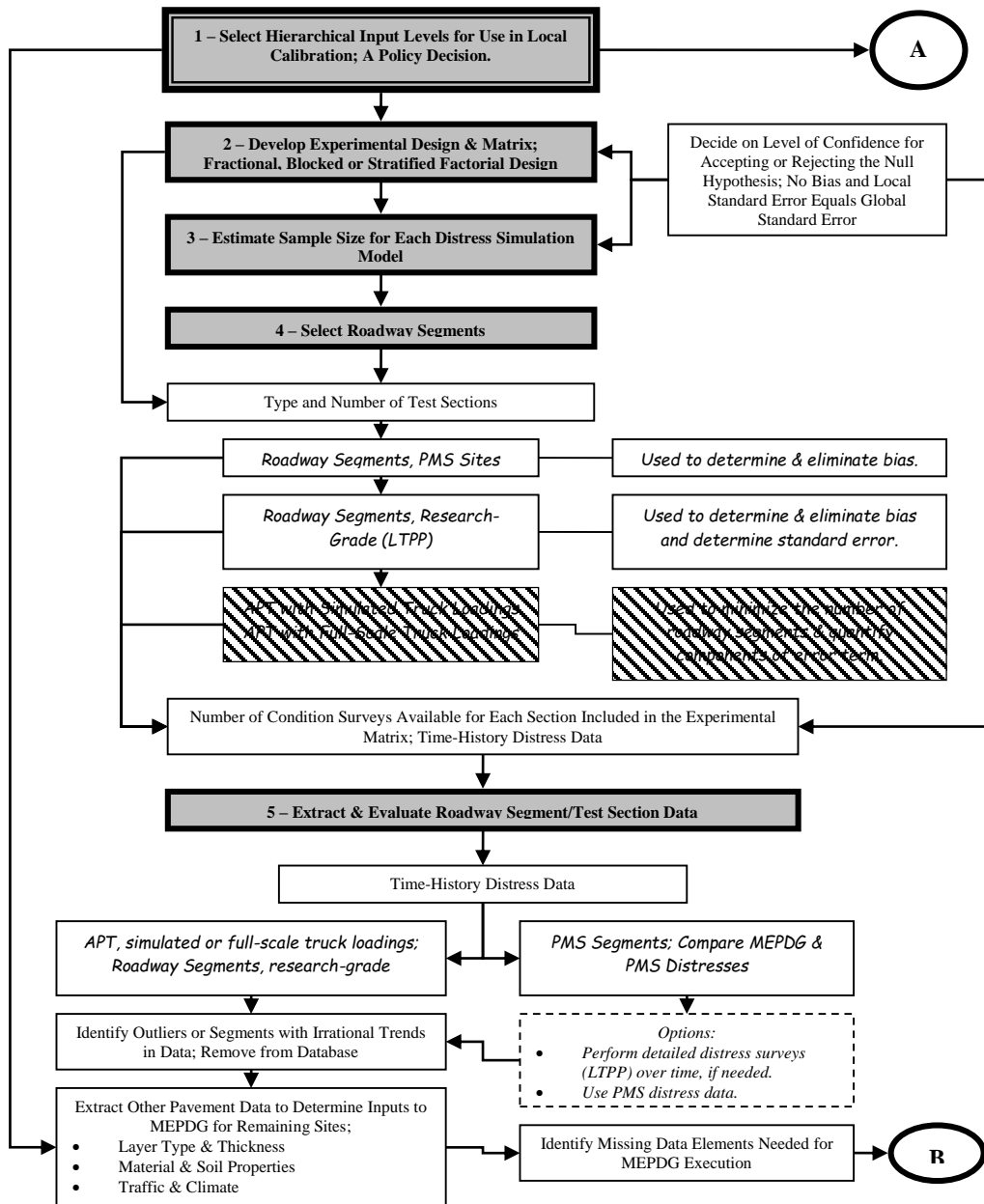


Figure A.2. Flow chart for the procedure and steps suggested for local calibration: steps 1-5 (NCHRP 2009)

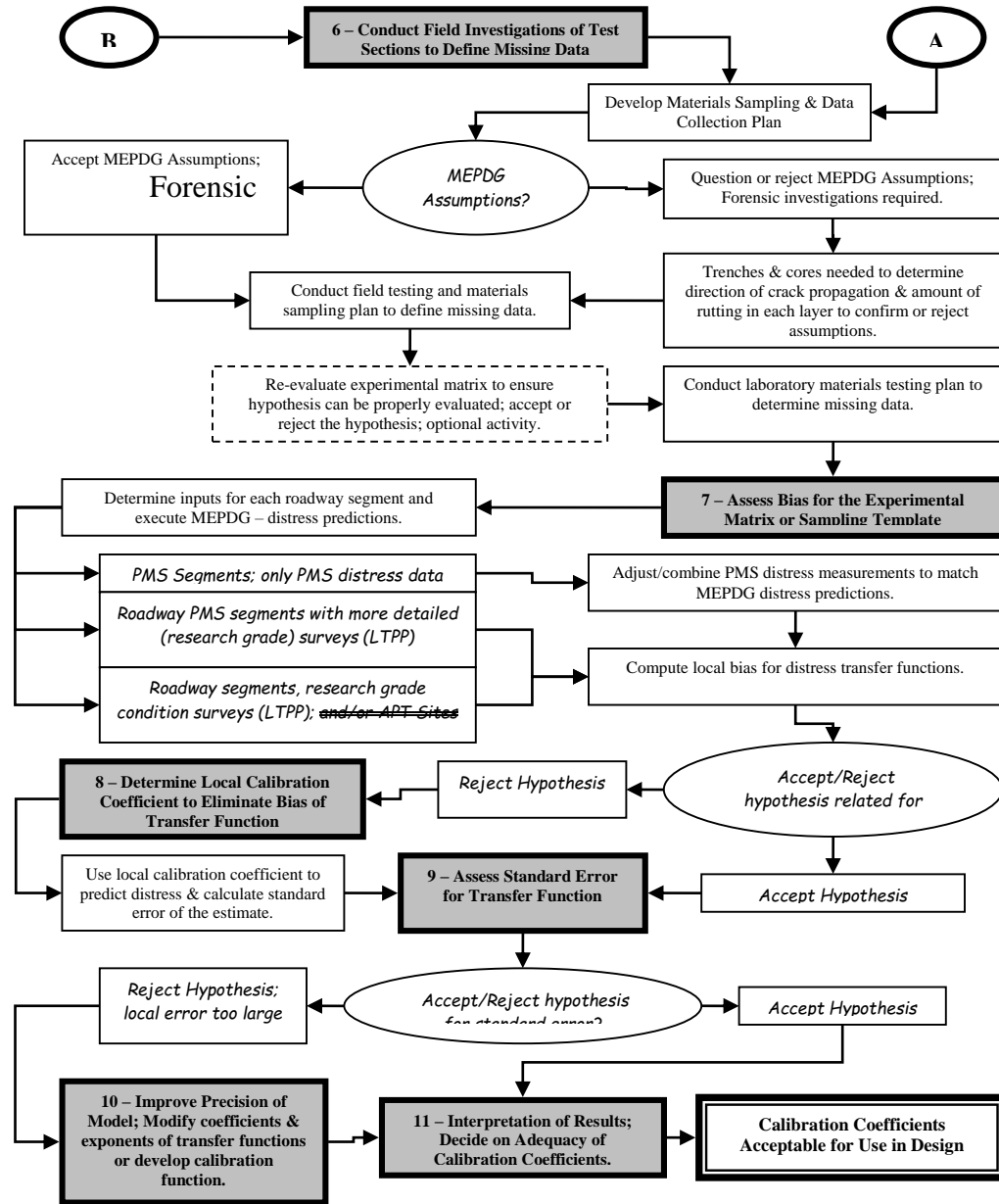


Figure A.3. Flow chart for the procedure and steps suggested for local calibration: steps 6-11 (NCHRP 2009)

Step 1: Select Hierarchical Input Level

The hierarchical input level to be used in the local validation-calibration process should be consistent with the way the agency intends to determine the inputs for day-to-day use. Some of input level 3 data could be available in the state Department of Transportation (DOT)

pavement management system (PMS). It is also important to point out that the calibration using level 1 and 2 input data is dependent upon material and mixture characteristics. Further the linkage of material and mixture characteristics to pavement performance is critical to the level 1 and 2 calibrations. The general information from which the inputs were determined for each input category is discussed in Step 5.

Step 2: Experimental Factorial & Matrix or Sampling Template

A detailed sampling template should be created considering traffic, climate, pavement structure and materials representing local conditions. The number of roadway segments selected for the sampling template should result in a balanced factorial with the same number of replicates within each category.

Step 3: Estimate Sample Size for Each Performance Indicator Prediction Model

The sample size (total number of roadway segments or projects) can be estimated with statistical confidence level of significance. The selection of higher confidence levels can provide more reliable data but increase the number of segments needed. The number of distress observations per segment is dependent on the measurement error or within segment data variability over time (i.e.; higher the within project data dispersion or variability, larger the number of observations needed for each distress). The number of distress measurements made within a roadway segment is also dependent on the within project variability of the design features and site conditions. NCHRP 1-40B project report (NCHRP 2009) provides the following equation in determination of the number of distress observations:

$$N = \left(\frac{z_{\alpha}(s_y)}{e_t} \right)^2 \quad (\text{A.1})$$

Where, $z_{\alpha} = 1.282$ for a 90 percent confidence interval; s_y = standard deviation of the maximum true or observed values; and e_t = tolerable bias. The tolerable bias will be estimated from the levels that are expected to trigger some major rehabilitation activity, which are agency dependent. The s_e/s_y value (ratio of the standard error and standard deviation of the measured values) will also be agency dependent.

Step 4: Select Roadway Segments

Roadway segments should be selected to cover a range of distress values that are of similar ages within the sampling template. Roadway segments exhibiting premature or accelerated distress levels, as well as those exhibiting superior performance (low levels of distress over long periods of time), can be used, but with caution. The roadway segments selected for the sampling template when using hierarchal input level 3 should represent average performance conditions. It is important that the same number of performance observations per age per each roadway segment be available in selecting roadway segments for the sampling template. It would not be good practice to have some segments with ten observations over 10 years with other segments having only two or three observations over 10 years. The segments with one observation per year would have a greater influence on the validation-calibration process than the segments with less than one observation per year.

Step 5: Extract and Evaluate Roadway Segment/Test Section Data

This step is grouped into four activities: (1) extracting and reviewing the performance data; (2) comparing the performance indicator magnitudes to the trigger values; (3) evaluating the distress data to identify anomalies and outliers; and (4) determining the inputs to the MEPDG. First, measured time-history distress data should be made from accelerated pavement testing (APT) or extracted from agency PMS. The extraction of data from agency PMS should

require a prior step of reviewing PMS database to determine whether the measured values are consistent with the values predicted by the MEPDG. NCHRP 1-40B project report (NCHRP 2009) demonstrated the conversion procedures of pavement distress measurement units between PMS and MEPDG for flexible pavements PMS database of Kansas Department of Transportation (KSDOT) and rigid pavements PMS database of Missouri Department of Transportation (MODOT). These examples in NCHRP 1-40B project report (NCHRP 2009) is reproduced in below.

For the flexible pavement performance data in KSDOT, the measured cracking values are different, while the rutting and International Roughness Index (IRI) values are similar and assumed to be the same. The cracking values and how they were used in the local calibration process are defined below.

Fatigue Cracking. KSDOT measures fatigue cracking in number of wheel path feet per 100-foot sample by crack severity, but do not distinguish between alligator cracking and longitudinal cracking in the wheel path. In addition, reflection cracks are not distinguished separately from the other cracking distresses. The PMS data were converted to a percentage value similar to what is reported in the Highway Performance Monitoring System (HPMS) system from Kansas. In summary, the following equation was used to convert KSDOT cracking measurements to a percentage value that is predicted by the MEPDG.

$$FC = \left(\frac{FCR_1(0.5) + FCR_2(1.0) + FCR_3(1.5) + FCR_4(2.0)}{8.0} \right) \quad (A.2)$$

All load related cracks are included in one value. Thus, the MEPDG predictions for load related cracking were combined into one value by simply adding the length of longitudinal cracks and reflection cracks for Hot Mix Asphalt (HMA) overlays, multiplying by 1.0 ft,

dividing that product by the area of the lane and adding that value to the percentage of alligator cracking predicted by the MEPDG.

Transverse Cracking. Another difference is that KSDOT records thermal or transverse cracks as the number of cracks by severity level. The following equation has been used by KSDOT to convert their measured values to the MEPDG predicted value of ft./mi.

$$TC = \left(\frac{TCR_o + TCR_1 + TCR_2 + TCR_3}{(10)(12)(52.8)} \right) \quad (\text{A.3})$$

The value of 10 in the above equation is needed because the data are stored with an implied decimal. The value of 12 ft. is the typical lane width, and the value of 52.8 converts from 100 foot sample to a per mile basis. Prior to 1999, KSDOT did not record the number or amount of sealed transverse cracking (TCR0). As a result, the amount of transverse cracks sometimes goes to “0”.

For the rigid pavement performance data in MODOT, the measured transverse cracking values are different from MEPDG, while the transverse joint faulting and IRI values are similar and assumed to be the same. The transverse cracking values and how they were used in the local calibration process are defined below.

Transverse Cracking. MEPDG requires the percentage of all Portland Cement Concrete (PCC) slabs with mid panel fatigue transverse cracking. Both MODT and LTPP describe transverse cracking as cracks that are predominantly perpendicular to the pavement slab centerline. Measured cracking is reported in 3 severity levels (low, medium, and high) and provides distress maps showing the exact location of all transverse cracking identified during visual distress surveys. Thus, the databases contain, for a given number of slabs within a 500-ft pavement segment, the total number of low, medium, and high severity transverse cracking.

Since LTPP does not provide details on whether a given slab has multiple cracks, as shown in Figure 4, a simple computation of percent slabs with this kind of data can be misleading.

Therefore, in order to produce an accurate estimate of percent slab cracked, distress maps or videos prepared as part of distress data collection were reviewed to determine the actual number of slabs with transverse “fatigue” cracking for the 500-ft pavement segments. Total number of slabs with transverse “fatigue” cracking for the 500-ft pavement segments. Total number of slabs was also counted. Percent slabs cracked was defined as follows:

$$\text{Percent Slabs Cracked} = \left(\frac{\text{Number of cracked slabs}}{\text{Total number of slabs}} \right) * 100 \quad (\text{A.4})$$

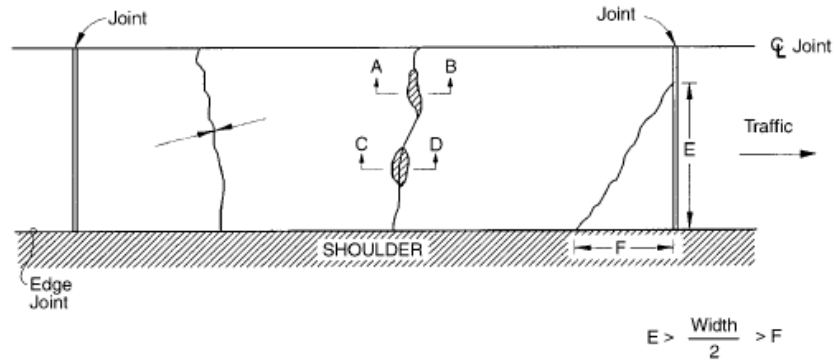


Figure A.4. LTPP transverse cracking (Miller and Bellinger 2003)

Transverse Joint Faulting. It is measured and reported by MODOT and LTPP as the difference in elevation to the nearest 1 mm between the pavement surfaces on either side of a transverse joint. The mean joint faulting for all joints within a 500-ft pavement section is reported. This is comparable to the MEPDG predicted faulting.

IRI. The values included in the MODOT PMS database are comparable to the MEPDG predicted IRI.

The second activity of step 5 is to compare the distress magnitudes to the trigger values for each distress. In other words, answer the question—Does the sampling template include

values close to the design criteria or trigger value? This comparison is important to provide answer if the collected pavement distress data could be properly utilized to validate and accurately determine the local calibration values. For example, low values of fatigue cracking measurements comparing to agency criteria is difficult to validate and accurately determine the local calibration values or adjustments for predicting the increase in cracking over time.

The distress data for each roadway segment included in the sampling template should be evaluated to ensure that the distress data are reasonable time-history plots. Any zeros that represent non-entry values should be removed from the local validation-calibration database. Distress data that return to zero values within the measurement period may indicate some type of maintenance or rehabilitation activity. Measurements should be taken after structural rehabilitation should be removed from the database or the observation period should end prior to the rehabilitation activity. Distress values that are zero as a result of some maintenance or pavement preservation activity, which is a part of the agency's management policy, should be removed but future distress observation values after that activity should be used. If the outliers or anomalies of data can be explained and are a result of some non-typical condition, they should be removed. If the outlier or anomaly cannot be explained, they should remain in the database.

The MEPDG pavement input database related to each selected roadway segment should be prepared to execute MEPDG software. The existing resource of these input data for level 3 analyses are agency PMS, traffic database, as-built plans, construction database files and etc. If adequate data for level 3 were unavailable, the mean value from the specifications was used or the average value determined for the specific input from other projects with similar condition. The default values of MEPDG could also be utilized in this case.

Step 6: Conduct Field and Forensic Investigations

Field and forensic investigations could be conducted to check the assumptions and conditions included in the MEPDG for the global (national) calibration effort. These field and forensic investigations include measuring the rutting in the individual layers, determining where the cracks initiated or the direction of crack propagation, and determining permanent curl/warp effective temperature and etc. The field and forensic investigations is not necessary if agency accepts the assumptions and conditions included in the MEPDG.

Step 7: Assess Local Bias from Global Calibration Factors

The MEPDG software is executed using the global calibration values to predict the performance indicators for each roadway segment selected. The null hypothesis is first checked for the entire sampling matrix. The null hypothesis in equation below is that the average residual error ($e_r = y_{Measured} - x_{predicted}$) or bias is zero for a specified confidence level or level of significance.

$$H_0 : \sum_{i=1}^n (y_{Measured} - x_{Predicted})_i = 0 \quad (\text{A.5})$$

It is helpful for assessment through making plots of a comparison between the predicted ($x_{predicted}$) and the measured values ($y_{Measured}$) and a comparison between the residual errors (e_r) and the predicted values ($x_{predicted}$) for each performance indicator (See Figure A.5).

Two other model parameters can be also used to evaluate model bias—the intercept (b_o) and slope (m) estimators using the following fitted linear regression model between the measured ($y_{Measured}$) and predicted ($x_{predicted}$) values.

$$\hat{y}_i = b_o + m(x_i) \quad (\text{A.6})$$

The intercept (b_o) and slope (m) estimators can provide not only accuracy quantity of each prediction but also identification of dependent factors such as pavement structure (new

construction versus rehabilitation) and HMA mixture type (conventional HMA versus Superpave mixtures) to each prediction. For illustration, Figure A.6 presents comparison of the intercept and slope estimators to the line of equality for the predicted and measured rut depths using the global calibration values.

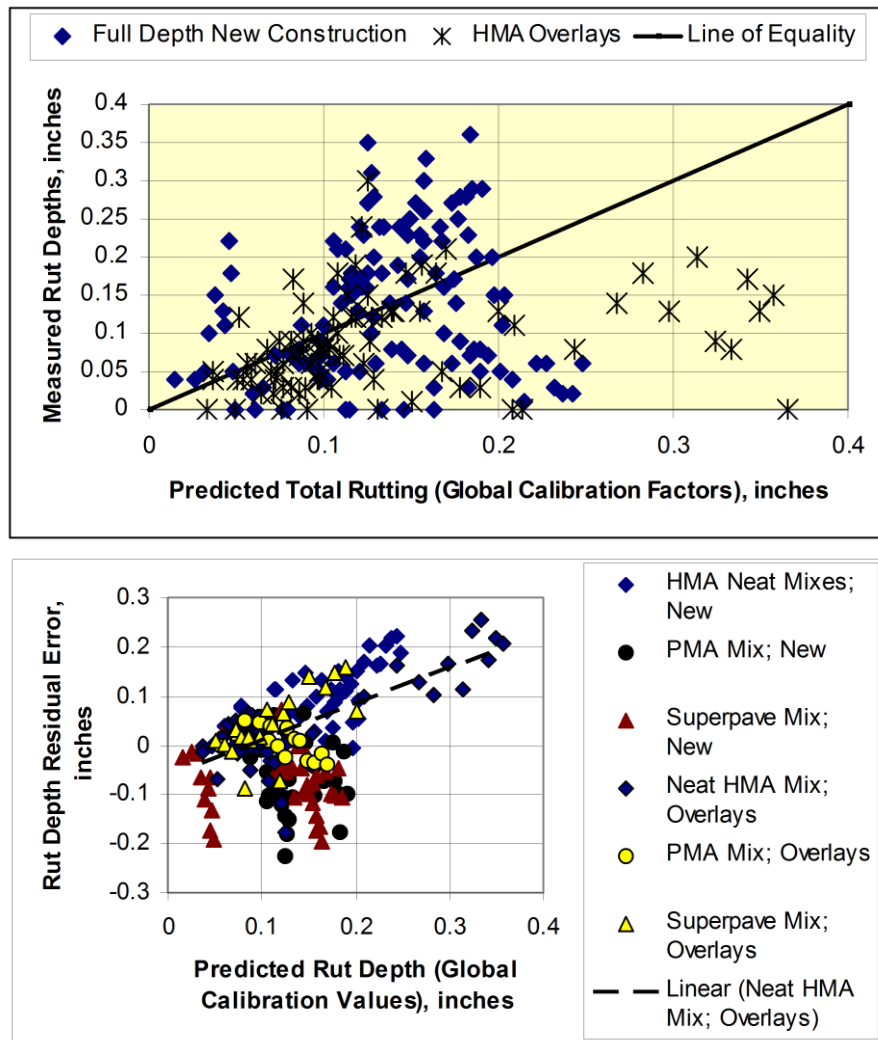
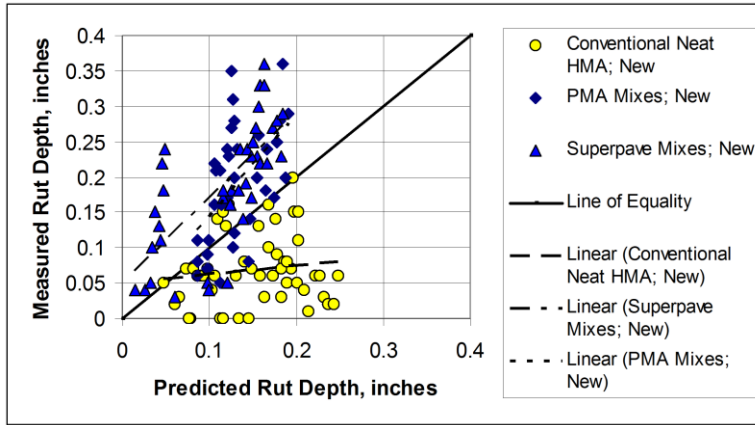
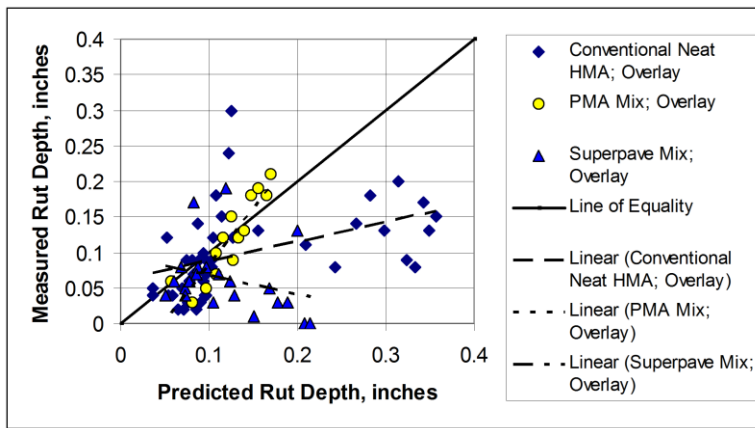


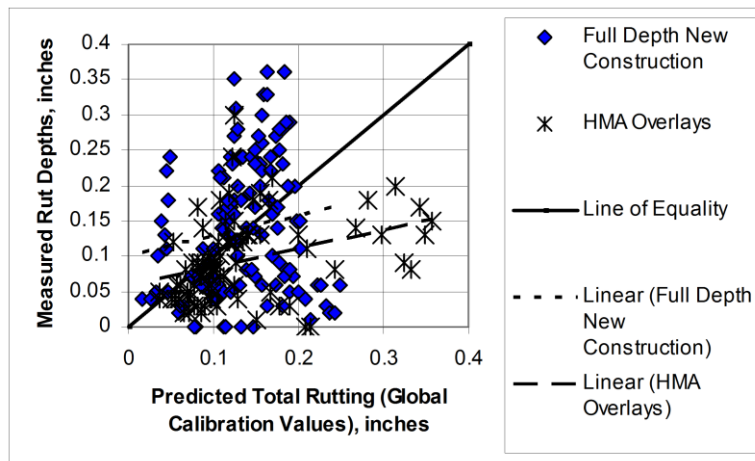
Figure A.5. Comparison of predicted and measured rut depths using the global calibration in KSDOT study (NCHRP 2009)



a. Intercept and slope estimators that are dependent on mixture type for the new construction PMS segments.



b. Intercept and slope estimators that are dependent on mixture type for the rehabilitation PMS segments.



c. Intercept and slope estimators that are structure dependent for the PMS segments.

Figure A.6. Comparison of the intercept and slope estimators to the line of equality for the predicted and measured rut depths using the global calibration values in KSDOT study (NCHRP 2009)

Step 8: Eliminate Local Bias of Distress Prediction Models

The MEPDG software includes two sets of parameters for local calibration of most performance indicator transfer functions. One set is defined as agency specific values and the other set as local calibration values. Figure A.7 shows a screen shot of the tools section where these values can be entered into the software for each performance indicator on a project basis. The default values of MEPDG performance indicator transfer functions are global calibration values for agency specific values (k_1 , k_2 , and k_3 in Figure A.7) and are one for local calibration values (β_1 , β_2 , and β_3 in Figure A.7). These parameters are used to make adjustments to the predicted values so that the difference between the measured and predicted values, defined as the residual error, is minimized. Either one can be used with success. Appendix A presents screen shots of the MEPDG software (Version 1.1) tools section for all of performance indicators of rehabilitated HMA pavement and new PCC pavement.

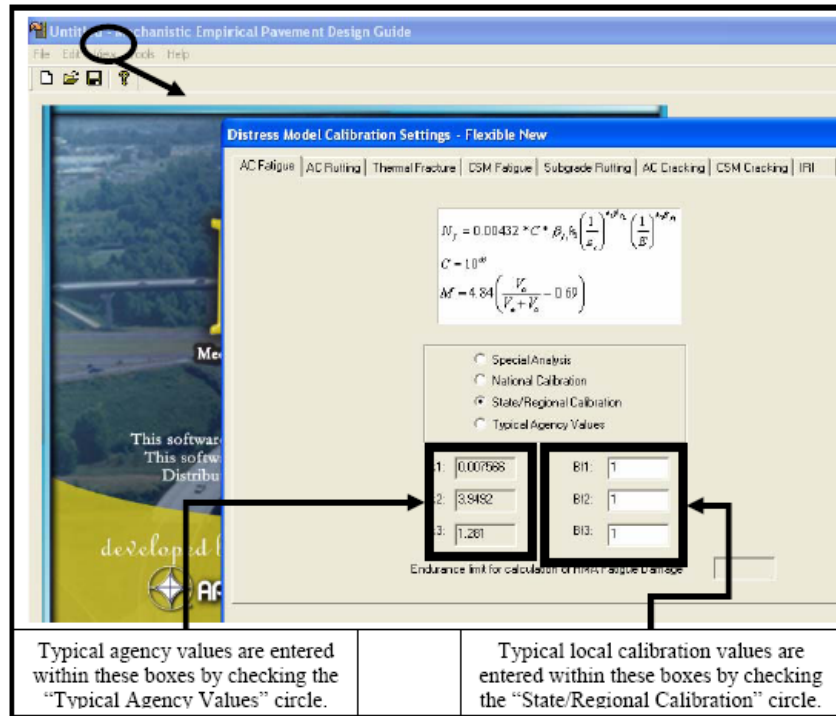


Figure A.7. Screen Shot of the MEPDG Software for the local calibration and agency specific values (Von Quintus 2008b)

NCHRP 1-40B project study (2009) lists the coefficients of the MEPDG transfer functions or distress and IRI prediction models that should be considered for revising the predictions to eliminate model bias for flexible pavements and HMA overlays. Table A.1 Table A.1. Calibration parameters to be adjusted for eliminating bias and reducing the standard error of the flexible pavement transfer functions (NCHRP 2009) from NCHRP 1-40B project study (2009) was prepared to provide guidance in eliminating any local model bias in the predictions. The distress specific parameters can be dependent on site factors, layer parameters, or policies of the agency.

Table A.1. Calibration parameters to be adjusted for eliminating bias and reducing the standard error of the flexible pavement transfer functions (NCHRP 2009)

(a) HMA pavements

Distress	Eliminate Bias	Reduce Standard Error
Rutting	k_{r1}, β_{s1} or β_{r1}	k_{r2}, k_{r3} , and β_{r2}, β_{r3}
Alligator cracking	C_2 or k_{f1}	k_{f2}, k_{f3} , and C_1
Longitudinal cracking	C_2 or k_{f1}	k_{f2}, k_{f3} , and C_1
Load related cracking – semi-rigid pavements	C_2 or β_{c1}	C_1, C_2 , and C_4
Thermal cracking	β_{t3}	β_{t3}
IRI	C_4	C_1, C_2 , and C_3

(b) PCC pavements

Distress	Eliminate Bias	Reduce Standard Error
Faulting	C_1	$C_2 - C_8$
JPCP transverse cracking	C_1 or C_4	C_2 and C_5
CRCP fatigue cracking	C_1	C_2
CRCP punchouts	C_3	C_4 and C_5
CRCP crack widths	C_6	C_6
JPCP IRI	C_4	C_1
CRCP IRI	C_4	C_1 and C_2

The process to eliminate the bias is applied to the globally calibrated pavement performance transfer functions found to result in bias from step 7. The process used to eliminate the bias depends on the cause of that bias and the accuracy desired by the agency. NCHRP 1-40B project study (NCHRP 2009) addresses three possibilities of bias and the bias elimination procedures corresponding to each possibility reproduced below.

1. The residual errors are, for the most part, always positive or negative with a low standard error of the estimate in comparison to the trigger value, and the slope of the residual errors versus predicted values is relatively constant and close to zero. In other words, the precision of the prediction model is reasonable but the accuracy is poor. In this case, the local calibration coefficient is used to reduce the bias. This condition generally requires the least level of effort and the fewest number of runs or iterations of the MEPDG with varying the local calibration values to reduce the bias. The statistical assessment described in step 7 should be conducted to the local calibrated pavement performance to check obtaining agency acceptable bias.
2. The bias is low and relatively constant with time or number of loading cycles, but the residual errors have a wide dispersion varying from positive to negative values. In other words, the accuracy of the prediction model is reasonable, but the precision is poor. In this case, the coefficient of the prediction equation is used to reduce the bias but the value of the local calibration coefficient is probably dependent on some site feature, material property, and/or design feature included in the sampling template. This condition generally requires more runs and a higher level of effort to reduce dispersion of the residual errors. The statistical assessment described in step 7 should be conducted to the local calibrated pavement performance to check obtaining agency acceptable bias.

3. The residual errors versus the predicted values exhibit a significant and variable slope that is dependent on the predicted value. In other words, the precision of the prediction model is poor and the accuracy is time or number of loading cycles dependent—there is poor correlation between the predicted and measured values. This condition is the most difficult to evaluate because the exponent of the number of loading cycles needs to be considered. This condition also requires the highest level of effort and many more MEPDG runs with varying the local calibration values to reduce bias and dispersion. The statistical assessment described in step 7 should be conducted to the local calibrated pavement performance to check obtaining agency acceptable bias.

Step 9: Assess Standard Error of the Estimate

After the bias was reduced or eliminated for each of the transfer functions, the standard error of the estimate (SEE, s_e) from the local calibration is evaluated in comparison to the SEE from the global calibration. The standard error of the estimate for each globally calibrated transfer function is included under the “Tools” section of the MEPDG software. Figure A.8 illustrates the comparison of the SEE for the globally calibrated transfer functions to the SEE for the locally calibrated transfer functions.

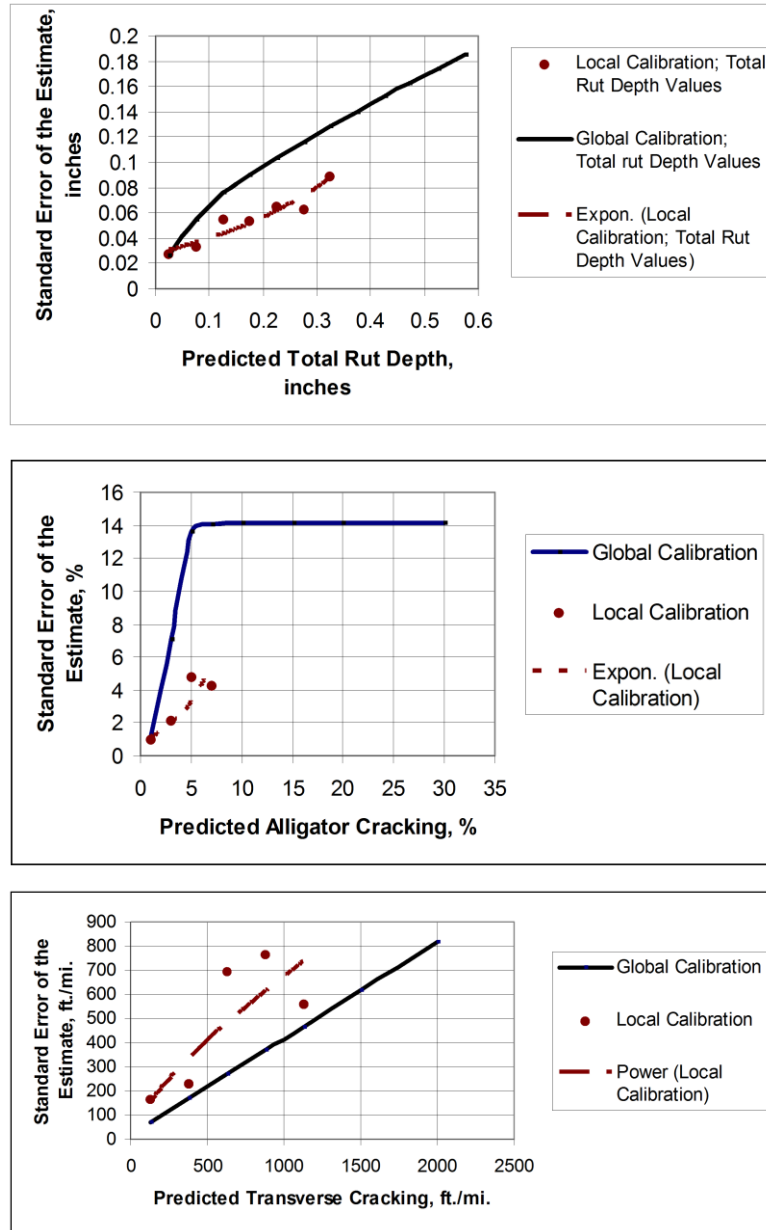


Figure A.8. Comparison of the standard error of the estimate for the global-calibrated and local-calibrated transfer function in KSDOT study (NCHRP 2009)

Step 10: Reduce Standard Error of the Estimate

If the SEE from the local calibration is found in step 9 to be statistically different in comparison to the SEE included in the MEPDG for each performance indicator, an statistical analysis of variance (ANOVA) can be conducted to determine if the residual error or bias is

dependent on some other parameter or material/layer property for the selected roadway segments. If no correlation would be identified, the local calibration factors determined from step 8 and the SEE values obtained from step 9 could be considered as the final products for the selected roadway segments. If some correlation to some parameters (for example, HMA mixture volumetric properties) would be identified, the local calibration values should be determined for each type in correlated parameters or new calibration function should be developed. NCHRP Project 1-40B and Von Quintus (2008b) documented HMA mixture specific factors used to modify or adjust the MEPDG global calibration factors for the rut depth and the bottom-up cracking transfer functions where sufficient data are available.

Step 11: Interpretation of Results and Deciding on Adequacy of Calibration Factors

The purpose of this step is to decide whether to adopt the local calibration values or continue to use the global values that were based on data included in the LTPP program from around the U.S. To make that decision, an agency should identify major differences between the LTPP projects and the standard practice of the agency to specify, construct, and maintain their roadway network. More importantly, the agency should determine whether the local calibration values can explain those differences. The agency should evaluate any change from unity for the local calibration parameters to ensure that the change provides engineering reasonableness.

NCHRP Synthesis 457 was issued in 2014 (NCHRP 2014) to document strategies for facilitating the implementation of MEPDG (and accompanying AASHTOWare Pavement ME Design™ software) and the reasons that some SHAs had not implemented MEPDG. This document is a product of surveys and follow-up questions with highway transportation agencies (U.S. state highway agencies, Puerto Rico, and the District of Columbia, and Canadian provincial and territorial governments). In total, 57 agencies [48 U.S. (92%) and nine Canadian

(69%) highway transportation agencies] provided responses to the agency survey. Among the 57 responding agencies, full implementation of the MEPDG was conducted by three agencies, forty-six indicated that they are in the process of implementation, and the remaining eight indicated that they have no plans at this time for implementing the MEPDG. The agencies were also requested to provide information about the pavement types they use.

New construction pavement types used by the responding agencies included thick asphalt pavement (46 agencies), JPCP (44 agencies), thin asphalt pavement (41 agencies), and semi-rigid pavement (29 agencies). Agencies also indicated designing full-depth asphalt pavements (21 agencies) and composite pavements (18 agencies), with nine agencies reported designing CRCP.

Responding agencies were also asked to provide information about pavement design methods they use. Table A.2 lists agency pavement design methods.

Table A.2. Agency Use of Pavement Design Methods (NCHRP 2014)

Method	New Construction		Rehabilitation		Number of Agencies
	Asphalt	Concrete	Asphalt	Concrete	
AASHTO 1972	7	2	5	1	7
AASHTO 1986	1	0	2	0	2
AASHTO 1993	35	23	31	19	39
AASHTO 1998 Supplement	4	11	4	8	13
AASHTO <i>MEPDG</i> ¹	12	10	10	7	13
Agency Empirical Procedure	7	1	9	3	13
WINPAS (ACPA 2012)	0	5	0	4	7
MS-1 (AI 1999)	1	0	3	0	3
ME-based Design Table or Catalog	1	3	0	2	3
Other ME Procedure	8	3	6	2	11
Other	5	7	7	8	14

¹A number of agencies indicated that the *MEPDG* is currently being used or under evaluation; however, only three agencies indicated that the *MEPDG* has been implemented.

Table A.3 presents a summary of agency responses about MEPDG use or planned use by pavement types.

Table A.3. Summary of MEPDG Use or Planned Use by Pavement Type (NCHRP 2014)

Pavement Type	Number of Responses
New asphalt pavement	45
New JPCP	39
Asphalt overlay of existing asphalt pavement	38
Asphalt overlay of existing JPCP	34
Asphalt overlay of existing fractured JPCP	27
Unbonded JPCP overlay of existing JPCP	22
JPCP overlay of existing asphalt pavement	21
Asphalt overlay of existing CRCP	15
Bonded overlay of existing JPCP	13
New CRCP	12
Asphalt overlay of existing fractured CRCP	11
Unbonded JPCP overlay of existing CRCP	11
CRCP overlay of existing flexible pavement	7
Unbonded CRCP overlay of existing JPCP	7
Bonded concrete overlay of existing CRCP	6
Unbonded CRCP overlay of existing CRCP	6

The agencies were also asked about their local calibration efforts. Table A.4 and Table A.5 list local calibration coefficients for agencies who conducted local calibration for concrete and asphalt pavements at the time of the survey.

Table A.4. Agency Local Calibration Coefficients—Concrete (NCHRP 2014)

Feature	MEPDG	Arizona	Colorado	Florida	Missouri
Cracking					
C1	2.0	2.0	2.0	2.8389	2.0
C2	1.22	1.22	1.22	0.9647	1.22
C4	1.0	0.19	0.6	0.5640	1.0
C5	-1.98	-2.067	-2.05	-0.5946	-1.98
Std. Dev.	¹	⁴	⁷	¹	¹
Faulting					
C1	1.0184	0.0355	0.5104	4.0472	1.0184
C2	0.91656	0.1147	0.00838	0.91656	0.91656
C3	0.002848	0.00436	0.00147	0.002848	0.002848
C4	0.000883739	1.1E-07	0.008345	0.000883739	0.000883739
C5	250	20000	5999	250	250
C6	0.4	2.309	0.8404	0.0790	0.4
C7	1.8331	0.189	5.9293	1.8331	1.8331
C8	400	400	⁸	400	400
Std. Dev.	²	⁵		²	²
Punchout					
C1	2.0	2.0	Not applicable	Not applicable	2.0
C2	1.22	1.22			1.22
C3	216.8421	85			216.8421
C4	33.15789	1.4149			33.15789
C5	-0.58947	-0.8061			-0.58947
Crack	¹	¹			¹
Std. Dev.	³	⁶		³	
IRI (CRCP)					
C1	3.15	3.15	Not applicable	Not applicable	3.15
C2	28.35	28.35			28.35
Std. Dev.	5.4	5.4			5.4
IRI (JPCP)					
J1	0.8203	0.6	0.8203	0.8203	0.82
J2	0.4417	3.48	0.4417	0.4417	1.17
J3	1.4929	1.22	1.4929	2.2555	1.43
J4	25.24	45.2	25.24	25.24	66.8
Std. Dev.	5.4	5.4	5.4	5.4	5.4

¹Pow(5.3116 x CRACK,0.3903) + 2.99

²Pow(0.0097 x FAULT,0.05178) + 0.014

³2 + 2.2593 x Pow(0.4882 x PO)

⁴Pow(9.87x CRACK,0.4012) + 0.5

⁵Pow(0.037 x FAULT,0.6532) + 0.001

⁶1.5 + 2.9622 x Pow(PO,0.4356)

⁷Pow(57.08 x CRACK, 0.33) + 1.5

⁸0.0831 x Pow(FAULT,0.3426) + 0.00521

⁹0.1 for A-7-6 soils

¹⁰0.001 for A-7-6 soils

¹¹3 for A-7-6 soils

Table A.5. Agency Local Calibration Coefficients—Asphalt (NCHRP 2014)

Feature	MEPDG	Arizona	Colorado	Missouri	Oregon
Cracking					
C1 Bottom	1.0	1.0	0.07	1.0	0.56
C1 Top	7.0	7.0	7.0	7.0	1.453
C2 Bottom	1.0	4.5	2.35	1.0	0.225
C2 Top	3.5	3.5	3.5	3.5	0.097
C3 Bottom	6000	6000	6000	6000	6000
C3 Top	0	0	0	0	0
C4 Top	1000	1000	1000	1000	1000
Std. Dev. Top	¹	¹	¹	¹	¹
Std. Dev. Bottom	²	²	¹²	²	²
Fatigue					
BF1	1	249.00872	130.3674	1	1
BF2	1	1	1	1	1
BF3	1	1.23341	1.2178	1	1
Thermal Fracture					
Level 1	1.5	1.5	7.5	0.625	1.5
Level 2	0.5	0.5	0.5	0.5	0.5
Level 3	1.5	1.5	1.5	1.5	1.5
Std. Dev. (Level 1)	³	³	³	³	³
Std. Dev. (Level 2)	⁴	⁴	⁴	⁴	⁴
Std. Dev. (Level 3)	⁵	⁵	⁵	⁵	⁵
Rutting (asphalt)					
BR1	1.0	0.69	1.34 ¹³		1.48
BR2	1.0	1.0	1.0		1.0
BR3	1.0	1.0	1.0		0.9
Std. Dev.	⁶	⁹	¹⁴	⁶	⁶
Rutting (subgrade)					
BS1 (fine)	1.0	0.37	0.84	0.4375	1.0
Std. Dev. (fine)	⁷	¹⁰	¹⁵	⁷	⁷
BS1 (granular)	1.0	0.14	0.4	0.01	1.0
Std. Dev. (granular)	⁸	¹¹	¹⁶	⁸	⁸
IRI					
C1 (asphalt)	40	1.2281	35	17.7	40
C2 (asphalt)	0.4	0.1175	0.3	0.975	0.4
C3 (asphalt)	0.008	0.008	0.02	0.008	0.008
C4 (asphalt)	0.015	0.028	0.019	0.01	0.015
C1 (over concrete)	40.8	40.8	40.8	40.8	40.8
C2 (over concrete)	0.575	0.575	0.575	0.575	0.575
C3 (over concrete)	0.0014	0.0014	0.0014	0.0014	0.0014
C4 (over concrete)	0.00825	0.00825	0.00825	0.00825	0.00825

¹200 + 2300/(1 + exp(1.072 - 2.1654 x LOG₁₀(TOP + 0.0001)))

²1.13 + 13/(1 + exp(7.57 - 15.5 x LOG₁₀(BOTTOM + 0.0001)))

³0.1468 x THERMAL + 65.027

⁴0.2841 x THERMAL + 55.462

⁵0.3972 x THERMAL + 20.422

⁶0.24 x Pow(RUT, 0.8026) + 0.001

⁷0.1235 x Pow(SUBRUT, 0.5012) + 0.001

⁸0.1447 x Pow(BASERUT, 0.6711) + 0.001

⁹0.0999 x Pow(RUT, 0.174) + 0.001

¹⁰0.05 x Pow(SUBRUT, 0.085) + 0.001

¹¹0.05 x Pow(BASERUT, 0.115) + 0.00110

¹²1 + 15(1 + exp(-1.6673 - 2.4656*LOG₁₀(BOTTOM+0.0001)))

¹³Under review

¹⁴0.2052 x Pow(RUT,0.4) + 0.001

¹⁵0.1822 x Pow(SUBRUT, 0.5) + 0.001

¹⁶0.2472 x Pow(BASERUT, 0.67) + 0.001

¹⁷0.01 for A-7-6 soil

FHWA Projects

Two research study supported by FHWA have been conducted to use (PMIS) data for local calibration of MEPDG. One is “*Using Pavement Management Data to Calibrate and Validate the New MEPDG, An Eight State Study* (FHWA 2006a, FHWA 2006b).” This study evaluated the potential use of PMIS on MEPDG calibrations from eight participated states: Florida, Kansas, Minnesota, Mississippi, New Mexico, North Carolina, Pennsylvania, and Washington. The study concluded that all the participating states could feasibly use PMIS data on MEPDG calibrations and others states not participating in this study could also do. It is recommended that each SHA should develop a satellite pavement management/pavement design database for each project being designed and constructed using the MEPDG in part of current PMIS used.

As following previous one, *FHWA HIF-11-026 research project the local calibration of MEPDG using pavement management system* (FHWA 2010a, FHWA 2010b) was conducted to develop a framework for using existing PMIS to calibrate the MEPDG performance model. One state (North Carolina) was selected from screening criteria to finalize and verify the MEPDG calibration framework based on the set of actual conditions. As following developed framework, local calibration of a selected state was demonstrated under the assumptions of both MEPD performance predictions established from NCHRP 1-37 A and distress measurements from a selected state. Note that NC DOT used **subjective distress rating** with severity in accordance to state DOT manual rather than LTPP manual. Table A.6 listed the assumptions used for MEPDG local calibration in this study.

Table A.6. List of assumptions in MEPDG local calibration of NC under FHWA HIF-11-026 research project (FHWA 2010)

Type	Performance Predictions ¹	Assumptions
HMA	Rutting	<ul style="list-style-type: none"> • Rutting measurement was assumed to progress from zero to the assumed numeric value over the life of the pavement in order to convert NCDOT subjective rut rating into an estimated measured value. <ul style="list-style-type: none"> ✓ Low severity – 0.5 in. (12.7 mm). ✓ Moderate severity – 1.0 in. ✓ High severity – Not applicable • Rut depth progression was based on the number of NCDOT rut depth ratings and distributed over the measurement period to best reflect the slope of the MEPDG predicted rut depth over time. • For HMA overlay, the rut condition prior to the applied overlay was selected.
	Alligator Cracking	<ul style="list-style-type: none"> • A sigmoid function form of MEPDG alligator cracking is the best representation of the relationship between cracking and damage. The relationship must be “bounded” by 0 ft² cracking as a minimum and 6,000 ft² cracking as a maximum². • Alligator cracking is to 50 percent cracking of the total area of the lane (6000 ft²) at a damage percentage of 100 percent². • Since alligator cracking is related to loading and asphalt layer thickness, alligator crack prediction is similar for a wide range of temperatures². • All load-related cracking was considered to initiate from the bottom up (alligator cracking). • The alligator cracking measurement was estimated from tensile strains at the bottom of the asphalt layer calculated from a layer elastic analysis program by inputting MEPDG asphalt dynamic modulus corresponding to the NCDOT measured alligator distress rating. • The estimated alligator cracking measurement was distributed over the age of the pavement section.

	Thermal Cracking	<ul style="list-style-type: none"> • The model will not predict thermal cracking on more than 50 percent of the total section length². • The maximum length of thermal cracking is 4224 ft/mi (400 ft/500 ft × 5280 ft/1mi)². • Cracks were assumed to be full-lane width (i.e., 12 ft) for all severity levels. • For each pavement section, the section length was divided by the reported NCDOT cracking frequency and multiplied by the crack length (assumed to be 12 ft) to obtain the total estimated crack length per pavement section. • As with rutting and alligator cracking, the distress severity from the last NCDOT survey was used to calculate the thermal cracking numeric value.
JPCP	Transverse Cracking	<ul style="list-style-type: none"> • JPCP in NCDOT was assumed to be designed on average perform to the selected design criteria (15 percent slab cracking) at the specified reliability (90 percent). • The layer properties for these design runs were selected primarily as default values, as were most of the traffic characteristics.
	Faulting	<ul style="list-style-type: none"> • The layer properties for these design runs were selected primarily as default values, as were most of the traffic characteristics.

¹Longitudinal cracking, reflection cracking, and smoothness were not considered in calibration due to lack of data and deficiency of model.

² The assumptions made from MEPDG performance models in NCHRP 1-37 A.

MEPDG/Pavement ME Design Local Calibration Studies in State Level

As apart to national level projects, multiple State level research efforts have been being conducted regarding the local calibration of the MEPDG involving each step described in NCHRP 1-40B study. However, not many research studies for MEPDG validation in local sections have been finalized because the MEPDG has constantly been updated through NCHRP

projects (2006a; 2006b) after the release of the initial MEPDG software (Version 0.7). This section summarizes up to date MEPDG local calibration research efforts at the State level.

Flexible Pavements

A study by Galal and Chehab (2005) in Indiana compared the distress measures of existing HMA overlay over a rubblized PCC slab section using AASHTO 1993 design with the MEPDG (Version 0.7) performance prediction results using the same design inputs. The results indicated that MEPDG provide good estimation to the distress measure except top-down cracking. They also emphasized the importance of local calibration of performance prediction models.

Montana DOT conducted the local calibration study of MEPDG for flexible pavements (Von Quintus and Moulthrop 2007). In this study, results from the NCHRP 1-40B (Von Quintus et al. 2005) verification runs were used to determine any bias and the standard error, and compare that error to the standard error reported from the original calibration process that was completed under NCHRP Project 1-37A (NCHRP 2004). Bias was found for most of the distress transfer functions. National calibration coefficients included in Version 0.9 of the MEPDG were used initially to predict the distresses and smoothness of the Montana calibration refinement test sections to determine any prediction model bias. These runs were considered a part of the validation process, similar to the process used under NCHRP Projects 9-30 and 1-40B. The findings from this study are summarized for each performance model as shown below:

- Rutting prediction model: the MEPDG over-predicted total rut depth because significant rutting was predicted in unbound layers and embankment soils.
- Alligator cracking prediction model: the MEPDG fatigue cracking model was found to be reasonable.

- Longitudinal cracking prediction model: no consistent trend in the predictions could be identified to reduce the bias and standard error, and improve the accuracy of this prediction model. It is believed that there is a significant lack-of-fit modeling error for the occurrence of longitudinal cracks.
- Thermal cracking prediction model: the MEPDG prediction model with the local calibration factor was found to be acceptable for predicting transverse cracks in HMA pavements and overlays in Montana.
- Smoothness prediction model: the MEPDG prediction equations are recommended for use in Montana because there are too few test sections with higher levels of distress in Montana and adjacent States to accurately revise this regression equation.
- Von Quintus (2008b) summarized the flexible pavement local calibration value results of the MEPDG from NCHRP project 9-30, 1-40 B, and Montana DOT studies listed in Table A.7. These results originally from Von Quintus (2008b) present in Table A.8 to Table A.9 for the rut depth, fatigue cracking, and thermal cracking transfer functions. These could be useful reference for states having similar conditions of studied sites. The detailed information of studied sites is described in Von Quintus (2008b).

Table A.7. Listing of local validation-calibration projects (Von Quintus 2008b)

Project Identification	Transfer Functions Included in the Local Validation and/or Calibration Efforts for Each Project				
	Rut Depths	Area Cracking	Longitudinal Cracking	Thermal Cracking	Smoothness or IRI
NCHRP Projects 9-30 & 1-40B; <i>Local Calibration Adjustments for HMA Distress Prediction Models in MEPDG Software</i> , (Von Quintus, et al., 2005a & b)	√	√	√		
Montana DOT, <i>MEPDG Flexible Pavement Performance Prediction Models for Montana</i> , (Von Quintus & Moulthrop, 2007a & b)	√	√	√	√	√
NCHRP Project 1-40B, <i>Examples Using Recommended Practice for Local Calibration of MEPDG Software</i> , Kansas Pavement Management Data, (Von Quintus, et al., 2008b)	√	√		√	√
NCHRP Project 1-40B, <i>Examples Using Recommended Practice for Local Calibration of MEPDG Software</i> , LTPP SPS-1 and SPS-5 Projects, (Von Quintus, et al., 2008b)	√	√		√	√

Table A.8. Summary of local calibration values for the rut depth transfer function (Von Quintus 2008b)

Project Identification		Unbound Materials/Soils, β_{s1}		HMA Calibration Values		
		Fine-Grained	Coarse-Grained	β_{r1}	β_{r3}	β_{r2}
NCHRP Projects 9-30 & 1-40B; Verification Studies, Version 0.900 of the MEPDG.		0.30	0.30	Values dependent on volumetric properties of HMA; the values below represent the overall range.		
		Insufficient information to determine effect of varying soil types.		6.9 to 10.8	0.65 to 0.90	0.90 to 1.10
Montana DOT; Based on version 0.900 of the MEPDG		0.30	0.30	Values dependent on the volumetric properties of HMA; the values below represent overall averages.		
				7.0	0.70	1.13
Kansas DOT; PM Segments; HMA Overlay Projects; All Mixtures (Version 1.0)		0.50	0.50	1.5	0.95	1.00
Kansas PM Segments; New Construction	Convent	0.50	0.50	1.5	0.90	1.00
	Superpave			1.5	1.20	1.00
	PMA			2.5	1.15	1.00
LTPP SPS-1 & SPS-5 Projects built in accordance with specification; conventional HMA mixtures (Version 1.0).		0.50	0.50	Value dependent on the air void & asphalt content		1.00
				1.25 to 1.60	0.90 to 1.15	1.00
LTPP SPS-1 Projects with anomalies or construction difficulties, unbound layers.		Values dependent on density and moisture content; values below represent the range found.		---	---	---
		0.50 to 1.25	0.50 to 3.0			

Table A.9. Summary of local calibration values for the area fatigue cracking transfer function (Von Quintus 2008b)

Project Identification		β_{f1}	β_{f2}	β_{f3}	C_2
NCHRP Projects 9-30 & 1-40B; Verification Studies, Version 0.900 of the MEPDG		Values dependent on the volumetric properties.			
		0.75 to 10.0	1.00	0.70 to 1.35	1.0 to 3.0
Montana DOT; Based on version 0.900 of the MEPDG, with pavement preservation treatments		Values dependent on the volumetric properties.			
		13.21	1.00	1.25	1.00
Northwest Sites; Located in States Adjacent to Montana, without pavement preservation treatments		Values dependent on the volumetric properties.			
		1.0 to 5.0	1.00	1.00	1.0 to 3.0
Kansas DOT; PM Segments; HMA Overlay Projects; All HMA Mixtures		0.05	1.00	1.00	1.00
Kansas DOT; PM Segments; New Construction	Conventional HMA Mixes	0.05	1.00	1.00	1.00
	PMA	0.005	1.00	1.00	1.00
	Superpave	0.0005	1.00	1.00	1.00
Mid-West Sites	LTPP SPS-1 Projects built in accordance with specifications	0.005	1.00	1.00	1.00
	LTPP SPS-1 Projects with anomalies or production difficulties	1.00	1.00	1.00	1.0 to 4.0
	LTPP SPS-5 Projects; Debonding between HMA Overlay and Existing Surface	0.005	1.00	1.00	1.0 to 4.0

Table A.10. Summary of the local calibration values for the thermal cracking transfer function (Von Quintus 2008b)

Project Identification		β_{t1}	β_{t2}	β_{t3}
Montana DOT; application of pavement preservation treatments.		---	---	0.25
Northwest Sites, located in states adjacent to Montana, but without pavement preservation treatments; appears to be agency dependent.		---	---	1.0 to 5.0
Kansas PM Segments; Full-Depth Projects	PMA	---	---	2.0
	Conventional	---	---	2.0
	Superpave	---	---	3.5
Kansas PMS Segments; HMA Overlay Projects	PMA	---	---	2.0
	Conventional	---	---	7.5
	Superpave	---	---	7.5
LTPP Projects; HMA produced in accordance with specifications	Conventional	---	---	Dependent on Asphalt Content & Air Voids
LTPP Projects; Severely aged asphalt	Conventional	---	---	7.5 to 20.0

Kang et al. (2007) prepared a regional pavement performance database for a Midwest implementation of the MEPDG. They collected input data required by the MEPDG as well as measured fatigue cracking data of flexible and rigid pavements from Michigan, Ohio, Iowa and Wisconsin State transportation agencies. They reported that the gathering of data was labor-intensive because the data resided in various and incongruent data sets. Furthermore, some pavement performance observations included temporary effects of maintenance and those observations must be removed through a tedious data cleaning process. Due to the lack of reliability in collected pavement data, the calibration factors were evaluated based on Wisconsin data and the distresses predicted by national calibration factors were compared to the field collected distresses for each state except Iowa. This study concluded that the default national calibration values do not predict the distresses observed in the Midwest. The collection of more reliable pavement data is recommended for a future study.

Schram and Abdelrahman (2006) attempted to calibrate two of MEPDG IRI models for the Jointed Plain Concrete Pavement (JPCP) and the HMA overlays of rigid pavements at the

local project-level using Nebraska Department of Roads (NDOR) pavement management data. The focused dataset was categorized by annual daily truck traffic (ADTT) and surface layer thickness. Three categories of ADTT were considered: low (0 – 200 trucks/day), medium (201 – 500 trucks/day), and high (over 500 trucks/day). The surface layer thicknesses considered ranged from 6 inches to 14 inches for JPCP and 0 to 8 inches for HMA layers. Results showed that project-level calibrations reduced default model prediction error by nearly twice that of network-level calibration. Table A.11 and Table A.12, as reported from this study, contain coefficients for the smoothness model of HMA overlays of rigid pavements and JPCP.

Table A.11. HMA overlaid rigid pavements' IRI calibration coefficients for surface layer thickness within ADTT (Schram and Abdelrahman 2006)

ADTT	Thickness	C1	C2	C3	N	R ²	SEE (m/km)
Low	2"-3"	0.1318	0.0018	0.3971	3	0.994	0.02
	4"-5"	0.0704	-0.0048	-2.8771	16	0.813	0.11
	5"-6"	-0.0038	0.2409	-4.6360	5	0.039	1.15
Medium	2"-3"	0.0639	0.1337	-0.7896	21	0.612	0.5
	3"-4"	0.0733	0.0282	1.4725	65	0.532	0.36
	4"-5"	0.0781	-0.0032	1.1116	82	0.546	0.31
	5"-6"	0.0649	0.0169	3.5543	84	0.535	0.31
	6"-7"	0.0794	-0.0312	4.3652	31	0.888	0.17
	7"-8"	0.0674	-0.0164	1.7122	19	0.674	0.13
	8"-9"	0.0683	0.0192	-3.6231	13	0.936	0.1
High	0"-1"	0.2019	0.1158	-10.0646	27	0.392	0.45
	2"-3"	0.1866	0.0498	-16.7082	19	0.565	0.6
	3"-4"	0.1835	-0.0579	8.1863	32	0.010	0.9
	4"-5"	0.1170	-0.0100	1.4057	101	0.299	0.51
	5"-6"	0.2422	0.0371	-23.4448	62	0.713	0.85
	6"-7"	0.0756	0.0127	0.9250	64	0.597	0.22
	7"-8"	0.0604	0.0574	-2.4936	7	0.624	0.2
	8"-9"	0.0578	0.0706	-10.9179	28	0.103	0.25
	9"-10"	0.1005	-0.0001	-0.5216	8	0.845	0.13

Table A.12. JPCP IRI calibration coefficients for surface layer thickness within ADTT (Schram and Abdelrahman 2006)

ADTT	Thickness	C1	C2	C3	C4	N	R ²	SEE (in/mi)
Low	6"-7"	0.0000	0.0000	1.0621	74.8461	33	0.434	26.885
	7"-8"	0.0000	0.0000	1.9923	46.9256	37	0.961	8.235
	8"-9"	0.8274	0.0000	0.0000	86.9721	39	0.904	14.465
	9"-10"	0.3458	0.0000	1.5983	64.3453	110	0.537	26.230
	10"-11"	0.0300	0.0000	3.4462	10.7893	37	0.893	17.280
	11"-12"	--	--	--	--	--	--	--
	12"-13"	--	--	--	--	--	--	--
	13"-14"	--	--	--	--	--	--	--
Medium	6"-7"	0.0000	0.0000	4.1422	0.0000	3	0.966	5.094
	7"-8"	0.0000	1.5628	0.0000	71.9009	22	0.968	9.952
	8"-9"	0.0000	0.0000	1.7162	53.0179	122	0.291	40.537
	9"-10"	0.1910	0.0000	0.9644	89.3990	609	0.686	24.945
	10"-11"	0.0000	0.0000	2.0945	73.1246	314	0.812	18.535
	11"-12"	0.0000	0.0090	1.3617	100.0000	27	0.792	10.166
	12"-13"	--	--	--	--	--	--	--
	13"-14"	0.0000	0.0100	2.2226	24.9354	4	0.924	3.948
High	6"-7"	--	--	--	--	--	--	--
	7"-8"	--	--	--	--	--	--	--
	8"-9"	0.0000	0.1376	0.4352	79.5526	46	0.151	48.576
	9"-10"	0.1561	0.0000	1.1024	62.9556	81	0.333	31.255
	10"-11"	0.0000	0.0000	1.6344	100.0000	228	0.653	22.295
	11"-12"	0.1125	1.8207	1.1678	100.0000	29	0.739	13.366
	12"-13"	0.0000	0.0000	1.5331	100.0000	151	0.719	17.724
	13"-14"	0.0100	0.0100	0.5184	0.0000	4	0.623	1.728
14"-15"	0.1904	0.0000	2.1387	51.4053	146	0.838	9.018	

Muthadi and Kim (2008) performed the calibration of MEPDG for flexible pavements located in North Carolina (NC) using version 1.0 of MEPDG software. Two distress models, rutting and alligator cracking, were used for this effort. A total of 53 pavement sections were selected from the LTPP program and the NC DOT databases for the calibration and validation process. Based on calibration procedures suggested by NCHRP 1-40B study, the flow chart was made for this study. The verification results of MEPDG performance models with national

calibration factors showed bias (systematic difference) between the measured and predicted distress values. The Microsoft Excel Solver program was used to minimize the sum of the squared errors (SSE) of the measured and the predicted rutting or cracking by varying the coefficient parameters of the transfer function. Table A.13 lists local calibration factors of rutting and alligator cracking transfer functions obtained in this study. This study concluded that the standard error for the rutting model and the alligator cracking model is significantly less after the calibration.

Table A.13. North Carolina local calibration factors of rutting and alligator cracking transfer functions (Muthadi and Kim 2008)

Recalibration	Calibration Coefficient	National Calibration	National Recalibration	Local Calibration
Rutting				
AC	k_1	-3.4488	-3.35412	-3.41273
	k_2	1.5606	1.5606	1.5606
	k_3	0.479244	0.479244	0.479244
GB	β_{GB}	1.673	2.03	1.5803
SG	β_{SG}	1.35	1.67	1.10491
Fatigue				
AC	k_1	0.00432	0.007566	0.007566
	k_2	3.9492	3.9492	3.9492
	k_3	1.281	1.281	1.281
	C_1	1	1	0.437199
	C_2	1	1	0.150494

The Washington State DOT (Li et al. 2009) developed procedures to calibrate the MEPDG (version 1.0) flexible pavement performance models using data obtained from the Washington State Pavement Management System (WSPMS). Calibration efforts were concentrated on the asphalt mixture fatigue damage, longitudinal cracking, alligator cracking, and rutting models. There were 13 calibration factors to be considered in the four related models. An elasticity analysis was conducted to describe the effects of those calibration factors on the pavement distress models. I.e., the higher the absolute value of elasticity, the greater impact the

factor has on the model. The calibration results of typical Washington State flexible pavement systems determined from this study presents in Table A.. This study also reported that a version 1.0 of MEPDG software bug does not allow calibration of the roughness model.

Table A.14. Local calibrated coefficient results of typical Washington State flexible pavement systems (Li et al. 2009)

Calibration Factor	Default	Calibrated Factors
AC Fatigue	B _{r1} 1	0.96
	B _{r2} 1	0.97
	B _{r3} 1	1.03
Longitudinal cracking	C1 7	6.42
	C2 3.5	3.596
	C3 0	0
	C4 1000	1000
Alligator cracking	C1 1	1.071
	C2 1	1
	C3 6000	6000
AC Rutting	B _{r1} 1	1.05
	B _{r2} 1	1.109
	B _{r3} 1	1.1
Subgrade Rutting	B _{s1} 1	0
IRI	C1 40	—
	C2 0.4	—
	C3 0.008	—
	C4 0.015	—

Similar to the study conducted in NC (Muthadi and Kim 2008), Banerjee et al. (2009) minimized the SSE between the observed and the predicted surface permanent deformation to determine the coefficient parameters (β_{r1} and β_{r3}) of HMA permanent deformation performance model after values based on expert knowledge assumed for the subgrade permanent deformation calibration factors (β_{s1}) and the HMA mixture temperature dependency calibration factors (β_{r2}). Pavement data from the Texas SPS-1 and SPS-3 experiments of the LTPP database were used to run the MEPDG and calibrate the guide to Texas conditions. The set of state-default calibration coefficients for Texas was determined from joint minimization of the SSE for all the sections after the determination of the Level 2 input calibration coefficients for each section. The results of calibration factors as obtained from this study are given in Figure A.9. Banerjee et al. (2011)

also determined the coefficient parameters (β_{r1} and β_{r3}) of rutting for rehabilitated flexible pavements under six of regional area in U.S.

Valesquez et al. (2009) evaluated the sensitivity of input parameters for pavement performance prediction models in Minnesota. Longitudinal cracking prediction of the nationally calibrated MEPDG were found to be poor.

Titus-Glover and Mallela (2009) investigated the implementation of NCHRP 1-37A ME design procedure in Ohio. The local calibration of rutting and IRI models of flexible pavement was implemented.

Souliman et al. (2010) presented the calibration of the MEPDG (Version 1.0) predictive models for flexible pavement design in Arizona conditions. This calibration was performed using 39 Arizona pavement sections included in the LTPP database. The results of calibration factors as obtained from this study are given in Table A.15.

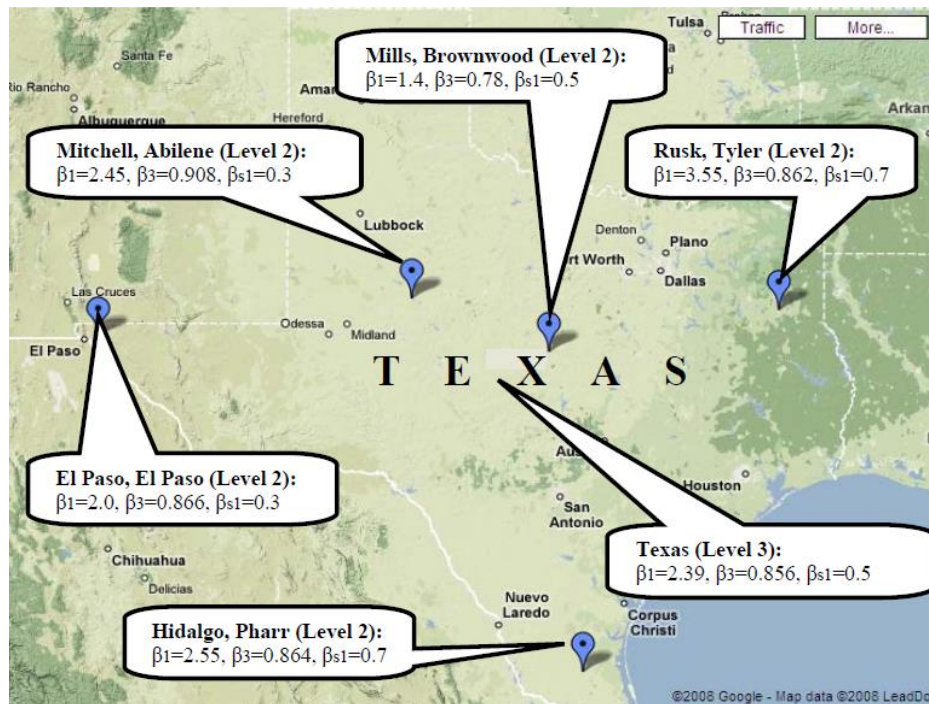


Figure A.9. Regional and state level calibration coefficients of HMA rutting depth transfer function for Texas (Banerjee et al. 2009)

Table A.15. Calibration coefficients of the MEPDG flexible pavement distress models in Arizona conditions (Souliman et al. 2010)

MEPDG Model	Coefficients before Calibration	Coefficients after Calibration	Net Effect of Calibration
Alligator Fatigue Transfer Function	$\beta_{fl} = 1$	$\beta_{fl} = 0.729$	Increased prediction
	$\beta_{f2} = 1$	$\beta_{f2} = 0.8$	
	$\beta_{f3} = 1$	$\beta_{f3} = 0.8$	
	$C_1 = 1.0$	$C_1 = 0.732$	
	$C_2 = 1.0$	$C_2 = 0.732$	
Longitudinal Fatigue Transfer Function	$\beta_{fl} = 1$	$\beta_{fl} = 0.729$	Decreased prediction
	$\beta_{f2} = 1$	$\beta_{f2} = 0.8$	
	$\beta_{f3} = 1$	$\beta_{f3} = 0.8$	
	$C_1 = 7.0$	$C_1 = 1.607$	
	$C_2 = 3.5$	$C_2 = 0.803$	
AC Rutting Model	$\beta_{r1} = 1$	$\beta_{r1} = 3.63$	Increased prediction
	$\beta_{r2} = 1$	$\beta_{r2} = 1.1$	
	$\beta_{r3} = 1$	$\beta_{r3} = 0.7$	
Granular base Rutting Model	$\beta_{gb} = 1$	$\beta_{gb} = 0.111$	Decreased prediction
Subgrade Rutting Model	$\beta_{sg} = 1$	$\beta_{sg} = 1.38$	Increased prediction
Roughness Model	$C_1 = 40$	$C_1 = 5.455$	Decreased prediction
	$C_2 = 0.4$	$C_2 = 0.354$	
	$C_3 = 0.008$	$C_3 = 0.008$	
	$C_4 = 0.015$	$C_4 = 0.015$	

Hoegh et al. (2010) utilized time history rutting performance data for pavement sections at the Minnesota Department of Transportation (MnDOT) full-scale pavement research facility (MnROAD) for an evaluation and local calibration of the MEPDG rutting model. Instead of an adjustment of the calibration parameters in current MEPDG rutting model, a modified rutting model was suggested to account for the forensic and predictive evaluations on the local conditions. This study demonstrated that current MEPDG subgrade and base rutting models grossly overestimate rutting for the MnROAD test sections. Instead of calibration of fatigue cracking performance model, Velasquez et al (2009) calibrated MEPDG fatigue damage model against MnPAVE which is mechanistic-empirical design based software calibrated in Minnesota. The alligator cracking predicted by the MEPDG was approximately 5 times greater than that predicted by MnPAVE. This difference has been minimized by setting up 0.1903 of fatigue damage model coefficient B_{fl} .

Glover and Mallela (2009) calibrated MEPDG rutting and IRI models by using LTPP data of Ohio roads. Due to lack data (no distress observation or record), the other distress predictions were not calibrated. Similar to Ohio study, Darter et al (2009) could calibrate only MEPDG rutting model due to lack of data. However, they found the national calibrated IRI model of flexible pavement produce good of fit between measured and prediction IRI and SEE approximately the same as that reported in NCHRP 1-37A study.

Some type of maintenance or rehabilitation activity can make actual distress measurements decrease in distress time-history plots (Kim et al 2010). Banerjee et al. (2010) found that the calculation factors of MEPDG permanent deformation performance models are influenced by maintenance strategies. Liu et al. (2010) suggested historical pavement performance model to account for rehabilitation or maintenance activity using piecewise approximation. The whole pavement serviceable life was divided into three zones: Zone 1 for the early age pavement distress, Zone 2 in rehabilitation stage, and Zone 3 for over-distressed situations. The historical pavement performance data were regressed independently in each time zone. This approach is able to accurately predict the pavement distress progression trends in each individual zone by eliminating the possible impacts from the biased data in the other zones. It is also possible to compare the pavement distress progression trends in each individual zone with the MEPDG incremental damage approach predictions.

Mamlouk and Zapata (2010) discussed differences between the Arizona Department of Transportation (ADOT) PMS data and the LTPP database used in the original development and national calibration of the MEPDG distress models. Differences were found between: rut measurements, asphalt cracking, IRI, and all layer back calculated moduli found from NDT measurements done by ADOT and those of the LTPP. Differences in distress data include types

of data measured, types of measuring equipment, data processing methods, units of measurements, sampling methods, unit length of pavement section, number of runs of measuring devices, and survey manuals used. Similar findings were reported in NC DOT PMS by Corley-Lay et al. (2010).

Hall et al (2011) also discussed differences in defining transverse cracking between the MEPDG and LTPP distress survey manual. The transverse cracking in MEPDG is related to thermal cracking caused by thermal stress in pavement while one in LTPP distress survey manual is the cracks predominately perpendicular to pavement centerline by various causes. Since the pavement sections selected in this study are generally in good condition for transverse cracking and rutting, local calibration coefficients were optimized for the alligator cracking and longitudinal cracking. In the local calibration of the smoothness model, some concerns aroused since this model is depended on other predicted distress. Therefore, the local calibration of this model was not carried out. Table A.16 compares the national default and locally-calibrated coefficients for different pavement prediction models:

Table A.16. Summary of calibration factors (Hall et al. 2011)

Calibration Factor	Default	Calibrated
Alligator cracking		
C1	1	0.688
C2	1	0.294
C3	6000	6000
Longitudinal cracking		
C1	7	3.016
C2	3.5	0.216
C3	0	0
C4	1000	1000
AC rutting		
β_{r1}	1	1.20
β_{r2}	1	1
β_{r3}	1	0.80
Base rutting		
Bs1	1	1
Subgrade rutting		
Bs1	1	0.50

The alligator-cracking and rutting models in the MEPDG for flexible pavement systems in North Carolina were locally calibrated (Jadoun 2011). The scope of this paper was determining rutting and fatigue model coefficients (k values) using the twelve most commonly used Hot Mix Asphalt (HMA) mixtures in North Carolina and evaluating the effectiveness of two recalibration methods used in attaining rutting and fatigue cracking model coefficients. The two calibration methods used in the recalibration procedure are Approach 1: generalized reduced gradient (GRG) and Approach 2: genetic algorithm (GA) methods. Using these two approaches, the following local calibration coefficients for rutting and alligator cracking were obtained:

Table A.17. Comparison between local calibration coefficients from Approach 1 and 2 (Jadoun 2011)

Distress Type	Parameter	Approach I-R	Approach II-R
Rutting	β_{r1}	13.1000	0.94750
	β_{r2}	0.40000	0.86217
	β_{r3}	1.40000	1.35392
	β_{gb}	0.30300	0.53767
	β_{sg}	1.10200	1.50000
Distress Type	Parameter	Approach I-F	Approach II-F
Alligator Cracking	β_{f1}	3.87800	3.50000
	β_{f2}	0.80000	0.72364
	β_{f3}	0.80000	0.60000
	C_1	0.24500	0.24377
	C_2	0.24500	0.24377

Local calibration of the mechanistic-empirical pavement design guide (MEPDG) for flexible pavement systems in New Mexico was performed using a total of 24 New Mexico pavement sections (Tarefder and Rodriguez-Ruiz 2013). As a result of this local calibration, rutting, alligator-cracking, longitudinal-cracking and roughness models were locally calibrated, determining the model coefficients that minimized the difference between predicted and measured distresses. The following coefficients were obtained as a result of this local calibration process:

- Total rutting: $\beta_{r1}=1.1$, $\beta_{r2}=1.1$, $\beta_{r3}=0.8$, $B_{GB}=0.8$, and $B_{SG}=1.2$;
- Alligator cracking: $C_1=0.625$, $C_2=0.25$, and $C_3=6,000$;
- Longitudinal cracking: $C_1=3$, $C_2=0.3$, and $C_3=1,000$;
- IRI: Site factor=0.015.

The following conclusions were documented in the paper:

- Using national coefficients, it was realized that rutting verification results had a significant bias that required initiating local calibration for this model. Only total rutting data were provided by NMDOT, so only this parameter could have been calibrated. As a result of local calibration, the standard error was mitigated and bias was eliminated.
- A significant bias was also found in the verification results for alligator cracking, so the model coefficients of C_1 , C_2 and C_3 were calibrated and sum-of-squares errors was decreased.
- The local calibration of longitudinal cracking was problematic, since most of the measured longitudinal cracking values were almost zero, making the model hard to calibrate. Although the error was reduced for the model, the improvement in the model accuracy was not as significant as for the rutting and alligator cracking models.
- As a result of IRI verification runs, it was realized that the models already produced accurate predictions, so it was determined that local calibration for this model did not really reduce the error.

Mallela et al. (2013) employed the local calibration procedure of Darwin ME for Colorado conditions. Based on the verification of the new and rehabilitated flexible pavement performance prediction models, the local calibration of alligator cracking, rutting, transverse cracking and smoothness (IRI) were recalibrated for Colorado conditions. As a result of local calibration, accuracy of pavement prediction models was significantly improved.

Williams and Shaidur (2013) implemented local calibration of alligator and longitudinal cracking and HMA rutting models for Oregon flexible pavement systems using trial-and-error and MS Solver optimization techniques. Darwin ME version 1.1 software was also used in local calibration. Using locally-calibrated models, better SEE values were obtained.

Zhou et al. (2013) compared the pavement performance predictions of MEPDG version 1.100 for some selected highways in Tennessee using distress values extracted from the Tennessee DOT PMS database for these highway sections. In that analysis, a new pavement design procedure was used rather than an overlay design procedure. The conclusions of this study are as follows: (1) An initial IRI value of 67.9 cm/km was used in this experiment taking into account the PSI history data of pavement sections used. (2) Utilizing Level 1 input data in the prediction of AC rutting gave accurate results, although in a case using Level 3 input data, SC rutting was overpredicted. Another overprediction was observed when Level 2 input data were used for rutting of base and subgrade. (3) Traffic input was another important factor in roughness prediction of MEPDG. (4) It was also found that, in making the prediction of PSI using MEPDG, the software was not sensitive enough in reflecting variations in climate, traffic, and materials. (4) The authors recommend implementing local calibration of MEPDG for Tennessee pavement systems to produce more accurate predictions.

Darter et al., (2014) employed the local calibration procedure of Darwin ME for Arizona conditions. Alligator cracking, fatigue, IRI, asphalt, and subgrade rutting models were locally calibrated using SAS statistical methods, and the accuracy of the models was significantly improved.

Rigid Pavements

While eleven U.S. state highway agencies have approved use of national calibration coefficients for their JPCP pavement performance prediction models, eight agencies adopted locally calibrated coefficients, according to a recent ACPA survey (Mu et al. 2015). Table A.18 shows which calibration coefficients have been adopted by state highway agencies for JPCP pavement performance prediction models.

Table A.18. Local calibration summary for JPCP pavement systems (Mu et al. 2015)

State	Cracking Model	Faulting Model	IRI Model
1. Arizona	3 of 5 Coeff. Changed	8 of 9 Changed	4 of 5 Changed
2. Colorado	NNC	9 of 9 Changed	NNC
3. Florida	4 of 5 Changed	2 of 9 Changed	1 of 5 Changed
4. Utah	NNC	NNC	NNC
5. Wyoming	NNC	NNC	NNC
6. Delaware	ONC	ONC	ONC
7. Indiana	ONC	ONC	ONC
8. Iowa	4 of 5 Changed	5 of 9 Changed	4 of 5 Changed
9. Kansas	ONC	ONC	ONC
10. Louisiana	1 of 5 Changed	1 of 9 Changed	ONC
11. Missouri	ONC	ONC	3 of 4 Changed
12. New York	ONC	ONC	ONC
13. North Carolina	ONC	ONC	ONC
14. Ohio	ONC	ONC	3 of 4 Changed
15. Oklahoma	ONC	ONC	ONC
16. Pennsylvania	ONC	ONC	ONC
17. South Dakota	ONC	ONC	ONC
18. Virginia	ONC	ONC	ONC
19. Washington	2 of 5 Changed	ONC	ONC

Note: NNC: new national calibration; ONC: original national calibration

The Washington State DOT (Li et al. 2006) developed procedures to calibrate the MEPDG (Version 0.9) rigid pavement performance models using data obtained from the WS PMS. Some significant conclusions from this study are as follows: (a) WSDOT rigid pavement performance prediction models require calibration factors significantly different from default values; (b) the MEPDG software does not model longitudinal cracking of rigid pavement, which is significant in WSDOT pavements; (c) WS PMS does not separate longitudinal and transverse cracking in rigid pavements, a deficiency that makes calibration of the software's transverse cracking model difficult; and (d) the software does not model studded tire wear, which is

significant in WS DOT pavements. This study also reported that: (a) the calibrated software can be used to predict future deterioration caused by faulting, but it cannot be used to predict cracking caused by the transverse or longitudinal cracking issues in rigid pavement, and (b) with a few improvements and resolving software bugs, MEPDG software can be used as an advanced tool to design rigid pavements and predict future pavement performance. The local calibration results of typical Washington State rigid pavement systems determined from this study are presented in Table A.19.

Table A.19. Calibration coefficients of the MEPDG (Version 0.9) rigid pavement distress models in the State of Washington (Li et al. 2006)

Calibration Factor		Default for			
		New Pavements	Undoweled	Undoweled – MP ^a	DBR ^{b,c}
Cracking	C ₁	2	2.4	2.4	2.4
	C ₂	1.22	1.45	1.45	1.45
	C ₄	1	0.13855	0.13855	0.13855
	C ₅	-1.68	-2.115	-2.115	-2.115
Faulting	C ₁	1.29	0.4	0.4	0.934
	C ₂	1.1	0.341	0.341	0.6
	C ₃	0.001725	0.000535	0.000535	0.001725
	C ₄	0.0008	0.000248	0.000248	0.0004
	C ₅	250	77.5	77.5	250
	C ₆	0.4	0.0064	0.064	0.4
	C ₇	1.2	2.04	9.67	0.65
	C ₈	400	400	400	400
Roughness ^d	C ₁	0.8203	0.8203	0.8203	0.8203
	C ₂	0.4417	0.4417	0.4417	0.4417
	C ₃	1.4929	1.4929	1.4929	1.4929
	C ₄	25.24	25.24	25.24	25.24

Notes:

- Mountain pass climate
- Dowel bar retrofitted
- DBR calibration factors are the same as default “restoration” values in NCHRP 1-37A software
- Roughness calibration factors are the same as the default values

Khazanovich et al. (2008) evaluated MEPDG rigid pavement performance prediction models for the design of low-volume concrete pavements in Minnesota. It was found that the faulting model in MEPDG version 0.8 and 0.9 produced acceptable predictions, whereas the cracking model had to be adjusted. The cracking model was recalibrated using the design and

performance data for 65 pavement sections located in Minnesota, Iowa, Wisconsin, and Illinois. The recalibrated coefficients of MEPDG 0.8 and 0.9 cracking model predictions in this study are (1) $C1 = 1.9875$, (2) $C2 = -2.145$. These values are recalibrated into $C1 = 0.9$ and $C2 = -2.64$ by using the MEPDG version 1.0 (Velasquez et al 2009). Since MEPDG software evaluated in these studies was not a final product, authors recommended that these values should be updated for the final version of the MEPDG software.

Darter et al. (2009) found that the national calibrated MEPDG model predicted faulting, transverse cracking and IRI well under Utah conditions with an adequate goodness of fit and no significant bias. Bustos et al. (2009) attempted to adjust and calibrate the MEPDG rigid pavement distress models in Argentina conditions. A sensitivity analysis of distress model transfer functions was conducted to identify the most important calibration coefficient. The $C6$ of joint faulting model transfer function and the $C1$ or $C2$ of cracking model transfer function were the most sensitive coefficients. Delgado et al (2011) also present local calibration coefficients of transverse cracking and faulting of JPCP in Chile.

The scope of (Titus-Glover and Mallela 2009) is to figure out if the global calibration factors of MEPDG adequately predict pavement performance in Ohio rigid pavements and initiating the local calibration process if needed. A validation study was employed for pavement prediction models to figure out which models give accurate pavement predictions. Based on the validation study, it was found out that smoothness model for the new jointed plain concrete pavement was needed to be locally calibrated. The new local calibration for the locally calibrated model can be seen in the table below (Table A.20):

Table A.20. New local calibration coefficients of the MEPDG rigid pavement distress models in the State of Ohio (Titus-Glover and Mallela 2009)

Pavement Type	JPCP Model IRI Local Calibration Coefficients			
	CRK (C1)	SPALL (C2)	TFAULT (C3)	SF (C4)
New JPCP	0.82	3.7	1.711	5.703

The scope of (Mallela et al. 2009) is to figure out if the global calibration factors of MEPDG adequately predict pavement performance in Missouri rigid pavements and initiating the local calibration process if needed. A validation study was employed for pavement prediction models to figure out which models give accurate pavement predictions. Based on the validation study, it was found out that smoothness model for the new jointed plain concrete pavement was needed to be locally calibrated. The new local calibration for the locally calibrated model can be seen in the table below:

Table A.21. New local calibration coefficients of the MEPDG rigid pavement distress models in the State of Missouri (Mallela et al. 2009)

Pavement Type	JPCP Model IRI Local Calibration Coefficients			
	CRK (C1)	SPALL (C2)	TFAULT (C3)	SF (C4)
New JPCP	0.82	1.17	1.43	66.8

Li et al. (2010) recalibrated MEPDG (version 1.0) for rigid pavement systems based on the local conditions of State of Washington. The first local calibration was conducted for WSDOT using MEPDG version 0.6. Since the software has evolved since then, initiation of recalibration was a necessity. As a result of recalibration process, following recalibrated local calibration coefficients were found out:

Table A.22. Recalibrated local calibration coefficients of the MEPDG for transverse cracking model models in the State of Washington (Li et al. 2010)

Calibration Factor		Elasticity	Default	Recalibration Results	
Rigid Pavement	Cracking	C1	-7.579	2	1.93
		C2	-7.079	1.22	1.177
		C3	0.658	1	1
		C4	-0.579	-1.98	-1.98

For the faulting and roughness models, the default calibration confidents gave good results. Therefore, the recalibration for these models were not conducted.

Mallela et al. (2013) employed the local calibration procedure of Darwin ME for Colorado conditions. The local calibration methodology consists of three steps: verification, calibration and validation. First, the researchers run the software using global calibration coefficients for all projects of rigid pavements to see the goodness of fit and bias between predicted and actual performance results of pavements. If the verification results give high goodness of fit and low bias, the global calibration coefficients are announced as local calibration coefficients. If not, local calibration process is started out to come up with better set of calibration coefficients giving the highest goodness of fit and lowest bias. The local calibration results also needed to be verified with validation process.

As a result of verification process, all of the global performance models for new JPCPs (transverse cracking, transverse joint faulting and smoothness (IRI)) performed good enough and it was determined that local calibration of models is not necessary for Colorado conditions. Namely, the global models gave good goodness of fit and bias and required no local calibration effort.

Darter at al. (2014) employed the local calibration procedure of Darwin ME for Arizona conditions. This methodology consists of three steps: verification, calibration, and validation.

First, the researchers run the software using global calibration coefficients for all rigid-pavement projects to determine the goodness of fit and the bias between predicted and actual performance results of pavements. If the verification results produce high goodness of fit and low bias, the global-calibration coefficients are taken as local-calibration coefficients. If not, a local-calibration process is initiated to seek a set of calibration coefficients that give the highest goodness of fit and lowest bias. The local-calibration results also must be verified through a validation process. For JPCP pavement systems, the verification of transverse cracking gave poor goodness of fit and bias, so local calibration of the transverse-cracking model was initiated. Possible causes of poor goodness of fit were also investigated. JPCPs with asphalt-treated or aggregate bases gave accurate transverse-cracking predictions compared to those constructed over lean concrete bases. In local calibration, SAS statistical software was used to determine model local-calibration coefficients that improved the model predictions, producing significantly better goodness of fit and lower bias. The goodness of fit of the faulting model was found to be fair but it overpredicted faulting with high bias, so local calibration was necessary for the faulting model. Again, SAS statistical software was used to determine model local coefficients that improved the model predictions with significantly better goodness of fit and lower bias. For the IRI model, as a result of verification the IRI values were overpredicted, so local calibration for this model was also necessary, with SAS statistical software used to determine model local coefficients that improved the model predictions with significantly better goodness of fit and lower bias.

Table A.23. Comparison of accuracy between global and ADOT calibrated MEPDG models for Arizona JPCP systems (Darter et al. 2014)

Pavement Type	Distress/IRI Models	Global Models		ADOT Calibrated Models	
		Global R ² (%)	Global Model SEE*	Arizona R ² (%)	Arizona SEE
New JPCP	Transverse cracking	20	9%	78	6%
	Transverse joint faulting	45	0.03 inch	52	0.03 inch
	IRI	35	25 inches/mi	81	10 inches/mi

Mu et al. (2015) summarizes the local calibration efforts of state highway agencies. At its time of that paper's publication, the local calibration process for JPCP had been finalized by 19 states, with 11 states accepting use of national calibration coefficients while the remaining 8 states adopted one or more new calibration coefficients. The paper also elaborates on the local calibration effort of each state adopting new calibration coefficients and their effectiveness. The paper concludes that, while the improvements with respect to bias reduction are significant, the precision (standard error of the estimate) was rarely improved. Second, the writers focused on distress prediction models, i.e., the transverse cracking, faulting and IRI models were evaluated using the new calibration coefficients adopted by 8 states as well as national calibration coefficients. Third, the writers emphasize the path dependence of the transverse cracking model, i.e., how using different calibration coefficients would result in the same effect as those predicted. Finally, the paper uses two hypothetical JPCP sections (one with low traffic volume, other one with high traffic volume) as case studies to determine why using new local calibration coefficients or national calibration coefficients predict different distress results. The paper's conclusions are as follows: (1) The local calibration process for JPCP was finished by 19 states, and 11 states accepted using national calibration coefficients. (2) The local calibration procedure is path dependent, meaning that using different calibration approaches would result in different

coefficients. (3) For those states adopting different calibration coefficients rather than national ones, the estimates' biases are mostly reduced while the standard error rarely decreased. (4) For those states adopting different calibration coefficients rather than national ones, the local calibration procedure results in less cracking but higher IRI predictions compared to predictions using national calibration coefficients.

Mallela et al. (2015) recalibrated the JPCP cracking and faulting models in the AASHTO ME design procedure under NCHRP 20-07 using corrected coefficient thermal expansion (CTE) values acquired through a new CTE test procedure (AASHTO T 336-09 2009). Lower CTE values were produced when the new test procedure was used (AASHTO T 336-09 2009) rather than the old test procedure (AASHTO TP 60-00 2004). The difference between erroneous and corrected CTE values were found to be $-0.8 / \text{in/in}/^\circ\text{F}$ on average, with a range of 0 to $-1.2 / \text{in/in}/^\circ\text{F}$. Table A.24 shows erroneous and corrected CTE values.

Table A.24. Comparison of erroneous CTEs (NCHRP 1-40D) and corrected CTEs (NCHRP 20-07) (Mallela et al. 2015)

Primary Aggregate Origin	Primary Aggregate Class	NCHRP 1-40D			NCHRP 20-07 (LTPP Projects with Single Coarse Agg. Type)			NCHRP 20-07 (LTPP Projects with Two or More Coarse Agg. Type)		
		Avg. CTE $10^{-6} / ^\circ\text{F}$	Std. Dev. $10^{-6} / ^\circ\text{F}$	No.	Avg. CTE $10^{-6} / ^\circ\text{F}$	Std. Dev. $10^{-6} / ^\circ\text{F}$	No.	Avg. CTE $10^{-6} / ^\circ\text{F}$	Std. Dev. $10^{-6} / ^\circ\text{F}$	No.
Igneous (Extrusive)	Andesite	5.3	0.5	23	NA	NA	NA	4.4	0.5	33
Igneous (Extrusive)	Basalt	5.2	0.7	47	4.4	0.5	18	4.4	0.6	87
Igneous (Plutonic)	Diabase	5.2	0.5	17	5.2	0.5	21	4.6	0.6	66
Igneous (Plutonic)	Granite	5.8	0.6	83	4.8	0.6	69	4.9	0.6	167
Metamorphic	Schist	5.6	0.5	17	4.4	0.4	17	4.7	0.7	24
Sedimentary	Chert	6.6	0.8	28	6.1	0.6	25	5.9	0.7	62
Sedimentary	Dolomite	5.8	0.8	124	5.0	0.7	30	4.9	0.6	195
Sedimentary	Limestone	5.4	0.7	236	4.4	0.7	160	4.4	0.6	425
Sedimentary	Quartzite	6.2	0.7	69	5.2	0.5	9	5.3	0.5	73
Sedimentary	Sandstone	6.1	0.8	18	5.8	0.5	7	5.2	0.6	29
	BF slag	—	—	—	—	—	—	4.8	0.7	22

Using the corrected CTE values, JPCP cracking and faulting models were calibrated using the LTPP database. The revised calibrated joint faulting model coefficients based on this study are presented in Table A.25.

Table A.25. Revised calibrated joint faulting model coefficients (Mallela et al. 2015)

Model Coefficients	Value
C1	0.51040
C2	0.00838
C3	0.00147
C4	0.008345
C5	5999
C6	0.8404
C7	5.9293
C8	400

The researchers compared slab thickness predictions using the faulting and transverse cracking model using erroneous CTE values (NCHRP 1-40 D) and corrected CTE values (NCHRP 20-07) (Figure A.26).

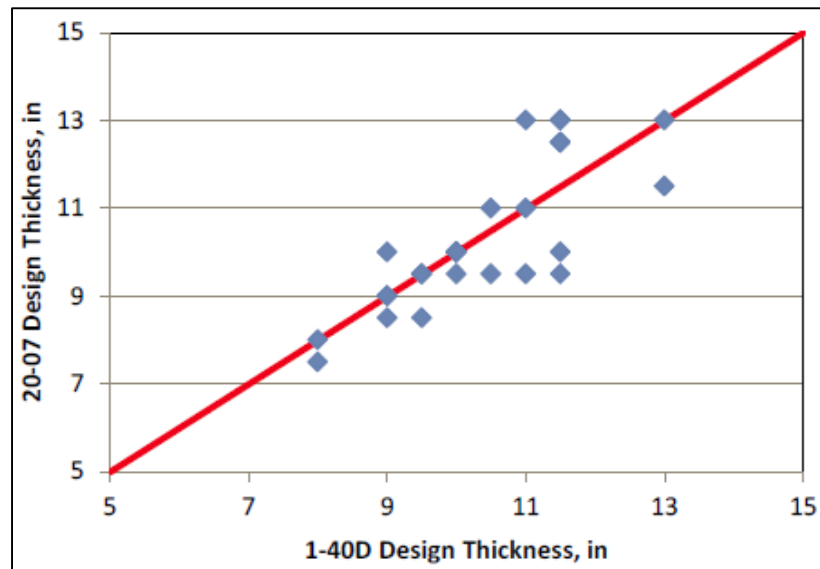


Figure A.10. 2007 and 2011 thickness designs for 13 projects at two levels of traffic each

APPENDIX B. DESIGN EXAMPLES OF NEW JPCP, NEW HMA AND HMA OVER JPCP PAVEMENTS USING PAVEMENT ME SOFTWARE

New Rigid Pavement

The design example of a new JPCP section in Des Moines, Iowa was performed using AASHTOWare Pavement ME Design software. The following input categories are required for the design procedure:

- Traffic inputs
- Climate inputs
- JPCP design properties
- Pavement structure related inputs
- Project specific calibration factors

The following inputs are used in this specific design example:

Design life

- Design life: 30 years
- Pavement construction month: September 2014
- Traffic open month: October 2014
- Type of design: new pavement – JPCP

Construction requirements

- A good quality of construction with an initial IRI between 50 and 75 in/mile (assume 63 in/mile for design purposes)

Traffic

- The two-way average annual daily truck traffic (AADTT) on this highway is estimated to be 5,000 trucks during the first year of its service.
- Two lanes in the design direction with 90% of the trucks in the design lane

- Truck traffic is equally distributed in both directions
- The operational speed is 60 mph
- The traffic increases by 2.0% of the preceding year's traffic (compounded annually)
- Vehicle class distribution: TTC 4

Performance Criteria

- Initial IRI (in/mi): 63
- Terminal IRI (in/mi): 172
- JPCP transverse cracking (percent slabs): 15
- Mean joint faulting (in): 0.12
- Reliability level for all criteria: 90%

Layer properties

- PCC Course: 10 in./MOR = 600 psi
- Non-stabilized Base: 6 in./Mr. = 35,000 psi
- Subgrade: semi-infinite thickness/Mr. = 10,000 psi

JPCP design properties

- PCC joint spacing: 20 ft.
- Sealant type: no sealant, liquid or silicone
- Doweled joints: 1.5 in. of dowel diameter
- Widened slab: 14 ft.
- Not tied shoulders

The following figures show the screenshots the design steps using Pavement ME Design:

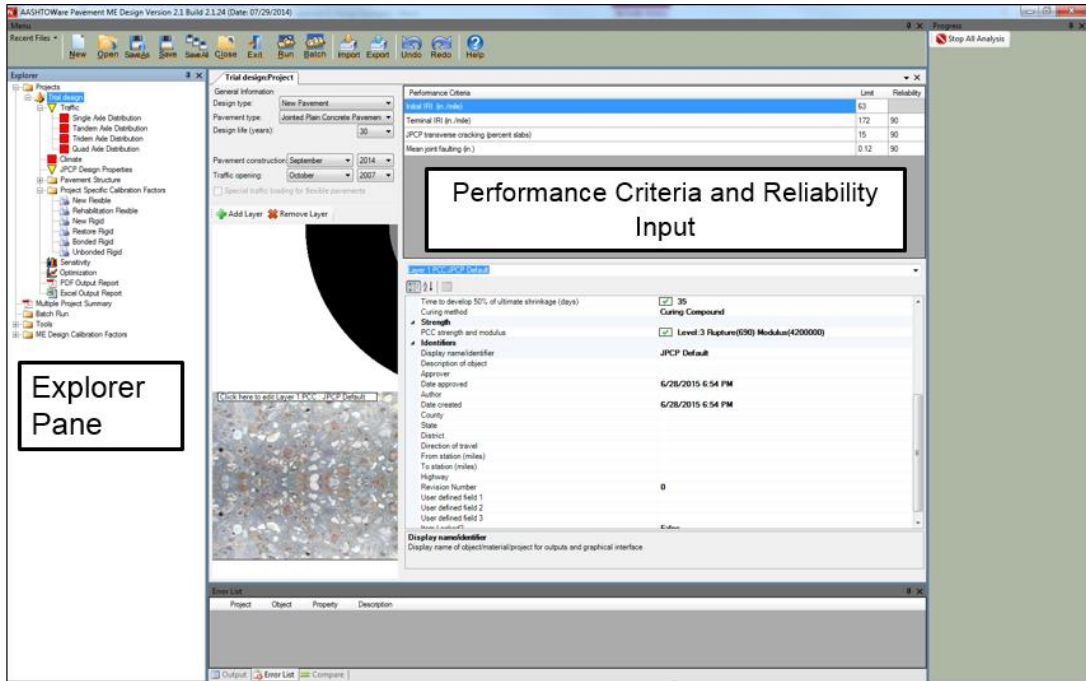


Figure B.1. General inputs, design criteria and reliability

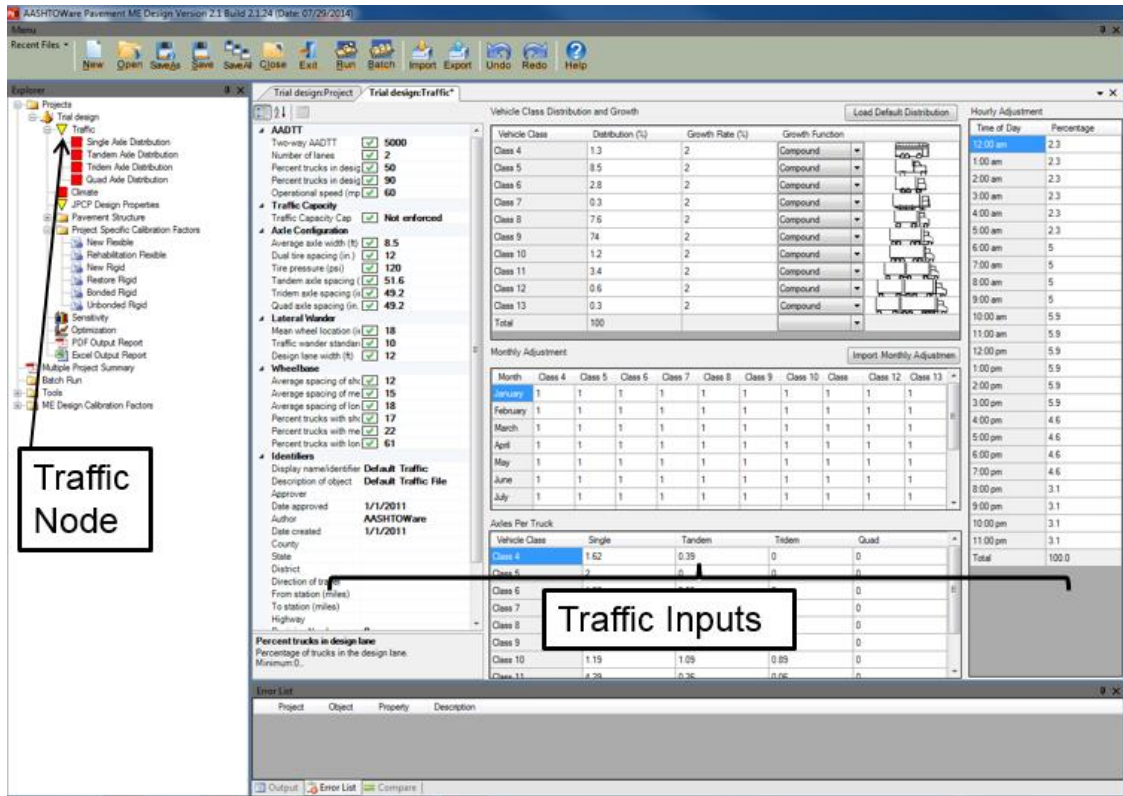


Figure B.2. Traffic inputs used in the design

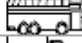
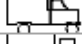
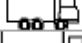

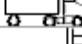
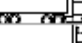



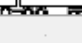
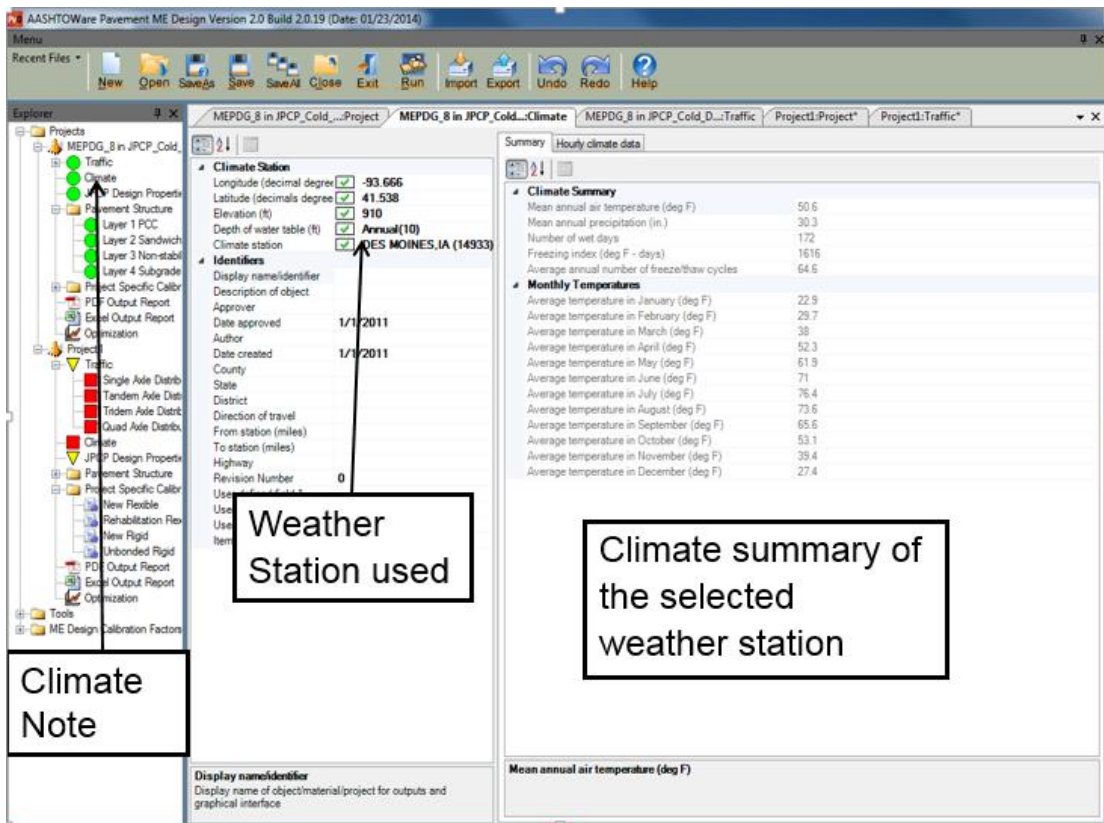
Vehicle Class Distribution and Growth				Load Default Distribution
Vehicle Class	Distribution (%)	Growth Rate (%)	Growth Function	
Class 4	1.3	2	Compound	
Class 5	8.5	2	Compound	
Class 6	2.8	2	Compound	
Class 7	0.3	2	Compound	
Class 8	7.6	2	Compound	
Class 9	74	2	Compound	
Class 10	1.2	2	Compound	
Class 11	3.4	2	Compound	
Class 12	0.6	2	Compound	
Class 13	0.3	2	Compound	
Total	100			

Figure B.3. Vehicle class distribution and growth used in the design



The screenshot shows the AASHTOWare Pavement ME Design software interface. The 'Climate Station' properties are displayed, including longitude (93.666), latitude (41.538), elevation (910), and climate station (Annual(10) QES MOINES, IA (14933)). A callout box labeled 'Weather Station used' points to the climate station selection. The 'Climate Summary' panel shows various climate data points, including mean annual air temperature (50.6 deg F), mean annual precipitation (30.3 in.), and monthly temperatures. A callout box labeled 'Climate summary of the selected weather station' points to this panel. A 'Climate Note' box is also visible at the bottom left.

Figure B.4. Climate input used in the design

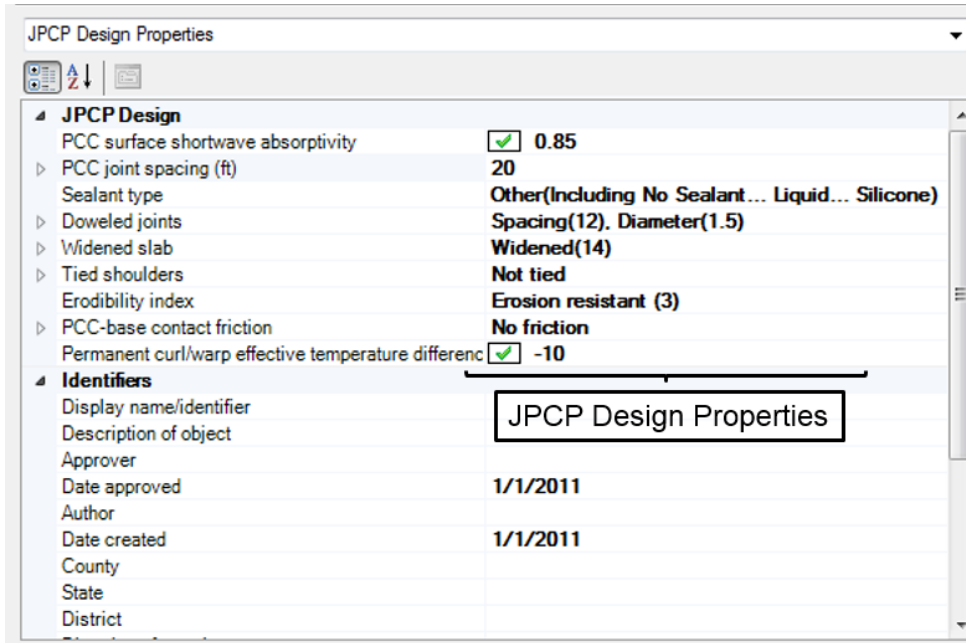


Figure B.5. JPCP design properties

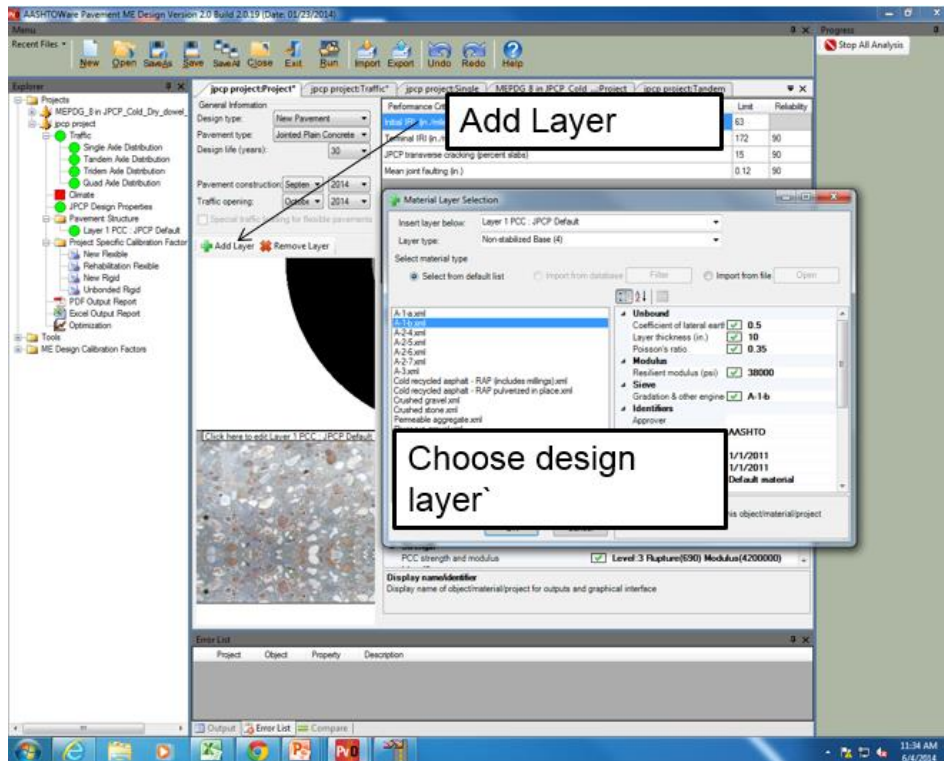


Figure B.6. Pavement structure input

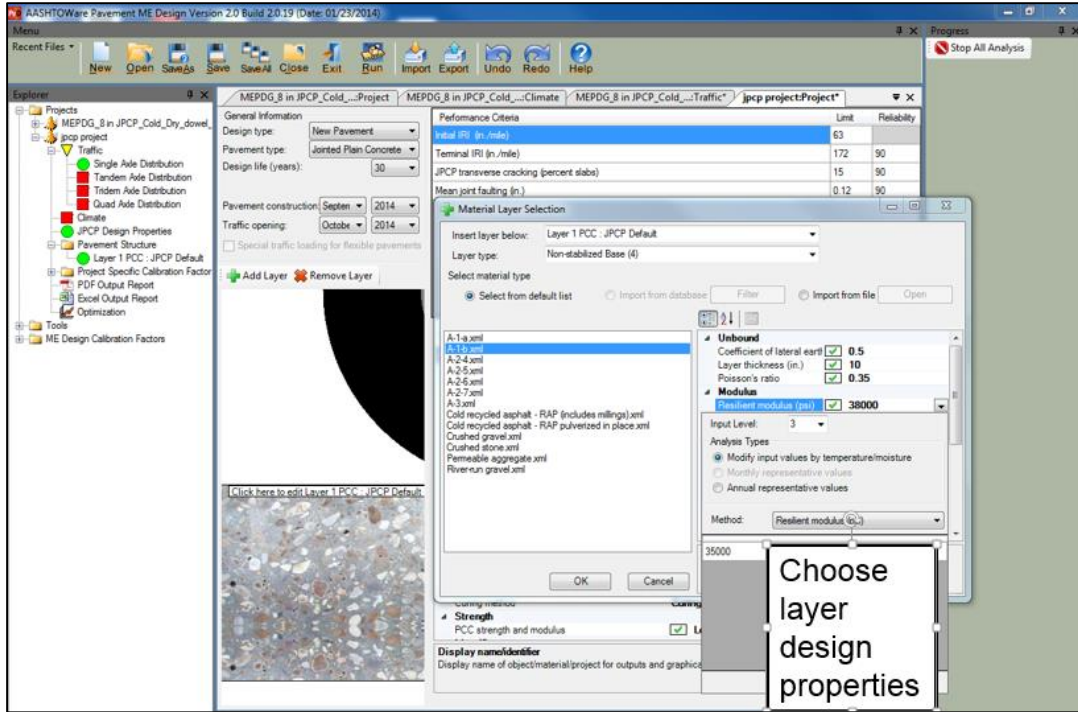


Figure B.7. Layer design properties

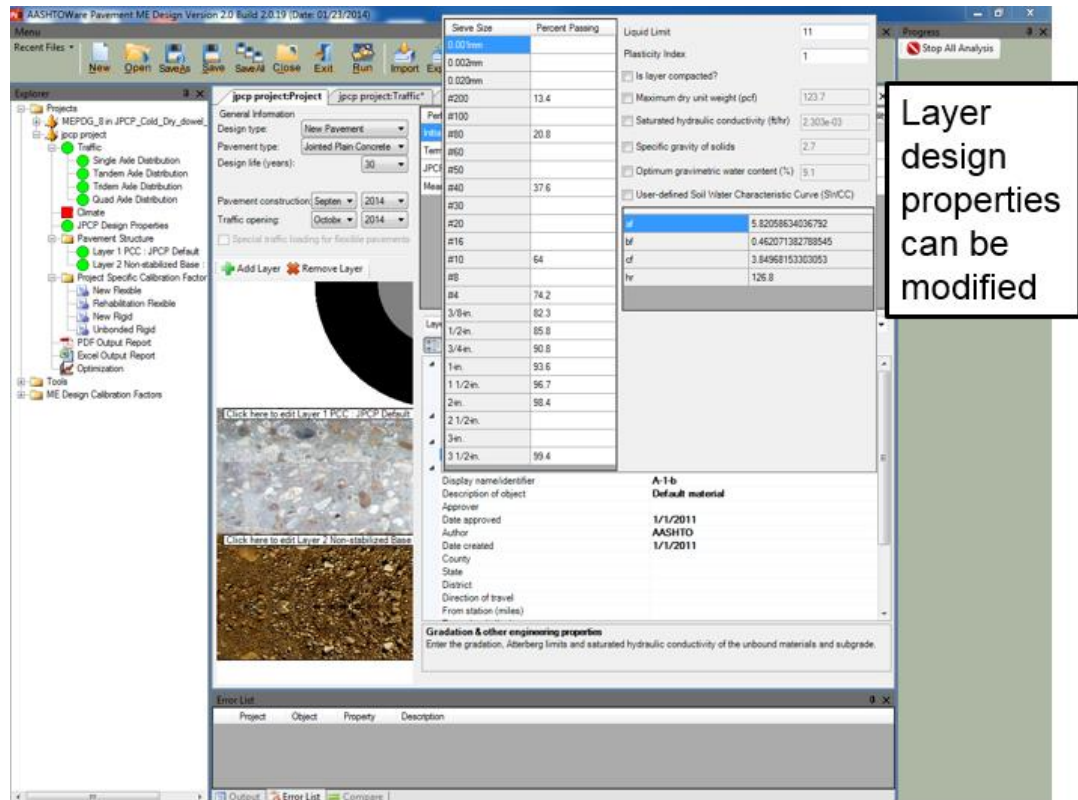


Figure B.8. Modification of layer design properties

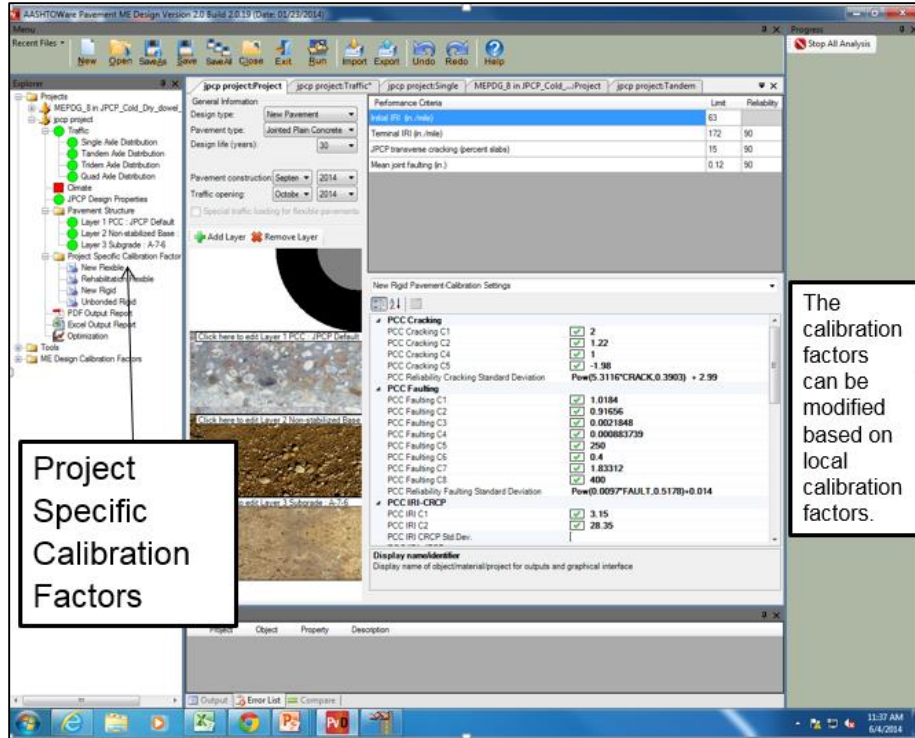


Figure B.9. Inputting local calibration coefficients

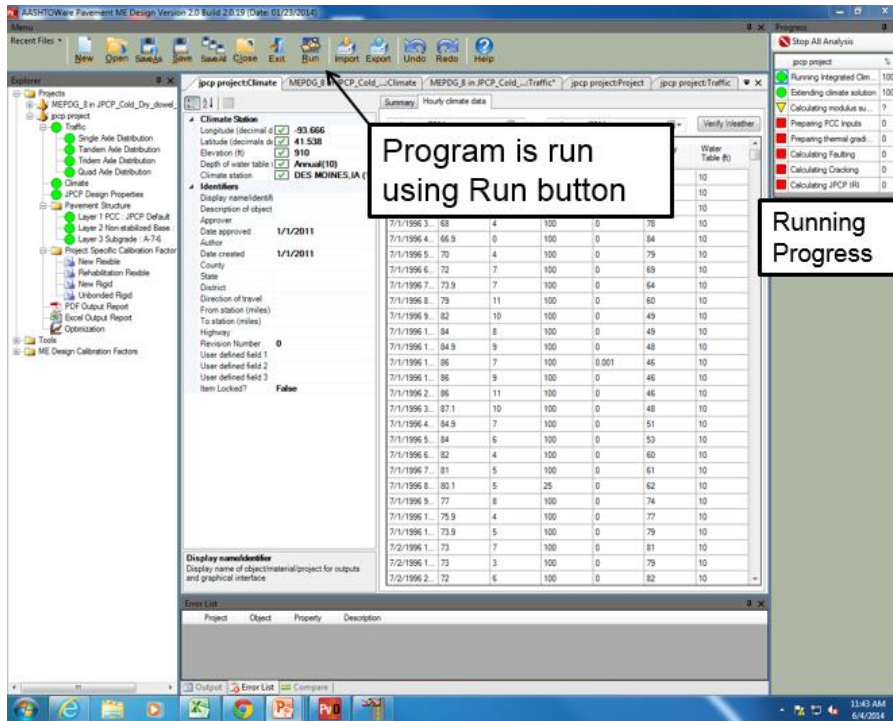


Figure B.10. Running the software

Once the run is completed, two kinds of output reports are generated:

- PDF output report
- Excel output report

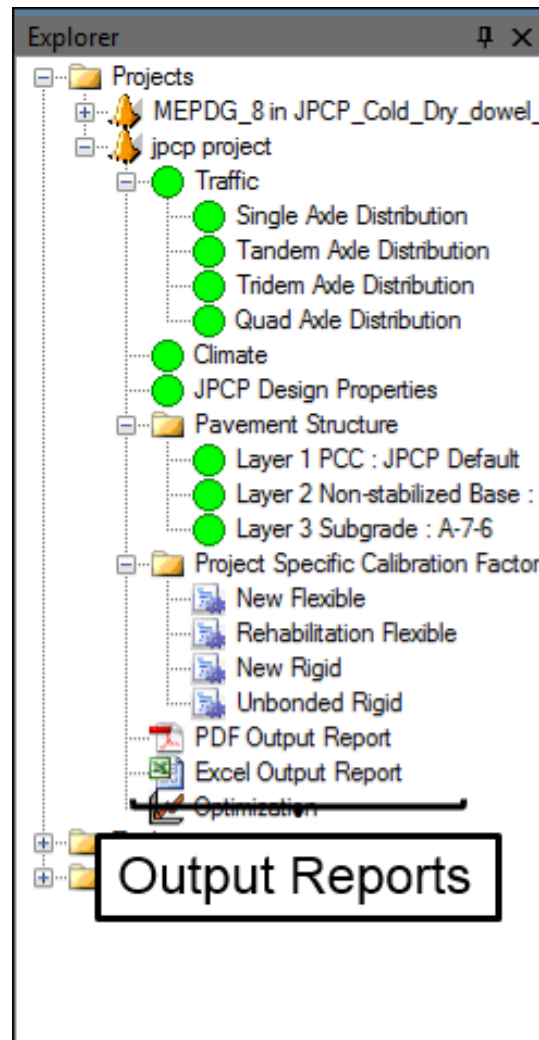


Figure B.11. Output reports

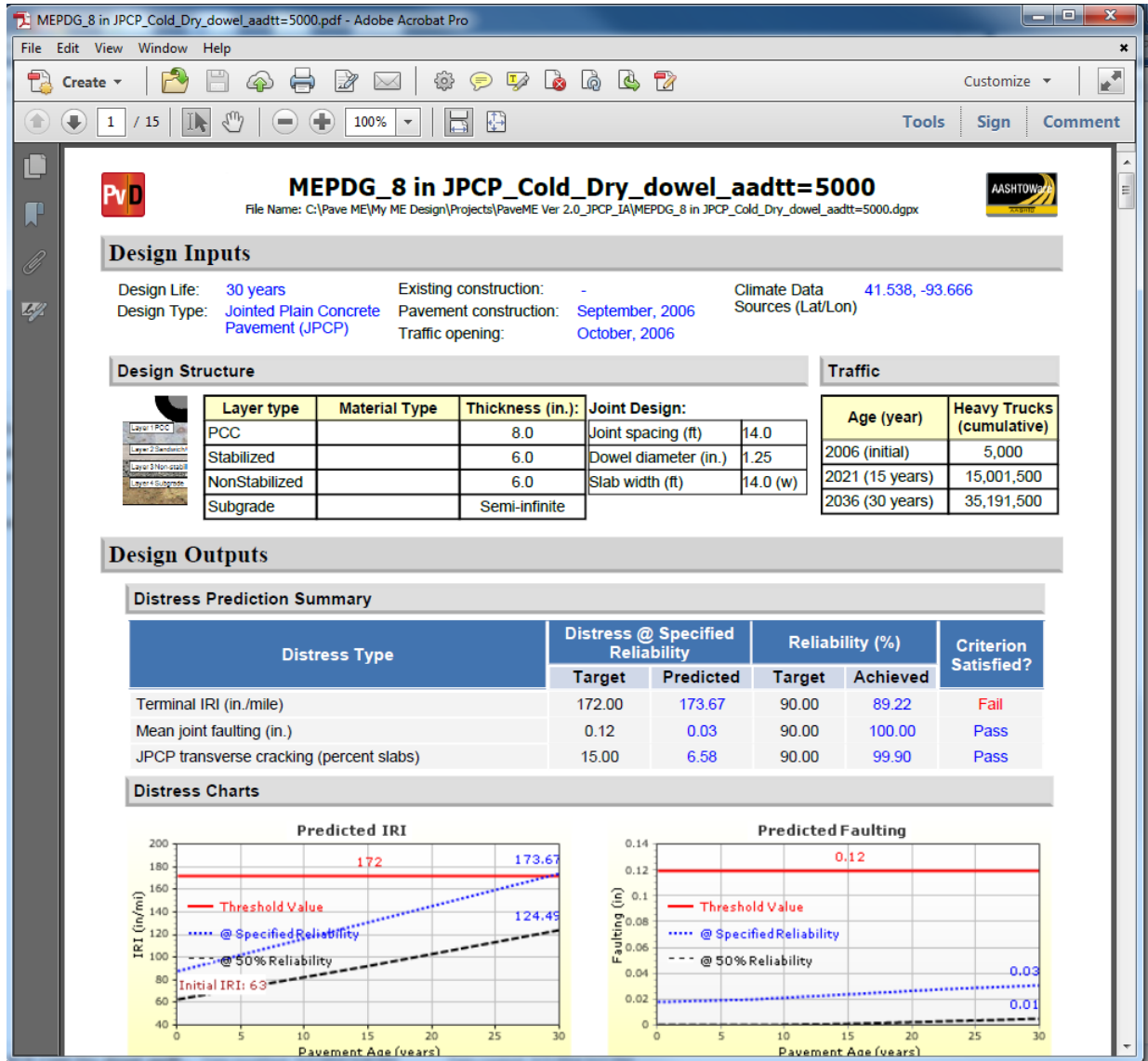


Figure B.12. PDF output report

If the trial fails, the designer can modify the design inputs based on the failed criteria by using optimization node.

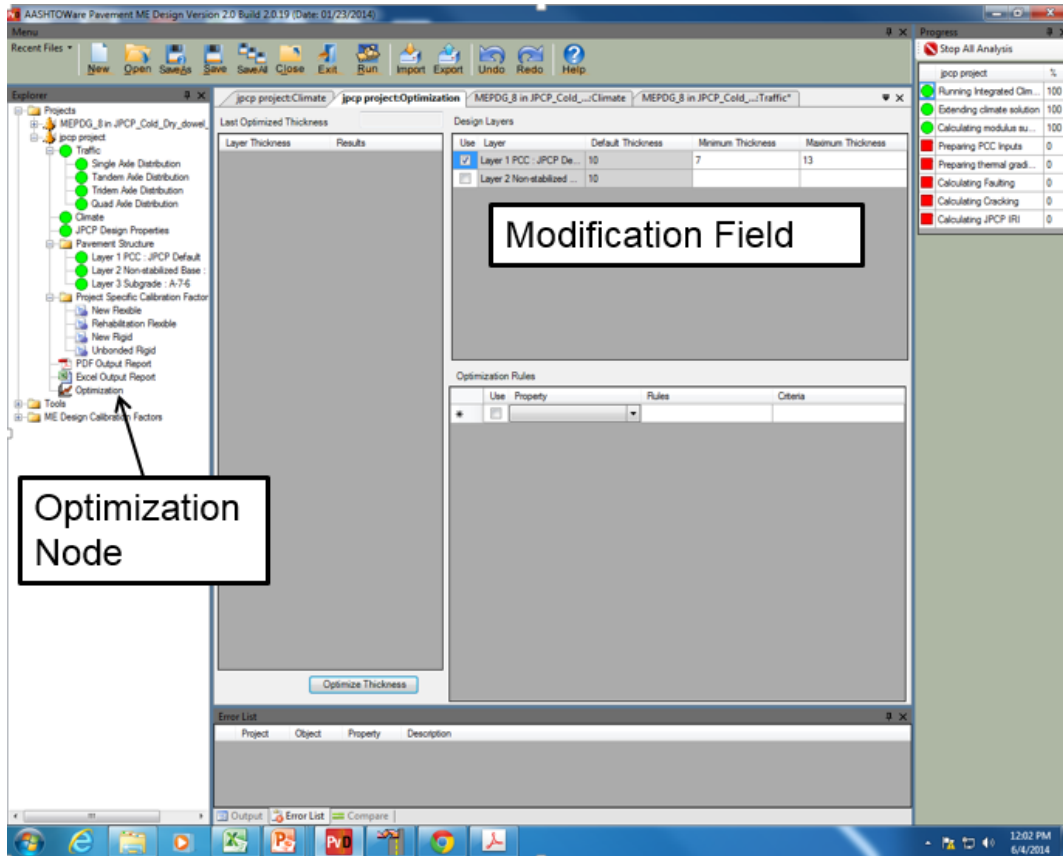


Figure B.13. Optimization tool

New HMA Pavement

The design of a new HMA pavement section in Des Moines, Iowa was performed using AASHTOWare Pavement ME software. The following input categories are required for the design procedure:

- Traffic inputs
- Climate inputs
- Pavement structure related inputs
- Project specific calibration factors

The following inputs are used in this specific design example:

Design life

- Design life: 20 years
- Base/Subgrade construction month: August 2014
- Pavement construction month: September 2014
- Traffic open month: October 2014
- Type of design: New pavement – flexible pavement

Construction requirements

- A good quality of construction with an initial IRI between 50 and 75 in/mile (assume 63 in/mile for design purposes)

Traffic

- The two-way average annual daily truck traffic (AADTT) on this highway is estimated to be 5,000 trucks during the first year of its service.
- Two lanes in the design direction with 90% of the trucks in the design lane
- Truck traffic is equally distributed in both directions
- The operational speed is 60 mph
- The traffic increases by 2.0% of the preceding year's traffic (compounded annually)
- Vehicle class distribution: TTC 4

Performance Criteria

- Initial IRI (in/mi): 63
- Terminal IRI (in/mi): 172
- AC top-down fatigue cracking (ft/mi): 2000
- AC bottom-up fatigue cracking (percent): 25
- AC thermal cracking (ft/mi): 1000

- Permanent deformation-total pavement (in): 0.75
- Permanent deformation-AC only (in): 0.25
- Reliability level for all criteria: 90 %

Layer properties

- HMA layer: 12 in./PG 58-28
- Subgrade (Fill/Borrow): 12 in. /Mr:10,000 psi
- Subgrade: semi-infinite thickness /Mr:10,000 psi

The following figures show the screenshots the design steps using Pavement ME Design:

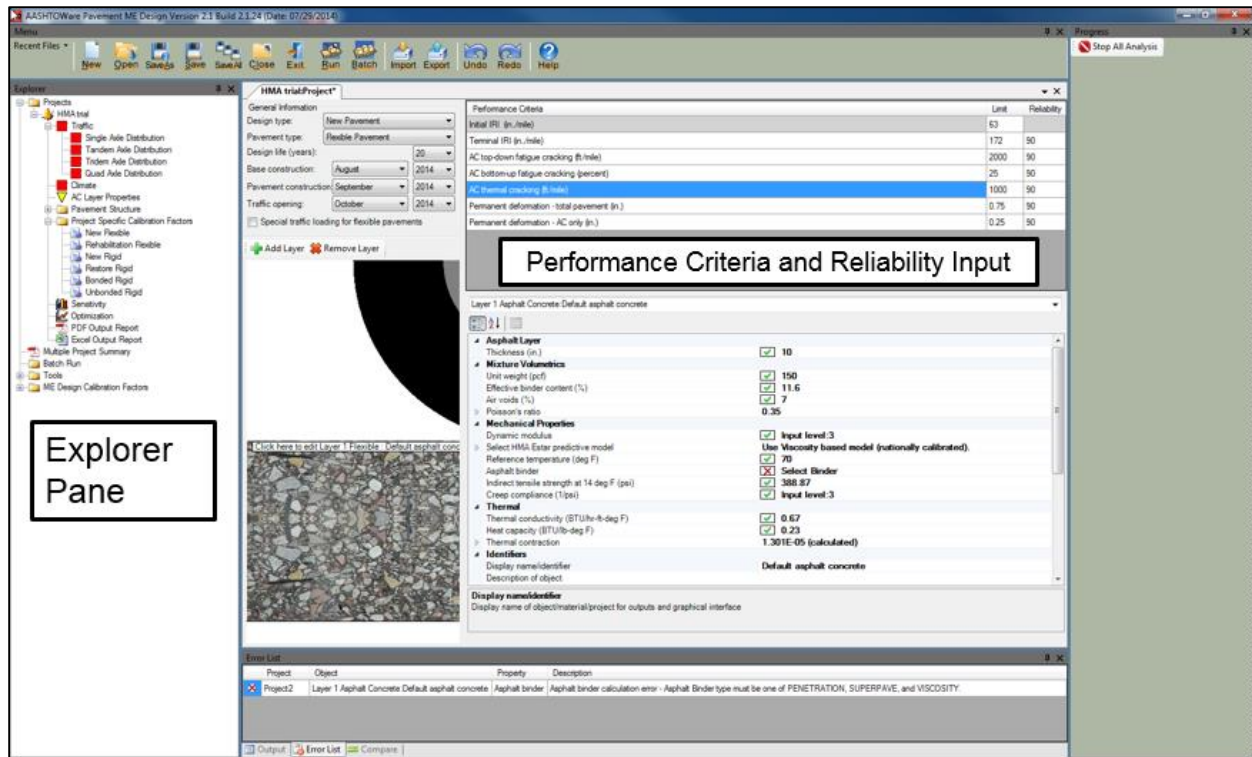


Figure B.14. General inputs, design criteria and reliability

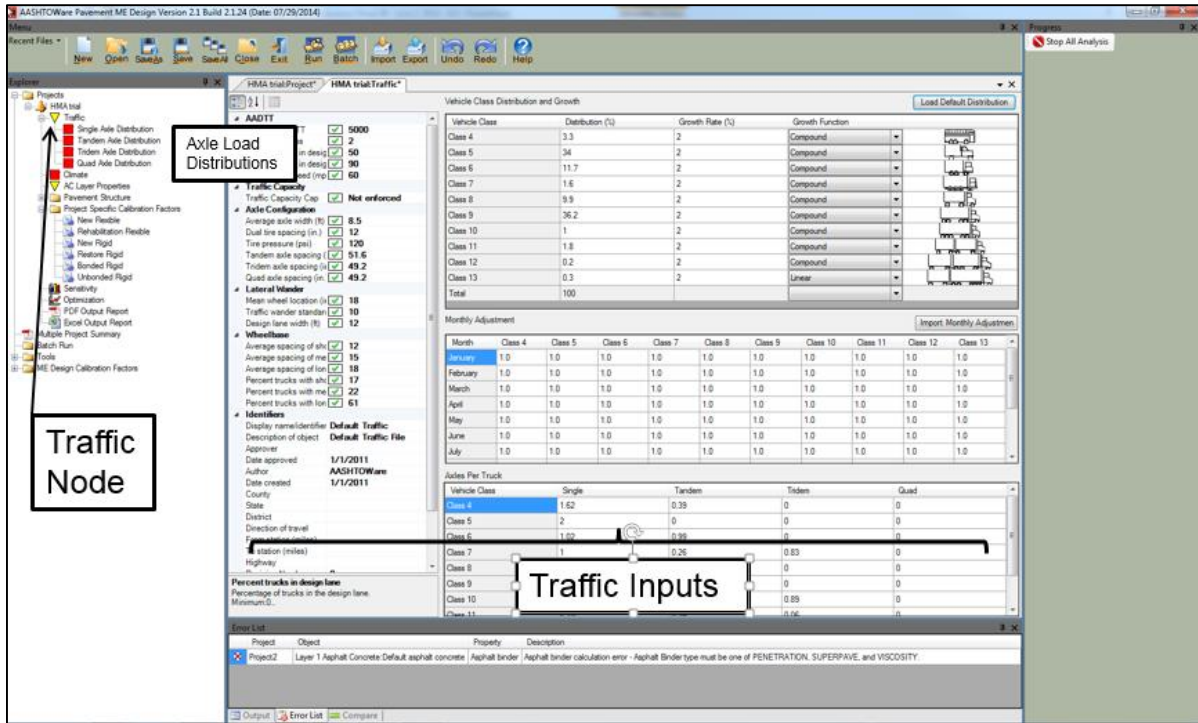


Figure B.15. Traffic inputs

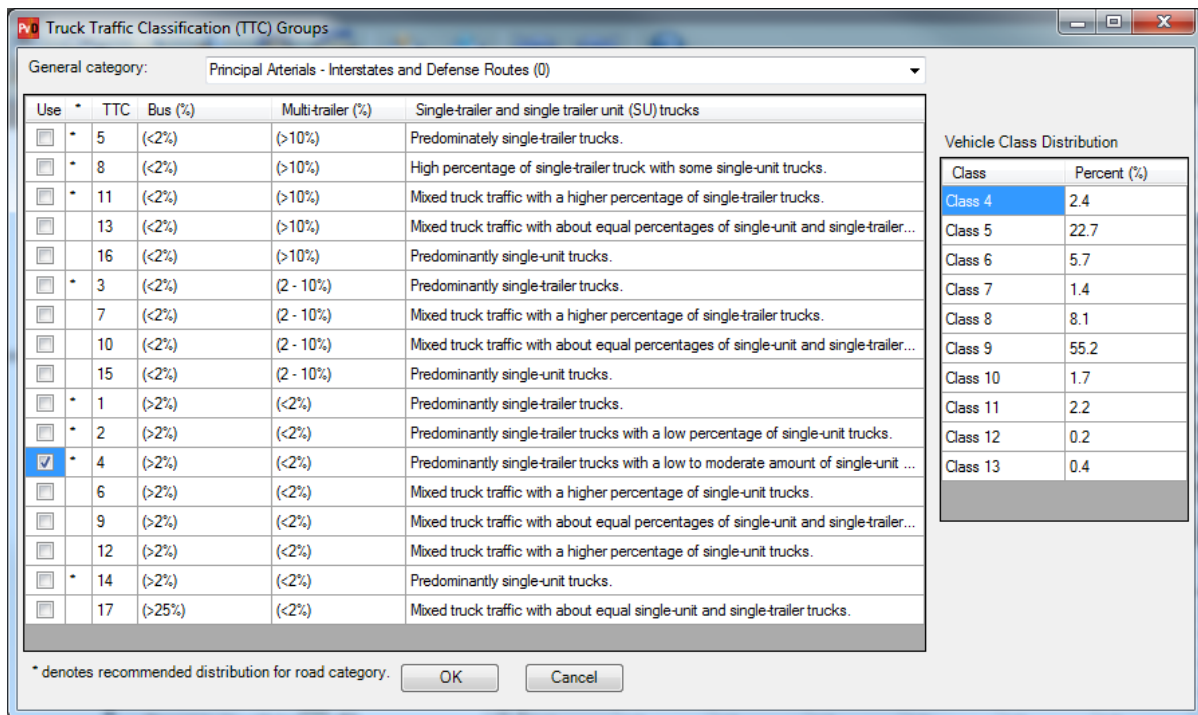


Figure B.16. Truck traffic classification

Hourly climatic database for USA and Canada to be used can be downloaded from www.me-design.com website.

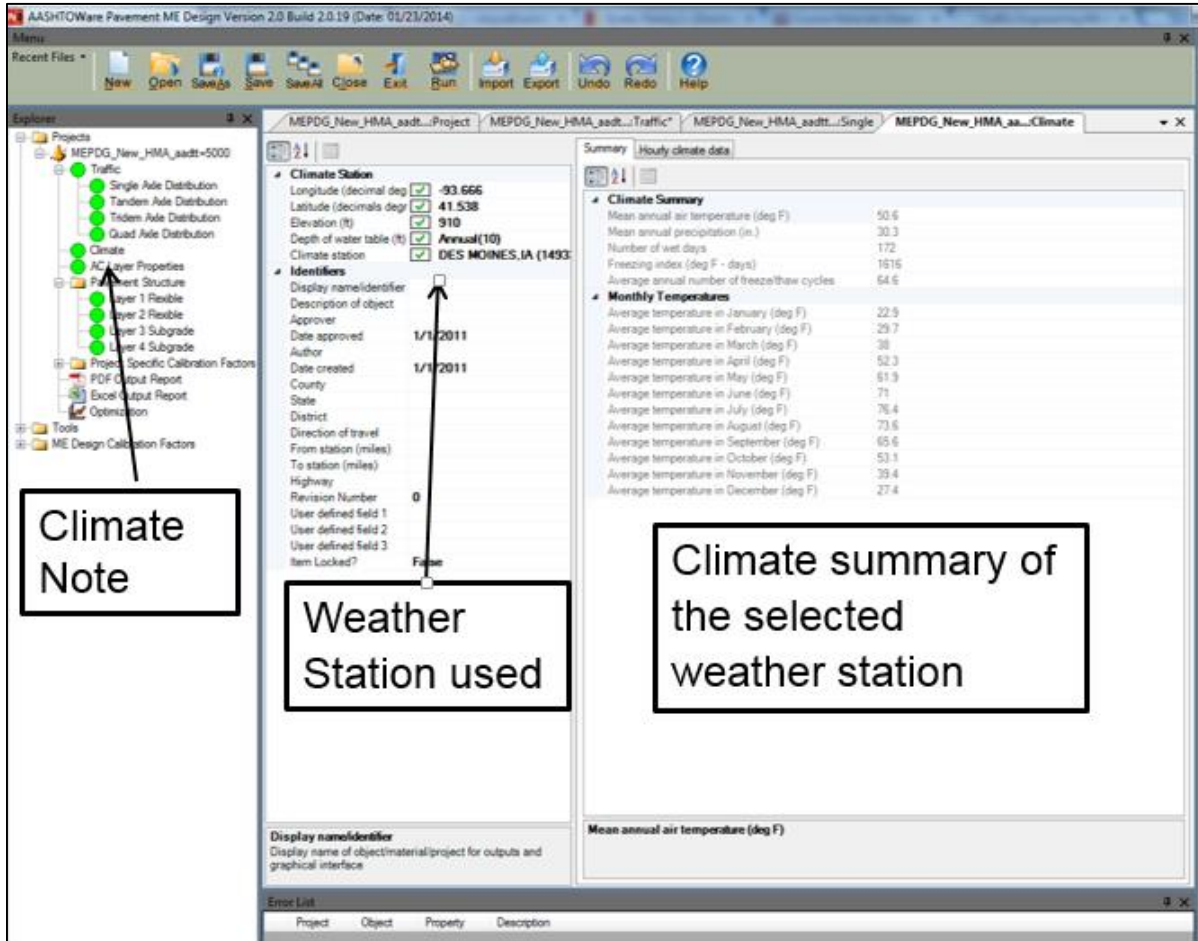


Figure B.17. Climate inputs

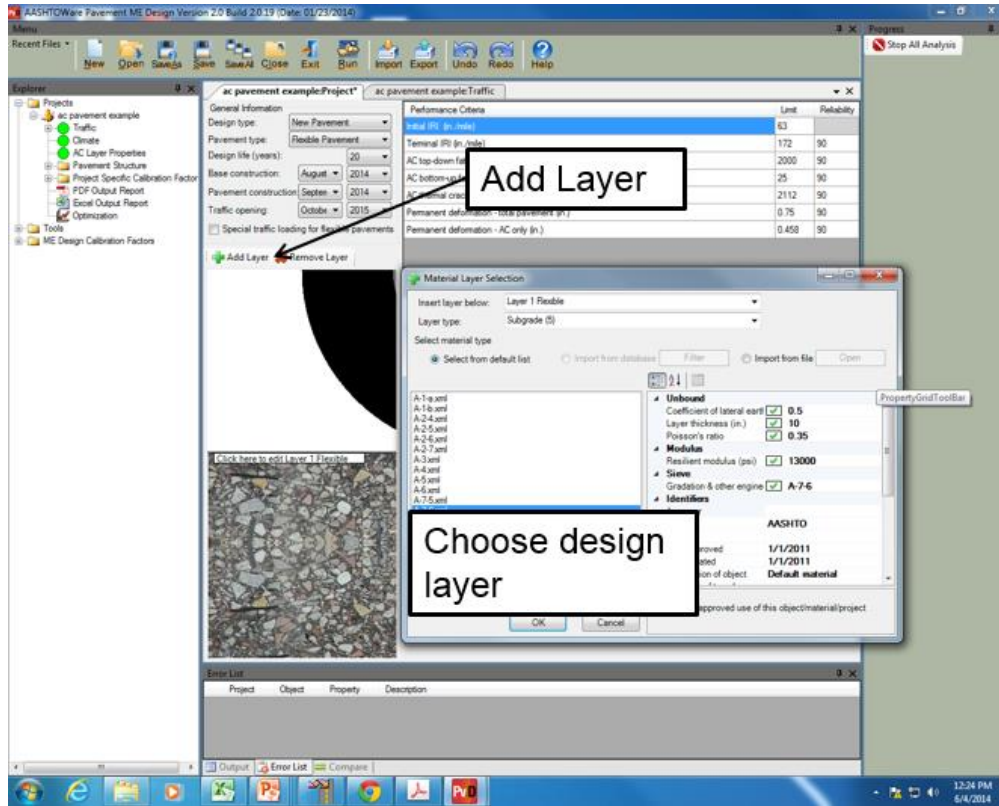


Figure B.18. Pavement structure input for new HMA

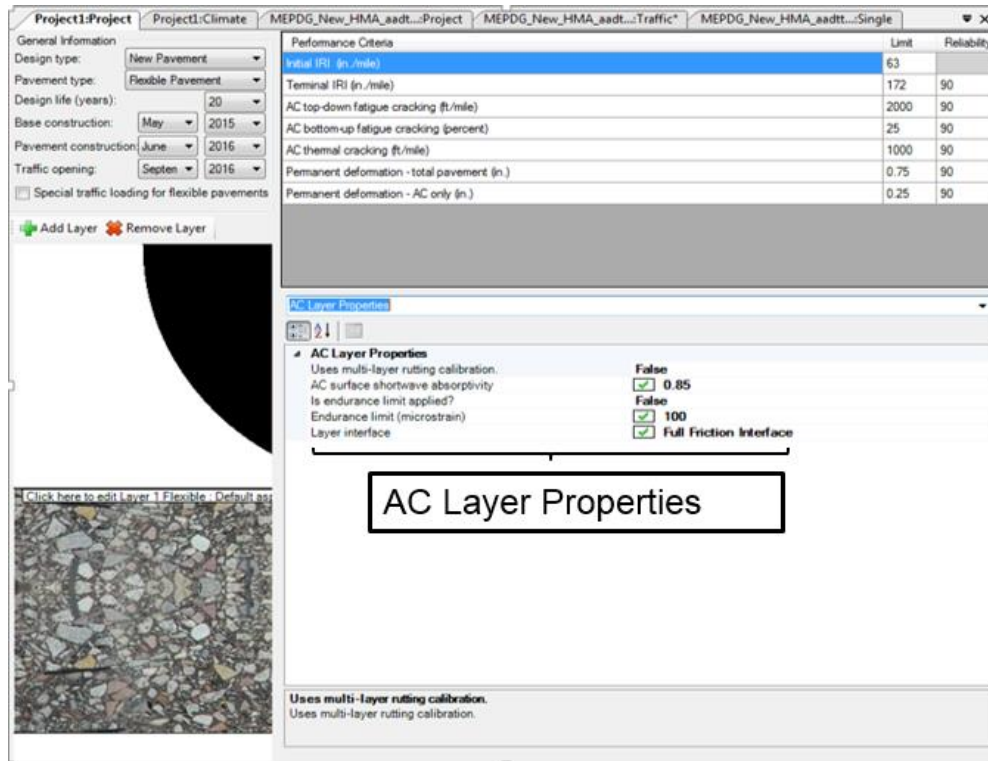


Figure B.19. AC layer properties

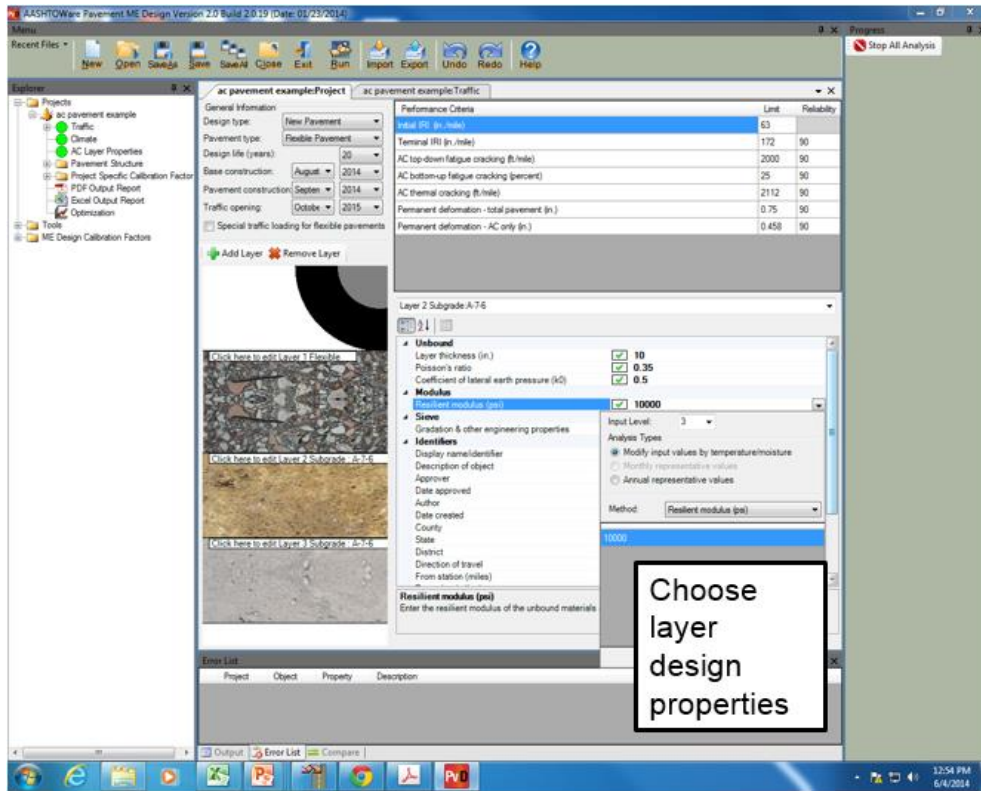


Figure B.20. Layer design properties

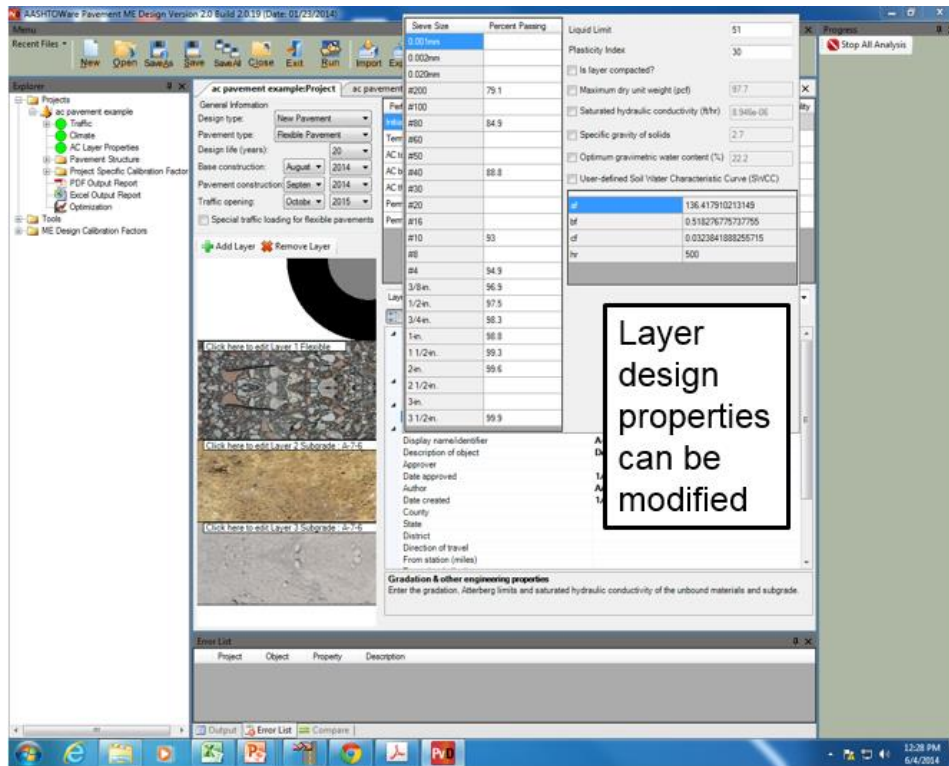


Figure B.21. Modification of layer design properties of new HMA pavement

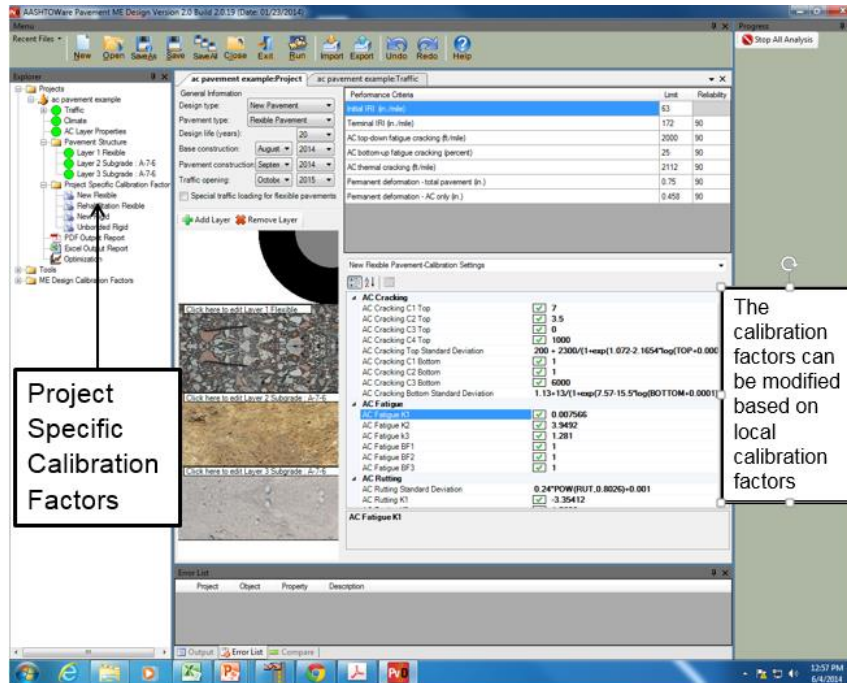


Figure B.22. Inputting HMA local calibration coefficients

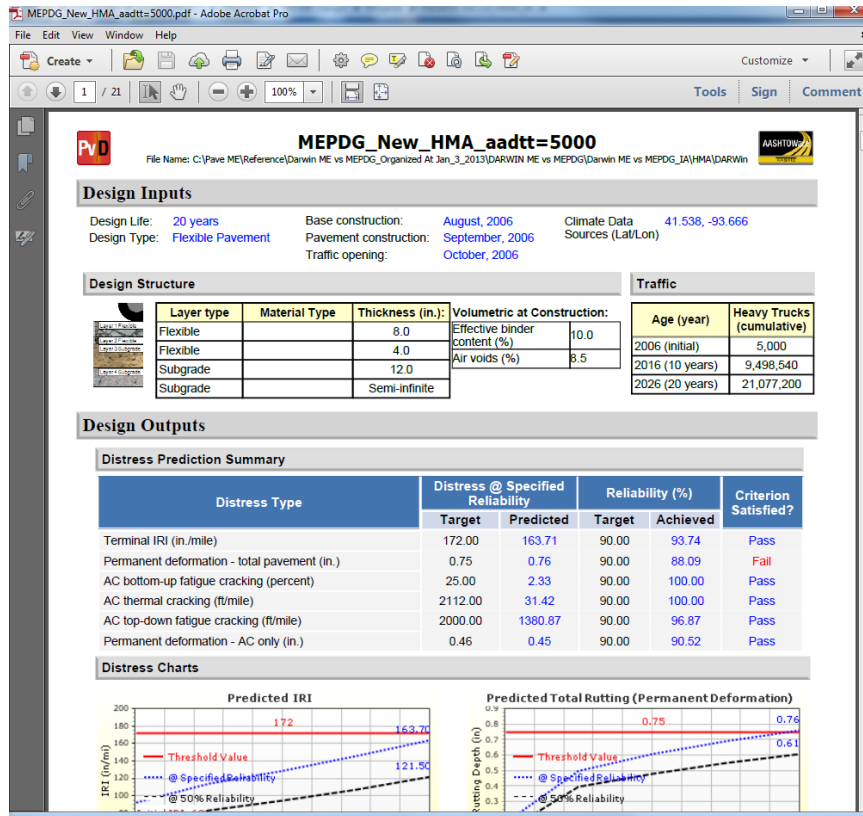


Figure B.23. PDF output report for new HMA pavement

HMA over JPCP Pavement

The design of a HMA over JPCP pavement section in Des Moines, Iowa was performed using AASHTOWare Pavement ME Design software. The following input categories are required for the design procedure:

- Traffic inputs
- Climate inputs
- Pavement structure related inputs
- Existing JPCP design properties
- Existing JPCP condition
- Project specific calibration factors

The following inputs are used in this specific design example:

Design life

- Design life: 30 years
- Existing construction: August 2014
- Pavement construction: September 2014
- Traffic opening: October 2014
- Type of design: Overlay– AC over JPCP

Construction requirements

- A good quality of construction with an initial IRI between 50 and 75 in/mile (assume 63 in/mile for design purposes)

Traffic

- The two-way average annual daily truck traffic (AADTT) on this highway is estimated to be 5,000 trucks during the first year of its service.

- Two lanes in the design direction with 95% of the trucks in the design lane
- Truck traffic is equally distributed in both directions
- The operational speed is 60 mph
- The traffic increases by 2.0% of the preceding year's traffic (compounded annually)
- Vehicle class distribution: TTC 4

Performance Criteria

- Initial IRI (in/mi): 63
- Terminal IRI (in/mi): 172
- AC top-down fatigue cracking (ft/mi): 2000
- AC bottom-up fatigue cracking (percent): 25
- AC thermal cracking (ft/mi): 1000
- Permanent deformation-total pavement (in): 0.75
- Permanent deformation-AC only (in): 0.25
- AC total cracking - bottom up + reflective (percent): 10
- JPCP transverse cracking (percent slabs): 15
- Reliability level for all criteria: 90 %

Layer properties

- HMA layer: 5 in./ PG 58-28
- Existing PCC layer: 10 in./ MOR = 600 psi
- Non-stabilized base: 5 in./ Mr =35,000 psi
- Subgrade: semi-infinite thickness / Mr = 10,000 psi
- JPCP design properties:
- PCC joint spacing: 20 ft.

- Sealant type: no sealant, liquid or silicone
- Doweled joints: 1.5 in. of dowel diameter
- Widened slab: 14 ft.
- Not tied shoulders
- Existing JPCP condition
- Percent slabs replaced/distressed (transverse cracks) before restoration: 15 %
- Percent slabs repaired/replaced after restoration: 0 %

The following figures show the screenshots the design steps using Pavement ME Design:

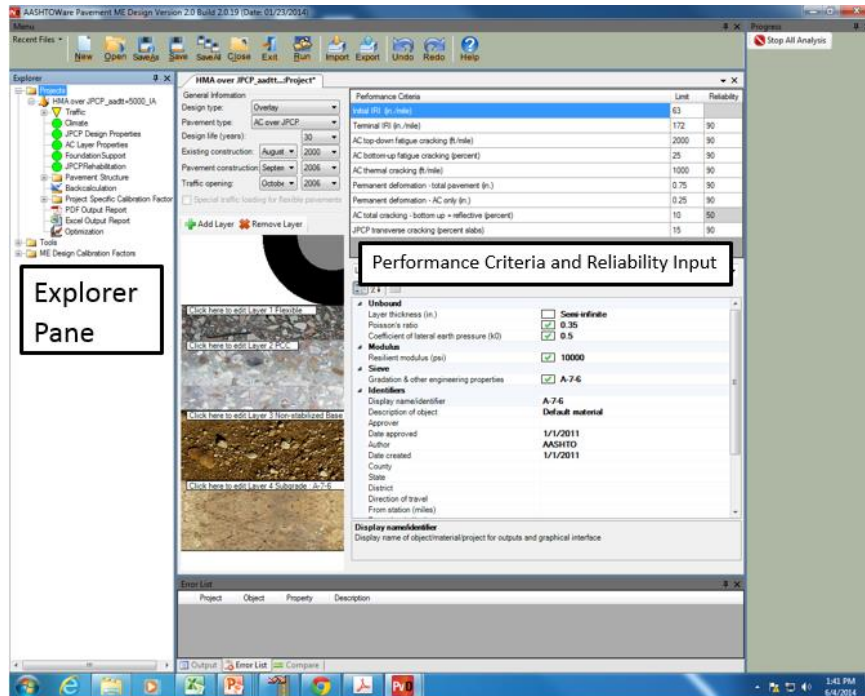


Figure B.24. General inputs, design criteria and reliability

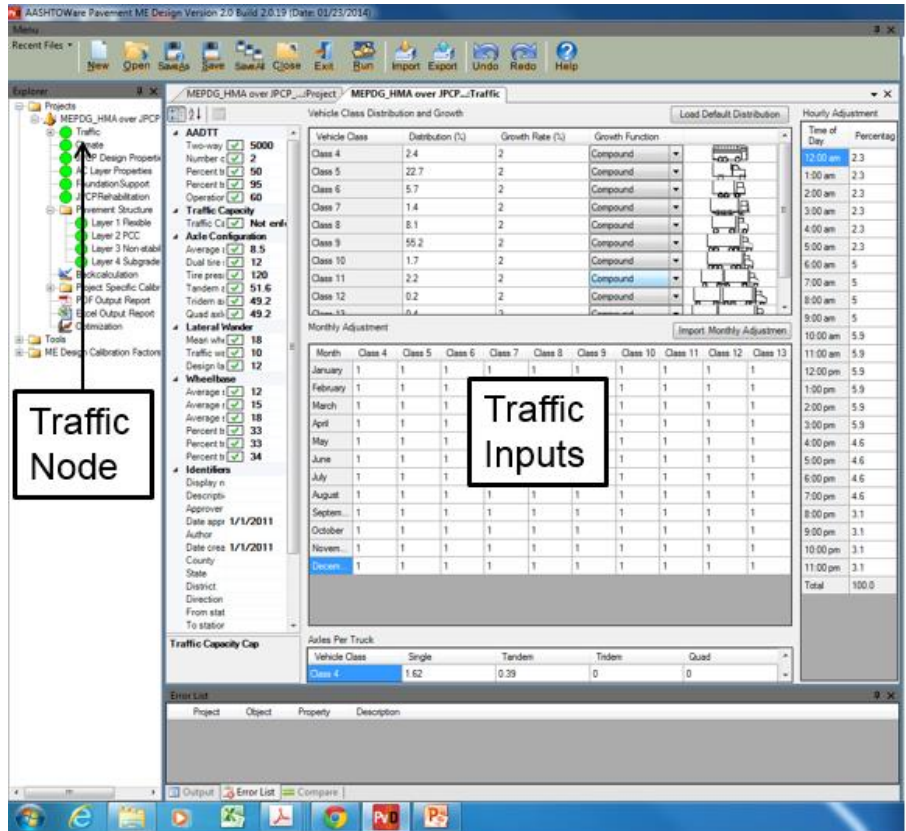


Figure B.25. Traffic inputs

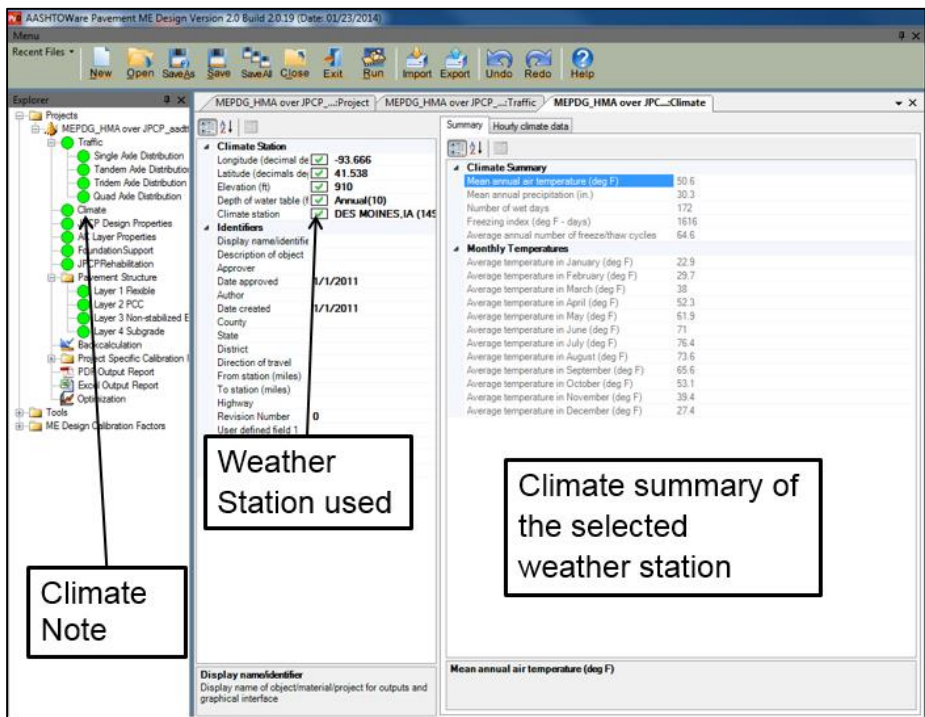


Figure B.26. Climate inputs

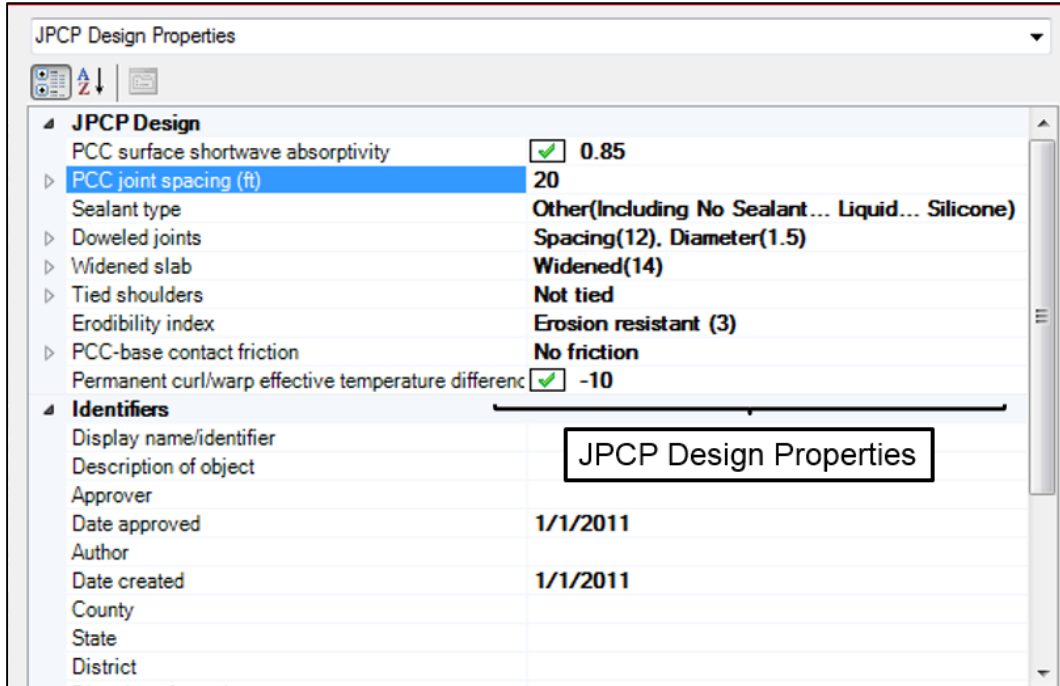


Figure B.27. JPCP design properties for the HMA over JPCP pavement

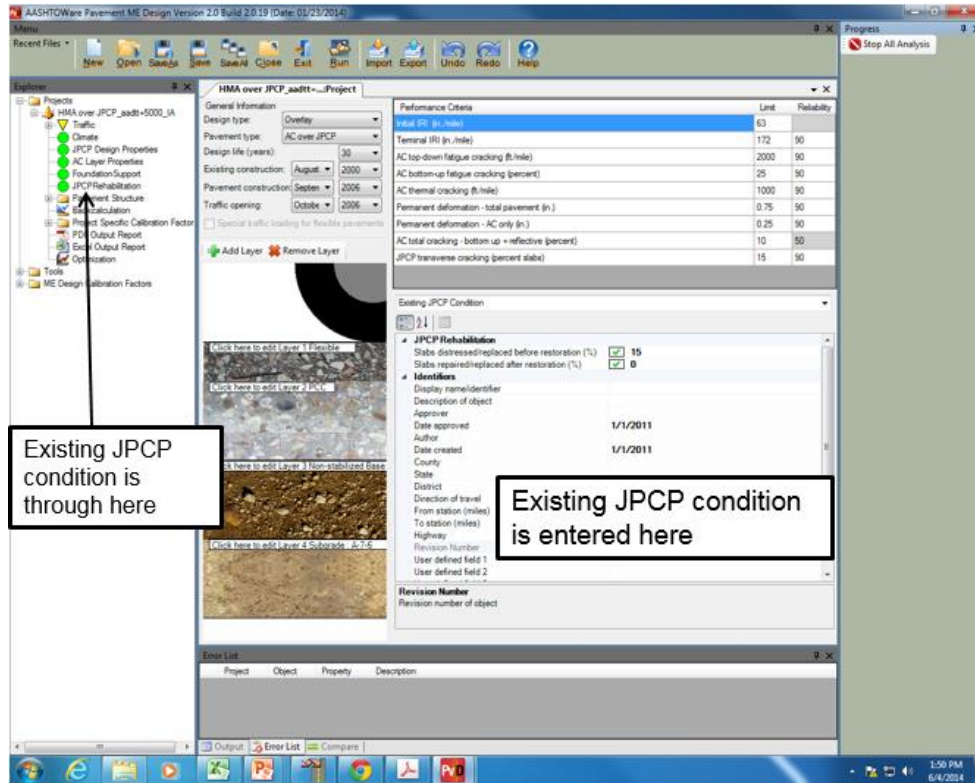


Figure B.28. Existing JPCP condition of the HMA over JPCP pavement

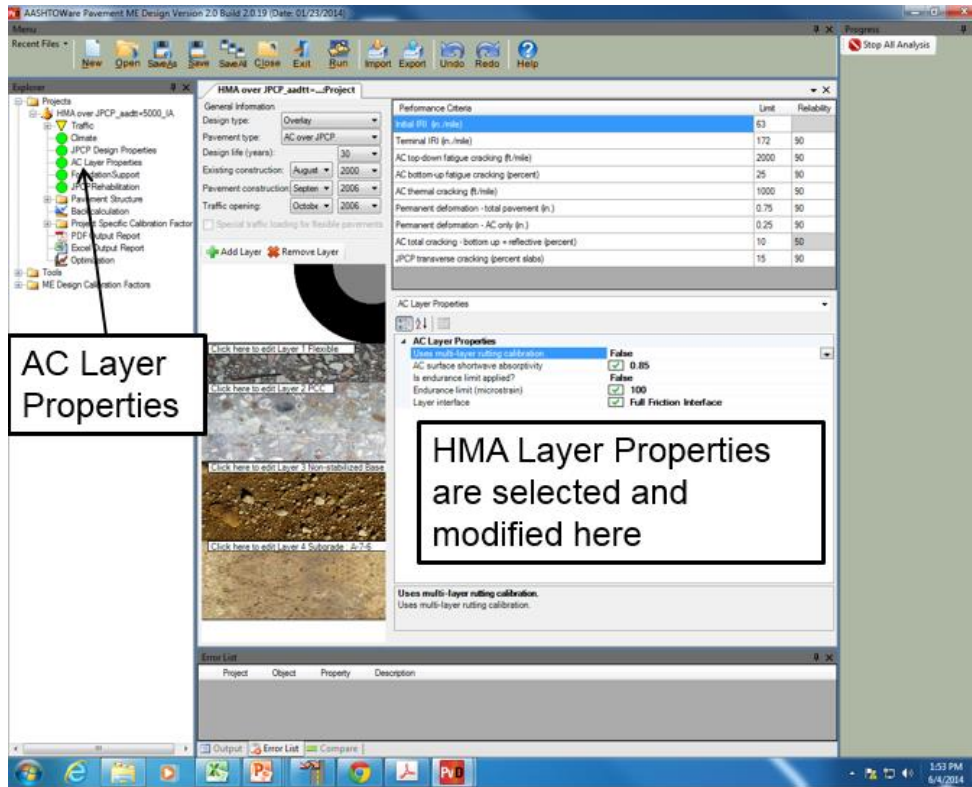


Figure B.29. AC layer design properties

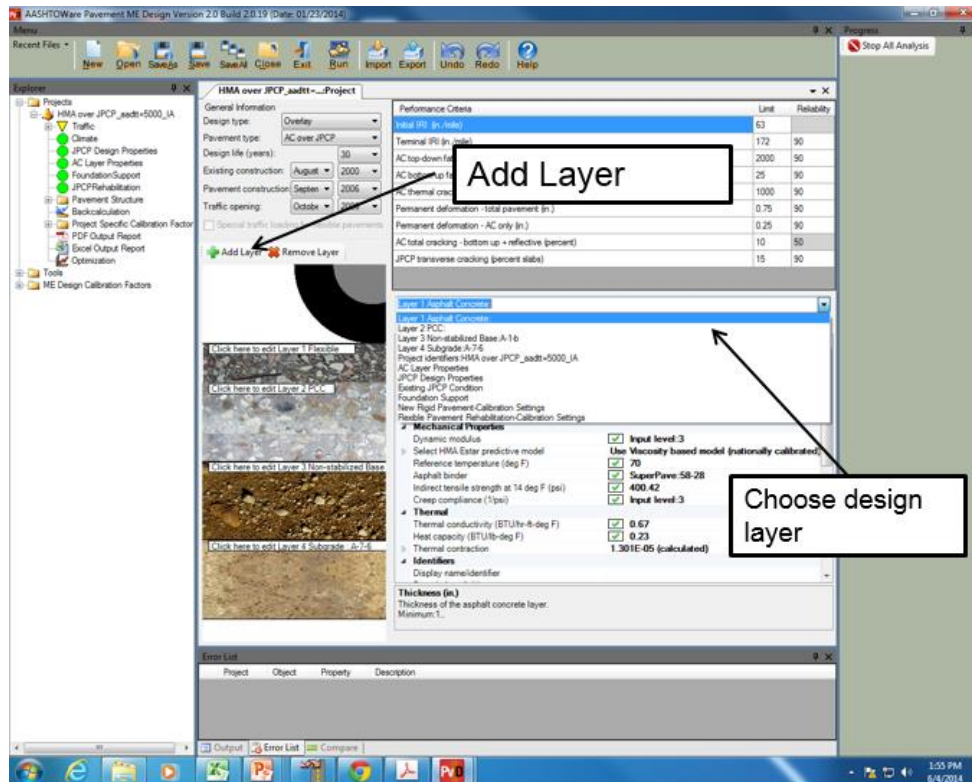


Figure B.30. Pavement structure input for the HMA over JPCP pavement

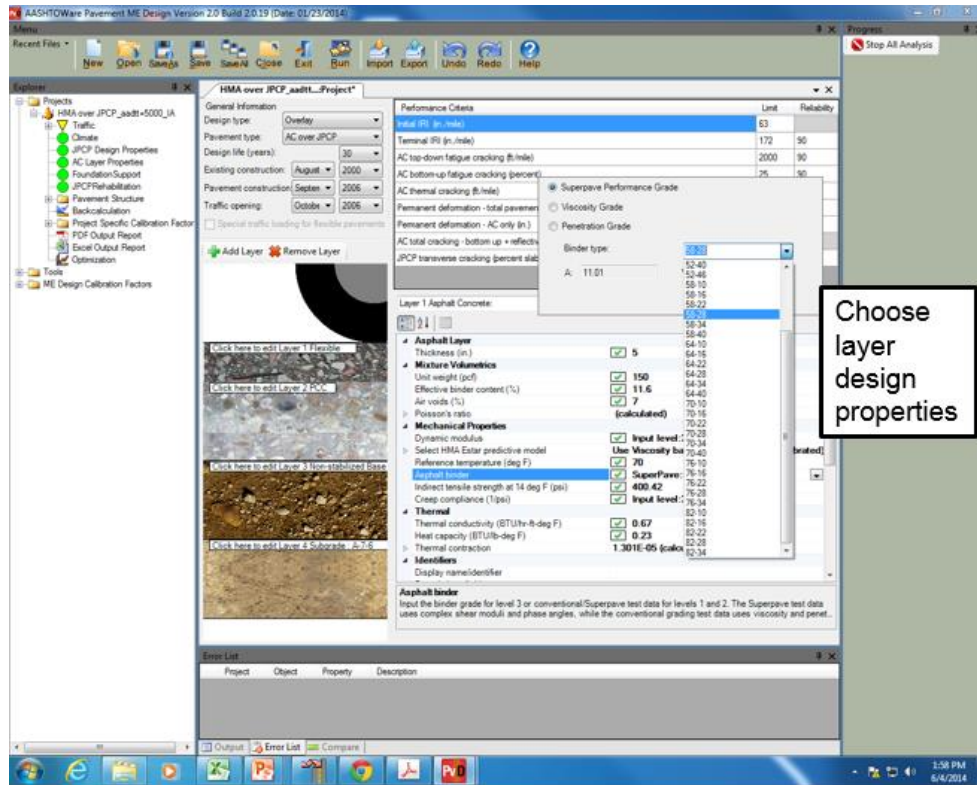


Figure B.31. Choosing layer design properties of the HMA over JPCP pavement

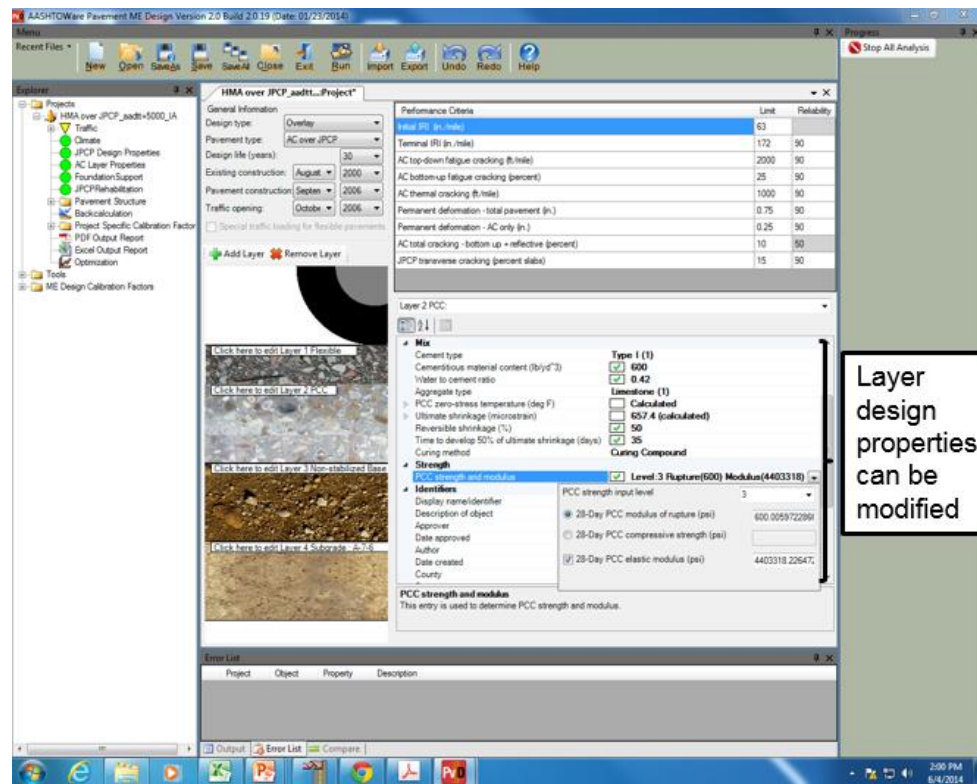


Figure B.32. Modification of layer design properties

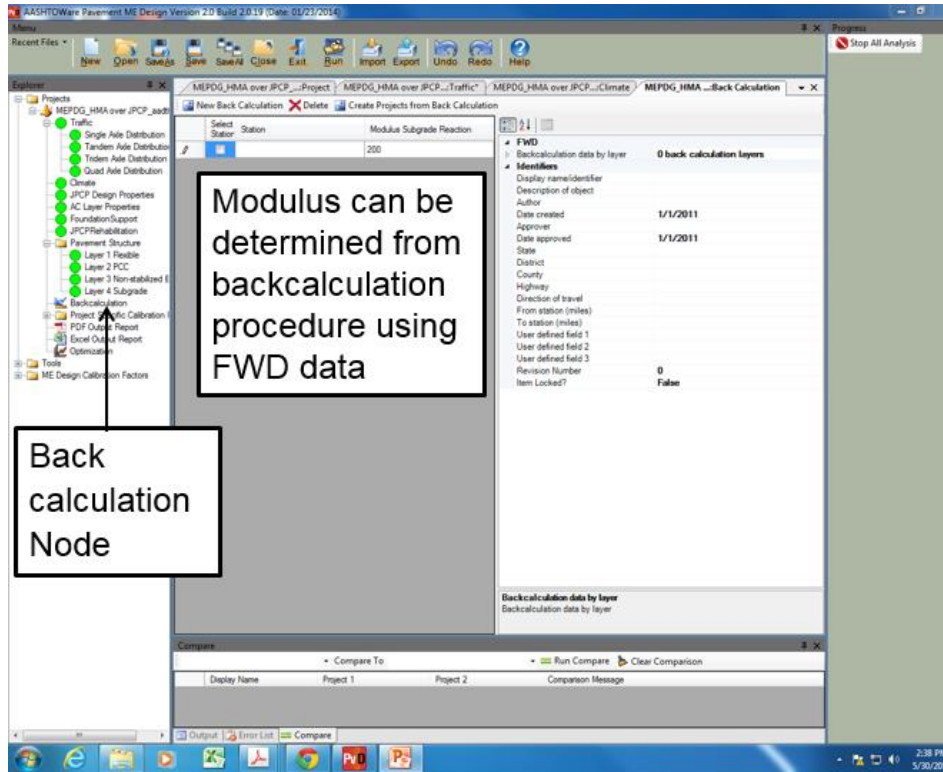


Figure B.33. Use of Back calculation Node

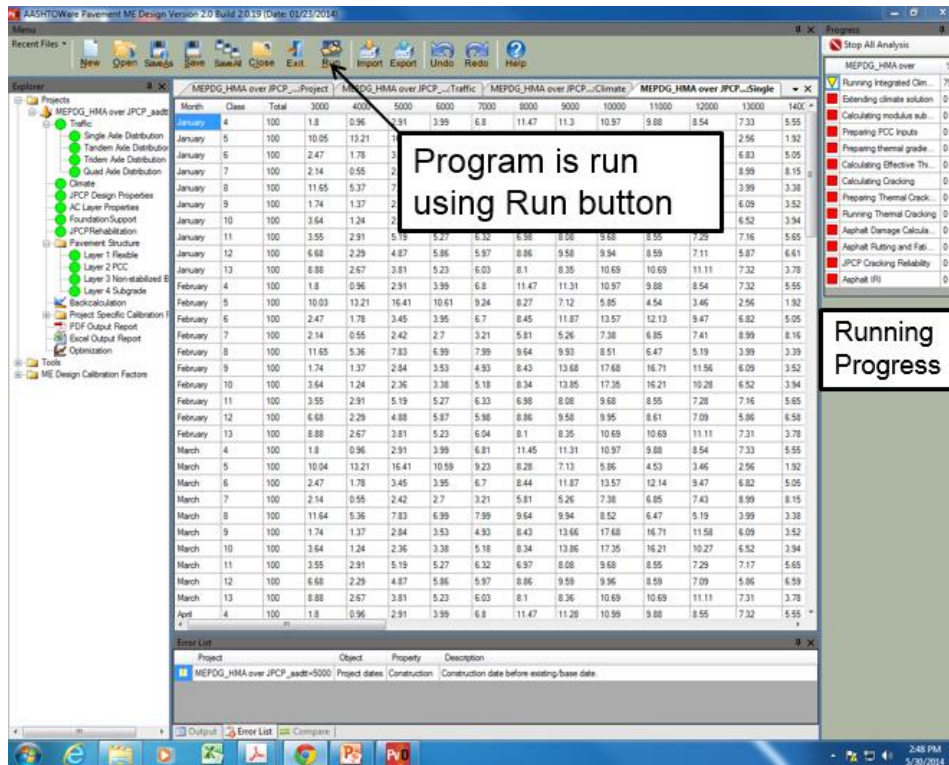


Figure B.34. Running the software

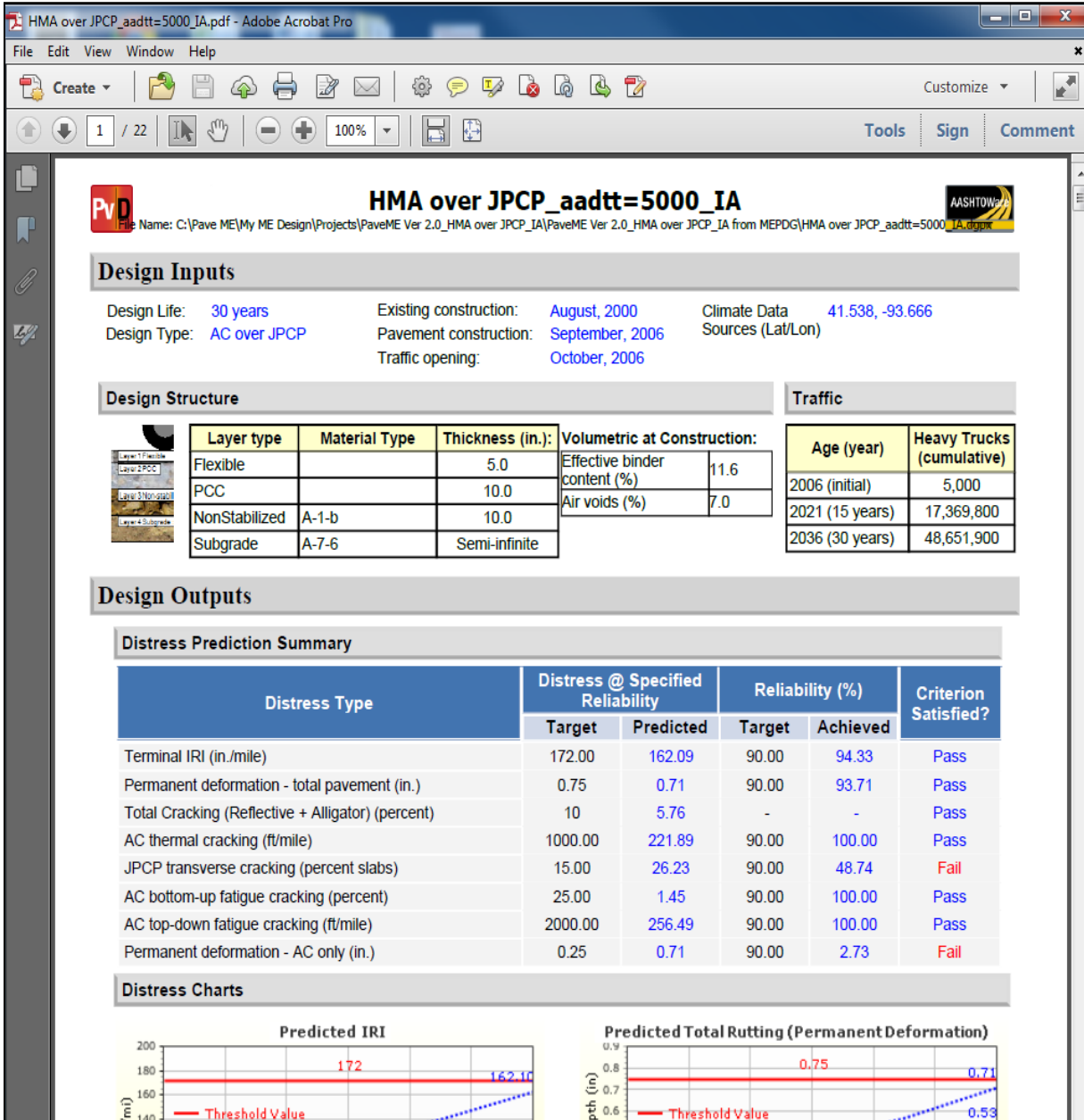


Figure B.35. PDF output report for the HMA over JPCP pavement

APPENDIX C: SENSITIVITY ANALYSIS OF LOCAL CALIBRATION COEFFICIENTS

Sensitivity analysis basically indicates the sensitivity (change) in an output (y) as a result of a change in the input (x). In this study, the sensitivity analysis of calibration coefficients of each pavement performance model was performed to understand which calibration coefficients play the major role in a model.

One-at-a-time sensitivity analysis (OAT) was utilized to quantify the sensitivity of each equation calibration coefficient in this study. OAT sensitivity study figures out the extent of change in the output as response to a change in only one input at a time. (NCHRP 2011). Two numerical parameters, a coefficient sensitivity index (S_{ijk}) and a coefficient-normalized sensitivity index (S^n_{ijk}), were calculated for each calibration coefficient to assess the sensitivity of each calibration coefficient quantitatively and compare the magnitudes of sensitivities amongst themselves.

The coefficient sensitivity index (S_{ijk}) can be calculated as follows (NCHRP 2011):

$$S_{ijk} = \left. \frac{\partial Y_j}{\partial X_k} \right|_i \cong \left. \frac{\Delta Y_j}{\Delta X_k} \right|_i \quad (\text{C1})$$

$$\left. \frac{\Delta Y_j}{\Delta X_k} \right|_i = \frac{Y_{j,i+1} - Y_{j,i}}{X_{k,i+1} - X_{k,i}} \quad \text{when } X_{j,i+1} > X_{j,i} \quad (\text{C2})$$

$$\left. \frac{\Delta Y_j}{\Delta X_k} \right|_i = \frac{Y_{j,i} - Y_{j,i-1}}{X_{k,i} - X_{k,i-1}} \quad \text{when } X_{j,i-1} < X_{j,i} \quad (\text{C3})$$

Where, Y_{ji} and X_{ki} are the values of the performance prediction j and calibration coefficient k evaluated at national calibration coefficient condition i in a model. The partial derivative in the coefficient of sensitivity index can be approximated into a standard central difference approximation (equation C1). The S_{ijk} implies the percentage change in performance prediction Y_j as a result of the percentage change in the calibration coefficient X_k at national calibrated condition i in the model. To exemplify the interpretation of S_{ijk} , the value of 0.5 of S_{ijk}

would imply that a 40% change in the calibration coefficient value of X_{ki} would cause a 20% change in performance prediction Y_{ji} . (NCHRP 2011)

For each calibration coefficient, X_k , two coefficient sensitivity indices (S_{ijk}) were calculated using the 20 % increased and 20 % decreased values of calibration coefficients ($X_{j,1.2i} > X_{j,i}$ and $X_{j,0.8i} < X_{j,i}$). To compare the coefficient sensitivity indices amongst calibration coefficients, the indices should be normalized. Note that, the normalization of S_{ijk} was performed using the associated national calibration coefficient. A “national coefficient” normalized sensitivity index (S_{ijk}^n) can be calculated as follows (NCHRP 2011):

$$S_{ijk}^n = \frac{\partial Y_j}{\partial X_k} \bigg|_i \left(\frac{X_{ki}}{Y_{ji}} \right) \cong \frac{\Delta Y_j}{\Delta X_k} \bigg|_i \left(\frac{X_{ki}}{Y_{ji}} \right) \quad (\text{C4})$$

New Rigid Pavement

In the sensitivity analysis of JPCP pavement performance models, a JPCP section representing typical Iowa JPCPs was determined. This pavement section is on I-29 highway with Mile-post (MP) numbers 76.54 to 90.72 in Harrison County, Iowa. The pavement section is composed of a 12 in. PCC layer with 4 in. granular subbase layer. It has 2 lanes with 3,104 projected annual average daily truck traffic (AADTT) in the construction year.

Table C.1 indicates the sensitivity analysis results of JPCP faulting model calibration coefficients. The negative sign of coefficient sensitivity index implies that as equation calibration coefficient increases, the faulting prediction decreases or vice versa. As can be seen in the table, C6 is the most sensitive coefficient in this model. Table C.2 and Table C.3 present the sensitivity analysis results of transverse cracking and IRI model coefficients, respectively. As can be seen from the tables, C1 and C4 are the most sensitive coefficients for transverse cracking and IRI models, respectively.

Table C.1. Summary of calibration coefficient sensitivity indices for JPCP faulting model

Calibration factors	Coefficient sensitivity index (S_{ijk})		Coefficient Sensitivity Index	Rank
	$X_{j,i+1} > X_{j,i}$	$X_{j,i-1} < X_{j,i}$		
C6	0.00335	0.00223	2.22	1
C1	0.00065	0.00058	1.24	2
C2	0.00046	0.00042	0.80	3
C3	0.17882	0.17882	0.78	4
C4	0.12794	0.12794	0.22	6
C7	0.00006	0.00006	0.22	5
C5	0.00000	0.00000	0.07	7

Table C.2. Summary of calibration coefficient sensitivity indices for JPCP transverse cracking model

Calibration Factors	Coefficient sensitivity index (S_{ijk})		Coefficient Sensitivity Index	Rank
	$X_{j,i+1} > X_{j,i}$	$X_{j,i-1} < X_{j,i}$		
C1	-201.03	-27.93	-2.58	1
C2	-320.49	-45.29	-2.52	2
C5	-8.96	-12.32	0.24	3
C4	-9.80	-10.25	-0.11	4

Table C.3. Summary of calibration coefficient sensitivity indices for JPCP IRI model

Calibration Factors	Coefficient sensitivity index (S_{ijk})		Coefficient Sensitivity Index	Rank
	$X_{j,i+1} > X_{j,i}$	$X_{j,i-1} < X_{j,i}$		
C4	1.66	1.66	0.20	1
C1	47.78	47.78	0.18	2
C2	0.95	0.95	0.0020	3
C3	0.04	0.04	0.0003	4

New HMA and HMA over JPCP

The same rutting, fatigue cracking, thermal cracking and IRI models are used in both HMA and HMA over JPCP pavement systems. Only difference between the models in these pavement systems is that in HMA over JPCP IRI model, reflective cracking predictions are also included in the IRI equations as a part of total transverse cracking predictions. Therefore, only

the sensitivity analysis of HMA pavement performance model calibration coefficients were presented here.

In the sensitivity analysis, an HMA section, representing typical Iowa HMA pavements was determined. This pavement section is on US 61 highway with Mile-post (MP) numbers 167.95 to 174.74 in Jackson County, Iowa. The pavement section is composed of 11 in. HMA layer with 12 in. subgrade layer. It has 2 lanes with 1,162 projected annual average daily truck traffic (AADTT) in the construction year.

Table C.4, Table C.5, Table C.6, Table C.7, Table C.8, Table C.9, and Table C.10 present the sensitivity analysis results of AC rutting, subgrade rutting, HMA fatigue, alligator (bottom-up) cracking, longitudinal (top-down) cracking, thermal cracking and IRI models for HMA and HMA over JPCP pavement types, respectively.

Table C.4. Summary of calibration coefficient sensitivity indices for HMA rutting model

Calibration Factors	Coefficient sensitivity index (S_{ijk})		Coefficient Sensitivity Index	Rank
	$X_{j,i+1} > X_{j,i}$	$X_{j,i-1} < X_{j,i}$		
BR2	2.11	0.51	9.65	1
BR3	1.94	0.50	8.94	2
BR1	0.14	0.14	1.00	3

Table C.5. Summary of calibration coefficient sensitivity indices for HMA subgrade rutting model

Calibration Factors	Coefficient sensitivity index (S_{ijk})		Coefficient Sensitivity Index	Rank
	$X_{j,i+1} > X_{j,i}$	$X_{j,i-1} < X_{j,i}$		
BS1	0.24	0.24	1.00	1

Table C.6. Summary of calibration coefficient sensitivity indices for HMA fatigue model

Calibration Factors	Coefficient sensitivity index (S_{ijk})		Coefficient Sensitivity Index	Rank
	$X_{j,i+1} > X_{j,i}$	$X_{j,i-1} < X_{j,i}$		
BF2	-1.54	-3183.455	-5153.72	1
BF3	46.51	1.49	77.67	2
BF1	-0.26	-0.39	-1.04	3

Table C.7. Summary of calibration coefficient sensitivity indices for HMA alligator (bottom-up) cracking model

Calibration Factors	Coefficient sensitivity index (S_{ijk})		Coefficient Sensitivity Index	Rank
	$X_{j,i+1} > X_{j,i}$	$X_{j,i-1} < X_{j,i}$		
C1_Bottom	-0.69	-1.81	-5.65	1
C2_Bottom	-0.24	-0.31	-1.24	2
C4_Bottom	0.00	0.00	1.00	3

Table C.8. Summary of calibration coefficient sensitivity indices for HMA longitudinal (top-down) cracking model

Calibration Factors	Coefficient sensitivity index (S_{ijk})		Coefficient Sensitivity Index	Rank
	$X_{j,i+1} > X_{j,i}$	$X_{j,i-1} < X_{j,i}$		
C1_Top	-0.04	-0.17	-9.54	1
C2_Top	-0.07	-0.18	-5.64	2
C4_Top	0.00	0.00	1.00	3

Table C.9. Summary of calibration coefficient sensitivity indices for HMA thermal (transverse) cracking model

Calibration Factors	Coefficient sensitivity index (S_{ijk})		Coefficient Sensitivity Index	Rank
	$X_{j,i+1} > X_{j,i}$	$X_{j,i-1} < X_{j,i}$		
K_Level 3	1155.9	2120.0	3.17	1

Table C.10. Summary of calibration coefficient sensitivity indices for HMA IRI model

Calibration Factors	Coefficient sensitivity index (S_{ijk})		Coefficient Sensitivity Index	Rank
	$X_{j,i+1} > X_{j,i}$	$X_{j,i-1} < X_{j,i}$		
C4	2366.67	2333.33	0.35	1
C1	0.38	0.38	0.15	2
C3	812.50	750.00	0.06	3
C2	0.00	0.00	0.00	4